PALEOSEISMOLOGY OF UTAH, VOLUME 4

SEISMOTECTONICS OF NORTH-CENTRAL UTAH AND SOUTHWESTERN WYOMING

by
Michael W. West

Special Study 82 **1994**
UTAH GEOLOGICAL SURVEY
a division of
UTAH DEPARTMENT OF NATURAL RESOURCES

STATE OF UTAH
Michael O. Leavitt, Governor

DEPARTMENT OF NATURAL RESOURCES
Ted Stewart, Executive Director

UTAH GEOLOGICAL SURVEY
M. Lee Allison, Director

UGS Board

Member	Representing
Russell C. Babcock, Jr. (chairman)	Mineral Industry
D. Cary Smith	Mineral Industry
Richard R. Kennedy	Civil Engineering
Jo Brandt	Public-at-Large
C. William Berge	Mineral Industry
Jerry Golden	Mineral Industry
Milton E. Wadsworth	Economics-Business/Scientific
Scott Hirschi, Director, Division of State Lands and Forestry	*Ex officio member*

UGS Editorial Staff

J. Stringfellow	Editor
Vicky Clarke, Sharon Hamre	Editorial Staff
Patricia H. Speranza, James W. Parker, Lori Douglas	Cartographers

UTAH GEOLOGICAL SURVEY
2363 South Foothill Drive
Salt Lake City, Utah 84109-1491
Phone: (801) 467-7970 Fax: (801) 467-4070

THE UTAH GEOLOGICAL SURVEY is organized into three geologic programs with Administration, Editorial, and Computer Resources providing necessary support to the programs. THE ECONOMIC GEOLOGY PROGRAM undertakes studies to identify coal, geothermal, uranium, hydrocarbon, and industrial and metallic mineral resources; to initiate detailed studies of the above resources including mining district and field studies; to develop computerized resource data bases, to answer state, federal, and industry requests for information; and to encourage the prudent development of Utah's geologic resources. THE APPLIED GEOLOGY PROGRAM responds to requests from local and state governmental entities for engineering geologic investigations; and identifies, documents, and interprets Utah's geologic hazards. THE GEOLOGIC MAPPING PROGRAM maps the bedrock and surficial geology of the state at a regional scale by county and at a more detailed scale by quadrangle. The Geologic Extension Service answers inquiries from the public and provides information about Utah's geology in a non-technical format.

The UGS manages a library which is open to the public and contains many reference works on Utah geology and many unpublished documents on aspects of Utah geology by UGS staff and others. The UGS has begun several computer data bases with information on mineral and energy resources, geologic hazards, stratigraphic sections, and bibliographic references. Most files may be viewed by using the UGS Library. The UGS also manages a sample library which contains core, cuttings, and soil samples from mineral and petroleum drill holes and engineering geology investigations. Samples may be viewed at the Sample Library or requested as a loan for outside study.

The UGS publishes the results of its investigations in the form of maps, reports, and compilations of data that are accessible to the public. For information on UGS publications, contact the Sales Office, 2363 South Foothill Drive, Salt Lake City, Utah 84109-1491, (801) 467-0401.

The Utah Department of Natural Resources receives federal aid and prohibits discrimination on the basis of race, color, sex, age, national origin, or handicap. For information or complaints regarding discrimination, contact Executive Director, Utah Department of Natural Resources, 1636 West North Temple #316, Salt Lake City, UT 84116-3193 or Office of Equal Opportunity, U.S. Department of the Interior, Washington, DC 20240.

Printed on recycled paper

**THE PUBLICATION OF THIS PAPER
IS MADE POSSIBLE WITH MINERAL LEASE FUNDS**

This publication is printed on recycled paper.

Paleoseismology of Utah, Volume 4

FOREWORD

This Utah Geological Survey (UGS) Special Study publication on Quaternary faulting along the north flank of the Unita Mountains in north-central Utah and southwestern Wyoming is the fourth report in the "Paleoseismology of Utah" Special Studies series. More than the usual "site-specific" trench study, this report presents a comprehensive evaluation and regional synthesis of the seismotectonic setting along the Utah - Wyoming border. Results of the study provide strong evidence for Quaternary normal-slip reactivation of thrust faults along the leading edge of the Wyoming part of the Sevier orogenic belt. In addition, fault-trenching studies like this one provide critical information on earthquake timing, recurrence, displacement, fault geometry, and related earthquake-induced hazards that can be used to characterize seismic-source zones and to evaluate the long-term earthquake potential and risk from active faults.

The author, Michael W. West, currently in private geologic consulting practice, is the former head of the U.S. Bureau of Reclamation's (USBR) Seismotectonic Section, which specializes in seismic-hazard evaluations of proposed and existing USBR dams. Work in the study area was initiated as part of a seismic-hazard evaluation for the Meeks Cabin and Stateline dams on the north flank of the Unita Mountains. Work continued with support from a number of oil companies as part of Mr. West's Ph.D. dissertation at the Colorado School of Mines. Funding to prepare this report for publication was provided through the UGS Mineral Lease Special Projects Program.

William R. Lund, Series Editor
Utah Geological Survey

also in this series

Utah Geological Survey Special Study 75, 1991, Paleoseismology of Utah, Volume 1: Fault behavior and earthquake recurrence on the Provo segment of the Wasatch fault zone at Mapleton, Utah County, Utah by W.R. Lund, D.P. Schwartz, W.E. Mulvey, K. E. Budding, and B.D. Black

Utah Geological Survey Special Study 76, 1991, Paleoseismology of Utah, Volume 2: Paleoseismic analysis of the Wasatch fault zone at the Brigham City trench site, Brigham City, Utah and the Pole Patch trench site, Pleasant View, Utah by S. F. Personius

Utah Geological Survey Special Study 78, 1991, Paleoseismology of Utah, Volume 3: The number and timing of Holocene paleoseismic events on the Nephi and Levan segments of the Wasatch fault zone, Utah by Michael Jackson

Utah Geological Survey Special Study 83, 1994, Paleoseismology of Utah, Volume 5: Neotectonic deformation along the East Cache fault zone, Cache County, Utah by James P. McCalpin

PALEOSEISMOLOGY OF UTAH, VOLUME 4

SEISMOTECTONICS OF NORTH-CENTRAL UTAH AND SOUTHWESTERN WYOMING

by
Michael W. West

PART III - NEOTECTONICS OF NORTH-CENTRAL UTAH AND SOUTHWESTERN WYOMING

METHODOLOGY . . . 22
Photogeologic and Field Mapping . . . 22
Scarp Profiling . . . 22
Trench Excavation and Logging . . . 22
Radiocarbon and Amino Acid Racemization Ages . . . 24
Radiocarbon Ages . . . 24
Introduction . . . 24
Sample collection, preparation, and laboratory dating . . . 25
Calibration . . . 25
Amino Acid Racemization Analysis . . . 25
Fault-Rupture Parameters . . . 26
Fault-Rupture Lengths . . . 26
Net Vertical Tectonic Displacements . . . 26
Scarp profiles . . . 26
Stratigraphic throw . . . 26
Colluvial-wedge stratigraphy . . . 26
Ages of Faulting and Recurrence Intervals . . . 26
Tectonic Slip Rates . . . 27
BEAR RIVER FAULT ZONE . . . 27
General Description . . . 27
Northern Scarps . . . 27
La Chapelle Scarp . . . 29
La Chapelle Trench . . . 29
Pre-fault stratigraphy . . . 29
Structure and post-fault stratigraphy . . . 29
Interpretation . . . 29
Lester Ranch Scarp . . . 33
Lester Ranch Trench . . . 33
Pre-fault stratigraphy . . . 33
Structure and post-fault stratigraphy . . . 33
Interpretation . . . 38
Lester Ranch South Trench . . . 38
Pre-fault stratigraphy . . . 38
Structure and post-fault stratigraphy . . . 40
Interpretation . . . 40
Austin Reservoir Scarp . . . 41
Austin Reservoir Irrigation Ditch . . . 41
Pre-fault stratigraphy . . . 42
Structure and post-fault stratigraphy . . . 42
Interpretation . . . 42
Sulphur Creek Scarp . . . 42
Sulphur Creek Trench . . . 45
Pre-fault stratigraphy . . . 45
Structure and post-fault stratigraphy . . . 46
Interpretation . . . 47
Deadman Creek Lineament . . . 48
Deadman Creek Scarp . . . 48
Big Burn Scarp . . . 48
Big Burn Trench . . . 48
Pre-fault stratigraphy . . . 51
Structure and post-fault stratigraphy . . . 51
Interpretation . . . 52
Little Burn Scarps . . . 52
Upper Little Burn Trench . . . 52

Pre-fault stratigraphy . . . 52
Structure and post-fault stratigraphy . . . 52
Interpretation . . . 53
Lower Little Burn Trench . . . 53
Pre-fault stratigraphy . . . 54
Structure and post-fault stratigraphy . . . 54
Interpretation . . . 54
Fault Rupture Characteristics . . . 55
Rupture Length . . . 55
Net Vertical Tectonic Displacements . . . 55
Age of Movement and Recurrence Intervals . . . 56
Tectonic Slip Rates . . . 59
Summary . . . 59
ABSAROKA FAULT . . . 59
Martin Ranch Scarp . . . 60
Upper Martin Ranch Trench . . . 60
Pre-fault stratigraphy . . . 61
Structure and post-fault stratigraphy . . . 61
Interpretation . . . 61
Lower Martin Ranch Trench . . . 61
Pre-fault stratigraphy . . . 62
Structure and post-fault stratigraphy . . . 62
Interpretation . . . 62
Deflection of the Bear River . . . 62
Fault Rupture Characteristics . . . 64
Rupture Length . . . 64
Net Vertical Tectonic Displacements . . . 64
Age of Movement and Recurrence Intervals . . . 64
Tectonic Slip Rates . . . 64
Summary . . . 64
DARBY-HOGSBACK FAULT . . . 64
Terrace Deformation . . . 64
Muddy Creek Lineament and Associated Scarps . . . 65
Elizabeth Ridge Scarps . . . 67
Elizabeth Ridge Trench . . . 67
Pre-fault stratigraphy . . . 68
Structure and post-fault stratigraphy . . . 68
Interpretation . . . 68
Drainage Basin Separation . . . 69
Fault-Rupture Characteristics . . . 69
Rupture Length and Vertical Tectonic Displacements . . . 70
Age of Movement and Recurrence Intervals . . . 70
Tectonic Slip Rates . . . 70
Summary . . . 70

PART IV - TECTONIC MODELS AND HAZARD ASSESSMENT

NEOTECTONIC MODELS . . . 71
Subsurface Structure . . . 71
Neotectonic Development of the Bear River Fault Zone . . . 71
Mechanical Relaxation . . . 71
Basement-Penetrating Faults . . . 72
Reactivation of Thrust Faults . . . 72
SEISMOGENESIS IN NORTH-CENTRAL UTAH, SOUTHWESTERN WYOMING, AND THE INTERMOUNTAIN SEISMIC BELT . . . 75
Seismogenesis in the ISB . . . 75

Geological Versus Seismological Models . . . 75
Conclusions . . . 78
SEISMOTECTONIC HAZARD ASSESSMENT . . . 78
Historic Seismicity . . . 78
Paleoearthquakes and Hazard Assessment . . . 79
Bear River Fault Zone . . . 79
Absaroka Fault . . . 80
Darby-Hogsback Fault . . . 80
Northeast-Striking Scarps . . . 81
Surface-Fault Rupture . . . 81
Secondary Seismotectonic Hazards . . . 81
Ground Tilt/Subsidence . . . 81
Liquefaction . . . 81
Earthquake-Induced Landslides . . . 81

PART V - CONCLUSIONS AND RECOMMENDATIONS

CONCLUSIONS . . . 82
RECOMMENDATIONS . . . 82
SELECTED REFERENCES . . . 84

FIGURES

Figure 1. Location map of detailed and reconnaissance study areas . . . 3
Figure 2. Western United States showing tectonic provinces and relationship of the project area to major neotectonic and volcanic features . . . 6
Figure 3. Generalized tectonic map of north-central Utah and southwestern Wyoming . . . 7
Figure 4. Generalized tectonic map of the Uinta Mountains anticline . . . 7
Figure 5. Back valleys of east-central Utah . . . 8
Figure 6. The Intermountain seismic belt . . . 10
Figure 7. Generalized stratigraphic section, north-central Utah and southwestern Wyoming . . . 12
Figure 8. Regional geologic map of north-central Utah and southwestern Wyoming . . . 13
Figure 9. Middle to Upper Paleozoic rocks exposed in the hanging wall of the North Flank fault . . . 13
Figure 10. Steeply dipping beds of the Frontier Formation . . . 15
Figure 11. Outcrop of Triassic Woodside(?) Shale with Mississippian Madison(?) Limestone in background . . . 15
Figure 12. Planar Gilbert Peak erosion surface capped by Bishop Conglomerate on Elizabeth Ridge . . . 16
Figure 13. Exposure of Bishop Conglomerate on Elizabeth Mountain . . . 16
Figure 14. Tectonic map of the project area and vicinity . . . 19
Figure 15. View to the south across Sulphur Creek in section 29, T. 14 N., R. 119 W . . . 19
Figure 16. Sub-vertical beds of the Hilliard Formation exposed in the hanging wall of the Absaroka thrust . . . 20
Figure 17. Northwest-southeast cross section across the Absaroka and Darby-Hogsback thrust plates . . . 21
Figure 18. Subsurface structure along the North Flank fault in T. 1 N., R. 7-8 E. . . . 21
Figure 19. Block diagram showing degradation of sub-vertical free face formed by surface rupture . . . 23
Figure 20. Water-filled sag pond at the base of the Lester Ranch scarp in section 24, T. 13 N., R. 119 W. . . . 23
Figure 21. Model for development of successive colluvial wedges and buried soils . . . 23
Figure 22. Excavation of the Lester Ranch trench in section 24, T. 13 N., R. 119 W. . . . 24
Figure 23. Gibbons and Dickey (1983) mapped apparent late Quaternary faults in southwestern Wyoming . . . 28
Figure 24. Map of neotectonic features in the project area . . . 28
Figure 25. Oblique aerial view to the south of right en echelon scarps near the northern end of the main Bear River fault zone . . . 28
Figure 26. Oblique aerial view to the southwest of a short late Quaternary scarp northeast of the main Bear River fault zone (section 15, T. 14 N., R. 118 W.) . . . 30

Figure 27. Oblique aerial view to the south of the southern end of the La Chapelle scarp 30
Figure 28A. Oblique aerial view to south of fault scarp impinging on the floodplain of La Chapelle Creek 31
Figure 28B. Floodplain alluvium is displaced along fault in upper center 31
Figure 29. View to the north along the La Chapelle scarp showing the trench site in section 19, T. 13 N., R. 118 W. 32
Figure 30. View of the La Chapelle trench near station 30 32
Figure 31. South wall of the La Chapelle trench showing the fault near station 28 33
Figure 32. Ground-level view to north of the Lester Ranch scarp 36
Figure 33. View to the south along the Lester Ranch scarp showing water-filled sag pond 36
Figure 34. Oblique aerial view to northeast of the Lester Ranch scarp displacing a strath-terrace surface 37
Figure 35. Detail of faulting exposed in the Lester Ranch trench 37
Figure 36. View of the Lester Ranch fault and tectonically stacked colluvial wedges and buried soils 39
Figure 37. View to the west away from the fault exposed in the Lester Ranch trench 39
Figure 38. Fault zone exposed in the south wall of the Lester Ranch South trench near stations 17-18 40
Figure 39. View of an excavation along the master fault plane in the north wall of the Lester Ranch South trench 41
Figure 40. View to the west away from the fault zone exposed in the Lester Ranch South trench 41
Figure 41. View to the southeast across Austin Reservoir showing the scarp dying out to the south (right) 42
Figure 42. View of the Austin Reservoir fault exposed in the irregular wall of an irrigation ditch 43
Figure 43. View to the north along the Sulphur Creek scarp near its northern end in section 35, T. 13 N., R. 119 W. 43
Figure 44. Oblique aerial view of the northern Sulphur Creek scarp displacing strath-terrace deposits 44
Figure 45. Oblique aerial view to the northeast of the Sulphur Creek scarp displacing bedrock of the Wasatch Formation . . 44
Figure 46. View to the east of the Sulphur Creek scarp and trench in section 35, T. 13 N., R. 119 W. 45
Figure 47. View of highly organic A-horizon (unit 4A) developed on fine-grained sag-pond sediments (unit 3) 46
Figure 48. Block of A-horizon (unit 5A) and colluvium (unit 5B) resting unconformably on buried A-horizon (unit 4A) . . . 47
Figure 49. Interfingering of slope colluvium (unit 6) transported from uphill to the right with scarp colluvium (unit 7) 47
Figure 50. Oblique aerial view to the northeast of the Big Burn scarp running from upper left to lower right 49
Figure 51. Oblique aerial view to the south showing the Big Burn scarp displacing a lateral moraine 49
Figure 52. Low-sun-angle view of the southern Big Burn scarp (synslope) 50
Figure 53. View of the Big Burn scarp and trench site 50
Figure 54. Buried A-horizon (unit 7) and pods of correlative soil (unit 9B) incorporated in a tectonically derived colluvial wedge (unit 9A) 51
Figure 55. View of the east wall of the Upper Little Burn trench showing imbrication of clasts and root penetration 53
Figure 56. Excavation of the Lower Little Burn trench in section 34, T. 2 N., R. 10 E. 54
Figure 57. Models for increasing scarp heights from north to south along the Bear River fault zone 55
Figure 58. Laboratory ages and calendar-calibrated radiocarbon ages, Bear River fault zone and Martin Ranch scarp 57
Figure 59. Development of soils and tectonically derived colluvial wedges with time 57
Figure 60. Soil-forming intervals in the Bear River and Absaroka fault zones 58
Figure 61. Fault windows for first and second surface-faulting events in the Bear River and Absaroka fault zones 58
Figure 62. Oblique aerial view to the northeast of the Martin Ranch scarp 60
Figure 63. Buried soil (unit 6) and overlying colluvial wedge (unit 7A), Upper Martin Ranch trench 61
Figure 64. Sketch map showing deflection of the Bear River along the trace of the Absaroka thrust 63
Figure 65. Apparent eastward-tilted strath-terrace surfaces in the far middle ground 65
Figure 66. Apparent down-to-the-west fault scarp displacing the Bigelow Bench surface and outwash/terrace gravels 66
Figure 67. View to the north along apparent fault scarp displacing the Bigelow Bench terrace/outwash surface 66
Figure 68. Vertical aerial view (1:34,500) of short scarps on the west flank and top of Elizabeth Ridge 67
Figure 69. Map showing postulated course of the Bear River 69
Figure 70. Map showing relationship of neotectonic features to former course of the Bear River and Muddy Creek 70
Figure 71. Geologic cross section A-A′ (plate I) showing subsurface structure of the Darby-Hogsback thrust plate 72
Figure 72. Hypothetical model for neotectonic development of the Darby-Hogsback and Absaroka thrust plates 74
Figure 73. Geologic cross section A-A′ (plate I) showing relationship of hypothetical 45° fault plane and M = 7.5 earthquake nucleating at a depth of 7.5 miles (12 km) to subsurface structure, the Bear River fault zone, and pre-existing thrust faults in the project area 76
Figure 74. Diagrammatic geologic cross section showing relationship of seismicity to various types of geologic structures in the ISB 77
Figure 75. Seismicity map of north-central Utah and southwestern Wyoming 78

TABLES

Table 1. Large earthquakes in the Utah region, 1850 through 1978 11
Table 2. Total net vertical tectonic displacements calculated from scarp-profile data, Bear River fault zone 34
Table 3. Net vertical tectonic displacement per event from scarp-profile data, Bear River fault zone 34
Table 4. Vertical displacement per event from total vertical stratigraphic offset, Bear River fault zone 34
Table 5. Single-event and total vertical displacement estimated from colluvial-wedge stratigraphy exposed in trenches, Bear River fault zone 35
Table 6. Comparison of vertical tectonic displacements per event from scarp-profile, stratigraphic offset, and colluvial-wedge stratigraphic data, Bear River fault zone 35
Table 7. Average slip rates based on total net vertical tectonic displacements 59
Table 8. Total and single-event net vertical tectonic displacement from scarp-profile data, Martin Ranch scarp 62
Table 9. Vertical displacement per event from total vertical stratigraphic offset, Martin Ranch scarp 62
Table 10. Vertical displacement estimated from colluvial-wedge stratigraphy, Martin Ranch scarp 63
Table 11. Comparison of vertical tectonic displacements per event from scarp-profile, stratigraphic offset, and colluvial-wedge stratigraphic data, Martin Ranch scarp, Absaroka fault 63
Table 12. Paleoearthquake magnitudes 79
Table 13. Estimates of paleoearthquake magnitudes from surface-rupture lengths and surface displacements 80
Table 14. Estimates of paleoearthquake magnitudes from rupture lengths and down-dip fault widths 80

PLATES
(in pocket)

Plate I. Neotectonic map of north-central Utah and southwestern Wyoming with hazard overlays
Plate II. Logs of the La Chapelle, Lester Ranch, and Lester Ranch South trenches
Plate III. Logs of the Austin Reservoir ditch and Sulphur Creek trench
Plate IV. Logs of the Big Burn, Upper Little Burn, and Lower Little Burn trenches
Plate V. Logs of the Upper Martin Ranch, Lower Martin Ranch, and Elizabeth Ridge trenches

APPENDICES

APPENDIX I. Scarp-profile data 89
APPENDIX II. Radiocarbon age determinations 93

PALEOSEISMOLOGY OF UTAH, VOLUME 4

SEISMOTECTONICS OF NORTH-CENTRAL UTAH AND SOUTHWESTERN WYOMING

by
Michael W. West
*Consulting Geologist**

ABSTRACT

Geomorphic evidence of late Quaternary faulting and related tectonic deformation is present north of the Uinta Mountains in Uinta County, Wyoming and Summit County, Utah. A major zone of late Quaternary normal faulting, termed the Bear River fault zone, extends over 25 miles (40 km) from southeast of Evanston, Wyoming to an apparent complex intersection with the North Flank fault of the Uinta Mountains in north-central Utah. The Bear River fault zone consists of well-defined scarps each about 1.9 to 2.2 miles (3.0 to 3.5 km) in length arranged in a right en echelon pattern. Major scarps trend N. 20° W. to N. 20° E. and show consistent, down-to-the-west displacement. Short, down-to-the-east scarps trend N. 15-20° W. and are interpreted to be antithetic faults. Near the south end of the fault zone, scarps in Pleistocene glacial deposits show strong angular discordance (70°) with the main north-northeast pattern of faulting. Late Quaternary movement is indicated by scarps ranging from <3 to 49+ feet (<1 to 15+ m) high in till, outwash, alluvium, and bedrock of the Eocene-age Wasatch Formation; beheading and reversal of streams and numerous sag ponds.

Neotectonic deformation results from regional east-west extension superimposed on the Darby-Hogsback and Absaroka thrust plates. Pre-existing thrust faults were reactivated in a normal sense and caused propagation of "new" listric normal faults over stress points, particularly at the transition from thrust ramps to flats in Jurassic salts and Cretaceous marine shales. The Bear River fault zone developed above the Darby-Hogsback ramp and has experienced recurrent, Holocene movement over a length of 21 to 25 miles (34 to 40 km) with net vertical tectonic displacements ranging from less than 3 feet to greater than 16 feet (<1 to >5 m) per event. Two distinct surface-faulting events are represented by scarps and associated scarp-derived colluvial deposits.

Ages of surface rupture were estimated by radiocarbon dating of tectonically buried and modern soil A-horizons and other organic material exposed in trenches excavated across late Quaternary fault scarps. Calibrated radiometric ages indicate surface-faulting events occurred at 4,620 ± 690 and 2,370 ± 1050 radiocarbon years before present (yr B.P.). Recurrence intervals, based on these ages, range from about 2,250 to over 2,370 years. Interpreted ages of surface-faulting events are not corrected for apparent mean soil residence time; thus, ages of surface-faulting events may be too old by several hundred years.

Surface rupture lengths of 21 to 25 miles (34 to 40 km), vertical tectonic displacements of <3 to >16 feet (<1 to >5 m) per event, and slip rates of 0.03 to 0.11 in/yr (0.8 to 2.7 mm/yr) are comparable to the Wasatch fault, a major earthquake source zone in the Intermountain seismic belt (ISB). Based on empirical relationships for seismogenic normal faults, the Bear River fault zone could have produced paleoearthquakes of surface wave magnitude $M_S = 7.5$. The mean age of latest surface rupture (2,370 yr B.P.) and minimum apparent recurrence interval (2,250 years) suggest a major earthquake could occur at any time in southwestern Wyoming and north-central Utah.

**Michael W. West*
Consulting Engineers and Geologists
Suite 290
8906 West Bowles Avenue
Littleton, CO 80123

The Martin Ranch scarp is coincident with the leading edge of the Absaroka thrust about 4.5 miles (7.2 km) to the west of the Bear River fault zone and developed in response to normal reactivation of the pre-existing thrust plane. Related tectonic deformation extending at least 0.6 mile (1 km) south of the Martin Ranch scarp deflected the channel of the Bear River. Scarp-derived colluvial deposits record one surface-faulting event over a length of 3.1 miles (5.0 km). Mean net vertical tectonic displacements for the single event range from 2.8 to 4.9 feet (0.8 to 1.4 m). The age of latest surface rupture is coeval with latest surface rupture in the Bear River fault zone, 2,370 ± 1,050 yr B.P.

Similar ages of movement suggest displacement along the Martin Ranch scarp occurred as a simultaneous response to east-west extension superimposed on pre-existing thrust and ramp-normal faults. Slip rates on the reactivated leading edge of the Absaroka thrust range from 0.02 to 0.03 in/yr (0.5 to 0.7 mm/yr).

Fault scarps displacing Pleistocene geomorphic surfaces and associated outwash/alluvium and regional, eastward tilt of terrace surfaces indicate the leading edge of the Darby-Hogsback thrust was also reactivated but now may be inactive due to development of the Bear River fault zone over the ramp structure to the west. Normal displacements along the leading edge of the Darby-Hogsback fault are believed responsible for apparent separation of the Bear and Green River drainage basins less than 600,000 years ago.

Research in southwestern Wyoming and north-central Utah in comparison with the Hebgen Lake and Borah Peak areas suggests different levels of maturity and tectonic/structural relationships exist with time and location in the ISB/eastern basin-and-range transition zone. Hebgen Lake and Borah Peak represent evidence of mature seismogenesis manifested by imposing fault-bounded mountain blocks and evidence of recurrent normal fault movements with great displacements. The Bear River fault zone and normally-reactivated thrust faults represent an early, youthful stage of seismogenesis in a thrust-faulted terrain. Continued tectonic deformation may produce fault-bounded mountain ranges with remnants of thrust plates preserved within the block similar to the Wasatch Range east of Salt Lake City. Major seismogenic faults, which may be "blind" sub-decollement structures in early stages of extension, eventually rupture the surface as 45° to 60° planar faults. The early tectonic relationship between regional extension and normally reactivated leading edges of thrust faults and ramp structures is destroyed with time. The idea that all late Quaternary surface faults in the ISB are steeply dipping and penetrate from ground surface to depths of 7.4 to 9.3 miles (12 to 15 km) may be an oversimplification that is applicable to certain seismically mature areas but cannot be applied unilaterally to all areas in the ISB/eastern basin-and-range transition zone.

PART I - INTRODUCTION

INTRODUCTION

This report describes results of neotectonic studies conducted in Summit County, Utah and Uinta County, Wyoming. The work was based originally on a seismotectonic hazard evaluation for the U.S. Bureau of Reclamation's (USBR's) Meeks Cabin and Stateline dams located about 26 miles and 35 miles (42 km and 57 km), respectively, southeast of Evanston, Wyoming (figure 1). A moderate to large earthquake in the vicinity of either dam would pose a threat to dam safety. Accordingly, the seismogenic potential of major faults in north-central Utah and southwestern Wyoming required evaluation.

The lack of macroseismicity and apparent isolation from major seismogenic structures initially suggested that regional seismic exposure in the project area was relatively low. Field geologic mapping conducted by the U.S. Geological Survey (USGS) for the Energy Lands Program (Gibbons and Dickey, 1983), however, disclosed evidence of potentially high earthquake hazard based on the presence of late Quaternary fault scarps. Other major faults related to development of the Wyoming thrust belt and uplift of the Uinta Mountains are also present in the area. A major earthquake occurring along one of these faults, associated ground deformation and related secondary effects would pose significant hazards to engineered works in the general study area. The presence of late Quaternary surface faulting indicated the need for careful evaluation of earthquake hazard/risk rather than reliance on existing literature and evaluation of historic seismicity.

As the study progressed, significant ideas developed regarding the evolution of seismogenic faulting in the thrust belt of north-central Utah and southwestern Wyoming. The accumulated data indicated late Quaternary tectonic extension was superimposed on and controlled by pre-existing thrust faults. Major late Quaternary deformation, 80 miles (129 km) east of the Wasatch Front, and apparent lack of evidence for significant pre-late Quaternary history of surface faulting also had implications for development of the transition between the eastern Basin and Range and the Middle Rocky Mountains/Colorado Plateau tectonic provinces.

Localization of extensional movement along pre-existing low-angle thrusts was also in apparent conflict with the prevailing model for large-magnitude earthquakes accompanied by surface faulting in the Intermountain seismic belt (ISB). The

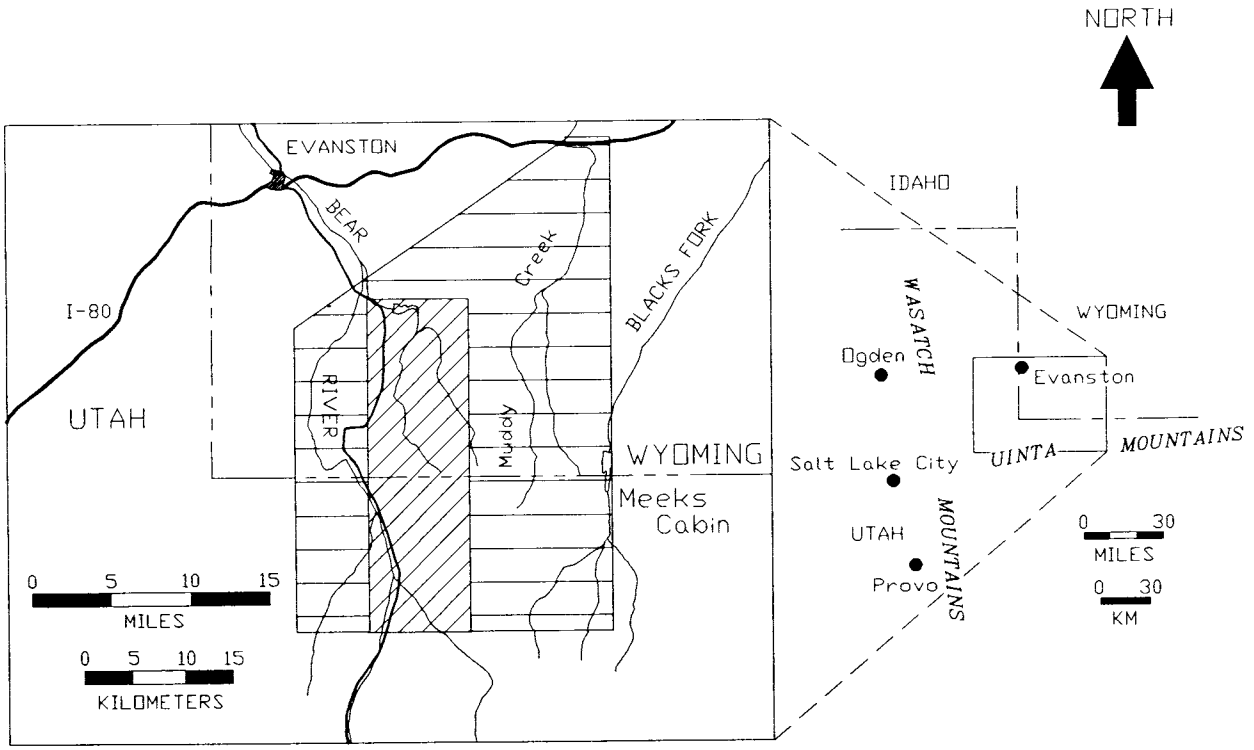

Figure 1. Location maps showing detailed (diagonal hatch) and reconnaissance (horizontal hatch) study areas in north-central Utah and southwestern Wyoming.

model relating surface faulting, subsurface structure, and earthquake magnitude was either more complex than previously thought or, alternatively, the seismogenic cycle is operating at different stages of development in various parts of the ISB. Detailed study of late Quaternary surface faulting in north-central Utah and southwestern Wyoming provided important clues to many of these questions.

Objectives

The objectives of the seismotectonic studies were:

1. to describe evidence for late Quaternary deformation in the thrust belt of north-central Utah and southwestern Wyoming including interpretation of trenches excavated across late Quaternary fault scarps,
2. to define spatial and temporal seismicity patterns with respect to major tectonic structures in the project area, and
3. to synthesize the results of field and office studies into a seismotectonic hazard assessment including specification of paleo-earthquake magnitudes, future expectable events, and delineation of related seismotectonic hazards which could be expected to affect the study area.

The regional tectonic significance of late Quaternary faulting and implications for seismogenesis in the ISB are summarized in related papers (West, 1992; 1993).

Scope of Studies

Field work was performed during the summers of 1983, 1984, and 1985. Field work in 1983-84 was sponsored by the USBR and included field mapping, fault trenching, and radiocarbon dating programs. Field work during 1985 was supported by research grants from Chevron USA and Marathon Oil Company and was devoted to additional field mapping and regional tectonic studies. In the spring of 1986, I spent several days in the field examining surface faulting and secondary deformation related to the 1959 Hebgen Lake earthquake near West Yellowstone, Montana and the 1983 Borah Peak earthquake near Mackay, Idaho. Field studies were supplemented by synthesis of regional tectonic literature, compilation of historic seismicity, and assessment of geologic factors controlling seismogenesis in the project area.

The scope of studies summarized in this report includes:

1. Aerial photo interpretation using natural color and false-color infrared photographs at scales of 1:24,000, 1:35,000, and 1:60,000. Known or suspected late Quaternary faults were mapped on air photos and selected for field evaluation.
2. Low sun-angle aerial overflight (morning sun) of late Quaternary scarps reported by Gibbons and Dickey (1983). The overflight was intended to supplement air photo interpretation, provide photographic documentation of tectonic features, and aid in selection of sites for field study.
3. Reconnaissance mapping of tectonic features within the

study area. Late Quaternary faults, lineaments, and related features were compiled on 1:24,000 and 1:100,000 scale topographic base maps.

4. Excavation and logging of trenches across known late Quaternary fault scarps. Ten trenches across seven scarps and one fortuitous "natural" exposure across an eighth scarp were logged at a scale of 1 inch = 1 meter (39.37 inches). Thirty-eight radiocarbon ages were obtained from modern and buried soil A-horizons associated with scarp-derived colluvial wedges. Three amino acid racemization ratios were also obtained from pre-fault alluvial sediments in one trench.

5. Measurement of sixteen scarp profiles at seven sites to aid in interpretation of vertical tectonic displacements.

The paper is divided into five parts. Part I describes the objectives and scope of studies, location and physiographic setting of the study area, and previous work relating to neotectonics. Regional tectonic setting, stratigraphy, and structure of north-central Utah and southwestern Wyoming are described in Part II. Late Quaternary tectonic deformation in the study area, the results of field studies, and analyses of fault-rupture parameters are described in Part III. An assessment of seismotectonic hazards is presented in Part IV. Conclusions and recommendations for future research comprise Part V.

LOCATION AND PHYSIOGRAPHY

Location

The study area encompasses 420 square miles (1,088 km^2) in north-central Utah and southwestern Wyoming, 104 miles (167 km) northeast of Salt Lake City, Utah. Detailed studies were concentrated along a zone of reported late Quaternary faulting (Gibbons and Dickey, 1983) extending from 10 miles (16 km) southeast of Evanston, Uinta County, Wyoming to the North Flank fault of the Uinta Mountains in Summit County, Utah about 29 miles (47 km) south of Evanston (figure 1). Reconnaissance studies encompassed an area extending from the Bear River on the west to the Blacks Fork River on the east and from Interstate 80 (I-80) connecting Evanston and Rock Springs on the north to the north flank of the Uinta Mountains on the south.

Evanston, the principal population center of the region, is the focus of oil exploration, oil field service, and ranching industries. The Anschutz Ranch East oil field is located about 15 miles (24 km) southwest of Evanston. Interstate 80 connects Evanston with Salt Lake City, a 1½ hour drive to the west, and the cities of Rock Springs, Rawlins, Laramie, and Cheyenne to the east. Wyoming Highway 89 and Utah 150 south of Evanston cross the Uinta Mountains via Bald Mountain Pass and connect Evanston with Kamas, Utah and U.S. Highway 40 beyond. Highways 89 and 150 provide principal access to the project area. Secondary county and Forest Service access roads link state highways with most of the study area. Meeks Cabin dam, the original focus of USBR-sponsored studies in the project area, is located on the Blacks Fork River in sections 10 and 11, T. 12 N., R. 117 W., Uinta County, Wyoming about 2 miles (3.3 km) north of the Wyoming-Utah state line.

Physiography

The topography of the study area is dominated by the Uinta Mountains, a major east-west mountain range paralleling the Utah-Wyoming border in north-central Utah. The crest of the Uintas, 38 miles (61 km) south of Evanston, rises to elevations of over 13,500 feet (4,115 m) and has been incorporated into the High Uintas Primitive Area administered by the U.S. Forest Service as part of the Wasatch National Forest. Major streams draining the north flank of the Uintas include the Bear River, Blacks Fork, Smiths Fork, and numerous smaller tributaries.

Near the Utah-Wyoming state line, topographic conditions change abruptly from mountainous terrain of relatively high relief to broad alluvial flats and rolling to steppe-like terrain. South of Evanston, the subdued terrain is traversed by hogbacks of moderate relief marking the topographic expression of the Cordilleran thrust belt in southwestern Wyoming. Elevations in the project area range from about 10,990 feet (3,350 m) on the north flank of the Uintas to 6,890 feet (2,100 m) near Evanston, a total relief of about 4,100 feet (1,250 m).

Differences in elevation account for the variety of vegetation in the project area. The Uinta Mountains between timberline and the Utah-Wyoming border support montane and subalpine assemblages including spruce, fir, lodgepole pine, and aspen. North of the border, montane and subalpine forests give way to grasses, sage, cottonwood, and widely scattered clumps of ponderosa pine and aspen on sheltered slopes.

PREVIOUS WORK

The geology, geophysics, and seismicity of the Uinta Mountains, Basin and Range Province, and Wyoming thrust belt have been described in numerous publications. Selected publications representative of literature relating to each area are summarized in the section on Regional Tectonics. Literature regarding seismotectonics of north-central Utah and southwestern Wyoming, however, is limited and deserves discussion.

The research summarized in this report was based on work by Gibbons and Dickey (1983) which indicated the presence of apparent late Quaternary faulting in southwestern Wyoming. Late Quaternary faulting in the region seemed implausible in terms of both published neotectonic literature and intense petroleum exploration activity in the Wyoming-Utah thrust belt.

The earliest reference to neotectonic features in the region appeared in 1928 with G.K. Gilbert's introduction of the term "back valleys" to describe apparent grabens east of the Wasatch Range. These grabens, including Morgan, Ogden, Cache, Keetley, Kamas, and Heber valleys, were studied by Eardley (1968), who concluded the back valleys developed by folding and subsequent basin-and-range-style faulting. In 1977, Stokes included the back valleys in a physiographic subprovince of the Middle Rocky Mountains termed the Wasatch Hinterland.

Since 1978, the Wasatch Front and the back valleys have been the subjects of study by Woodward-Clyde Consultants (Cluff and others, 1980; Swan and others, 1980, 1982, and 1983), the USBR (Sullivan and others, 1988), the USGS (Hays and Gori, 1992), and the Utah Geological Survey (UGS) (Jackson, 1991; Lund and others, 1991; Personius, 1991). Woodward-Clyde Consultants, under contract to the USGS, studied the late Quaternary history of the Wasatch fault in the Salt Lake City area. The USBR conducted a regional study of neotectonics in the back valleys of the Wasatch Hinterland as part of a hazard assessment for various features of the Central Utah Project (Sullivan and others, 1988). The USGS and UGS conducted a number of studies related to earthquake hazard/risk along the Wasatch Front in north-central Utah (Hays and Gori, 1992).

Several studies of regional extent cover all or parts of north-central Utah and southwestern Wyoming. Witkind (1975) released an open-file report showing known and suspected active faults in Wyoming. Late Quaternary faulting reported by Gibbons and Dickey (1983), however, does not appear on this map. The nearest zone of Quaternary faulting to that reported by Gibbons and Dickey is approximately 45 miles (73 km) to the north along the Rock Creek and related faults. A similar Quaternary fault map of Utah (Anderson and Miller, 1979), likewise, does not show faulting in north-central Utah along the southern extension of faulting reported by Gibbons and Dickey. Seismic regionalization of the Basin and Range Province (Thenhaus and Wentworth, 1982) indicates the presence of "short" late Quaternary fault scarps with apparent vertical displacements of about 3 feet (1 m) in an area encompassing extreme southwestern Wyoming and part of north-central Utah. Presumably, portrayal of these reported late Quaternary faults was based on work by Gibbons and Dickey (1983).

In addition to regional studies, Hansen (1969, 1984, 1986) mentions Quaternary movement on faults bounding the north flank of the Uinta Mountains and the possibility of a seismically-induced landslide on the Middle Fork of the Blacks Fork River a few miles south of Meeks Cabin dam. A paper by Hansen (1985) on distribution of warm- and cold-water fish species postulates neotectonic separation of the Green and Bear River drainage basins in the area between the Bear River and Blacks Fork. An early version of the Geologic Map of Utah (Stokes and Madsen, 1961) shows the North Flank fault south of Evanston cutting the youngest Quaternary map units including alluvium along the Bear River valley. The pattern of faulting, however, implies a drafting error and was apparently discounted by Anderson and Miller (1979) in their compilation.

A literature review disclosed five references, two published and three unpublished, to late Quaternary faulting south of Evanston. The first of these papers (Eardley, 1959), published in an Intermountain Association of Petroleum Geologists guidebook, discusses the Sulphur Creek oil field and shows a pattern of normal faulting similar to that reported by Gibbons and Dickey (1983). A thesis by Nixon (University of Utah, M.Sc., 1955) shows apparent late Quaternary normal faults in the Hilliard Flat area southeast of Evanston but no significance is attached to their presence. Lamerson (1982), also shows a system of faults similar to those reported by Gibbons and Dickey (1983) cutting late Quaternary deposits. Lamerson's paper discusses the mechanics of normal faulting in the thrust belt and attributes it primarily to mechanical relaxation. Late Quaternary faults also appear on a proprietary photogeologic map prepared by a division of Petroleum Information (Dixon, personal communication, 1984) and on an unpublished geologic map of southwestern Wyoming prepared by M'Gonigle and Dover (in press) of the U.S. Geological Survey. This latter work is probably based, at least in part, on Gibbons and Dickey's open-file report and includes other apparent late Quaternary faults. None of these documents/publications relate apparent late Quaternary normal faulting to potential earthquake hazards.

Based on a review of current literature, Gibbons and Dickey (1983) should be given credit for recognition of a major late Quaternary fault zone in southwestern Wyoming. The discovery is remarkable because considerable attention has been focused on earthquake hazards in the ISB and adjacent areas.

ACKNOWLEDGMENTS

Field work in 1983-84 was sponsored by the U.S. Bureau of Reclamation (USBR), Denver, Colorado as part of Safety Evaluation Existing Dams (SEED) studies for Meeks Cabin and Stateline dams, Lyman Project. Carol Krinsky and Edward M. Baltzer of USBR assisted with trench logging. Krinsky, in particular, described soil profiles and collected samples for laboratory and radiocarbon analyses.

Field logistical support for the trenching program was provided by the Bonneville Projects Office and the Upper Colorado Regional Office of USBR. Carol Wiens provided archaeological/environmental clearances for the trench sites, and Evan Rudd arranged right-of-way for trenching on private property. Aaron Martin, Lamar Lester, Neldon Barker, and J.R. Broadbent kindly provided permission for trenching on their property. Jerry Green, Evanston District Forest Ranger, and Bernard Asay, Mineral Resource Ranger, assisted with trenching operations in the Wasatch National Forest.

Radiocarbon samples from the 1983 trenching program were prepared by Rolf Kihl, Institute of Arctic and Alpine Research (INSTAAR), University of Colorado. Radiocarbon dating of these samples was performed by Geochron Laboratories, Krueger Enterprises, Inc. under the direction of Harold Krueger. Samples from the 1984 trenching program were prepared and dated by Beta Analytic, Inc. under the direction of Dr. Murray Tamers. Dr. Gifford Miller of INSTAAR provided amino acid racemization ratios for three land snails from the La Chapelle trench.

Field work during the 1985 season was sponsored by grants from Chevron USA, Inc. and Marathon Oil Company. The study also benefitted from discussions with several geologists familiar with the stratigraphy and structure of the area including Joe Dixon (Champlin), Frank Royse and Paul Lamerson (Chevron), Art Berman (Amoco), Bill Glover (Marathon), Ray Durkan and David Hay (Exxon), Steve Bell (Sun), Jim Case (Wyoming Geological Survey), Wallace Hansen (USGS), Ken Pierce (USGS), Ernie Anderson (USGS), Russ Wheeler (USGS), Tony Crone (USGS), Mike Machette (USGS) and Tim Hait (USGS retired) among others. Hunt Oil Company of Denver and Exxon

USA kindly released reflection seismic lines across the project area.

Drs. Robert Smith and Walter Arabasz of the University of Utah provided valuable insight into various aspects of earthquake occurrence in the Intermountain seismic belt. Through their generosity, I was allowed access to the University of Utah earthquake data base.

Dr. Clarence R. Allen of the California Institute of Technology provided technical review of this paper on behalf of the Utah Geological Survey (UGS). Hopefully, Dr. Allen's comments and criticisms are reflected in the final manuscript. Finally, I would like to thank the UGS, specifically William R. Lund and Douglas A. Sprinkel, for making publication of this paper possible.

PART II - REGIONAL GEOLOGY

REGIONAL TECTONICS

North-central Utah and southwestern Wyoming lie at the intersection of three major structural/tectonic elements in the western United States: (1) the east-trending Uinta Mountains anticline, (2) the eastern margin of the Basin and Range tectonic province, and (3) the thrust belt of the western Cordillera (figures 2 and 3). Late Quaternary surface faulting in the project area bears apparent relationships to all three structural provinces.

The following sections provide a framework for neotectonic studies by outlining the characteristics of each major structural element in the project area. An overprinted zone of intraplate seismicity, the Intermountain seismic belt (ISB), is also discussed. Possible tectonic relationships conclude the description of regional tectonics and seismicity.

Uinta Mountains Anticline

The Uinta Mountains anticline (figure 4) is a compound upwarp extending from the Wasatch Front across north-central Utah into northwestern Colorado. Total axial length is about 198 miles (320 km) and maximum width is about 47 miles (75 km). The plunging west end of the anticline is well-exposed near Kamas, Utah. West of Kamas, the anticline is believed to continue in the subsurface at least through the Cottonwood uplift in the central Wasatch Range and perhaps beyond. A series of mid-Tertiary stocks and associated eruptive rocks, decreasing in age from east to west, appears to be localized along the subsurface extension of the anticlinal axis. Near the east end of the anticline in northwestern Colorado, the uplift breaks up into a series of subsidiary folds, swings to the southeast, and merges with the predominant northwest-southeast structural grain of the Southern Rocky Mountains.

In cross section, the Uinta anticline is asymmetrical with the north limb exhibiting steeper dip than the south limb. Both limbs have been modified by thrust faults termed the North Flank and Uinta Basin systems. The North Flank system includes the North Flank fault along the western third of the range, the Henrys Fork fault along the central third, and the Uinta/Sparks faults along the eastern third. The Uinta Basin system includes the Uinta Basin Boundary fault along the south flank of the range and a series of subsidiary faults east of Vernal, Utah including the Willow Creek, Island Park, Disaster, Mitten Park, Wolf Creek, and Yampa faults near Dinosaur National Monument. A complex zone of faulting is also present immediately north of the anticlinal axis along much of the length of the range. This system is termed the Crest fault in the western half of the range but has not been formally named in the eastern half. The South

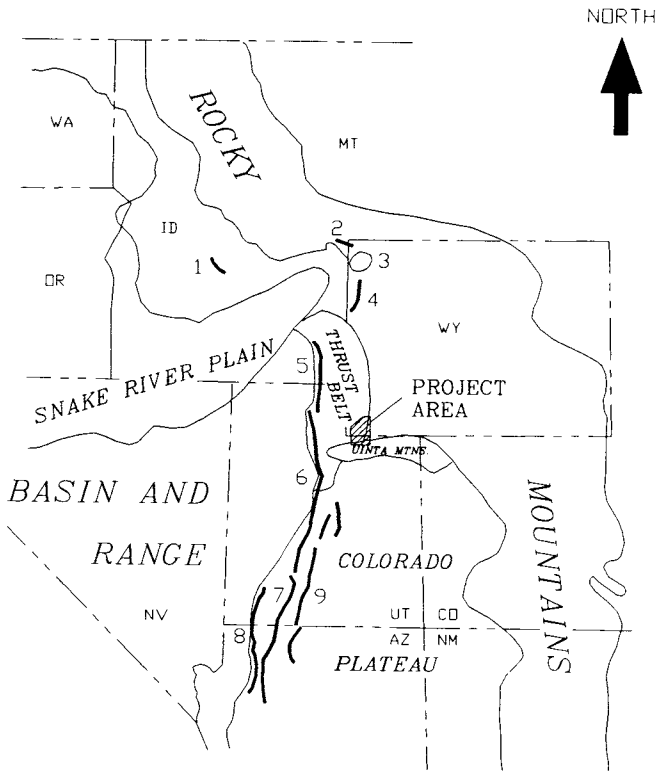

Figure 2. Map of part of the western United States showing tectonic provinces and relationship of the project area to major neotectonic and volcanic features. 1) Lost River fault, Borah Peak; 2) Hebgen Lake fault; 3) Yellowstone caldera; 4) Teton fault; 5) East Cache fault; 6) Wasatch fault; 7) Sevier fault; 8) Hurricane fault; 9) Paunsaugunt fault; (modified from Smith and Sbar, 1974).

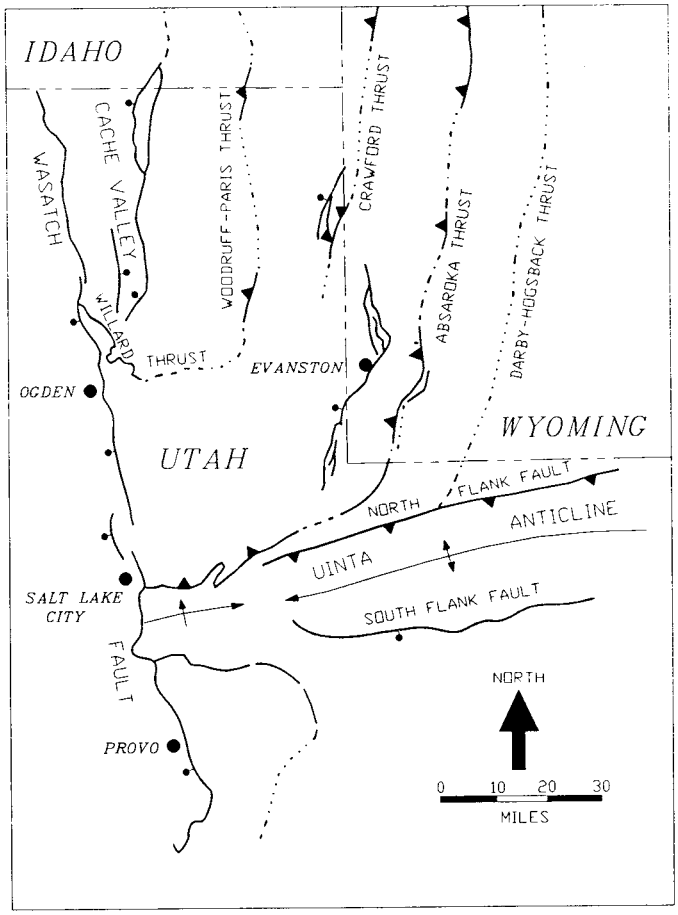

Figure 3. Generalized tectonic map of north-central Utah and southwestern Wyoming showing major structural features at the intersection of the eastern margin of the Basin and Range, thrust belt, and Uinta Mountains anticline (Crittenden, 1974).

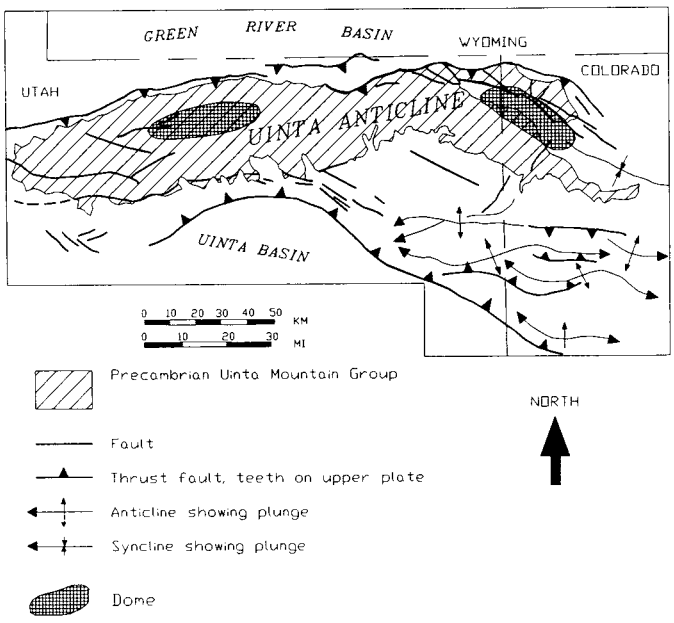

Figure 4. Generalized tectonic map of the Uinta Mountains anticline (Hansen, 1986).

Flank normal fault delineates the south flank of the Uinta Mountain anticline north of the Uinta Mountain Boundary thrust.

Hansen (1984) divides the Uinta anticline into east and west domes aligned along the anticlinal axis (figure 4). A shallow structural saddle oriented roughly along a north-south line connecting the towns of Vernal and Manila separates the east and west domes. Both structural domes are coincident with positive gravity anomalies believed to reflect dense Precambrian rock at relatively shallow depths beneath the domes. The largest gravity anomaly, a 20+ milligal differential, is associated with the eastern dome. According to Hansen (1984), the eastern dome has also experienced greater relative uplift and dissection than the western dome.

The North Flank fault system comprises a complex set of overlapping reverse and thrust faults separating the Uinta Mountains anticline from adjacent basins and uplifts to the north. From west to east, the system includes the North Flank, Henrys Fork, Uinta, and Sparks faults. In general, maximum displacement occurs in the medial portions of each fault and decreases sharply toward either end. Adjacent faults overlap such that decreasing displacement on one fault is accompanied by increasing displacement on the adjacent fault (Ritzma, 1971).

Maximum stratigraphic displacement on the North Flank system appears to have occurred on the Uinta fault. Hansen (1969) estimates 33,990± feet (10,360 ± m) of displacement on the Uinta fault. Ritzma (1971), however, believes displacement on the Uinta fault to be about 39,990 feet (12,190 m) east of the Colorado-Utah border. Displacement on the North Flank fault along the western third of the range is estimated by Hansen (1969) to be 25,000 feet (7,620 m). Displacements cited for the Henrys Fork and Sparks faults are 12,000 and 18,000 feet (3,660 and 5,490 m), respectively.

Basin and Range Province

The Basin and Range Province (figure 2) encompasses 300,000 square miles (780,000 km^2) in 10 western states or roughly 8 percent of the surface area of the United States (Eaton, 1979). Stewart (1971) describes basin-and-range structure "as a system of horsts and grabens produced by the fragmentation of a crustal slab above a plastically extending substratum." In general, the horsts and grabens are systematically distributed throughout the province in a north-trending structural grain. Typical horst-to-horst or graben-to-graben spacing averages 15 to 20 miles (24 to 32 km).

Considerable east-west extension is required to produce basin-and-range structure. Stewart (1971) estimates an average of 1.5 miles (2.4 km) of extension for each major valley or a total of 30 to 60 miles (48 to 97 km) for the entire province. He further postulates that most of this extension took place in the last 17 million years and perhaps in the last 7 to 11 million years. Strain rates calculated from these figures yield values of 0.1 to 0.6 in/yr (2.5 to 15.2 mm/yr).

According to Eaton (1979), the crust of the province is divisible into three layers: (1) an upper listrically faulted surface layer, (2) a thin, intermediate ductile layer, and (3) a more rigid, "dike-riven" lower layer. The intermediate ductile layer is of

particular interest because it appears to control many of the anomalous features of the province, especially in tectonically active areas. Eaton envisions this layer as ranging in depth from 3.1 to 9.3 miles (5 to 15 km) and in thickness from 0 to 1.9 miles (0 to 3 km). Zones of locally high fluid pore pressures may be associated with the ductile layer producing low seismic velocities and high electrical conductivities.

Faulting and earthquake activity are assumed to be confined to the upper brittle layer; the intermediate layer absorbs fault displacements through ductile flow. The fragmented nature of the upper layer also appears to offer a partial explanation for the regional gravity low associated with the province. Intrusion of the lower layer by basaltic magmas may account for the anomalously high heat flow characteristic of the region.

Eaton (1979) divides the Basin and Range Province into discrete subprovinces based on physiographic, geologic, and geophysical properties. These subdivisions include: (1) the Great Basin, (2) the Rio Grande rift, (3) the Mexican highlands, (4) the Sonoran Desert, and (5) the Salton trough. Although all of these subprovinces contain common elements, further discussion is confined to the Great Basin, its eastern margin and transition into the Middle Rocky Mountains and Colorado Plateau provinces.

The Great Basin

The Great Basin is characterized by interior drainage, relatively high rates of surface faulting, regionally low Bouguer gravity values, hydrothermal circulation, and thin crust. The eastern physiographic margin of the basin is defined by the Wasatch Front (figure 3) in central Utah; although, the tectonic margin is believed to be transitional through the Wasatch Hinterland some distance east of the Wasatch Range. Active surface faulting and moderately high rates of seismicity distinguish the Great Basin from tectonically dormant or less active portions of the Basin and Range Province.

The Wasatch and Cache Valley faults define the physiographic boundary of the eastern Great Basin. The faults separate highly deformed rocks of the Great Basin on the west from the relatively stable cratonic block on the east. The Wasatch/Cache Valley systems together define the Wasatch Front.

The Wasatch fault (figure 3) extends from Gunnison, Utah into southern Idaho, a distance of 230 miles (370 km) (Smith and Sbar, 1974; Smith, 1978; Arabasz, Smith, and Richens, 1979, 1980). It is a down-to-the-west normal fault with a minimum displacement of more than 36,000 feet (11 km; Parry and Bruhn, 1987) exhibiting unequivocal evidence of recurrent, late Quaternary movement. The trace of the fault along most of its length is marked by scarps in Pleistocene and Holocene deposits.

Population centers along the Wasatch fault (figure 2), notably Salt Lake City, Ogden, and Provo, have stimulated a concentrated effort to assess seismotectonic hazards along the Wasatch Front (Cluff and others, 1980; Swan and others, 1980, 1982, 1983; Hays and Gori, 1992). These studies have shown the fault to be capable of producing earthquakes of M_L=7.5± with recurrence intervals ranging from 500 to 5,200 years. Single-event displacements range from 2.6 to 12.0 feet (0.8 to 3.7 m) with cumulative net tectonic displacement since mid-Holocene of 32.8 to 36.0 feet (10 to 11 m). Holocene slip rates range from 0.004 to 0.12 in/yr (0.1 to 3.0 mm/yr).

Back Valleys of the Wasatch Hinterland

G.K. Gilbert (1928) introduced the term "back valleys" to describe grabens east of the Wasatch Front (figure 5). Eardley (1968) concluded these grabens developed from basin-and-range style faulting and tilting. The area east of the Wasatch Front including the major back valleys was subsequently defined as the Wasatch Hinterland subprovince of the Middle Rocky Mountains by Stokes (1977). The principal back valleys include Morgan, Ogden, Cache, Keetley, Kamas, and Heber Valleys.

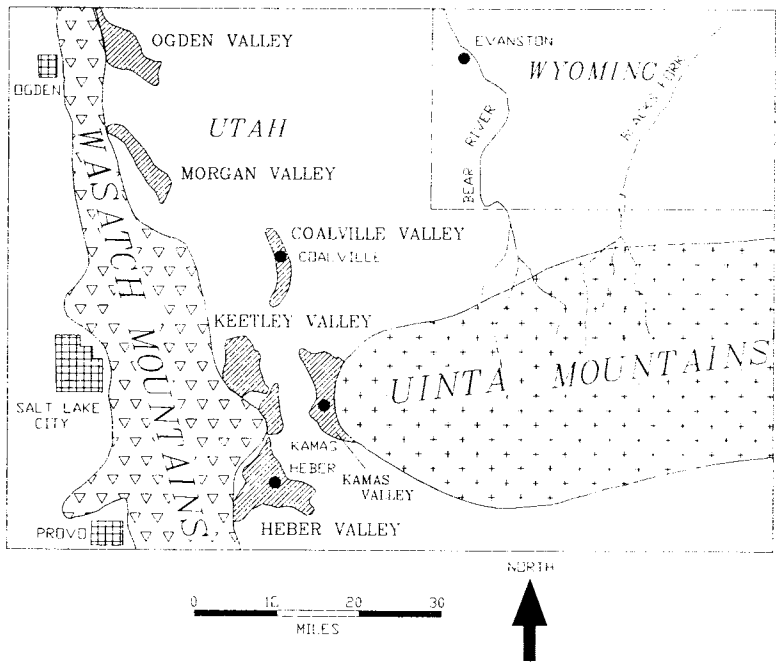

Figure 5. Back valleys of east-central Utah, shown in diagonal cross-hatched pattern, are fault-bounded, sediment-filled, structural basins representing the transition from the eastern Basin and Range Province into the Middle Rocky Mountains and Colorado Plateau Provinces.

In general, the back valleys are believed to represent a transition from the Basin and Range Province into relatively stable cratonic rocks of the Middle Rocky Mountains and Colorado Plateau. Structural attitudes in Oligocene and Miocene rocks flanking the valleys suggest initial development by folding. Present physiography, however, indicates subsequent development of the basins was controlled by normal faulting. Moreover, the basins are associated with closed gravity lows resulting from relatively thick, low-density valley fill, reinforcing the interpretation of fault-bounded structural basins.

The back valleys, particularly Heber, Keetley, and Morgan

have been studied by the USBR as part of a regional seismotectonic hazard evaluation for the Central Utah Project (Nelson and Martin, 1982; Sullivan and others, 1988). These studies suggest that although many back-valley faults have recurrent Quaternary histories, few show evidence of post-Bonneville (20,000 years+) movement (Nelson and Martin, 1982). Van Arsdale (1979a, 1979b), however, reported fault scarps in alluvial fans in the Strawberry Valley about 56 miles (90 km) southeast of Salt Lake City and 25 miles (40 km) due east of the Wasatch fault. Subsequent studies, including trenching by USBR (Nelson and Martin, 1982), demonstrated the Strawberry and Stinking Springs faults have experienced surface offset in Holocene time and are capable of generating earthquakes in the magnitude range of $M_L = 6.5$ to 7.0.

Cordilleran Thrust Belt

The Cordilleran thrust belt extends from northern Canada through western Montana, Idaho, Wyoming, and Utah (figures 3 and 4). The province is characterized along its length by imbricate, westward dipping thrust faults in Paleocene and older rocks. Recent large oil and gas discoveries in the Wyoming thrust belt have focused intense exploration activity on the region.

The thrust belt in Wyoming comprises a broad salient, convex to the east, extending from the Snake River Plain on the north through west-central Wyoming into north-central Utah and beyond on the south (figures 3 and 4). Major thrust faults, from west to east, include the Paris, Crawford, Absaroka, Darby-Hogsback, and Prospect faults. The thrust belt strikes southeasterly on emergence from beneath the Snake River Plain. At Jackson, Wyoming, the strike of major thrust faults swings rather abruptly to the south. The Prospect fault disappears near LaBarge, Wyoming, and the Darby-Hogsback fault becomes the easternmost thrust in the belt.

In southwestern Wyoming near Evanston, the thrust belt swings to the west and wraps around the plunging nose of the Uinta Mountains anticline. The eastern thrusts in this area are either abruptly terminated against the North Flank fault of the Uintas or swing sharply to the west and parallel the North Flank fault in a structurally complex and poorly understood zone of shearing and tear faulting.

The Wyoming thrust belt shares common characteristics with other major thrust belts of the world (Dixon, 1982; Wiltschko and Dorr, 1983): (1) a thick wedge of sediments is present off the craton margin, (2) thrust faults cut up-section through successively younger rocks, some of which were derived from erosion of older thrust sheets, (3) the lowest thrust is generally the youngest at a given locality, (4) deformation is brittle, and (5) decollements follow weak, incompetent horizons. Thrust faults characteristically cut through weak horizons at shallow angles and through more competent rocks at steep angles.

Dixon's (1982) synthesis of thrust-belt structure, based largely on interpretation of high density reflection seismic data from the Snake River Plain to the Uinta Mountains, defined a regional "near-basement" seismic reflector, the Cambrian-age Flathead Sandstone and an underlying autochthon dipping to the west at 200 to 300 feet/mile (38 to 57 m/km). The decollement surface is apparently located in weak shale/claystones of the Cambrian Gros Ventre Group; Precambrian rocks are not involved in thrusting. This interpretation is based on the recognition of unfaulted Flathead Sandstone on seismic records. Decollements also occur in weak units, principally Jurassic salt beds and Cretaceous shales.

In cross section, the thrust faults are imbricate, westward dipping with leading (surface) edges of older thrusts almost directly over trailing (decollement) edges of younger thrusts. Steeply dipping ramps form in competent Paleozoic bedrock units including the Bighorn Dolomite, Madison Limestone, and Wells Formation. Ramps also tend to develop in the Jurassic Nugget Sandstone. Subthrust sequences are relatively simple with little or no deformation apparent on seismic records. Suprathrust deformation, however, is exceedingly complex with intense folding and imbricate faulting especially near the leading edges of the thrusts (Dixon, 1982; personal communication, 1984).

Several workers (Armstrong, 1968; Blackstone, 1977; Dixon, 1982; Wiltschko and Dorr, 1983 among others) note the presence of post-thrusting normal faults within the Wyoming thrust belt. According to Wiltschko and Dorr (1983), normal faults both listric to thrusts and displacing thrusts are present in the region. All normal faulting is believed to post-date thrusting and is associated with either mechanical relaxation and/or basin-and-range extension. Basement-penetrating normal faults would be expected to cross-cut pre-existing thrust faults. Dixon (personal communication, 1984) believes at least part of the apparent normal faulting, particularly normal faults which do not penetrate basement rock (listric to thrust faults), are simple mechanical relaxation features resulting from adverse geometries in weak Cretaceous shales. He does not require regional extension to develop these normal faults.

Intermountain Seismic Belt

The ISB is a zone of seismic activity roughly corresponding to the eastern margin of the Basin and Range Province from Arizona through central Utah, eastern Idaho, western Wyoming, and into Montana (figure 6). Arabasz and Smith (1981) estimate the length of the ISB to be more than 800 miles (1,300 km) and the width to range from 62 to 124 miles (100 to 200 km). The ISB can be divided into several distinct segments based on temporal and spatial occurrence of seismicity. Most low-magnitude seismic activity, however, is diffuse and shows only a weak relationship to known or suspected surface tectonic features. Focal depths are generally less than 9.3 to 12.4 miles (15 to 20 km). Earthquake swarm sequences are relatively common and appear to be associated with zones of high heat flow and/or geothermal activity. Large magnitude earthquakes, greater than $M_L = 7$, have occurred infrequently in historic times despite the presence of well-documented Pleistocene and Holocene fault scarps in many parts of the ISB. Accordingly, recurrence intervals for surface-faulting events are inferred to be long, generally greater than 1,000 years (Arabasz and Smith, 1981), an inference subsequently supported by Swan and others (1980, 1982, 1983).

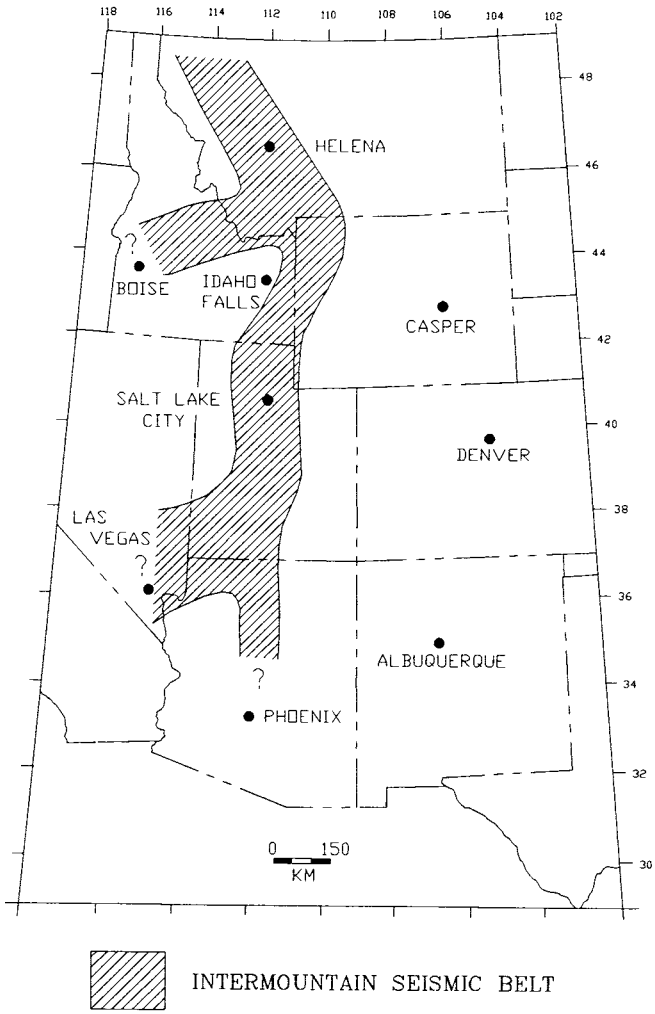

Figure 6. The Intermountain Seismic Belt roughly corresponds to the eastern margin of the Basin and Range Province. Low-to-moderate-magnitude seismic activity within the belt is diffuse and shows a weak relationship to known tectonic features.

The predominant state of stress over most of the ISB is west- to northwest-oriented extension virtually identical to the stress field in the Great Basin. Focal plane mechanisms generally reflect a similar stress regime, and mapped late Quaternary normal faults are consistent with east-west extension. Variations in stress orientation, however, have been noted locally within the ISB, suggesting a more complex stress field. Part of the complexity may be attributable to pre-existing structure interacting with contemporary basin-and-range extension.

Seismicity

Earthquake activity in the ISB has been monitored since the settlement of Utah by the Mormons in 1847. Systematic instrumental monitoring of seismicity, however, dates only from 1950. Computer calculated locations date from the early 1960s, and telemetered seismic nets were established in the 1970s (Arabasz and Smith, 1981). Since 1850, fifteen earthquakes of magnitude $M_L = 6$ or greater have occurred in the Utah area (table 1). Large magnitude earthquakes and the relatively high rates of occurrence of smaller magnitude events establishes the ISB as one of the areas of highest seismic risk in the conterminous U.S., excluding California and Nevada.

Arabasz and Smith (1981) report relatively low rates of crustal strain compared to plate boundaries, and background seismic flux four to six times lower than in the California-Nevada seismic zone. Crustal stresses appear to be in the range of 0.01 to 100 bars and are generally comparable to values computed for intraplate earthquakes elsewhere.

Temporal and spatial occurrence of seismicity within the ISB define discrete segments along its length. Smith and Sbar (1974) described these segments in detail:

1. Northwestern Montana - scattered events along north- to northwest-trending normal faults near Flathead Lake.
2. Western Montana - major earthquake swarm in 1935 accompanied by $M_L = 6.2$ and 6.0 events, in 1925, an $M_L = 6.2$ event occurred 50 miles (80 km) southeast of Helena.
3. Butte, Montana to Yellowstone Park - pronounced seismic activity southeast of Butte and along the Madison Range extending into Yellowstone Park. The 1959 $M_L = 7.1$ Hebgen Lake earthquake produced surface faulting. At Yellowstone, the ISB swings from southeast to south.
4. South of Yellowstone Park - seismicity diminishes at the east end of the Snake River Plain.
5. Southeastern Idaho - seismicity is associated with the Grand Valley fault, and earthquake swarms occur near the Caribou Range.
6. Cache Valley and Wasatch fault zones to Salt Lake City - diffuse seismicity.
7. Salt Lake City to south-central Utah - seismicity diminishes; no earthquakes $>M_L = 3.5$ occurred in this segment between 1961 and 1970.
8. South-central Utah to northern Arizona - seismic activity increases near the southern end of the Wasatch Front. $M_L = 6+$ earthquakes have occurred in this area and are believed to be associated with the Sevier, Tushar, and Hurricane faults.
9. Northern Arizona - ISB is defined by the Paunsagaunt fault; ISB apparently dies out in Quaternary lava flows on the north rim of the Grand Canyon.

Tectonics

The relationship between seismicity and tectonics in the ISB is poorly understood, a paradox considering the prevalence of late Pleistocene and Holocene surface faulting in the area. Low- to moderate-magnitude seismicity in the ISB tends to be diffuse and is only loosely associated with scarps produced by surface faulting. This point is well-illustrated in a discussion by Arabasz and Smith (1981) concerning 5½ years of monitoring by a 43 station net along the Wasatch Front. Very few small magnitude events could be associated with the Wasatch fault over its 230 mile (370 km) length, "despite the fact that . . . this fault zone has been the most active locus of surface faulting in the eastern Great Basin during Holocene time . . ." Seismicity, instead, occurs in diffuse zones a few tens of miles east and west of the Wasatch Front. Similar patterns of seismicity have been ob-

Table 1.
Large earthquakes in the Utah region 1850 through 1978 (Arabasz and Smith, 1979).

DATE	N LAT.	W. LONG.	I (MMI)	MAG. (M_L)	LOCATION
Nov. 10, 1884	42.4	111.3	8	6*	Bear Lake
Dec. 5, 1887	37.1	112.5	7	5.5*	Kanab
Aug. 1, 1900	40.0	112.1	7	5.5*	Eureka
Nov. 13, 1901	38.8	112.1	9	6.5*	Richfield
Nov. 17, 1902	37.4	113.5	8	6*	Pine Valley
Oct. 5, 1909	41.8	112.7	8	6*	Hansel Valley
May 22, 1910	40.8	111.9	7	5.5*	Salt Lake City
May 13, 1914	41.2	112.0	7	5.5*	Ogden
Sept. 29, 1921	38.7	112.2	8	6*	Elsinore
Oct. 1, 1921	38.7	112.2	8	6*	Elsinore
Mar. 12, 1934	41.7	112.8	9	6.6*	Hansel Valley
July 21, 1959	37.0	112.5	6	5.5+	UT-AZ border
Aug. 30, 1962	42.0	111.7	7	5.7	Cache Valley
Aug. 16, 1966	37.5	114.2	6	5.6	UT-NV border
Mar. 27, 1975	42.1	112.5	8	6.0	UT-ID border

I = Epicentral Modified Mercalli Intensity
** = Local magnitude (M_L) estimated from epicentral intensity*

served in relation to other major late Quaternary surface faults including those in Cache Valley, Star Valley, Bear Lake Valley, and along the east flank of the Teton Range. Microearthquake monitoring in the Hebgen Lake area following the 1959 event produced similar results.

Arabasz and Smith (1981) note the apparent difficulty of correlation of diffuse background seismicity with geologic structure in the ISB and adjacent areas. They attribute lack of correlation to four factors: (1) uncertain subsurface structure, (2) apparent discordance between surface fault patterns and fault slip at depth, (3) a lack of historic (within last 140+ years) surface rupture, and (4) inadequate focal depth resolution from regional seismic monitoring. Arabasz (personal communication, 1985) states that historic seismicity is of little value in defining either active or potentially active faults and seismic risk in the ISB. Moreover, statistical relationships do not accurately predict either the magnitude or frequency of occurrence of large earthquakes.

Schwartz and Coppersmith (1984) applied Allen's (1968) characteristic earthquake concept to the ISB: seismogenic faults tend to generate earthquakes of generally the same magnitude and surface-rupture parameters. Between major surface-faulting events, a seismogenic fault may not produce smaller magnitude events with greater frequency of occurrence. Accordingly, frequency-magnitude relationships often cited in earthquake hazard studies may provide valuable information for larger regions but have little, if any, application to smaller areas and specific fault zones. Use of historical frequency-magnitude relationships could result in serious underestimation of earthquake hazard/risk in areas where seismogenic faults are present.

In lieu of historic seismicity data, assessment of seismic hazard/risk must be based on geologic evaluation of fault history, minimum age of movement, recurrence interval, and surface-rupture parameters, tectonic slip per event, and rupture length. Studies conducted along the Wasatch fault suggest estimates of large earthquakes based on geological data would exceed those based on historic seismicity by an order of magnitude or more (Schwartz and Coppersmith, 1984, 1986).

REGIONAL STRATIGRAPHY

The study area is underlain by a sequence of Phanerozoic sedimentary rocks ranging in thickness from 30,000 to 40,000 feet (9,100 to 12,200 m) and in age from Cambrian to Miocene. These sedimentary rocks were deposited over a complex of Precambrian crystalline and meta-sedimentary rocks now exposed in the core of the Uinta Mountains anticline. Unconsolidated surficial deposits of Quaternary age mantle bedrock over much of the project area. Figure 7 (Lamerson, 1982) summarizes stratigraphic terminology, lithologies, and unit thicknesses in the southern part of the Wyoming thrust belt. The areal distribution of stratigraphic units and major structural features are illustrated on figure 8.

Pre-Quaternary Stratigraphy

Outcrops of Precambrian rocks in the project area are confined to the core of the Uinta Mountains anticline in Utah. Paleozoic and lower Mesozoic rocks deformed by Laramide

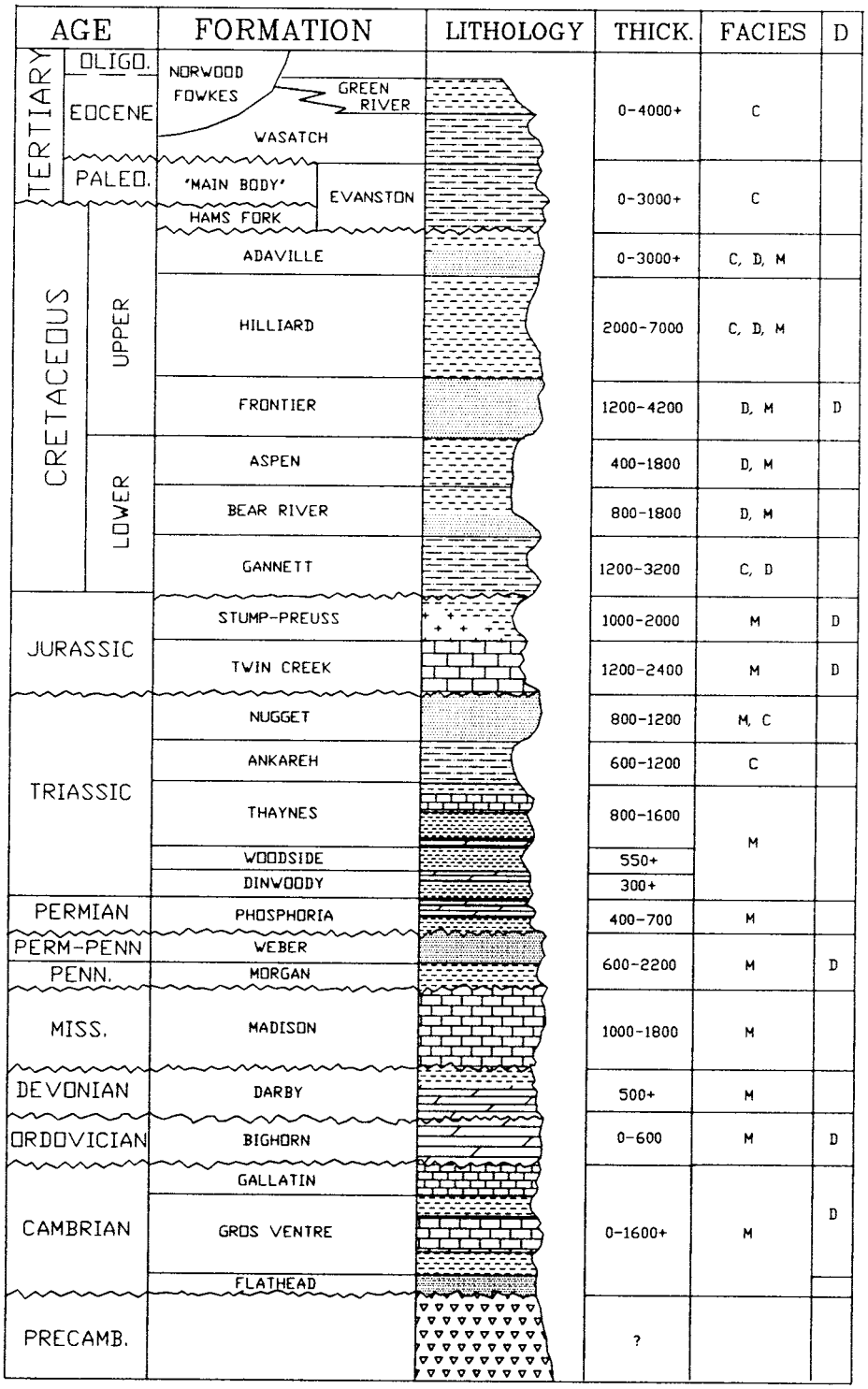

Figure 7. Generalized stratigraphic section, north-central Utah and southwestern Wyoming, showing age, nomenclature, lithology, thickness, facies, and detachment potential (Lamerson, 1982). Facies: C) continental; D) deltaic; M) marine. D in column on right indicates unit is detachment.

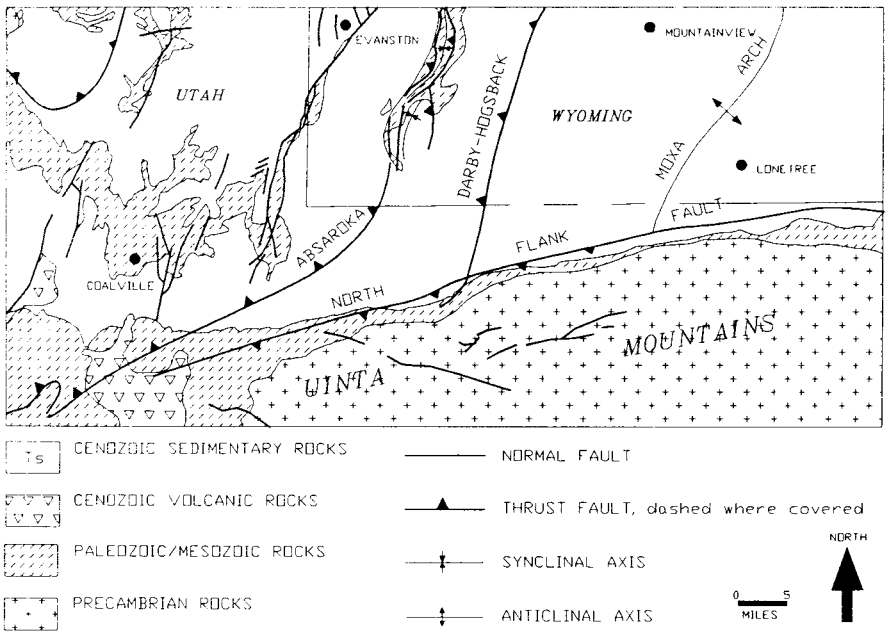

Figure 8. Regional geologic map of north-central Utah and southwestern Wyoming (Blackstone and Ver Ploeg, 1981).

faulting crop out in a narrow belt on the north flank of the Uintas. Jurassic to Paleocene-age rocks are exposed in the thrust belt about 6 miles (10 km) southeast of Evanston near the north end of the study area. Eocene to Miocene fluvial and lacustrine rocks comprise the uppermost bedrock units over the central part of the project area. Older rocks are exposed in "windows" eroded through the Tertiary cover.

Precambrian Rocks

The oldest rocks exposed in the Uinta Mountains belong to the Archean Red Creek Quartzite. According to Hansen (1969, 1984), the Red Creek Quartzite is exposed only in the eastern part of the Uinta Mountains, thereby implying greater relative uplift of the eastern Uinta dome over the western.

Overlying the Red Creek Quartzite are rocks of the Proterozoic-age Uinta Mountain Group or Belt Series equivalent. In general, these rocks comprise a sequence of low-grade, metasedimentary units deposited successively in terrestrial, shoreline margin, and marine environments. Total thickness of conglomerates, sandstones, quartzites, and shales in the Uinta Mountain Group is estimated by Hansen (1969) to be on the order of 23,950 feet (7,300 m).

Paleozoic Rocks

Middle to upper Paleozoic rocks are exposed in a narrow outcrop belt on the north flank of the Uinta Mountains as shown in figure 9. These rocks include the Mississippian Madison Limestone, the Mississippian/Pennsylvanian Round Valley Formation or equivalent units (Brazer Dolomite, Amsden Formation), the Weber Quartzite, and the Permian Park City/ Phosphoria Formations. Cambrian through Devonian units are not exposed in the study area.

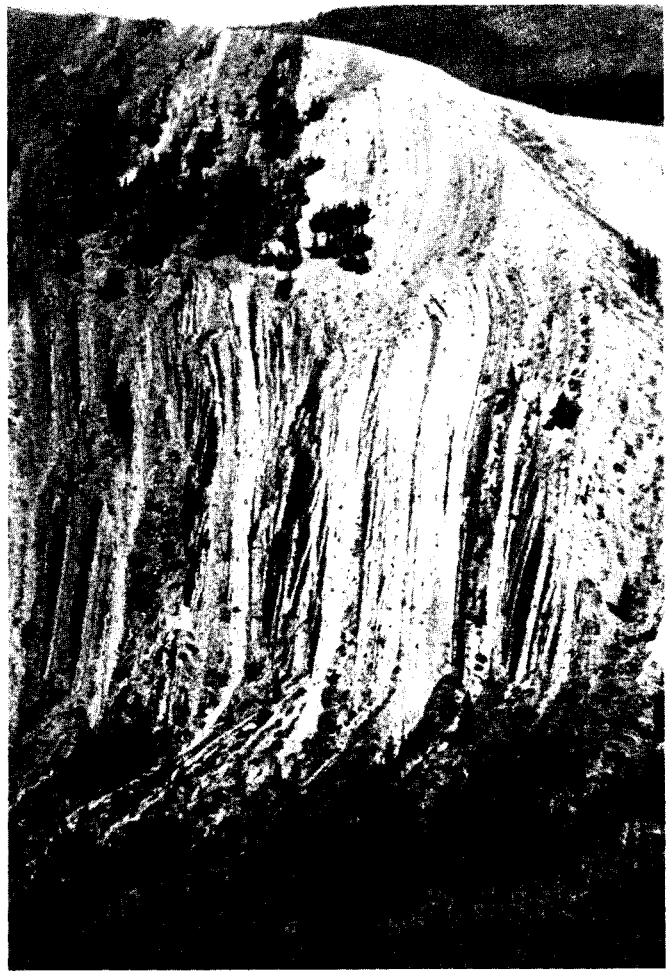

Figure 9. Middle to upper Paleozoic rocks exposed in the hanging wall of the North Flank fault of the Uinta Mountains. View is from Table Top to the east across the West Fork, Blacks Fork River.

Mesozoic Rocks

Jurassic to Cretaceous rocks are well-exposed in steeply dipping hogbacks (figure 10) associated with the trace of the Absaroka thrust in the northern part of the project area. These units include in ascending stratigraphic order the Jurassic Preuss and Stump Formations; the Triassic Woodside(?) Shale (figure 11); the Lower Cretaceous Gannet Group, Bear River and Aspen Formations; the Upper Cretaceous Frontier Formation and Hilliard Shale; and the Lazeart, Adaville, and Evanston Formations undivided.

Tertiary Rocks

Fluvial and lacustrine rocks of Tertiary age cover most of southwestern Wyoming to depths ranging from 0 to 3,280 feet (0 to 1,000 m) or more locally. These rocks include in ascending stratigraphic order: the Eocene Wasatch, Green River, and Bridger Formations; the Oligocene Bishop Conglomerate; and the Miocene Browns Park Formation. Except for the Bridger and Browns Park Formations, which are either absent or not exposed in the study area, the Tertiary units are important to evaluation of the Neogene and Quaternary structural development of the project area and are discussed below.

Wasatch Formation: The Wasatch Formation in southwestern Wyoming comprises a 2,590 to 3,280+ foot (790 to 1,000+ m) thick sequence of fluvial claystones, shales, siltstones, lenticular sandstones, and conglomerates. Studies indicate the Wasatch Formation was deposited on a paleotopographic surface cut on older Mesozoic and Tertiary strata. Thicknesses, therefore, appear to vary widely from absent to a thin veneer on paleotopographic highs to much greater thicknesses in presumed paleo-lows. Much of the topographic relief in the thrust belt at the north end of the study area appears to be related to exhumation of the paleo-surface by removal of the overlying Wasatch beds.

Lines and Glass (1975) divide the Wasatch Formation into seven members in southwestern Wyoming. Unfortunately, no reliable maps exist showing contact relationships between the various members. Moreover, members have not been defined in the subsurface through either geological or geophysical logging. No effort was made during this study to define specific members for two reasons. First, bedrock of the Wasatch Formation area is, for the most part, relatively nondescript and poorly exposed. Many of the lithologic units, particularly the sandstones, are lenticular and are of limited extent both areally and vertically within the section. Second, a relatively small stratigraphic section is exposed over a large area due to the gentle regional dip.

Green River Formation: The Eocene Green River Formation consists of about 630 to 700 feet (192 to 213 m) of lacustrine shales, marlstones and limestones. Discrepancies in stratigraphic terminology and reported unit thicknesses exist between various authors. Hansen (1984) subdivides the Green River Formation into three members in ascending stratigraphic order: the Tipton, Wilkins Peak, and Laney Members. Lines and Glass (1975), in the Fossil Basin of southwestern Wyoming, divide the Green River into the Fossil Butte and Angelo Members. Farther to the east along the western margin of the Green River basin, equivalent members include the basal Fontenelle Tongue and unnamed middle and upper tongues.

The basal Tipton Member of the Green River Formation interfingers with the upper Wasatch Formation near Piedmont Reservoir west of the inferred trace of the Darby-Hogsback thrust. Reconnaissance observations in this area suggest the Wasatch/Green River contact may be one of the few useful (identifiable) stratigraphic markers in the study area. The main body of the Green River Formation lies east of the inferred trace of the Darby thrust. The Bridger Formation conformably overlies and interfingers with the Green River on the higher divides.

Bridger Formation: The Bridger Formation consists of about 2,300 feet (700 m) of gray to pink siltstones and sandstones with interbedded tuffs, cherty limestones, and conglomerates. Lines and Glass (1975) indicate the Bridger Formation caps stream divides south and east of the project area. Large parts of the areas inferred to be underlain by the Bridger Formation, especially close to the Uinta Mountains, are mantled by Quaternary glacial deposits. Bryant (personal communication, 1984) indicates the Bishop Conglomerate directly overlies the Wasatch Formation in the Deadman Mountain quadrangle, implying the Green River and Bridger Formations are locally absent.

Bishop Conglomerate and the Gilbert Peak erosion surface: The Bishop Conglomerate caps smooth, gently northward sloping divides on the north flank of the Uinta Mountains (figure 12). It consists of poorly indurated, crudely stratified sandy gravels, cobbles, and boulders deposited in fluvial and debris-flow environments (figure 13). Clasts are derived predominantly from quartzites of the Uinta Mountain Group with subordinate clasts derived from Paleozoic units outcropping along the north flank of the range. According to Hansen (1984), volcanic ashes derived from sources in southern Utah and central Nevada are present locally within the conglomerate. Potassium-argon dates on biotite and hornblende from these ashes yield ages of about 29 million years.

The Bishop Conglomerate was deposited on a smooth surface cut on the underlying bedrock units which extended from the flanks of the Uinta Mountains to the north, east, and south. Bradley (1936) used the term "Gilbert Peak erosion surface" to describe this feature. At its maximum development during Oligocene time, the erosion surface probably extended from the flanks of the Uintas to near the centers of the adjacent basins, distances of 50 to 56 miles (80 to 90 km) (Hansen, 1984). Remnants of the surface and capping Bishop Conglomerate are present in the Green River basin, 31 to 50 miles (50 to 80 km) north of the Uintas. Topographically, the erosion surface was a vast, perhaps in excess of 9,650 square miles (25,000 km^2), smooth plain with little if any topographic relief. Bradley (1936) envisioned the erosion surface forming in a semi-arid environment by laterally scouring streams.

The development of the Gilbert Peak erosion surface and deposition of the Bishop Conglomerate argue for a long period of crustal stability following the Laramide orogeny and before the onset of Neogene-Quaternary deformation. The uniform nature of the erosion surface makes it an ideal datum by which to detect the effects of subsequent tectonism.

Figure 10. *Steeply dipping beds of the Frontier Formation exposed in hogbacks in the hanging wall of the Absaroka thrust north of Sulphur Creek. View is to the north in section 28, T. 14 N., R. 119 W.*

Figure 11. *Outcrop of Triassic Woodside (?) Shale in foreground with Mississippian Madison (?) Limestone in background exposed along the trace of the North Flank fault. Photographer is standing on Bishop Conglomerate at the south end of Table Top on the west side, West Fork of the Blacks Fork River. View is to the south in section 28, T. 2 N., R. 11 E.*

Figure 12. Planar Gilbert Peak erosion surface capped by Bishop Conglomerate on Elizabeth Ridge in section 35, T. 3 N., R. 11 E. View is to the south toward the Uinta Mountains.

Figure 13. Exposure of Bishop Conglomerate on Elizabeth Mountain. View is to the northwest in section 20, T. 3 N., R. 11 E.

Browns Park Formation: The Browns Park Formation consists of about 1,200 feet (366 m) of white to light-gray, tuffaceous sandstones, siltstones, and quartzites with conglomerate near the base. Winkler (1970) suggests the Browns Park Formation is a remnant of Tertiary sediments shed from uplifted mountain ranges through the central Rockies and Wyoming basin. Differential uplift and temporal variations account for the many topographic and structural settings in which the Browns Park Formation is found. Near the distal edges, Browns Park sediments coalesced to form a more or less continuous blanket extending tens of miles from adjacent uplifts. Locally, Browns Park sediments overlie the Gilbert Peak erosion surface and the Bishop Conglomerate. In other areas, however, the Browns Park was deposited in valleys eroded after development of the Gilbert Peak erosion surface (Winkler, 1970).

In most areas, the basal Browns Park Formation consists of conglomeratic facies believed to have been derived from the Bishop Conglomerate. Where the Browns Park overlies the Bishop, the two units are conformable and the contact is gradational. Overlying the basal conglomerate is a sequence of rhyolitic tuffs, tuffaceous sandstones, siltstones, and quartzites. Individual lithologic units are discontinuous and reflect local variations in sedimentary regime.

Potassium-argon dates from tuffaceous beds (Winkler, 1970) range from 41 to 12 million years. Postulated source areas for air-fall tuffs include the Yellowstone-Absaroka volcanic center, the San Juan Mountains of southwestern Colorado, and the Keetley volcanic field of east-central Utah, although the latter is andesitic in composition.

The Browns Park Formation, due to its friable nature, typically forms subdued, soil mantled slopes with little or no outcropping bedrock. Terrace and glacial deposits locally overlie the Browns Park Formation. The Browns Park Formation reportedly underlies glacial deposits in the vicinity of Meeks Cabin dam (Lines and Glass, 1975).

Quaternary Stratigraphy

Bedrock north of the Uinta Mountains is extensively mantled by unconsolidated surficial deposits of Pleistocene to Holocene age. These deposits include tills and related outwash deposits from alpine glaciations of the high Uintas, alluvium capping terraces and flooring modern stream drainages, and landslides.

Glacial Deposits

The Uinta Mountains underwent multiple glaciations during the Pleistocene. According to early workers (Blackwelder, 1915; Richmond, 1957, 1964, 1965), up to three pre-Wisconsin advances and two separate, but distinct, Wisconsin advances

were recorded. In this stratigraphic scheme, pre-Wisconsin glaciations were referred to collectively as pre-Bull Lake. The early and late Wisconsin glaciations were termed Bull Lake and Pinedale, respectively, after their type localities in the Wind River Mountains of north-central Wyoming.

Recently, several workers (Pierce, 1979; Porter and others, 1983) have demonstrated that the early Wisconsin glaciation traditionally termed Bull Lake is actually 150,000 to 140,000 years old and, therefore, pre-Wisconsin in age. The late Wisconsin or Pinedale glaciation ranges in age from 40,000 years to about 12-14 thousand years. Pinedale glaciers reached their maximum extent at least once and possibly twice prior to 25,000 years and reached another maximum about 20,000 years ago (Porter and others 1983).

Pre-Bull Lake deposits: The existence of pre-Bull Lake glacial deposits in the Uinta Mountains, as in other western mountain ranges, appears to be questionable. Atwood (1909) recognized two glaciations of the Uintas and suggested the possibility of a third (pre-Bull Lake?). In 1936, Bradley defined glacial deposits of the "Little Dry Stage" (pre-Bull Lake) based on tills found on Little Dry Creek south of Mountainview, Wyoming. Schoenfeld (1969) found no concrete evidence for pre-Bull Lake glaciation of the Uintas near Burnt Fork, about 40 miles (64 km) east of the Bear River. Isolated remnants of till, however, were found beyond the limits of Bull Lake moraines suggesting the possibility of pre-Bull Lake glaciation. No evidence of pre-Bull Lake till was found during the course of field studies conducted for this project.

Schlenker (1988) studied the glacial stratigraphy and geomorphology of the Blacks Fork drainage basin. He believes Bigelow Bench, a gently northward sloping surface capped by Uinta Mountain Group gravels may be equivalent to Bradley's (1936) "Little Dry Stage" glaciation and, therefore, is pre-Illinoian in age. The gravels appear to grade southward into tills suggesting Bigelow Bench was once part of an areally extensive outwash plain. The age of Bigelow Bench is important because it may constrain the onset of neotectonic deformation in the project area.

Bull Lake deposits: Atwood (1909), Bradley (1936), and Schoenfeld (1969) all recognize evidence for at least one Bull Lake (Illinoian) glaciation. Schoenfeld (1969) presents evidence for two distinct Bull Lake advances based on cross-cutting relationships between moraines containing broadly similar tills and "steps" in correlative outwash deposits.

Bull Lake outwash has been mostly eroded or covered by subsequent Pinedale till and outwash deposits in areas close to the north flank of the Uinta Mountains. A broad outwash plain, however, is preserved on Hilliard Flat about 3.5 miles (5.6 km) north of the lowest terminal moraines. These deposits, in an abandoned valley of the Bear River, may be Bull Lake outwash based on topographic position above outwash deposits clearly grading into Pinedale moraines. The material consists of poorly sorted, crudely stratified, lenticular gravels, cobbles, and scattered boulders with lenses of coarse sand. Clast lithology is predominantly sub-rounded Uinta Mountain Group quartzites. The deposits exhibit a mature soil profile with a strongly developed textural B-horizon and Stage II-III calcium carbonate.

Pinedale deposits: Pinedale (Wisconsin) tills are widely distributed in lateral, terminal, and recessional moraines in the major glaciated valleys on the north flank of the Uinta Mountains. Atwood (1909) and Bradley (1936) both recognized glacial deposits which would later be correlated with the Pinedale stade. Richmond (1965) divided the Pinedale of the Uinta Mountains into three separate glacial advances, early, middle, and late, each characterized by distinct, mappable tills. Schoenfeld (1969), working in the Burnt Fork area, supports at least a three-fold division of the Pinedale based on morphology and suggests the possibility of two additional Pinedale advances.

Pinedale tills are found in sharp-crested lateral moraines and in pitted terminal/recessional moraines along the major stream valleys including the Hayden Fork, East Fork, and the three major forks of the Blacks Fork. Pinedale outwash plains are present downstream of correlative tills in all of the major glaciated valleys. The Bear River Valley upstream of Hilliard Flat is an excellent example of a Pinedale outwash surface. Along Utah Highway 150 south of the Wyoming line, a broad outwash plain with several distinct terraces can be seen clearly grading into Pinedale terminal moraines deposited by glaciers in the Hayden Fork and East Fork valleys.

Terrace Alluvium

In addition to major outwash plains, alluvium in strath and cut-and-fill terraces is present along the Bear River, Blacks Fork, and their tributaries. Most of the strath terraces cap bedrock divides at elevations above Hilliard Flat and are inferred, therefore, to range from pre-Bull Lake to middle or early Pleistocene in age. Cut-and-fill terraces form the inter-valley walls of most modern drainages in the project area and are interpreted to be post-Pinedale or Holocene in age. No effort has been made to map or correlate post-Pinedale terraces in detail.

Most of the older strath-terrace deposits appear to be broadly similar in composition, generally consisting of sandy gravels and cobbles with a few widely scattered boulders. The clasts are subrounded to rounded and are mainly quartzites and other resistant lithologies derived from the Uinta Mountain Group. The deposits are poorly sorted, crudely stratified, and range in thickness from a thin residuum to several meters. Where exposed, soil development appears to be mature with strong textural B-horizons and Stage II-III+ calcium carbonate. Many of the major terrace surfaces appear to consist of several subordinate surfaces, possibly resulting from climatic fluctuations and/or Quaternary tectonism.

Alluvium in cut-and-fill terraces exposed in stream banks along modern drainages consists primarily of finer grained sands, silts, and clays with lenses of gravels and cobbles deposited by storm events. Terrace surfaces typically exhibit weakly developed A/C profiles. Buried A-horizons in low terraces associated with modern floodplains are common in the project area.

Landslides

Much of southwestern Wyoming and north-central Utah is underlain by Late Cretaceous and Tertiary marine/fluvial clay shales. These deposits exhibit low peak and residual shear strengths and are prone to landsliding, especially with the intro-

duction of water. Accordingly, landslides ranging in age from earliest post-Pinedale to historic are common in the area. The greatest concentration of large-scale landsliding, however, appears to be in moderately steep, forested areas between the north flank of the Uinta Mountains and the semi-arid plains to the north.

Soil Development and Chronosequences

No complete studies of soil development and/or soil chronosequences have been undertaken in the project area.

Schoenfeld (1969) in his study of the Quaternary geology of the Burnt Fork area concluded that relative age dating techniques, presumably including soil development, were of little value in the Uinta Mountains due to the abundance of quartzites in the parent material. This, however, does not appear to be the case, based on observations regarding soil development in the project area. Deposits of significantly different ages show apparent differences in soil development both in color and clay content of B-horizons and in calcium carbonate accumulation in Bk-horizons.

Similar findings were reached by Martin and others (1985) regarding studies of soil development near Taskeech and Upper Stillwater dams on the south flank of the Uinta Mountains. They concluded that sufficient amounts of iron, clay, and carbonate derived from Paleozoic through Tertiary sedimentary rocks exposed on the south flank of the Uintas were present to define age-dependent variations in soil development. Time spans required for soil profile development on the south flank of the Uinta Mountains were inferred to be comparable to time spans for similar soil development in granitic terrains of the Rocky Mountains (Martin and others, 1985).

REGIONAL STRUCTURE

Principal structures of the project area (figure 14) include the Absaroka and Darby-Hogsback thrusts of the Wyoming-Utah thrust belt, the North Flank fault of the Uinta Mountains, and late Quaternary normal faults described by Gibbons and Dickey (1983). The geology of thrust and Laramide faulting is discussed in the following sections. Late Quaternary normal faults southeast of Evanston and their relationships to older structures are discussed in later sections of this report.

Thrust Faults

Absaroka Thrust

The project area lies mainly on the Darby-Hogsback plate between the Darby-Hogsback thrust on the east and the Absaroka thrust on the west (figure 14). The Absaroka thrust, the older of the two faults, roughly delineates the western boundary of the project area and is defined by an outcrop belt of steeply dipping Jurassic to Cretaceous sediments (Nixon, 1955; Lines and Glass, 1975; Lamerson, 1982). These units, exposed along Sulphur Creek west of Sulphur Creek Reservoir (figure 10), include in ascending stratigraphic order the Preuss Formation, Stump Formation, Gannet Group, Bear River Formation, Aspen Formation, Frontier Formation, and Hilliard Shale.

The Absaroka thrust is exposed at the surface in this area and consists of two strands. The western strand strikes about N. 22° E. and dips vertically. The eastern strand juxtaposes Frontier Formation on the west against Hilliard Shale on the east and strikes N. 35° E. with a 70° dip to the northwest. South of Sulphur Creek both strands pass beneath Bull Lake(?) outwash and related deposits mantling Hilliard Flat (figures 15 and 16). A series of hogbacks on the west side of Hilliard Flat defines the general position of the Absaroka thrust between Sulphur Creek and the Bear River Valley to the south.

Southwest of Hilliard Flat, the Absaroka thrust reappears on the east slope of the Bear River Valley. The fault trace is covered by Pinedale outwash, recent alluvium, and fan deposits along the river floodplain and passes out of the project area to the southwest. Change in strike to the southwest probably reflects the buttressing effect of the Uinta Mountains a few kilometers to the south.

North of Sulphur Creek, the trace of the Absaroka thrust swings sharply to the northeast and crosses I-80 about 9.9 miles (16 km) east of Evanston. Subsurface geophysical mapping by Dixon (1982) suggests the swing to the northeast is a function of change in strike rather than change in dip. Cook (1977) reports an almost vertical dip on the Absaroka fault in the Aspen Tunnel area about 3.5 miles (5.6 km) northeast of Sulphur Creek Reservoir. Beutner (1977) suggests changes in strike within the thrust belt reflect geometric irregularities in the craton margin.

Darby-Hogsback Thrust

The Darby-Hogsback thrust, youngest of the major thrust faults in southwestern Wyoming, is inferred to lie about 11 miles (18 km) east of the Absaroka thrust. Traditional interpretations indicate the trace of the fault is covered by the Eocene Wasatch and Green River Formations and is not exposed at the surface. The trace of the Darby-Hogsback thrust beneath Tertiary sediments closely subparallels the strike of the Absaroka thrust through the project area. Near its southern end, close to the North Flank fault of the Uintas, structural relationships become unclear. Based on the tendency of other thrust faults, it seems likely the Darby-Hogsback swings sharply to the west-southwest and parallels the north flank of the Uintas, perhaps as a tear fault. No evidence exists to suggest that the Darby-Hogsback fault actually intersects or cuts the North Flank fault. Blackstone and Ver Ploeg (1981) show the Darby-Hogsback thrust swinging sharply to the southwest paralleling the North Flank fault of the Uinta Mountains (figure 8). The trace of the Darby-Hogsback is inferred to lie beneath the hanging wall of the North Flank fault. Definitive interpretation, however, is hindered by the cover of Pleistocene glacial deposits and widespread landsliding on the north flank of the Uintas.

Near the north end of the project area, the Darby-Hogsback thrust swings abruptly to the northeast in parallel with the Absaroka thrust, lending credibility to pre-existing control on thrust fault geometry. Dixon's (1982) subsurface interpretations show no appreciable change in dip to account for the swing of the fault trace to the northeast.

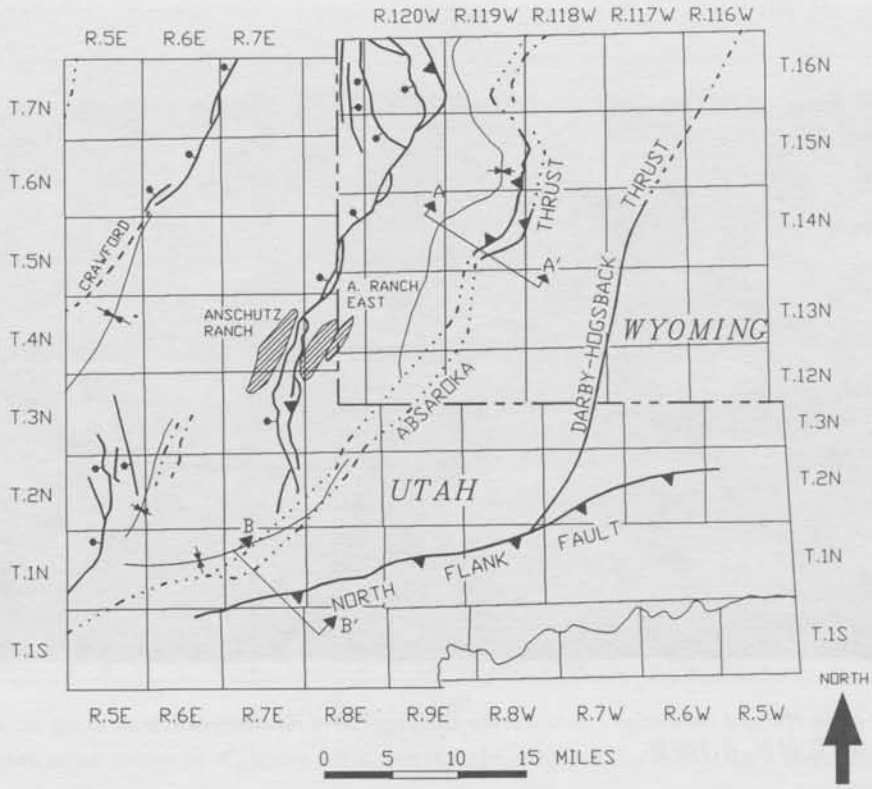

Figure 14. Tectonic map of the project area and vicinity showing the Darby-Hogsback and Absaroka thrust plates north of the Uinta Mountains. (Lamerson, 1982).

Figure 15. View to the south across Sulphur Creek in section 29, T. 14 N., R. 119 W. The leading edge of the Absaroka thrust passes beneath outwash and terrace alluvium on the extreme left of view. Hogbacks in the hanging wall of the Absaroka thrust are visible on the skyline. Stream bank in right-center of photograph is shown in figure 16.

Figure 16. Sub-vertical beds of the Hilliard Formation exposed in the hanging wall of the Absaroka thrust along the south side of Sulphur Creek. View is to the south in section 29, T. 14 N., R. 119 W.

Subsurface Structure

High density reflection seismic data interpreted by Dixon (1982) and Lamerson (1982) provide the best picture of subsurface structure in southwestern Wyoming (figure 17). Both the Absaroka and Darby-Hogsback thrusts are related to a westward dipping decollement in Cambrian Gros Ventre shales at a depth of about 22,000 + feet (6700 + m) below the Bear River Valley. The trailing edge of the Darby-Hogsback thrust lies almost directly (vertically) below the leading edge of the Absaroka thrust, a common geometrical relationship for adjacent thrusts in the thrust belt (Dixon, personal communication, 1984). Both the Absaroka and Darby-Hogsback thrusts exhibit ramp structures primarily in competent Paleozoic rocks. The crest of the Darby-Hogsback ramp lies approximately 8 miles (13 km) west of the subsurface trace of the thrust and 3 to 4 miles (4.8 to 6.5 km) east of the surface trace of the Absaroka thrust. The ramp crest generally parallels the leading edge of the Darby-Hogsback along strike through southwestern Wyoming. Accordingly, the trend of the ramp crest is inferred to mimic the abrupt change in strike to the northeast characteristic of both the Darby-Hogsback and Absaroka faults.

North Flank Fault

The North Flank fault of the Uinta Mountains (figures 8 and 14) defines the southern limit of the study area. It is a high-angle reverse fault juxtaposing meta-sedimentary rocks of the Uinta Mountain Group and overlying Paleozoic and lower Mesozoic rocks on the south against sharply upturned middle to late Mesozoic and early Tertiary(?) sediments on the north (figures 9 and 18). Reconnaissance studies along the North Flank fault between Moffit Pass and the West Fork, Blacks Fork River, suggest the fault is actually composed of several strands across a zone 330 feet (100 m) or more wide. Slivers of light-gray (Madison?) limestone and tan quartzose sandstones (Weber Quartzite?) were noted at several locations. Thin bands of red shale thought to be derived from the Triassic Woodside Formation are also present locally (figure 11). Individual fault planes are not exposed, so dip could not be determined.

On the drainage divide between the West Fork of the Blacks Fork River and Mill Creek, red shales are in apparent contact with the Bishop Conglomerate in a saddle marking the trace of the North Flank fault zone (figure 11). Gray (Madison?) limestones abut the red shales a few tens of feet to the south. Unfortunately, contact relationships, particularly between the red shales and Bishop Conglomerate, could not be established as either depositional or fault related.

Little information is currently available concerning the subsurface configuration of the North Flank fault zone in the project area. Sohio recently completed a major exploration effort (Christmas Meadows Project) on the Darby-Hogsback plate near its apparent intersection with the Uinta Mountains. At least two exploration wells were drilled in the footwall of the North Flank fault, but none of the data have been released.

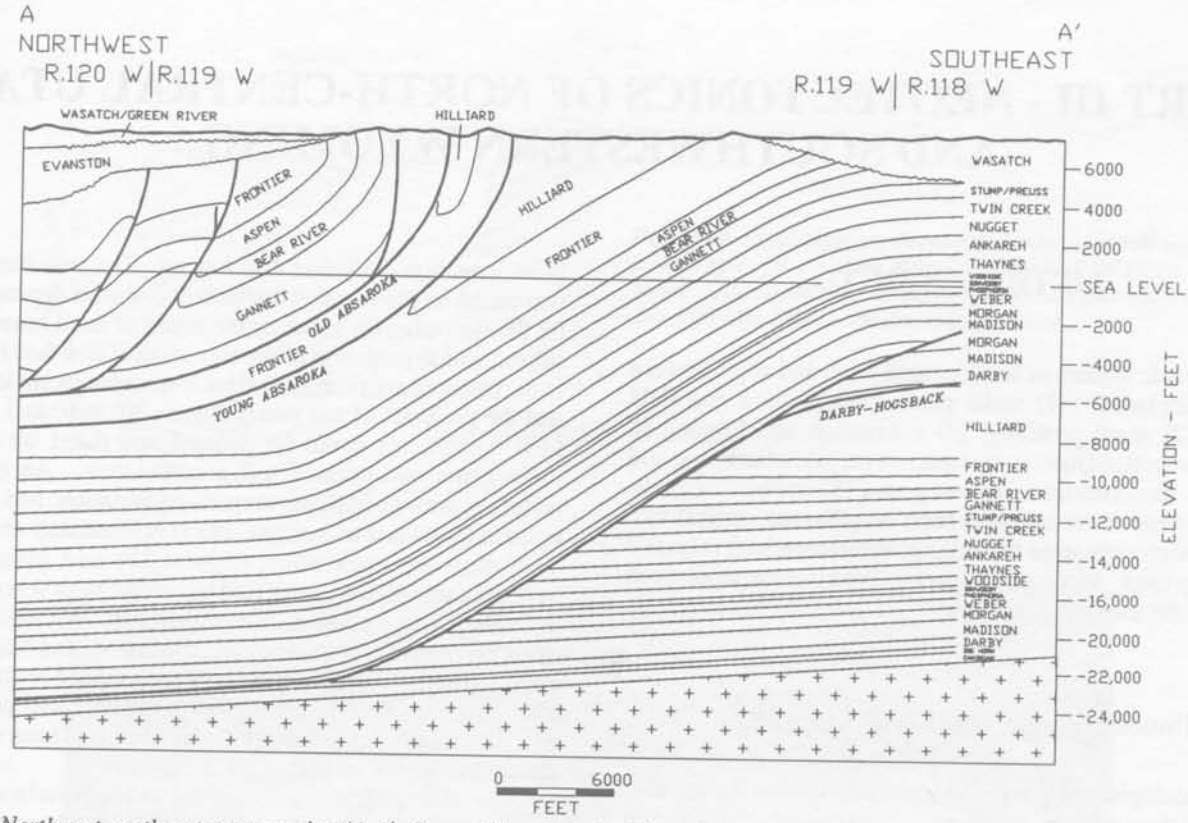

Figure 17. Northwest-southeast cross section (A-A', figure 14) across the Absaroka and Darby-Hogsback thrust plates north of Sulphur Creek Reservoir (Lamerson, 1982).

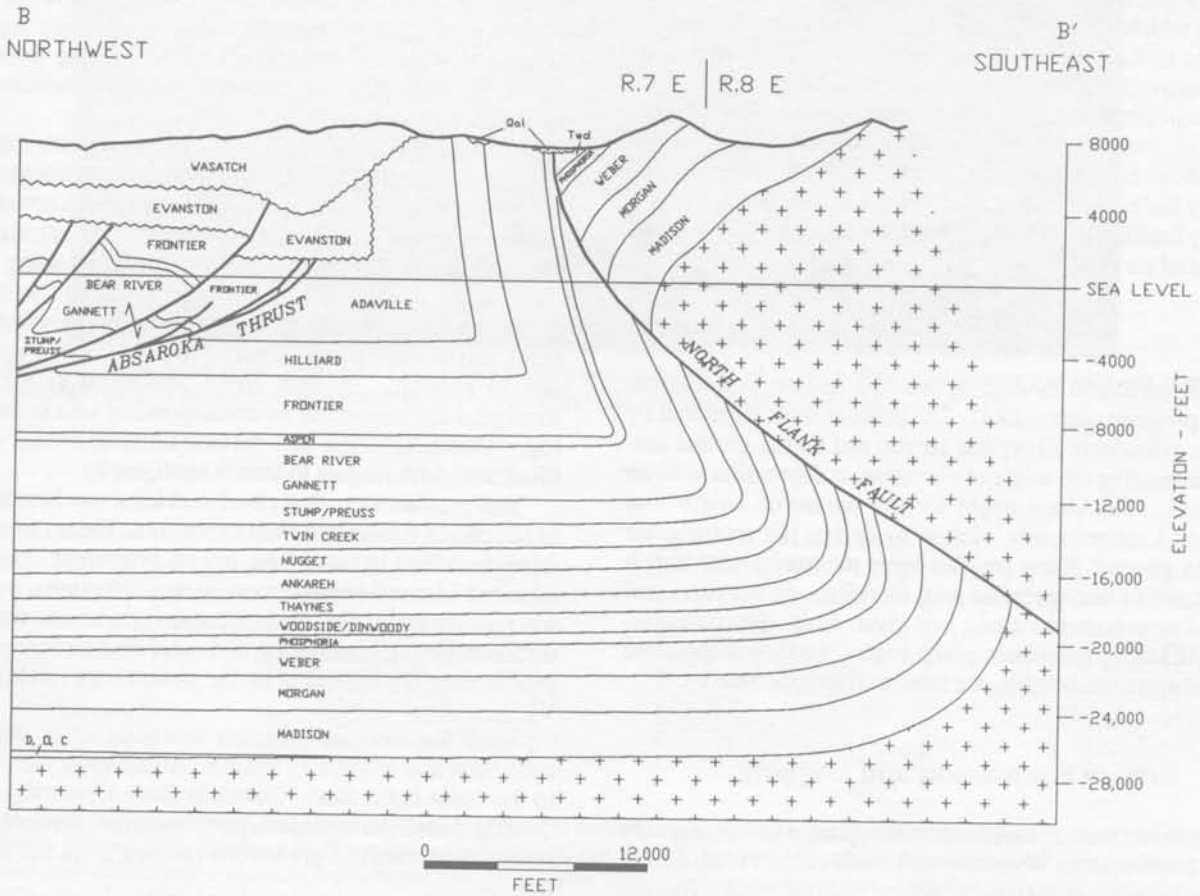

Figure 18. Subsurface structure along the North Flank fault in T. 1 N., R. 7-8 E. (B-B', figure 14). The "old" and "young" Absaroka thrust faults are present to the northwest (left) (Lamerson, 1982).

PART III - NEOTECTONICS OF NORTH-CENTRAL UTAH AND SOUTHWESTERN WYOMING

METHODOLOGY

Neotectonic studies in north-central Utah and southwestern Wyoming included: (1) aerial photo interpretation and field mapping, (2) scarp profiling, (3) excavation and logging of trenches across late Quaternary fault scarps, (4) radiocarbon and amino acid racemization age dating, and (5) analysis of fault-rupture parameters including rupture lengths, net vertical tectonic displacements, ages of faulting, recurrence intervals, and tectonic slip rates. Methodologies employed in these studies are outlined in the following sections.

Photogeologic and Field Mapping

Photogeologic mapping was conducted using false-color infrared photography at scales of 1:60,000 and 1:35,000 and natural color photography at a scale of 1:20,000. The primary objective of photogeologic interpretation was to identify possible faults which appeared to offset Quaternary-age deposits or geomorphic surfaces. Lineaments identified on air photos were compared to available geologic mapping to aid in interpretation. Apparent topographic scarps and photogeologic lineaments associated with late Quaternary faulting were compiled on aerial photograph overlays for subsequent field checking. Late Quaternary faults and other features believed to be related to late Quaternary faulting were mapped on a reconnaissance basis and are illustrated on plate I.

Scarp Profiling

Sixteen scarp profiles were measured in conjunction with the trenching program (appendix I). The profiles were measured by placing an extendable fiberglass survey rod on the ground surface and measuring the angle of elevation or depression with an Abney level. The slope angle for the measured length was recorded and subsequently plotted to derive the topographic profile. In general, scarp profiles were measured near trench sites as an aid to interpretation and, therefore, do not represent minimums or maximums along any given fault. Scarp characteristics, including maximum scarp angles, surface slopes, and offsets and apparent heights, are tabulated in appendix I.

Trench Excavation and Logging

Ten trenches were excavated across apparent late Quaternary scarps in southwestern Wyoming and north-central Utah during the 1983-84 field seasons. A fortuitous "natural" fault exposure in an irrigation ditch was also logged. The trenching program was based on the fact that distinctive colluvial deposits develop on the downthrown block as the result of fault movement and subsequent degradation of the sub-vertical free face (figure 19). In the project area, pronounced back-tilting adjacent to the scarps and the presence of sag ponds (figure 20) indicated successive fault movements could be defined and dated by alternating colluviation and organic soil accumulation. An example of recurrent normal-fault movement, colluviation, and soil development (Schwartz and others, 1983) is illustrated on figure 21.

Following excavation (figure 22) and installation of hydraulic shores, horizontal and vertical control was established by nailing a string line to one trench wall. Stations one meter apart horizontally were marked, numbered, and flagged along the string line. Geologic contacts were mapped by measuring in X-Y directions from the string line. Stratigraphic units defined by logging were described using a standardized form specifically developed for the project.

As anticipated, natural and man-made subsurface exposures in the Bear River fault zone showed clear evidence of recurrent fault displacements highlighted by scarp-derived colluvial wedges and buried A-horizons. Several trenches exhibited evidence of stacked, tectonic colluvial wedges separated by organic-rich buried A-horizons formed in sag pond environments. Samples from modern and buried A-horizons were collected for radiocarbon dating.

The log of each trench excavated during the 1983-84 field seasons and the irrigation ditch exposure are presented on plates II through V. Individual trench-log explanations are stratigraphically correct and illustrate development of lithostratigraphic and soil stratigraphic units with time. Corresponding laboratory radiometric ages are included where available. In some cases, geologic features or events, for example a period of soil development, can be inferred but direct stratigraphic evidence is missing due to erosion. In such cases, the event is shown in the stratigraphic column but no corresponding unit is shown on the log. Unconformities and surface-faulting events are clearly illustrated with respect to trench stratigraphy.

Soil profiles were described in at least one location in seven of the eleven subsurface fault exposures. Three or more profiles were described in two of the trench exposures. Data recorded included Munsell color(s), consistency, plasticity, composition, soil classification, clay films, structure, carbonate stage, horizon thickness/depth, boundaries, and other standard properties. Soil profile sites are indicated on the trench logs (plates II through V).

Each horizon was sampled in the field for additional examination and laboratory testing. All samples were transmitted to the Soils Laboratory, Colorado State University for testing. Tests included percentage organic material, percentage soil carbonate, and material gradations ranging from 0.5 microns to 2 mm.

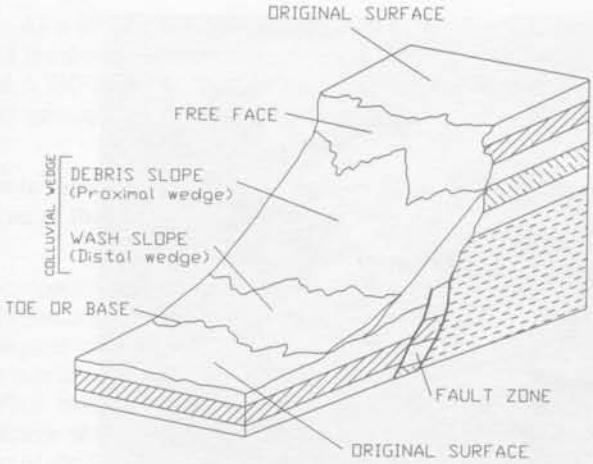

Figure 19. *Block diagram showing degradation of sub-vertical free face formed by surface rupture along a normal fault (Wallace, 1977). A colluvial wedge consisting of debris (proximal) and wash (distal) facies develops with time on the downthrown block.*

Figure 20. *Water-filled sag pond at the base of the Lester Ranch scarp in section 24, T. 13 N., R. 119 W. The presence of such sag ponds suggested that fault movements could be radiometrically dated using organic materials obtained from trench exposures.*

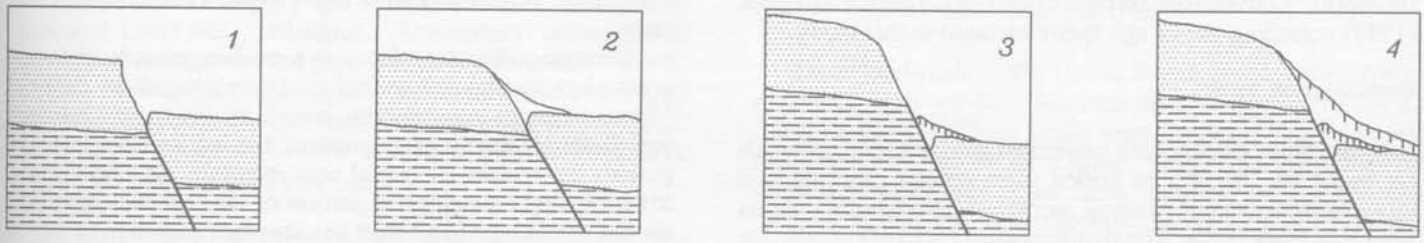

Figure 21. *Model for development of successive colluvial wedges and buried soils resulting from recurrent movement on a normal fault (Schwartz and others, 1983). (1) initial displacement and formation of sub-vertical free face; (2) erosion of free face, development of colluvial wedge and surface soil; (3) second fault displacement creating rejuvenated free face; (4) erosion of rejuvenated free face, burial of first colluvial wedge and resident soil by second colluvial wedge; development of new surface soil.*

Figure 22. Excavation of the Lester Ranch trench in section 24, T. 13 N., R. 119 W. Trenches were excavated by backhoe, and trench walls were supported by hydraulic shoring.

Radiocarbon and Amino Acid Racemization Ages

The well-preserved nature of tectonically buried soils and the fortuitous presence of detrital charcoal, other organic material, and landsnails in pre- and post-fault sediments allowed application of radiocarbon and amino acid racemization techniques to the study of faulting in the project area. The primary objectives of these studies were: (1) to estimate the age of individual surface-faulting events, (2) to establish recurrence intervals and slip rates, (3) to determine age of latest movement, and (4) to establish temporal continuity (or conversely segmentation) along late Quaternary faults in the project area.

Methodologies are described in the following sections. Radiocarbon laboratory results are presented in appendix II. Interpretation of data and applications to analysis of surface-rupture parameters for individual faults are presented later in the report. Conventions recommended by Colman and others (1987) regarding use of age terms are used in this study.

Radiocarbon Ages

Introduction: Ages of fault movement and recurrence intervals are based on ^{14}C ages of buried soils, detrital charcoal, and miscellaneous organic material recovered from trenches across late Quaternary faults. The significance of each radiometric age is affected by (1) inherent limitations of the radiocarbon method and (2) interpretation with respect to geological materials and events. Of the two types of error, geological misinterpretation is the greatest potential problem.

Taylor (1987) discusses sources of error and uncertainty inherent to the radiocarbon method. Principal sources of error include: (1) compositional factors, (2) experimental and statistical factors, and (3) systemic factors. Compositional factors include contamination where foreign carbon is introduced to the sample by accident or some unrecognized natural process and fractionation of carbon isotopes under natural conditions.

Errors may also be introduced by experimental and statistical factors. A radiocarbon-age calculation requires four values: (1) the background count rate, (2) the count rate of the contemporary standard, (3) the count rate of the "unknown" sample, and (4) the decay constant of ^{14}C which is directly related to the half-life (Taylor, 1987). Items 1 through 3 are experimentally measured under common operating conditions. Due to the random nature of radioactive decay, variations in experimentally measured values can be expected for the same sample. According to Taylor (1987), the laboratory "date" is not a specific point in time, rather it is an artifact of experimentally determined count rates.

Because radioactive decay is a random process, statistical constraints are imposed on analysis of counting data. Decay of ^{14}C nuclei over a long counting period, ideally an infinitely long period, should approximate a normal distribution when counting periods are broken into equal time intervals. In a normal distribution, approximately 68 percent of the separate count rates should not deviate more than one standard deviation (1 sigma) from the average count rate. Hence, a reported laboratory date of 5,570± 80 radiocarbon years before present (yr B.P.) indicates the age equivalent for the measured counting rates would fall between 5,490 and 5,650 yr B.P. approximately 68 percent of

the time. At a 95 percent confidence level (2 sigma) the age equivalent for the measured counting rates would fall between 5,410 and 5,730 yr B.P. At a 98 percent confidence level (3 sigma) the age equivalent would fall between 5,330 and 5,810 yr B.P.

Systemic factors derive from violations of the fundamental assumptions of the radiocarbon method:

1. The concentration of ^{14}C in each carbon reservoir has remained constant over the radiocarbon time scale.
2. Complete and rapid mixing of ^{14}C has occurred in carbon reservoirs worldwide.
3. Carbon isotope ratios in samples have only been altered by radioactive decay since sample materials ceased to be an active part of the reservoir (since death of the organism).
4. The half-life of ^{14}C is accurately known.
5. Natural levels of ^{14}C can be measured to meaningful levels of accuracy and precision.

For the purposes of this study, assumptions 4 and 5 are accepted without further discussion. Assumptions 1, 2 and 3, however, are subject to significant variations which affect geologic interpretation and calendar-year calibration of radiocarbon ages. Departures from these assumptions produce long-term (secular) and short-term (de Vries) variations between laboratory radiocarbon dates and calendar dates (Taylor, 1987). Secular variations are believed to result from (1) changes in the production of ^{14}C due to cosmic ray activity and changes in the magnetic fields of the earth and sun, and (2) variations in the carbon cycle caused by environmental and climatic factors. Secular variation between AD 1 and AD 1,000 produces radiocarbon dates that may be up to 100 calendar years too old. Between AD 1 and 6000 BC, secular effects may produce radiocarbon dates that may be up to 800 years too young (Klein and others, 1982; Stuiver and Kra, 1986).

In addition to long-term secular variations, short-term variations, the de Vries effect, are also present. The cause of the de Vries effect is believed to be related to short-term fluctuations in cosmic ray activity and magnetic fields. The de Vries effect can produce radiocarbon dates that are too old or too young by 200+ years (Taylor, 1987). The combination of the de Vries effect and statistical error effectively eliminate a simple additive (or subtractive) correction for secular variation (Taylor, 1987).

Other systemic factors include the Suess effect and the atom bomb effect. The Suess effect involves the depletion of ^{14}C in the late nineteenth century and is believed to be the result of increased fossil fuel combustion. Atmospheric detonation of thermonuclear weapons has produced large amounts of "bomb" carbon. Neither the Suess effect or bomb carbon is considered a significant problem in this study, assuming that very "young" carbon has not been mixed with "old" carbon by bioturbation or some other unrecognized process.

Sample collection, preparation, and laboratory dating: The radiocarbon dating program for this study included 33 samples obtained from buried and modern A-horizons adjacent to faults exposed in trenches and 5 samples of detrital charcoal and other organic material contained in pre- and post-fault sediments. All samples were obtained from trench exposures after logging and interpretation had been completed. The samples were removed as carefully as possible from the trench wall, sealed in plastic bags, placed on ice, and transported to cold storage in Denver. Two to four samples weighing about 5 pounds (2.5 kg) each were obtained from the base of each buried or modern A-horizon. Smaller samples of detrital charcoal and/or other organic material were also obtained where possible. Rodent skulls and bones were collected but proved to be of insufficient quantity for dating.

Bulk samples from modern and buried A-horizons, in all cases, were obtained from the lower 10-15 cm of the horizon. Consistent sampling at the base of the horizon, it was believed, would (1) provide an approximation of the maximum age of the horizon, (2) reduce problems of interpretation caused by the apparent mean residence time for the entire soil horizon, and (3) reduce problems of interpretation caused by comparison of ages obtained from different elevations in the same or correlative horizons.

Soil samples from each sampling site were visually inspected, and samples with high organic contents were selected for pre-treatment. Soil samples from the 1983 trenching program were prepared by Rolf Kihl, Institute of Arctic and Alpine Research (INSTAAR), University of Colorado and submitted to Geochron Laboratories Division, Krueger Enterprises, Inc. for age determinations. Samples from the 1984 field program were prepared and dated by Beta Analytic, Inc.

Sample location and ages in radiocarbon years before present (yr B.P.) are shown on individual trench logs (plates II through V), and are tabulated in appendix II. No discrepancies in ages are apparent which can be attributed solely to differences in procedures employed by the two laboratories. No control samples, however, were tested to allow direct comparison.

Calibration: Each laboratory radiocarbon age obtained from this study was calendar-calibrated using the methods outlined by de Jong and others, (1986); Linick and others (1986); and Pearson and Stuiver (1986). Calibration methods cited in these papers are based on direct comparison of radiocarbon ages to dendrochronologically determined ages of wood samples. A 2 sigma error was used for the reported laboratory value and for the resulting calendar age. Laboratory and calendar-calibrated ages are listed in appendix II.

Amino Acid Racemization Analysis

Three landsnails of the Genus *Oreohelix* cf. *strigosa* were recovered from pre-fault fluvial sediments exposed in the La Chapelle trench. These snails were analyzed for amino acid racemization ratios by Dr. Gifford Miller at INSTAAR. No dates were calculated from these samples, but racemization ratios are believed to be consistent with a late Pleistocene to early Holocene age. Land snail sampling sites are shown on the La Chapelle trench log. A discussion of the significance of amino acid racemization ratios is included under La Chapelle trench stratigraphy.

Fault-Rupture Parameters

Data obtained from geologic mapping, scarp profiling, trenching, and dating studies were used to define fault-rupture parameters including surface-rupture lengths, net vertical tectonic displacements, ages of faulting, recurrence intervals and slip rates, for each proven or suspected late Quaternary structure in the project area.

Fault-Rupture Lengths

Fault-rupture lengths were obtained directly from mapping of late Quaternary fault scarps and related deformation depicted on plate I. Actual surface rupture (ground breakage) was measured directly and accurately from geologic mapping of fault scarps. In some cases, however, deformation (warpage, tilting, and monoclinal folding) associated with surface rupture may extend some distance beyond the zone of actual ground breakage defined by the presence of fault scarps. In such cases, both the minimum length of actual ground breakage and the maximum length of related deformation were measured and/or estimated. Rupture lengths for individual faults are summarized in the sections on the Bear River fault zone, Absaroka fault, and Darby-Hogsback fault.

Net Vertical Tectonic Displacements

Estimates of total and single-event net vertical tectonic displacements for late Quaternary faults were based on (1) geometric analysis of scarp profiles, (2) measurement of stratigraphic offsets in trench exposures, and (3) interpretation of colluvial-wedge stratigraphy in trench exposures. Estimates of net vertical tectonic displacements for individual faults are summarized in later sections of the report.

Scarp profiles: Total net vertical tectonic displacements from scarp-profile data (table I.1, appendix I) were calculated using standard methods outlined by McCalpin (1982). The results of these calculations are summarized in tables I.2 and I.3 (appendix I). Total net vertical tectonic displacements shown in table I.2 are based on scarp height, maximum scarp angle, surface-slope angle, and either measured or estimated fault dip. Similar values in table I.3 are calculated from surface offset, surface-slope angle, and either measured or estimated fault dip. Differences in apparent total vertical tectonic displacements are attributed to uncertainties in parameter measurement. Single-event net vertical tectonic displacements were obtained by dividing total displacement by the number of events defined by trench stratigraphy.

Calculation of net vertical tectonic displacements from scarp profiles is complicated by extensive back-tilting, antithetic faulting, and graben formation extending 2 to 2.5 miles (3 to 4 km) away from the main zone of surface rupture. After analysis of the tectonic setting and deformation associated with surface faulting, it was concluded that none of the scarp profiles accounted for more than very localized tectonic deformation adjacent to the fault scarps. Conventional scarp-profiling techniques using survey rod and level are inadequate to characterize broad secondary deformation of the type present in the project area. Precise leveling and/or photogrammetric techniques appear to be the only viable techniques to characterize secondary deformation over wide zones.

In addition to broad, local areas of back-tilting and antithetic faulting, the region has been subjected to eastward tectonic tilt which could serve to add further uncertainty to interpretation of vertical tectonic displacements from topographic profiles. The effect of both broad, local deformation and regional tectonic tilt on scarp profiles may be to increase apparent net vertical tectonic displacements over actual values.

Stratigraphic throw: Estimates of total and single-event net vertical tectonic displacements were obtained from direct measurement of stratigraphic throw between correlative units in trench exposures. Obvious effects of back-tilting, antithetic faulting and graben development in trench exposures were eliminated where possible. The total effect of secondary deformation on estimates of stratigraphic throw could not be completely eliminated for reasons outlined in the preceding paragraphs.

Colluvial-wedge stratigraphy: Estimates of single-event vertical tectonic displacement were derived from the maximum thickness of the scarp-derived colluvial wedge preserved on the downthrown block (Ostenaa, 1984). Ideal slope degradation models suggest that material is symmetrically eroded off the free face and deposited at the base of the scarp. According to Ostenaa (1984), the thickness of the colluvial wedge should approach 1/2 the height of the initial free face for large surface displacements. The height of the free face that produced the colluvial wedge, therefore, should be about 2 times the thickness of the associated wedge. This method allows estimation of vertical displacements for each simple wedge identified in trench exposures. The effects of secondary deformation adjacent to the scarp, however, cannot be directly accounted for, suggesting estimates of vertical tectonic displacement based on colluvial-wedge geometry alone may be high.

Ages of Faulting and Recurrence Intervals

Most radiocarbon ages used in the analysis of ages of surface rupture and recurrence intervals were obtained from buried and modern soil A-horizons; hence, interpretation is complicated by the time it took the soil to develop in place, lateral and vertical variations in soil horizons caused by bioturbation, translocation of organic compounds, unavoidable differences in sampling techniques, and uncertainties introduced by the radiocarbon method itself. The apparent mean residence time (AMRT) age of a soil, therefore, is calculated from the total ^{14}C activity of various fractions in a bulk soil sample (Geyh and others, 1971; Martel and Paul, 1974; Matthews, 1980; Machette and others, 1992). The resulting age is a function of a complex suite of environmental factors controlling the development of the soil and sampling/pretreatment techniques.

In all cases, bulk samples of modern and buried A-horizons were obtained from the lower 10-15 cm of each horizon. The rationale was that an AMRT age from the base of the horizon would provide an estimate of the maximum age of the horizon

and, therefore, a minimum age for the underlying deposit or event. Hindsight indicates this approach was an oversimplification. Due to the nature of the soil-forming process, environmental factors and sampling techniques, the resulting AMRT ^{14}C age for a sample from the base of the horizon probably does not represent the maximum age of the horizon. Instead, it represents an age younger than the inception of soil formation and younger than the age of fault surface rupture. The data collected for this study do not provide a reasonable quantitative basis for taking this difference into account.

To partially compensate for this problem and to increase the confidence level in radiocarbon ages, the laboratory error for each AMRT and charcoal laboratory age was multiplied by a factor of two (2 x sigma) to arrive at a geologically more meaningful AMRT age. For example, an AMRT laboratory age of 1,000 ± 50 yr B.P. indicates a 68 percent probability that the actual radiocarbon age falls between 950 and 1,050 yr B.P. An AMRT age of 1,000 ± 100 yr B.P. (2 x sigma) indicates a 95 percent probability that the radiocarbon age falls between 900 and 1,100 yr B.P. The use of ± 2 sigma provides a higher confidence level and some compensation for uncertainties in interpretation of AMRT ages for soils.

Still greater confidence in interpretation is afforded by multiple subsurface exposures along fault strike and multiple dates from correlative soils. Where multiple exposures and age determinations are available, the data should average out discrepancies and provide more reliable estimates of the ages of soil development and, as a result, the ages of surface-faulting events than a single set of dates obtained from a single trench exposure.

Tectonic Slip Rates

Tectonic slip rates for individual faults were calculated from net vertical tectonic displacements and ages of movement. The resulting values were compared to documented slip rates for other late Quaternary faults in the western United States as a means of gauging relative degree of fault activity.

BEAR RIVER FAULT ZONE

Principal neotectonic features of north-central Utah and southwestern Wyoming include: (1) a zone of late Quaternary faulting (figure 23) originally described by Gibbons and Dickey (1983) and termed the Bear River fault zone by West (1984), (2) a scarp coincident with the leading edge of the Absaroka thrust and apparent tectonic deflection of the Bear River, and (3) apparent normal fault scarps along and near the subsurface trace of the Darby-Hogsback thrust. Evidence for late Quaternary deformation in each of these areas (figure 24) is discussed in this and the following two sections on the Absaroka and Darby-Hogsback faults.

General Description

In 1983, Gibbons and Dickey described significant late Quaternary faulting in southwestern Wyoming. A well-developed zone of faulting was mapped from about 12 miles (19 km) southeast of Evanston almost due south to an apparent termination 1.5 miles (2.4 km) north of the Wyoming-Utah line as shown on figure 23.

Initial reconnaissance mapping for this study disclosed a zone of late Quaternary fault scarps exhibiting evidence of co-seismic, basin and range-style surface faulting with associated sag ponds, beheaded drainages, and antithetic scarps. Numerous sag ponds along the scarps implied successive fault movements would be recorded by alternate scarp colluviation and organic soil formation (figures 20 and 21). Geologic study of these sag ponds, it was believed, would provide a detailed displacement history with supporting radiometric ages.

The height of late Quaternary fault scarps reported by Gibbons and Dickey (1983) increases from north to south, reaching maximum development just north of the Wyoming-Utah state line (figure 23). Subsequent air photo interpretation and field mapping for this study demonstrated that late Quaternary faulting continues southward into Utah and intersects a family of scarps sub-paralleling the trace of the North Flank fault zone (figure 24). The northern (Wyoming) scarps are separated from the southern (Utah) scarps by a gap of 4 miles (6.5 km).

The Bear River fault zone, as defined by this study, extends over 21 to 25 miles (34 to 40 km) from southeast of Evanston, Wyoming to the north flank of the Uinta Mountains in north-central Utah. In general, the fault zone comprises distinct individual scarps each about 1.9 to 2.2 miles (3.0 to 3.5 km) in length, arranged in a right-stepping en echelon pattern. Major scarps trend N. 20° W. to N. 20° E. and show consistent down-to-the-west displacement. Scarps of lesser down-to-the-east displacements, interpreted to be antithetic structures, trend N. 15-20° W. Near the south end of the fault zone, scarps in Pinedale and Bull Lake glacial deposits show strong angular discordance (70°) with the main north-northeast pattern of faulting.

Geomorphic evidence of recent movement includes scarps ranging from less than about 1.5 to 49 + feet (0.5 to 15 + m) high in a variety of deposits including till, outwash, and alluvium; beheading and reversal of stream drainages; and numerous water-filled sag ponds. Fault displacement of youngest floodplain alluvium and modification of stream courses were noted in widely separated stream drainages. Evidence of late Quaternary movement is described in the following sections.

Northern Scarps

The northern end of the main Bear River fault zone consists of three right-stepping en echelon scarps (figure 25) 1.1 to 1.7 miles (1.8 to 2.7 km) in length and trends about N. 15° E. (figure 24 and plate I). The scarps offset bedrock of the Wasatch Formation and, although distinct on air photos, are subdued at ground level. Scarp heights decrease rapidly to the north, and the northernmost scarp apparently dies out before reaching the old Piedmont railroad grade (county road in section 29, T. 14 N., R. 118 W.).

A short late Quaternary scarp (figure 26), similar to those in the Bear River fault zone, was mapped by Gibbons and Dickey

Figure 23. Gibbons and Dickey (1983) mapped apparent late Quaternary faults in southwestern Wyoming north of the state line as part of the Energy Lands Program of the U.S. Geological Survey.

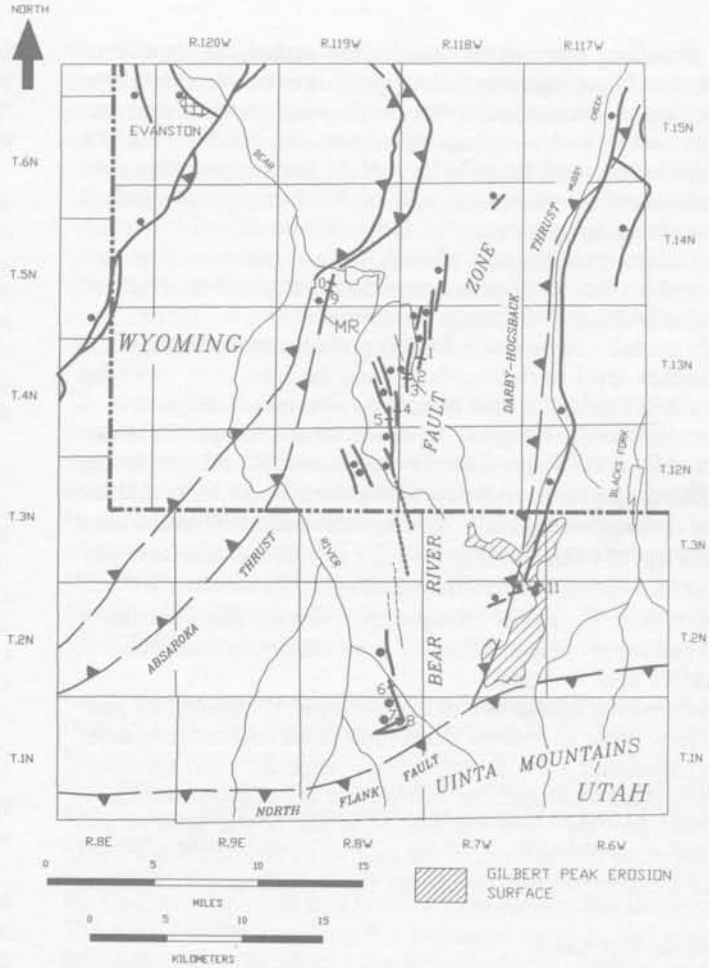

Figure 24. Map of neotectonic features in the project area. The Bear River fault zone is located between the Darby-Hogsback and Absaroka thrusts. 1=La Chapelle trench/scarp profile. 2=Lester Ranch trench/scarp profiles. 3=Lester Ranch South trench/scarp profiles. 4= Austin Reservoir ditch exposure. 5=Sulphur Creek trench-scarp profile. 6=Big Burn trench/scarp profile. 7=Upper Little Burn trench/scarp profile. 8=Lower Little Burn trench/scarp profile. 9=Upper Martin Ranch (MR) trench/scarp profile. 10=Lower Martin trench/scarp profile. 11= Elizabeth Ridge trench/scarp profiles.

Figure 25. Oblique aerial view to the south of right en echelon scarps near the northern end of the main Bear River fault zone (sections 6 and 7, T. 13 N., R. 118 W.). Note the large stock pond impounded against the scarp. Local ranchers have used late Quaternary fault scarps for dam construction in the project area due to "ideal" topographic conditions afforded by the scarps.

(1983) about 3.0 miles (4.8 km) northeast of the main zone of faulting (figure 24 and plate I). This scarp, apparently only a few hundred yards long, trends about N. 45° E. and is defined by a low scarp in bedrock and a sagebrush lineament. Although separated from the main Bear River fault zone, it was almost certainly produced by the same stress field and probably is contemporaneous with the main zone of surface faulting to the southwest. This scarp defines the maximum northern limit of surface faulting in the Bear River fault zone.

La Chapelle Scarp

The La Chapelle scarp, at 2.4 miles (3.8 km), is one of the longest in the Bear River fault zone (figure 24 and plate I). It trends N. 5° E. mainly in bedrock of the Wasatch Formation on the east side of the La Chapelle Valley (figure 27). A related scarp trending N. 13° E. displaces part of the La Chapelle floodplain in section 18, T. 13 N., R. 118 W. (figure 28A and B). The meander belt of the pre-fault stream channel is clearly visible on the upthrown side of the block. The present channel of La Chapelle Creek over a distance of about 0.6 miles (1 km) lies against the scarp and is locally eroding it. Displacement of floodplain alluvium here and at Deadman Creek in the southern part of the fault zone provides direct geomorphic evidence of late Holocene movement.

La Chapelle Trench

The La Chapelle trench was excavated in August 1984 and was originally intended to expose Eocene Wasatch Formation bedrock on either side of the fault. The specific objective of trenching was to provide stratigraphic correlation of Eocene-age bedrock units across the fault and, if correlatable, the net vertical tectonic displacement in bedrock. Comparison of post-Eocene net vertical tectonic displacement with Holocene net vertical tectonic displacement from this and other trenches, would provide evidence for the age of initial surface rupture. Coeval displacements in Eocene and Holocene units would indicate that initial surface rupture occurred in the Holocene and that the Bear River fault zone is a "new" tectonic feature. Lack of stratigraphic correlation across the fault and/or post-Eocene displacements in excess of Holocene values would indicate a longer history of faulting than that recorded solely by Quaternary deposits in the project area.

The La Chapelle fault along most of its length appears to displace Wasatch bedrock based on nearby outcrops and soil colors. The trench site, in the NW¼SW¼, section 19, T. 13 N., R. 118 W., was selected on the crest of a topographic rise in what appeared to be residuum/colluvium developed on claystone bedrock (figure 29). The scarp at the trench site is approximately 16.5 feet (5 m) high based on surface offset and has a maximum scarp angle of 12 degrees. The trench was oriented in a N. 84° W. direction, was 154 feet (47 m) long and 9.8 feet (3.0 m) deep at its deepest point. Seven radiocarbon samples and three land snails (Genus *Oreohelix*) were obtained for dating. In addition to stratigraphic logging and sampling, four soil profiles were described.

Pre-fault stratigraphy: The La Chapelle trench (figure 24 and plate I) exposed a sequence of late Quaternary-age fluvial sediments apparently deposited on an erosion surface cut on bedrock of the Wasatch Formation. No bedrock, however, was exposed in the trench, negating the primary objective of trenching at this location. Nevertheless, trench exposures provided an interesting and complex picture of faulting, fault-related colluviation, and soil development.

The fluvial sediments consist of interbedded sands, gravelly sands and clays derived predominantly from local source areas in terrain to the south and east. These materials are interpreted to have been deposited in a low energy stream or fan environment as evidenced by their fine-grained, well-sorted nature and graded bedding. Radiocarbon ages obtained from charcoal and layered organic material and amino acid racemization ratios obtained from landsnails are consistent with an apparent late Pleistocene to early Holocene age.

Logging of fluvial sediments was based on lithologic and stratigraphic characteristics. These units are designated 1 through 6 on the La Chapelle trench log. Units believed to be correlative across faults exposed in the trench are designated by letters A, B and C. A soil developed on the fluvial sediments and is at least partially preserved on the upthrown block. Soil profile 4 describes the original resident soil profile prior to faulting.

Structure and post-fault stratigraphy: Two distinct sub-vertical fault zones separated by a horizontal distance of 8.9 feet (2.7 m) were disclosed by the trench. Based on interpreted displacement of the original surface soil, both faults appear to have ruptured the surface during the initial surface-faulting event. Scarp-derived colluvial material (unit 8) buried the original surface soil on the intermediate and downthrown blocks as shown in figure 30. A second soil (unit 9) developed on the stabilized colluvial wedges (figure 31) and was subsequently displaced by a second surface-faulting event and buried by scarp-derived colluvial deposits (unit 10). The second buried soil at a location on the downthrown block was laboratory dated at about 3,400 yr B.P. (appendix 2). Following the second event, loess was deposited against the scarp by prevailing westerly winds. Much of this loess and the underlying scarp colluvium have been extensively bioturbated by burrowing animals making interpretation of colluvial-wedge stratigraphy and second event displacement history difficult. A third and final soil, laboratory dated at about 2,300 yr B.P., developed across the scarp.

Interpretation: The La Chapelle trench shows evidence of two surface-faulting events displacing late Pleistocene to earliest Holocene fluvial sediments. The presence of two fault planes and disruption of the uppermost colluvial wedge by burrowing animals complicate interpretation of individual fault displacements. Estimates of total net vertical tectonic displacement across the fault zone yield figures of 15.1 to 16.7 feet (4.6 to 5.1 m; table 2) distributed across both faults. Estimates of vertical tectonic displacement per surface-faulting event range from 5.2 to 8.5 feet (1.6 to 2.6 m) resulting in a mean of 6.9 feet (2.1 m). Total and single-event displacement data are summarized in tables 2 through 6.

Figure 26. Oblique aerial view to southwest of short, late Quaternary scarp northeast of the main Bear River fault zone (section 15, T. 14 N., R. 118 W.). Vegetation contrast is caused by bedrock in upthrown (left) block juxtaposed against tectonically derived colluvium and loess on the down-thrown (right) block.

Figure 27. Oblique aerial view to the south of the southern end of the La Chapelle scarp (section 29, T. 13 N., R. 118 W.).

Figure 28. ***A.*** *Oblique aerial view to south of fault scarp (lower right corner) impinging on floodplain of La Chapelle Creek (section 18, T. 13 N., R. 118 W.).* ***B.*** *Floodplain alluvium is displaced along fault in upper center of oblique aerial view to south (section 18, T. 13 N., R. 118 W.). Present channel is eroding scarp due to back-tilting of the downthrown block. Former meandering stream channel is preserved on top of upthrown block. The main La Chapelle scarp is visible near the top of the lower photo.*

Figure 29. View to the north along the La Chapelle scarp showing the trench site in section 19, T. 13 N., R. 118 W.

Figure 30. View of the La Chapelle trench near station 30 showing tectonically derived colluvial wedge (unit 8B) resting on buried soil (unit 7). Flags on string are one meter apart.

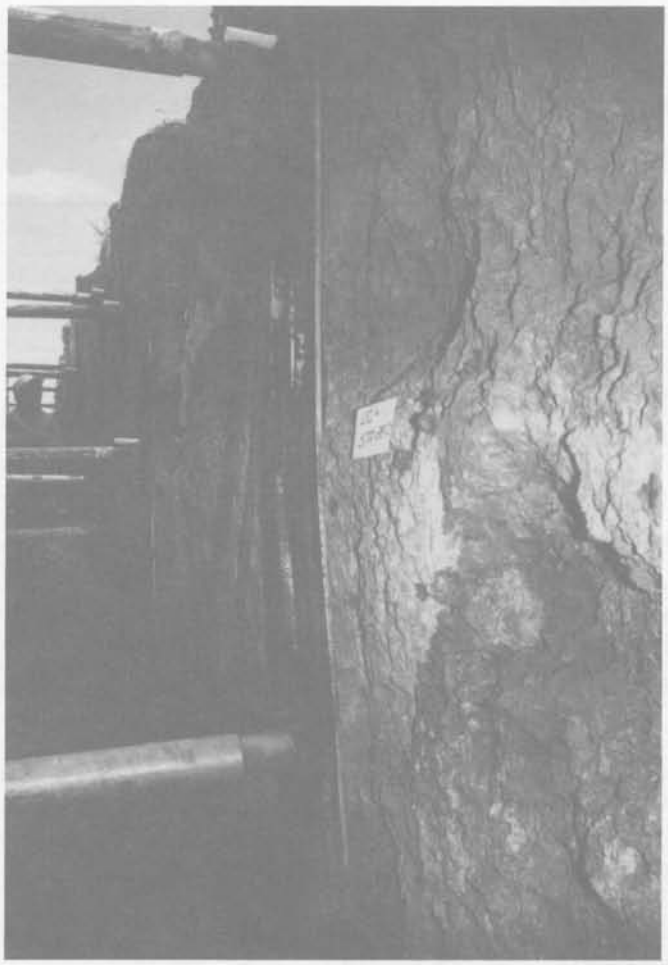

Figure 31. South wall of the La Chapelle trench showing the fault near station 28, truncation of buried soil (unit 7), and fissuring adjacent to the fault. Index card on trench wall is 3 x 5 inches.

Lester Ranch Scarp

The Lester Ranch scarp, trending about N. 14° E. over a distance of 2.3 miles (3.7 km), lies mainly west of the La Chapelle floodplain (figure 24 and plate I). The fault displaces strath terrace gravels over most of its length and, as a result, produces a prominent topographic scarp (figure 32). The scarp averages about 13 to 16.5 feet (4 to 5 m) in height along its central sector with slope angles ranging from 15 to 24 degrees. One sag pond containing water (figure 33) and several dry, closed depressions are present along the scarp. The Blacks Fork Sheep Trail (road) passes through an apparent breach in the scarp (figure 34) on the west side of the La Chapelle Valley. The breach is apparently related to a short, right en echelon step in the scarp.

Near its north end, the scarp impinges on the La Chapelle floodplain. Although no evidence for physical offset of the floodplain could be found at the site, a slight tonal variation along strike on air photos suggests continuation of the fault to the north. A short lineament and local deformation in Wasatch Formation bedrock on the east side of the valley support this interpretation.

Several northwest-striking air-photo lineaments are present in the area west of the Lester Ranch scarp (plate I). On air photos, these lineaments are clear and sharp but could not be located with certainty on the ground, probably due to very small surface displacements. The similarity of these lineaments to antithetic scarps further to the south suggest they, too, are of antithetic origin.

Lester Ranch Trench

The Lester Ranch trench was excavated in 1983 near a water-filled sag pond in the center of section 24, T. 13 N., R. 119 W. (figure 24 and plate I). The site was selected due to its proximity to the sag pond, the presence of Quaternary terrace deposits along the scarp and ease of access. It was believed proximity to the sag pond (figures 33 and 34) would aid in interpretation of fault-related sedimentation and provide samples for radiocarbon dating. The possibility of high ground-water levels which would interfere with trenching, however, was a concern.

The scarp near the trench ranges from about 13.1 to 13.8 feet (4.0 to 4.2 m) high (figure 23) and exhibits maximum scarp angles averaging 15 degrees. The trench was oriented in a N. 85° W. direction. Trench length and maximum depth were 93 and 11.8 feet (28.5 and 3.6 m), respectively.

Pre-fault stratigraphy: The trench in the upthrown block disclosed coarse gravel-cobble alluvium overlying bedrock of the Wasatch Formation. A well-developed soil with strong textural B-horizon and a Stage III to III+ Bk-horizon was present on the alluvium. Wasatch Formation bedrock exposed in the trench comprised mainly grayish olive, friable, medium- to coarse-grained sand with lenses of sandy shale. Indurated pods of sandstone were present within the friable sands.

Structure and post-fault stratigraphy: A distinct fault plane striking N. 12° E. and dipping 76° northeast was noted about two-thirds of the way down the scarp. The orientation of the fault plane implied high-angle reverse displacement (figure 35). Carbonate-filled fractures in bedrock on the upthrown side, however, suggested gravitational creep or overtoppling of the free face as an explanation for the apparent reverse orientation. Brown clay gouge with horsetailing carbonate-rich shear planes defined the position of the fault on the trench wall. No slickensides, however, could be found on the shear planes.

On the downthrown side of the fault, at least two tectonically stacked colluvial wedges separated by buried, organic-rich A-horizons were present in a classic exposure illustrated in figure

Table 2.
Total net vertical tectonic displacements calculated from scarp-profile data, Bear River fault zone.

SCARP	TOTAL NET VERT. TECTONIC DISPLACEMENT* (meters)
La Chapelle	4.6 - 5.1
Lester Ranch	3.9 - 11.3
Sulphur Creek	6.7 - 8.6
Big Burn	2.9 - 12.7
Upper Little Burn	4.8 - 7.2
Lower Little Burn	0.8 - 1.4

**See appendix I. tables I.2 and I.3 for explanation.*
To convert meters to feet multiply by 3.28.

Table 3.
Net vertical tectonic displacement per event from scarp-profile data, Bear River fault zone.

TRENCH	TOTAL NET VERT. TECTONIC DISPLACEMENT (meters)	NET VERT. DISPLACEMENT/EVENT (meters)
La Chapelle	4.6 - 5.1	2.3 - 2.6
Lester Ranch	4.0 - 5.5	2.0 - 2.7
Lester Ranch South	3.9 - 4.1	2.0 - 2.0
Austin Res. Ditch	- -	- -
Sulphur Creek	6.7 - 8.6	3.3 - 4.3*
Big Burn	9.7 - 12.7	4.8 - 6.3*
Upper Little Burn		
Upper Scarp	0.6 - 2.7	0.3 - 1.4*
Lower Scarp	2.7 - 4.4	1.4 - 2.2*
Total	4.8 - 7.2	2.4 - 3.6*
Lower Little Burn	0.8 - 1.4	0.4 - 0.7*
		0.8 - 1.4**

**Assumes two equal-displacement scarp-forming events*
***Assumes single scarp-forming event*
To convert meters to feet multiply by 3.28

Table 4.
Vertical displacement per event from total vertical stratigraphic offset, Bear River fault zone.

TRENCH	TOTAL VERT. STRAT. OFFSET (meters)	VERTICAL DISPLACEMENT/EVENT (meters)
La Chapelle	3.2 - 4.7	1.6 - 2.4
Lester Ranch	6.3	3.1
Lester Ranch South	3.9 - 5.9	2.0 - 2.9
Austin Res. Ditch	1.2 - 1.5	0.6 - 0.8
Sulphur Creek	>5.7	>2.8*
Big Burn	- -	- -
Upper Little Burn	2.0 - 2.2	1.0 - 1.1*
Lower Little Burn	- -	- -

**Assumes two equal-displacement scarp-forming events*
To convert meters to feet multiply by 3.28

Table 5.
Single-event and total vertical displacement estimated from colluvial-wedge stratigraphy exposed in trenches, Bear River fault zone.

TRENCH	EVENT 1		EVENT 2		TOTAL ESTIMATED VERTICAL DISPLACEMENT (meters)
	WEDGE THICKNESS (meters)	ESTIMATE DISPLACEMENT (meters)	WEDGE THICKNESS (meters)	ESTIMATED DISPLACEMENT (meters)	
La Chapelle	- -	- -	- -	- -	- -
Lester Ranch	0.7 - 1.2	1.4 - 2.3	0.7 - 1.0	1.3 - 2.0	2.7 - 4.3
Lester Ranch South	- -	- -	- -	- -	- -
Austin Reservoir Ditch	0.7 - 1.0	1.4 - 2.0	0.4 - 0.4	0.7 - 0.8	2.1 - 2.8
Sulphur Creek - Interp. 1**	1.3	2.50	2.1 - 2.4	4.2 - 4.7	6.7 - 7.1
Sulphur Creek - Interp. 2**	- -	- -	3.4 - 3.6	6.7 - 7.2	13.4 - 14.4*
Big Burn	- -	- -	1.9	3.9	7.7*
Upper Little Burn	- -	- -	- -	- -	- -
Lower Little Burn	0.7 - 0.9	1.4 - 1.8	0.50	1.0	2.4 - 2.8

**See section on Sulphur Creek trench for explanation of alternative interpretations.*
***Estimated displacement for second event multiplied by 2 to arrive at total estimated displacement.*

Table 6.
Comparison of vertical tectonic displacements per event summarized from scarp-profile, stratigraphic offset, and colluvial-wedge stratigraphic data, Bear River fault zone.

SCARP	VERTICAL TECTONIC DISPLACEMENT					
	SCARP PROFILES (meters)	STRAT. OFFSET (meters)	COLLUVIAL WEDGE STRAT. (meters)	MIN.	MAX. (meters)	MEAN
LaChapelle	2.3 - 2.6	1.6 - 2.4	- -	1.6	2.6	2.1
Lester Ranch North	2.0 - 2.7	3.13	1.30 - 2.3	1.3	3.1	2.2
Lester Ranch South	2.0 3.7 - 5.7	2.0 - 2.9 - -	- - - -	2.0 3.7	2.9 5.7	2.5 4.7
Austin Reservoir	- -	0.6 - 0.8	0.7 - 2.0	0.6	2.0	1.3
Sulphur Creek #1*	3.3 - 4.3**	>2.8	2.5 - 4.7	2.5	4.7	3.6
Sulphur Creek #2*	3.3 - 4.3**	>2.8	6.7 - 7.2	>2.8	7.2	5.0
Big Burn	4.8 - 6.3**	- -	3.9	3.9	6.3	5.1
Upper Little Burn Lower scarp Total	 1.4 - 2.2** 4.8 - 7.2**	 1.0 - 1.1** - -	 - - - -	 1.0 4.8	 2.2 7.2	 1.6 6.0
Lower Little Burn	0.4 - 0.7** 0.8 - 1.4***	- - - -	1.0 - 1.8 1.0 - 1.8	0.4 0.8	1.8 1.8	1.1 1.3

**See section on Sulphur Creek trench for explanation of alternative interpretations.*
***Assumes two equal displacement scarp-forming events.*
****Assumes single scarp-forming event.*
To convert meters to feet multiply by 3.28.

Figure 32. Ground-level view to north of the Lester Ranch scarp in sections 13 and 24, T. 13 N., R. 119 W. Note cow on top of scarp for scale.

Figure 33. View to the south along the Lester Ranch scarp showing water-filled sag pond in section 24, T. 13 N., R. 119 W. The Lester Ranch trench was excavated just beyond the sag pond.

Figure 34. Oblique aerial view to northeast of the Lester Ranch scarp displacing a strath-terrace surface (section 24, T. 13 N., R. 119 W.). Note the water-filled sag pond and the Blacks Fork Sheep Trail (road) passing through a right en echelon step in the scarp.

Figure 35. Detail of faulting exposed in the Lester Ranch trench. The fault, marked by clay gouge, appears to exhibit a high-angle reverse geometry. Cracking and gravitational over-toppling of Wasatch Formation bedrock in the free face has overturned the fault from its original high-angle normal to the apparent high-angle reverse orientation. Flags on string are one meter apart.

36. The colluvial wedges contained mainly gravel-cobble debris derived from the terrace deposit overlying bedrock on the upthrown side of the fault. Individual clasts adjacent to the fault plane were rotated into imbricated positions. Near the top of the fault plane, a small lens of Wasatch-derived colluvium was present in the uppermost colluvial wedge. Modern slope colluvium derived from the Wasatch Formation and the overlying terrace deposit cover the fault. These deposits and the modern surface soil are unbroken by faulting.

Two distinct buried A-horizons, formed on successive colluvial wedges, could be traced westward away from the fault until they merged with the modern surface soil (figure 37). Faulting down-dropped the original surface soil relative to the free face, and scarp colluviation subsequently buried it. Once the scarp slope stabilized, the next soil began to form on the colluvial wedge and was, itself, displaced by faulting and buried by scarp colluviation. After the second event, slope colluvium and the modern surface soil covered the fault. The lateral continuity of the buried soils and the fact that all three soils merge away from the fault support the interpretation of two discrete scarp-forming events separated by periods of relative stability.

The nature of the buried soils presented some problems of interpretation especially concerning apparent age. Both of the buried A-horizons appeared to be relatively fresh and not much different from the modern surface soil. According to Nelson (personal communication, 1983), it is unlikely that fresh-looking organic material would be preserved in a buried, well-drained, semi-arid terrestrial environment for more than a few thousand years. Very little well-preserved organic material has been found of early Holocene age and virtually none of late Pleistocene age (Nelson, personal communication, 1983). This fact, coupled with the excellent state of preservation, suggested the buried A-horizons were probably less than five thousand years old.

The apparent youthfulness of the buried A-horizons, however, was contradicted by their association with textural B-horizons. This association suggested a much greater time span would have been required for soil development, perhaps 10,000 years or more. The evidence appeared to be in conflict. Deposition of loess against the west-facing scarps by prevailing westerly winds, however, offers a possible explanation. Clay- and silt-rich loess derived from terrain to the west was deposited against the scarp after the slope had begun to reach equilibrium. This material formed an incipient B-horizon on which the overlying A-horizon developed. Influx of loess may accelerate the formation of a B-horizon giving the appearance of greater antiquity, especially in soils less than about 125,000 years old (Colman, 1982; Shroba and Birkeland, 1983; Sullivan and others, 1988). This interpretation seems to explain the contradictions regarding soil development observed in the Lester Ranch trench.

The Lester Ranch trench was not deep enough to fully expose correlative strath-terrace deposits on the downthrown block or the complete vertical sequence of colluvial wedges and buried soils adjacent to the fault. Attempts to dig deeper by hand were unsuccessful due to the high ground water in the area.

Three radiocarbon samples were taken from the base of the modern A-horizon, and one each from the two buried soils. A laboratory age of about 2,800 yr B.P. was obtained from the base of the modern soil. Laboratory ages of about 4,200 and 4,800 yr B.P. were obtained from the intermediate and lowest buried A-horizons, respectively (appendix II).

Interpretation: Two surface-faulting events, highlighted by tectonically-stacked colluvial wedges and buried organic soils, were exposed in the Lester Ranch trench. Estimates of total net vertical tectonic displacement from scarp-profile data range from 15.1 to 16.7 feet (4.6 to 5.1 m; table 2). Surface offset, stratigraphic offset, and geometry of colluvial wedges suggest single-event vertical tectonic displacements of 4.3 to 10.2 feet (1.3 to 3.1 m; table 6).

Lester Ranch South Trench

The Lester Ranch South trench was excavated in 1984 as a follow-up to the 1983 trench across the same scarp. High ground-water levels in 1983 precluded complete exposure of correlative strath-terrace alluvium and scarp-derived colluvial wedges on the downthrown side of the scarp. Some doubt remained as to the number of surface-faulting events recorded by colluvial-wedge stratigraphy. Consequently, a new trench was located about 820 feet (250 m) to the south (S½ section 24, T. 13 N., R. 119 W.) in a relatively well-drained area overlooking the confluence of the Willow Creek and La Chapelle valleys (figure 24 and plate I). The geologic setting of the 1984 site was similar to the 1983 site. It was believed the clarity of the 1983 exposure could be repeated at a well-drained site allowing complete exposure of fault-related stratigraphy on the downthrown block.

The scarp at the trench site ranges from about 13 to 18 feet (4 to 5.5 m) high based on projection of the lower terrace surface across the fault plane(s). The upper surface has been largely destroyed by erosion. Maximum scarp angle is 20.5 degrees. The trench, oriented in a N. 84° W. direction, was 115 feet (35 m) long and 12.5 feet (3.8 m) deep at its maximum. Seven radiocarbon samples were obtained and dated from this trench. One soil profile at station 22 (plate II) was also described and sampled.

Pre-fault stratigraphy: The Lester Ranch South trench (plate II) exposed a section of Wasatch Formation bedrock overlain by a patchy veneer of pre-terrace loess, Wasatch-derived colluvium/lag deposits, alluvial channel fill, and remnants of strath-terrace alluvium. Proximity to the La Chapelle and Willow Creek valley slopes, however, resulted in partial stripping of the terrace alluvium from the bedrock surface on the upthrown fault block. A thicker section of alluvium, part of the original terrace deposit, is preserved on the downthrown block. A soil characterized by a well-defined A-horizon and Stage III calcium carbonate developed across the original undisplaced terrace surface and was preserved on top of the alluvium in the downthrown block.

A number of units (1A through 1R) in the Wasatch Formation were defined based on lithology, color, and stratigraphic relationships. Attempts to correlate bedrock units from the upthrown to downthrown blocks were unsuccessful. Accordingly, mappable units on the upthrown block are designated by letters A through I and on the downthrown block by J through R. The apparent lack of correlation may be related to partial

Figure 36. *View of the Lester Ranch fault and tectonically stacked colluvial wedges and buried soils exposed in the Lester Ranch trench. The original surface soil is visible near the bottom of the trench and is overlain by a colluvial wedge and resident soil. A second colluvial wedge capped by the modern soil is present in the upper part of the exposure. Colluvial wedges and buried soils provide evidence of two surface faulting events. Flags on string are one meter apart.*

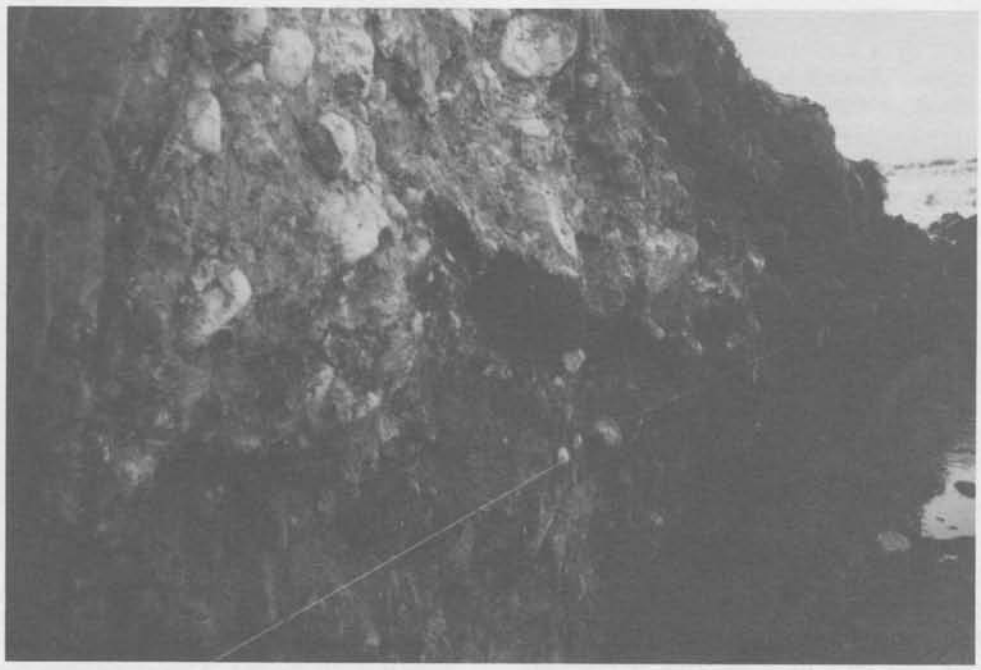

Figure 37. *View to the west away from the fault exposed in the Lester Ranch trench. Colluvial wedges thin and pinch out away from the fault. Soils, defining the upper and lower boundaries of the colluvial wedges, merge away from the fault. Note ground water in the bottom of the trench. Flags on string are one meter apart.*

erosion of bedrock on the upthrown block and the lenticular nature of Wasatch sediments. It is conceivable, but not likely, that large vertical displacements in bedrock exceeding the throw in terrace alluvium could account for the apparent lack of correlation.

Two interesting features were noted in the Wasatch Formation on the upthrown block. First, apparent pedogenic structure in unit 1E suggests Wasatch bedrock was subaerially exposed for a period of time during its depositional history. Secondly, this period of depositional stability was interrupted by channeling, in-filling, and soft sediment deformation represented by units 1A and 1B. These features are believed to be contemporaneous with Wasatch deposition because no Uinta Mountain Group detritus characteristic of younger Quaternary-age units is present.

Structure and post-fault stratigraphy: Unlike the single fault plane exposed in the Lester Ranch trench, faulting exposed in the south trench was complex (figure 38). At least three distinct fault planes were recognized along with several minor faults and a zone of intense shearing in bedrock. The main fault plane (figure 39) strikes N. 8-10° E. and dips to the west at 80-83° and could be traced to within 3.3 feet (1.0 meter) of the ground surface. Other fault planes showed evidence of overturning or overtoppling to the west due to slumping and gravitational creep along the free face following surface rupture.

Fault-related stratigraphy was also far more complex than in the original Lester Ranch trench, although a generally similar picture of surface faulting and colluviation emerged (figure 40). Original surface displacement along the main fault and secondary faults displaced the Wasatch Formation, overlying terrace deposits and surface soil horizons. An A-horizon, developed on the original terrace surface and preserved on the downthrown block, was laboratory dated at about 4,800 yr B.P. (appendix II). The free face degraded by a combination of slumping and scarp-derived colluviation. A well-defined slump block and crown scarp were defined on the upthrown block. The basal portion of the slump was marked by a distinct slip surface cutting into the underlying bedrock units. Portions of the slump block and slip surface apparently were preserved between the secondary fault planes west of the main fault. The location of the toe of the slump, however, was unclear.

The surface soil on the downthrown block was buried by a colluvial wedge largely derived from terrace alluvium on the upthrown surface. Stabilization of the scarp-derived colluvial wedge allowed a new soil to form across the degraded scarp. Two soil horizons, an A and A/B(?), were mapped on top of the original colluvial wedge. It is unclear, based on stratigraphic relationships, whether these horizons are part of the same profile or are two separate profiles separated by a storm or possibly a small surface-faulting event. The laboratory radiometric age of the upper horizon was about 3,000 yr B.P. A sample from the lower horizon(s) yielded a laboratory age of about 3,700 to 3,800 yr B.P., suggesting the horizons represent either different soils or different ages within the same soil. The intimate relationship between the horizons and lack of a discrete intervening lithostratigraphic unit argues against a major surface-faulting event. It is plausible that both horizons are part of the same soil, and the difference in ages reflects the mean residence time for the soil.

Following development of the soil on the first colluvial wedge, a second surface-faulting event occurred. This event displaced the base of the slump block along both the main and secondary faults. A second colluvial wedge formed burying the soil on top of the first scarp-derived colluvial wedge. Material incorporated in the second colluvial wedge was derived from both terrace alluvium and Wasatch bedrock exposed in the free face of the scarp. The modern surface soil profile developed on the tectonically-derived colluvial wedge, slope colluvium, and remnants of the original terrace deposit preserved on the upthrown block. The radiometric age of the base of the modern A-horizon ranges between about 1,300 and 1,600 yr B.P.

Interpretation: The Lester Ranch South trench shows evidence of two surface-faulting events. Displacement along multiple

Figure 38. Fault zone exposed in the south wall of the Lester Ranch South trench near stations 17-18. The master fault plane is visible along the left side of the photo. Wasatch Formation bedrock to the right of the plane is highly sheared. A low-angle shear plane, possibly related to a pre-existing slump block, is visible in the upper part of the photo. Note penny for scale.

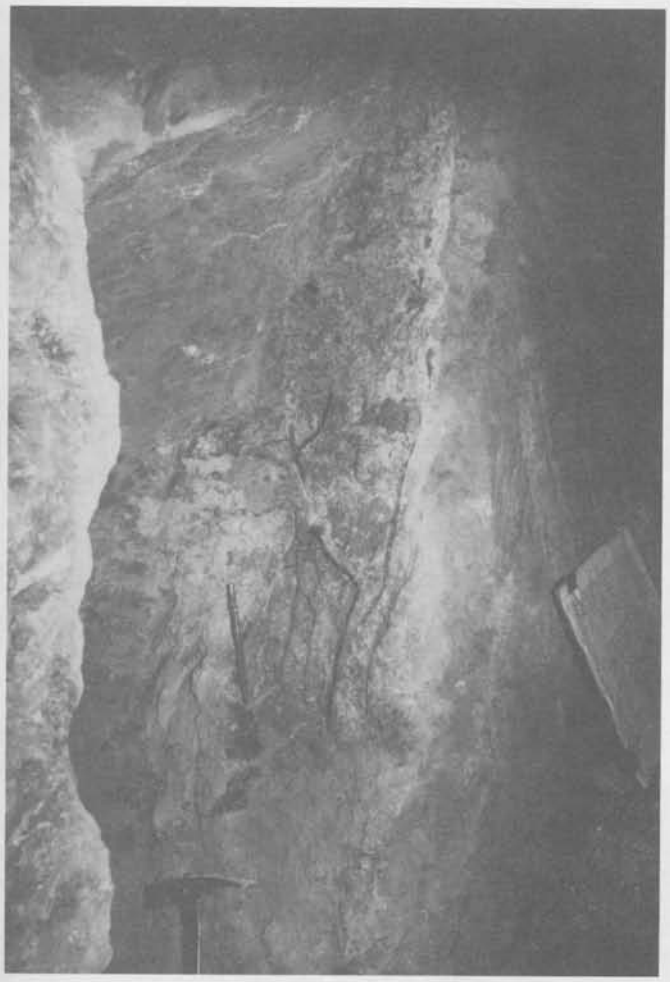

Figure 39. View of an excavation along the master fault plane in the north wall of the Lester Ranch trench. No slickensides were found along sheared surfaces. Notice rootlets preferentially growing along shear planes.

Figure 40. View to the west away from the fault zone exposed in the Lester Ranch South trench. Two tectonically stacked colluvial wedges separated by a buried A-horizon are clearly visible.

fault planes effectively precludes estimates of vertical displacement per event based on colluvial-wedge stratigraphy. Estimates of net vertical tectonic displacements for each event from geologic data and surface offsets range from 6.6 to 9.5 feet (2.0 to 2.9 m; table 6).

Austin Reservoir Scarp

The Austin Reservoir scarp (figure 41) forms the next right en echelon segment of the fault zone (figure 24 and plate I). Austin Reservoir Dam, a small earthen embankment, was built on the scarp where it crosses the stream valley. Presumably, faulting offset the channel and formed a natural dam which was subsequently breached and later rebuilt and enlarged by local ranchers. The fault displaces bedrock of the Wasatch Formation, strikes N. 15° W. to due north, and measures 1.3 miles (2.1 km) in length. North of Austin Reservoir the scarp is an anti-slope feature; south of the reservoir it is synslope.

The Austin Reservoir scarp provides one of the few "natural" subsurface exposures in the project area. Irrigation ditches constructed to replenish the reservoir have been allowed to spill over the scarp producing gullies several feet deep. The scarp-forming fault, scarp-derived colluvial wedges, buried organic material and a deep fissure on the downthrown side of the fault are all visible in a remarkable exposure in the northern wall of one of the ditches.

Austin Reservoir Irrigation Ditch

The fault which produced the Austin Reservoir scarp (figure 24 and plates I and III) is exposed in the irregular wall of an irrigation ditch eroded across the scarp. This exposure was

Figure 41. View to the southeast across Austin Reservoir showing the scarp dying out to the south (right). The Austin Reservoir fault is exposed in the two gully-like irrigation ditchs in section 36, T. 13 N., R. 119 W. The fault exposure in the southern ditch was logged as part of this study.

logged on a reconnaissance level as part of 1983 field studies but was not sampled for radiometric dating. Additional logging was performed and samples of organic soils for radiometric dating were collected in 1984. Only one age, however, was obtained from the base of the modern A-horizon on the upthrown block.

The irrigation ditch exposure is located in the W½ section 36, T. 13 N., R. 119 W. (figure 24 and plate I). The fault and related stratigraphy is exposed in the north wall of the ditch. The south wall is obscured by a slump block and colluvium.

Pre-fault stratigraphy: Claystones of the Wasatch Formation overlain by colluvium are exposed in the ditch wall. For the most part, primary bedrock sedimentary features have been obliterated by shearing. The colluvium consists of 20-45 percent gravels derived from Uinta Mountain Group and Wasatch lithologies in a sandy to silty clay matrix. The original pre-fault surface soil is preserved in the exposure.

Structure and post-fault stratigraphy: The Austin Reservoir ditch is a unique exposure in the project area (figure 42) because the fault is clearly visible and can be traced into bedrock of the Wasatch Formation. Maximum vertical throw on the bedrock surface is approximately 5 feet (1.5 m) or roughly the estimated height of the surface scarp. Unfortunately, bedrock on either side of the fault is badly sheared and distorted, preventing correlation of bedrock units across the fault.

The fault plane strikes N. 13° W. and dips 53° to the southwest. Near the top of the exposure, the fault plane appears to steepen to a vertical or slightly overturned position probably as the result of gravitational creep and/or overtoppling of the scarp free face. Radiating, open fissures in bedrock on the upthrown side of the fault suggest overtoppling as a likely mechanism. No slickensides were found on the fault plane.

A remarkable stratigraphic sequence is preserved on the downthrown block west of the fault plane. The pre-fault A-horizon developed on colluvium mantling the bedrock surface was displaced downward and subsequently buried by colluvium derived from the free face of the scarp. Back-tilting and/or a small antithetic fault caused development of a synform trough adjacent to the fault plane. Both the displaced A-horizon and overlying colluvial wedge show the effects of warping and back-tilting. Secondary ground cracking produced a 4.9 foot (1.5 m) deep fissure about 6.6 feet (2 m) to the west of the fault. Loess and modern A-horizon material have subsequently infilled both the scarp face and the fissure.

A second buried A-horizon and colluvial wedge indicate a second surface-faulting event. A sample obtained from the base of the A-horizon on the upthrown side of the fault yielded a radiocarbon age of about 800 yr B.P. (appendix II).

Interpretation: The Austin Reservoir scarp records two surface-faulting events, each producing vertical displacements ranging from 2.0 to 6.6 feet (0.6 to 2.0 m; table 6). The age of faulting is interpreted to be late Holocene based on the single laboratory radiocarbon age and the virtually unmodified buried A-horizon preserved adjacent to the fault.

Sulphur Creek Scarp

The Sulphur Creek scarp, 2.7 miles (4.4 km) long, is a complex of at least three right en echelon scarps in the central part of the fault zone (figure 24 and plate I). Near its north end, the Sulphur Creek scarp dies out in terrace alluvium, although warping of the terrace surface is evident for some distance beyond disappearance of the actual scarp (figure 43). The south end of the scarp is terminated by a post-fault landslide complex. The abrupt termination of the scarp by landsliding suggests

Figure 42. View of the Austin Reservoir fault exposed in the irregular wall of an irrigation ditch in section 36, T. 13 N., R. 119 W. The lowermost buried soil (unit 3A) and overlying colluvial wedge (unit 4) are visible to the left of the fault-produced step in Wasatch Formation bedrock. A second colluvial wedge is obscured by shadow. Note the in-filled fissure on the downthrown block. The thick organic soil on the downthrown block is believed to be related to accumulation of loess against the scarp.

Figure 43. View to the north along strike of the Sulphur Creek scarp near its northern end in section 35, T. 13 N., R. 119 W. Scarp dies out in foreground but warpage and back-tilting to the east (right) of the strath terrace is visible in the middle groud.

faulting continues to the south and is contiguous with the Deadman Creek and Big Burn scarps in the southern part of the fault zone.

The main Sulphur Creek scarp trends from N. 22° W. to N. 7° W. and ranges in height from 33+ feet (10+ m) near the southern end to <3 feet (<1 m) at the northern end before dying out in terrace alluvium. The scarp is notable because of its increasing height in a north to south direction and its pronounced effect on drainage. The northern quarter of the Sulphur Creek fault displaces gravel-cobble alluvium (figure 44); the southern three-quarters displaces claystone/shale bedrock of the Wasatch Formation (figure 45). In general, bedrock scarps appear more subdued and eroded than similar scarps in terrace gravels, indicating the importance of material as a control of scarp morphology.

The Sulphur Creek scarp offsets two stream drainages which once drained the area from southwest to northeast (figure 45 and plate I). Vertical fault movement blocked the drainages so that east-flowing streams impinge against the scarp, flow along the base of the scarp and eventually exit the area to the northwest.

Figure 44. Oblique aerial view of the northern Sulphur Creek scarp displacing strath-terrace deposits in the middle ground. View is to the northeast in section 35, T. 13 N., R. 119 W. A second right en echelon scarp is visible to the upper left. Austin dam was constructed on the scarp and was enlarged in 1985.

Figure 45. Oblique aerial view to the northeast of the Sulphur Creek scarp displacing bedrock of the Wasatch Formation (section 2, T. 12 N., R. 119 W.). The pond at right-center was formed by blockage of a stream channel which originally flowed to the east and joined the larger drainage near the top of the picture.

Sag ponds mark the position of former channels on the downthrown side of the scarp, and the displaced channel thalwegs are visible on the upthrown block.

Several other scarps and lineaments were noted in the vicinity of the Sulphur Creek scarp. The most important of these is a series of down-to-the-east antithetic scarps striking about N. 20° W. (figure 24 and plate I). Displacements are considerably smaller, generally less than 3 feet (1 m), than on the main part of the Bear River fault zone. Antithetic scarps, however, can be traced through terrace deposits and Wasatch Formation bedrock for distances of over 1.8 miles (2.9 km). One of the longest antithetic scarps splits from the Sulphur Creek scarp near its north end in section 35, T. 13 N., R. 119 W.

A graben-like structure and associated air-photo lineament are present about 1.2 miles (1.9 km) west of the Sulphur Creek scarp in sections 9, 10, and 15, T. 12 N., R. 119 W. The graben and lineament are believed to be related to antithetic movement resulting from displacement in the main part of the fault zone (plate I). These features trend N. 18-28° W. and show clear evidence of surface displacement although substantially less than on the Sulphur Creek scarp.

Sulphur Creek Trench

The Sulphur Creek trench was excavated in 1984 in the SE¼SE¼ section 35, T. 13 N., R. 119 W. (plate I). The trench site was selected because of the well-defined, simple nature of the scarp and the apparent presence of displaced strath-terrace deposits similar to the Lester Ranch sites (figure 46). The trench was oriented in a N. 89° W. direction and was 85 feet (26 m) long. Maximum trench depth was 15.1 feet (4.6 m) near station 15. Seven radiocarbon samples were obtained and dated from the Sulphur Creek trench. A single soil profile was described in the trench between stations 15 and 16.

The northern end of the scarp in the vicinity of the trench site parallels the eastern edge of a strath terrace and is anti-slope in aspect. The anti-slope aspect complicates estimates of scarp height and surface displacements based on scarp profile measurements. Using the surface uphill (west) of the scarp, the scarp appears to range from about 15.1 to 18.4 feet (4.6 to 5.6 m) in height. The effect of localized back-tilting and graben formation cannot be accurately estimated. Maximum scarp angle is 15 degrees.

Pre-fault stratigraphy: Variegated claystone, siltstone, and sandstone bedrock of the Wasatch Formation was exposed in the upthrown fault block (plate III) and was overlain by remnants of gravel-cobble terrace alluvium. It was unclear whether this material represented in-place alluvium or colluvial material transported downslope from the terrace surface to the west. A colluvial origin seems to be a likely interpretation.

The Sulphur Creek trench presents certain difficulties in interpretation mainly because the trench on the downthrown side of the scarp did not reach either bedrock or material that could be unequivocally identified as alluvium/colluvium overlying bedrock. Consequently, several interpretations are possible. The interpretation presented on the trench log and discussed below makes use of available data, including radiometric dating and comparison to fault histories developed from other trenches in the project area.

The key question is the origin of the cobbly deposit (unit 2), overlying fine-grained sediments (unit 3) and the buried soil (unit 4A - 4C). One interpretation suggests that these materials represent the original pre-fault alluvial/colluvial material and resident soil overlying bedrock. The alternative interpretation is

Figure 46. View to the east of the Sulphur Creek scarp and trench in section 35, T. 13 N., R. 119 W. The scarp in this area is anti-slope in aspect.

that these deposits are tectonically derived and the soil developed on a colluvial wedge in a sag pond environment. The latter interpretation, as discussed below, is preferred.

Structure and post-fault stratigraphy: The Sulphur Creek trench exposed several small faults and shear zones in the upthrown block. The main fault zone is expressed as a truncation of bedrock in an abrupt downward step from east to west across the scarp. The fault zone itself, however, was not exposed because the downthrown bedrock surface was not uncovered despite the 15+ foot (4+ meter) depth of the trench. Shearing in bedrock is difficult to detect in Wasatch claystones without stratigraphic markers. Several of the smaller faults in the upthrown block dip to the east and appear to have a high-angle, reverse sense of displacement. This apparent reverse orientation is attributed to post-fault mass movement along the scarp free face and overtoppling of coherent bedrock blocks.

The lowermost stratigraphic unit (unit 2) exposed in the downthrown block is a sandy gravel-cobble material composed of Uinta Mountain quartzites. This unit was examined carefully for evidence of primary fluvial stratification or other features that would unequivocally correlate it with the original terrace alluvium. No such features were found and the lack of any internal sorting implies the unit is of colluvial origin. The overlying fine-grained unit and resident soil are equally puzzling. If the underlying gravel-cobble unit is part of the original in-place terrace deposit, then the fine-grained unit must be overbank material and/or a cap of loess deposited prior to faulting. If the coarse unit is colluvium derived from the original strath terrace to the west, the overlying fine-grained material is a combination of slopewash and loess. Neither interpretation is particularly satisfying.

The A-horizon of the soil developed on top of the fine-grained unit (unit 3) is the most highly organic of any soil encountered in the project area (figure 47). This seems anomalous considering the topographic position and well-drained nature of the unfaulted terrace surface. The most plausible explanation suggests the cobble unit is part of a scarp-derived colluvial wedge associated with a surface-faulting event. The overlying fine-grained unit is sag-pond fill, and the organic-rich soil was formed in a poorly drained sag-pond environment. This interpretation has some important ramifications concerning vertical tectonic displacements as discussed later.

Samples of the buried organic A-horizon yielded laboratory ages of about 3,900 to 4,000 yr B.P. (appendix II). Following formation of this soil, a second surface-faulting event displaced it and a second colluvial wedge formed. Parts of the cobble colluvium and overlying organic soil toppled off the free face of the scarp within a short time of surface rupture, perhaps a few seconds to several hours, and became incorporated in the colluvial wedge at the base of the free face as illustrated in figure 48. Discontinuous pods of soil resting on top of the intact organic A-horizon, unit 5A, yielded laboratory ages of about 4,100 to 4,200 yr B.P. The discontinuous pods of soil, therefore, are part of the original soil developed across the pre-existing scarp and sag pond prior to the second surface-faulting event.

Units 6 and 7 represent colluviation from the slope uphill of the scarp and degradation of the Wasatch Formation bedrock in the free face of the scarp, respectively (figure 49). The tongue of slope colluvium, unit 6, was probably deposited directly on top of the organic A-horizon as the result of localized back-tilting into the scarp. Organic material obtained from this colluvial tongue was laboratory dated at about 4,200 yr B.P. The massive wedge of plastic, Wasatch-derived clay (unit 7) forms the main

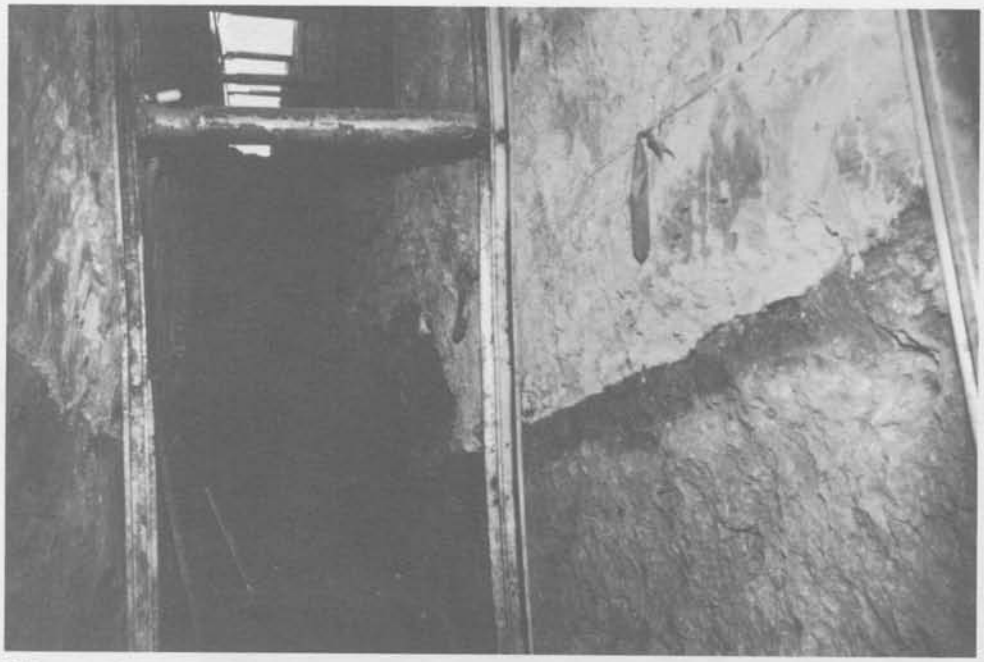

Figure 47. View of highly organic A-horizon (unit 4A) developed on fine-grained sag-pond sediments (unit 3) in the Sulphur Creek trench. Scarp colluvium (unit 7) derived from the Wasatch Formation, exposed in the free face, overlies the buried A-horizon. Back-tilting of the soil horizon into the fault is clearly visible in this photo. Flags on string are one meter apart.

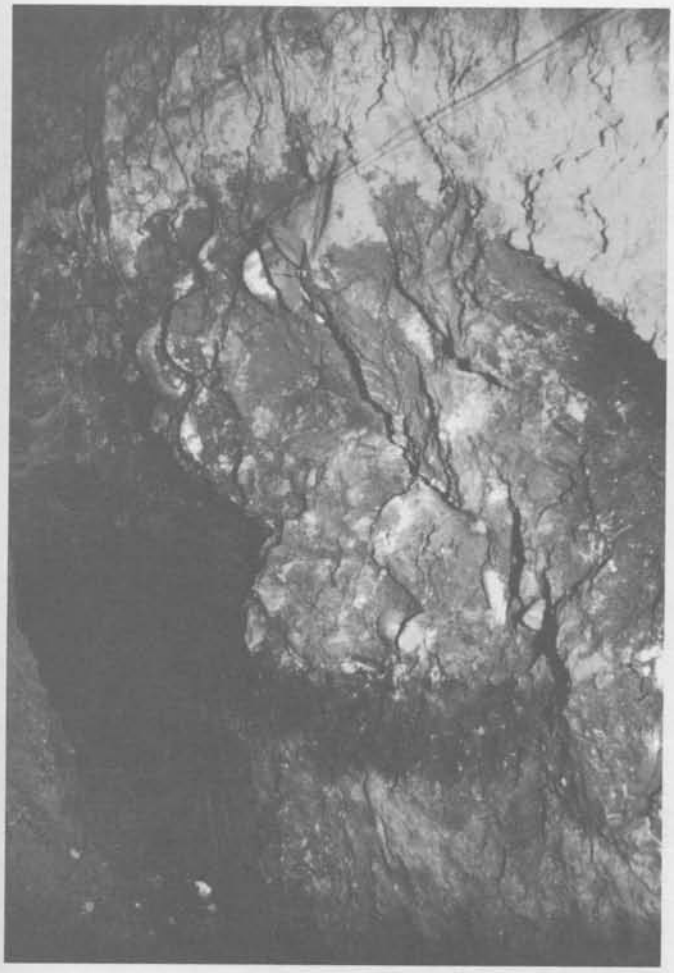

Figure 48. Block of A-horizon (unit 5A) and colluvium (unit 5B) resting unconformably on buried A-horizon (unit 4A). Units 4A and 5A are correlative. Units 5A and 5B toppled off the free face within a short time of a surface event, resulting in the angular, discordant relationship depicted in this photo.

Figure 49. Interfingering of slope colluvium (unit 6) transported from uphill to the right with scarp colluvium (unit 7) derived from the scarp free face to the left. Both units were deposited across the surface of the down-faulted soil (unit 4A).

body of the scarp-derived colluvial wedge. A second tongue of slope colluvium (unit 9) from uphill to the west interfingers with the Wasatch-derived scarp colluvium.

A small remnant of a buried A-horizon (unit 8) was noted on top of the basal Wasatch-derived colluvial wedge suggesting a period of stability and an unconformity between unit 7 and units 9/10. The possibility that this unconformity represents another surface-faulting event was considered but discarded because other characteristic evidence of surface rupture is absent in the trench and timing of postulated surface rupture is inconsistent with other trenches. Unfortunately, the potential significance of this soil was not recognized at the time of logging, and no radiocarbon age was obtained.

Units 9 and 10 represent slope colluviation from the west and the continued degradation of the scarp free face. Overtoppling of coherent bedrock blocks on the scarp caused open fissures to develop behind the free face. These fissures were filled by both bedrock-derived material and colluvium. Slope colluviation and development of the modern surface soil across the scarp represent the final stages of scarp history. As in other trenches, loess appears to have been deposited against the scarp, especially near the west end of the trench. Laboratory ages obtained from the modern A-horizon on the scarp slope range from about 3,000 to 3,800 yr B.P. (appendix II). The wide range in ages may reflect the mean residence time of the surface soil or the soil forming period represented by unit 13 plus unit 9 discussed in the preceding paragraph.

Interpretation: The Sulphur Creek trench shows evidence of one to three surface-faulting events depending on stratigraphic interpretation. The single surface-faulting event interpretation is based on the assumption that units 5, 7, and 10 are part of a single large colluvial wedge and that the organic-rich soil (unit 4A) developed on the pre-fault surface. At the other extreme, three surface-faulting events could be represented by three colluvial wedges and resident soils: (1) units 2, 3, and 4, (2) units

7 and 8, and (3) units 10 and 13. The preferred interpretation, based on stratigraphy and dating, is that two surface-faulting events separated by the organic soil horizon are recorded.

The laboratory age of about 3,800 yr B.P. obtained from the base of the modern A-horizon (unit 13B) on the scarp slope is inconsistent with trench stratigraphy. This laboratory age is fundamentally equivalent to laboratory ages from the buried A-horizon, unit 4A, 4.9 feet (1.5 m) deeper in the trench. An error in sampling, laboratory dating, or reporting could account for the apparent problem. As an alternative explanation, it is conceivable that remnants of the pre-fault surface soil (equivalent to unit 4A) from the upper block were incorporated into the modern surface soil thus yielding a similar laboratory age.

Estimates of single-event net vertical tectonic displacements range from 8.2 to 23.6 feet (2.5 to 7.2 m; table 6). Uncertainty is increased by the anti-slope nature of the scarp and difficulties in stratigraphic interpretation. The maximum single-event displacements estimated from the Sulphur Creek trench, however, are consistent with apparent scarp heights further to the south. An important question is whether apparent scarp heights were formed by two events or more than two. The Sulphur Creek trench does not provide a unique solution.

Deadman Creek Lineament

Between the south end of the Sulphur Creek scarp and the Deadman Creek lineament, evidence of late Quaternary faulting is obscured by late Holocene to historic landsliding in weak Wasatch Formation bedrock and overlying surficial deposits. The recency and complexity of landsliding makes it virtually impossible to trace late Quaternary faults through the area or to draw conclusions about the causes of mass movement. No evidence indicates that landsliding was triggered by surface-fault rupture or strong ground shaking. Landsliding, whatever the cause, probably postdates faulting because of the apparent absence of late Quaternary tectonic scarps in the area. The continuity of normal faulting in the subsurface is confirmed, however, by reflection seismic data and interpretation of normal faulting (Hay, personal communication, 1987) in Exxon's Mill Creek Federal No. 1 well (section 27, T. 3 N., R. 10 E.).

South of the Mill Creek floodplain (sections 3 and 10, T. 2 N., R. 10 E.) a distinct drainage lineament along Deadman Creek marks the inferred position of the Bear River fault zone (figure 24 and plate I). The lineament can be traced from the Mill Creek floodplain to a point 2.2 miles (3.5 km) to the south. At the south end of the lineament, Deadman Creek changes course abruptly from N. 5° W. to N. 30° E. Aside from the linear nature of the drainage, no geomorphic evidence of late Quaternary faulting could be identified. The spatial relationship of this lineament, however, to the Deadman Creek and Big Burn scarps to the south, both of unequivocal tectonic origin, argues circumstantially for a tectonic origin. A short (0.4 mile; 0.6 km) lineament north of the Mill Creek floodplain (section 34, T. 3 N., R. 10 E.) appears to be a northern continuation of the Deadman Creek lineament. A second lineament, 0.4 mile (0.6 km) long, parallels the main Deadman Creek lineament to the west.

Deadman Creek Scarp

The Deadman Creek fault, 0.5 miles (0.8 km) southwest of the Deadman Creek lineament, displaces Pinedale glacial deposits on the east side of the East Fork, Bear River Valley and can be traced 2.2 miles (3.6 km) along a strike ranging from N. 22° W. to almost due north. Scarp heights and angles are difficult to estimate due to the synslope position of the scarp on steep, wooded slopes. Near the northern end, however, the fault displaces Holocene floodplain alluvium along the channel of Deadman Creek and causes a local reversal of drainage. Scarp height in alluvium appears to be about 10 to 13 feet (3 to 4 m). A large sag pond is present in the former channel of Deadman Creek west of the scarp.

Big Burn Scarp

The Deadman Creek fault dies out rapidly to the south as displacement is taken up by the Big Burn fault located about 0.4 miles (0.6 km) to the southwest in a right en echelon pattern (figure 24 and plate I). The Big Burn scarp, named after a major forest fire in 1980, trends N. 17° W. in Pinedale till and outwash along the East Fork of the Bear River. The scarp is the most impressive late Quaternary tectonic feature in the project area with a height of 49+ feet (15+ m) and maximum scarp angles locally exceeding 30° (figure 50). From the ground, the scarp forms an imposing rampart traceable for 2 miles (3.2 km) from near the East Fork of the Bear River over the crest and down the reverse slope of the western Pinedale lateral moraine in East Fork Valley (figures 51 and 52). A linear depression apparently formed by ground cracking and subsidence parallels the base of the scarp from the crest of the moraine northward. The main scarp splits into two subsidiary scarps where it crosses the moraine crest. At the south end, the Big Burn scarp appears to merge or terminate abruptly against a second family of scarps trending N. 40-50° E., sub-parallel to the North Flank fault about 1.3 miles (2.1 km) to the south (figure 24 and plate I).

Big Burn Trench

A trench was excavated across the Big Burn scarp in the NE¼W¼ section 27, T. 2 N., R. 10 E. (figure 24 and plate I). This site was selected because of a closed, dry depression at the base of the scarp (figure 53). Recurrent movements on the fault, it was postulated, would be recorded by alternate scarp colluviation and sag-pond sedimentation. Trench excavation proved difficult, however, due to the loose, non-cohesive nature of the tills and derivative colluvium. Consequently, the depth of excavation was limited, and one trench wall was sloped back to provide a safe working environment. The height and steepness of the scarp prevented the back-hoe from creating a continuous exposure across the entire scarp. The upper end of the trench reached only to about the mid-point of the scarp slope.

The scarp at the trench site is about 40.4 feet (12.3 m) high and has a maximum scarp angle of 31 degrees. The trench, about 121 feet (37 m) long, was oriented in a N. 82° E. direction and reached a maximum depth of 7.5 feet (2.3 m).

Figure 50. Oblique aerial view to the northeast of the Big Burn scarp running from upper to lower right across photo (section 27, T. 2 N., R. 29 E.). Scarp is 12-15 meters high. Note vehicles for scale.

Figure 51. Oblique aerial view to the south showing the Big Burn scarp (arrow) displacing a lateral moraine on the west (right) side of the East Fork, Bear River (south half, T. 2 N., R. 10 E.). Discordant set of scarps (arrows) sub-paralleling the North Flank fault are visible in shadow beyond the moraine crest.

Figure 52. Low-sun-angle view of the southern Big Burn scarp (synslope) on the west slope of the lateral moraine shown in figure 51 (section 34, T. 2 N., R. 10 E.

Figure 53. View of the Big Burn scarp and trench site. Lower part of the trench was excavated through a closed, dry sag pond. Due to caving, the south (right) wall was laid back.

Pre-fault stratigraphy: The Big Burn trench (plate IV) was excavated in glacial deposits of inferred Pinedale age. The bulk of the deposits in and near the trench site are inferred to be tills based on surface morphology and limited exposures of in-place material. In general, the tills consist of a non-sorted, non-stratified mixture of cobbles and boulders in a silty to slightly clayey sand matrix.

Structure and post-fault stratigraphy: The Big Burn trench was simultaneously a disappointment and a significant exposure. The greatest disappointment was the lack of decipherable stratigraphic record in the sag pond at the base of the scarp and the inability to clearly expose the fault on the scarp itself. The sag pond contained fine-grained deposits derived from surrounding slopes but no evidence of scarp colluviation or appreciable organic soil development. A peaty A-horizon with detrital charcoal near its base, however, was present at the ground surface. Thin, discontinuous sedimentary layering within the sag-pond sediments suggested episodic sedimentation but could not be related to recurrent fault displacement.

The fault was poorly exposed in the extreme upper end of the trench. A zone of scattered, imbricate clasts separated till at the upper end of the trench from colluvial deposits further down the scarp slope. The depth of excavation and limited exposure east of the fault zone prevented a conclusive interpretation. Position of the imbricate zone near the mid-point of the scarp, however, is consistent with a fault interpretation.

Several significant features were found in the trench, considering the nature of the materials. Most important of these were remnants of buried A-horizons adjacent to the fault on the downthrown side (figure 54). One of these horizons (unit 7) formed a more or less continuous layer in a nearly horizontal position. A second, less continuous buried A-horizon (unit 9B) appeared to be resting on the first at a discordant angle. Several other pods and discontinuous layers of buried A-horizon material were also noted near the fault. No appreciable compositional difference existed between the various pods and layers suggesting they were all derived from the same soil. The discordant horizon appears to have toppled off the free face immediately after fault displacement and came to rest on the correlative A-horizon down-dropped by faulting.

Several discernible colluvial wedges derived either from free face colluviation and/or normal slope colluviation were noted in the lower part of the scarp. At the base of the scarp, colluvial material (units 4 and 9D) appears to have filled an open fissure probably produced at the time of faulting. This fissure fill coincides with the nearly continuous linear depression observed along the scarp base. No evidence was found to suggest the depression and in-filled sediments were related to post-faulting stream erosion and deposition. The depression and in-filling are the result of ground cracking and secondary deformation associated with surface-faulting. Two episodes of fissure in-filling are suggested by differences in composition of material and nearly vertical contacts. The location of fissures between the sag pond and the scarp slope may account for the lack of scarp colluviation in the depression. Colluvial material was intercepted by open fissures and filled them instead.

Radiocarbon samples were collected (1) from detrital charcoal at the base of the modern A-horizon in the sag pond area,

Figure 54. Buried A-horizon (unit 7) and pods of correlative soil (unit 9B) incorporated in a tectonically derived colluvial wedge (unit 9A) are visible in the north wall of the Big Burn trench. Flags on string are one meter apart.

(2) from modern A-horizon on the scarp slope, (3) from colluvium downslope of the inferred fault, and (4) from layers and pods of buried A-horizon adjacent to the fault near the upper end of the trench. Laboratory ages obtained from three samples of buried A-horizon material ranged from about 2,900 to 3,400 yr B.P. All of the buried soils were probably derived from a single, continuous soil developed on the scarp prior to the last fault event. A radiocarbon age of about 2,200 yr B.P. was obtained from scarp colluvium further downslope.

Radiocarbon ages of about 1,000 and 1,200 yr B.P. were obtained on detrital charcoal from the base of the modern A-horizon in the sag pond and from the modern A-horizon on the scarp slope, respectively. A radiocarbon age of about 800 yr B.P. was also obtained from modern colluvium associated with the surface soil.

Interpretation: The Big Burn trench shows clear evidence of a single surface-faulting event, but at least one other can be inferred on the basis of scarp height and colluvial stratigraphy. Single-event net vertical tectonic displacement appears to range from 12.8 to 20.7 feet (3.9 to 6.3 m; table 6).

Little Burn Scarps

At the southern end of the Big Burn scarp, the main north-south Bear River fault zone impinges on a discordant family of scarps trending N. 40-50° E. The angle of intersection between the two sets of scarps is about 70° and is remarkably abrupt. The northeast-trending scarps sub-parallel the trace of the North Flank fault before disappearing in younger deposits on the east side of Hayden Fork Valley. Scarp heights range from less than 3 feet (1 m) to apparently 100+ feet (30+ m) along the major scarp that marks the terminus of the Bear River fault zone. The fault associated with this scarp appears to displace a Bull Lake(?) lateral moraine based on relative position of the moraine crest on either side of the scarp. Two smaller scarps, termed the Little Burn scarps (figure 24 and plate I) after a small forest fire in the 1960s, exhibit a left-stepping en echelon pattern, scarp heights of 4.9 to 11.5 feet (1.5 to 3.5 m) and scarp angles ranging from 13.0 to 27.5 degrees.

Small-scale geologic mapping of the North Flank fault (Hintze, 1980) suggests these northeast-striking scarps are coincident with the Laramide North Flank fault. Air-photo interpretation for this study suggests, however, that the main trace of the North Flank fault actually lies about 1.3 miles (2.1 km) to the south. Preliminary 1:250,000 mapping by Bryant of the USGS (personal communication, 1984) is in agreement with this latter interpretation. Based on available mapping, the Little Burn scarps are not on the main trace of the North Flank fault. This interpretation must be qualified to the extent that the North Flank fault is poorly exposed and may comprise several imbricate planes which could extend north of the main trace.

Upper Little Burn Trench

The Upper Little Burn trench was excavated in 1984 across one of the two Little Burn scarps trending N. 55° E. on the downthrown block of the Big Burn scarp near its southern end (figure 24 and plate I). The trench site is located in the NE¼SE¼ section 34, T. 2 N., R. 10 E. on the northernmost of the two scarps 426 feet (130 m) west of the Big Burn scarp.

The site was selected to provide information on the age of discordant scarps and possible relationships to the Bear River fault zone and the North Flank fault. The trench was located in a left-stepping transition zone between two scarps. The uppermost (southern) scarp along the projection of the trench axis is about 2.6 feet (0.8 m) in height and exhibits a maximum slope angle of 11.5 degrees. The lowermost (northern) scarp is about 15.4 feet (4.7 m) high with a maximum slope angle of 24.5 degrees. The surface on which the scarps are located slopes to the north at 4.5°, and total surface offset is estimated to be about 17.7 feet (5.4 m). The trench, about 62 feet (19 m) long, was oriented in a N. 30° W. direction. Maximum depth was 5.9 feet (1.8 m). The loose nature of the glacial materials necessitated sloping the west wall back for safety. The east wall was maintained in a vertical position.

Pre-fault stratigraphy: Both of the smaller scarps are inferred to displace tills and overlying glaciofluvial deposits of probable kame-terrace origin. The age of these deposits has not been established. Location of the site inside (with respect to the main valley axis) a Bull Lake lateral moraine and outside the main Pinedale lateral moraine along the East Fork of the Bear River suggests the deposits are most likely of early Pinedale or Bull Lake age. The scarps cut a gently northward-sloping surface probably formed by ice-marginal meltwater between the main valley glacier and the lateral moraine to the west. The terrace-like surface has been partially dissected by modern drainage development.

The Upper Little Burn trench (plate IV) exposed moderately indurated till overlain by a sequence of meltwater-deposited sands and gravels. In general, the tills consisted of non-sorted, non-stratified clayey to silty sand with scattered gravels and cobbles. Color ranged from dull orange (2.5 YR 6/4; Munsell color notation) to dull reddish brown (2.5 YR 4/4) which contrasted sharply with overlying, lighter colored sands and gravels. The meltwater deposits included stratified, relatively clean, well-sorted sands, gravelly sands and sandy gravels. Distinct graded bedding was characteristic of the glaciofluvial units. The contact between the meltwater deposits and the underlying tills was irregular, but whether this irregularity is due to primary depositional processes or post-depositional deformation and displacement is unknown.

Structure and post-fault stratigraphy: Five major shear zones and several smaller features interpreted to be possible faults were noted in the trench. The complexity of deformation is attributed to step faulting in the en echelon transition zone between the two scarps. Total vertical tectonic displacement is manifested by a series of small step faults as the southern scarp dies out and the northern scarp reaches maximum displacement.

Individual faults showed little evidence of shearing due to the generally coarse-grained nature of the faulted deposits. Faults were recognized by: (1) lateral truncation of lithostratigraphic units, (2) lateral truncation of primary sedimentary features such as bedding and/or stratigraphic contacts, (3) loose, structureless zones, and (4) subvertical imbrication of clasts (figure 55). A large root system was noted in the fault zone mapped between stations 9 and 10, a feature common-

Figure 55. View of the east wall of the Upper Little Burn trench showing imbrication of clasts and roof penetration along loose zones created by shearing.

ly observed along fault/shear zones in unconsolidated deposits. Strongly imbricated clasts were observed in the large shear zone between stations 13 and 14 and near the upper end of the trench (station 17). Steps in the upper till (unit 1) surface mapped between station 2 and 9 may be related to faulting but, with a single exception at station 2, could not be traced into the overlying deposits. Back-tilting is apparent especially in glaciofluvial units near the southern end of the trench.

Surface displacements produced multiple zones of fissuring which were subsequently filled by loose sand (unit 4B) derived from the glaciofluvial deposits. Scarp-derived colluvial wedges (units 5 and 6) probably formed rapidly after surface displacements occurred due to the generally loose, non-cohesive nature of the faulted sediments, especially the glaciofluvial sands and gravels. In some cases, colluvial wedges could be associated with either early or late faulting events based on stratigraphic relationships. Colluvial-wedge material was also subdivided into proximal and distal facies (units 5A and 5B) where appropriate. Multiple step faults in the trench and the lack of well-defined zones of shearing complicate interpretation of fault history in the Upper Little Burn trench.

The colluvial wedge (unit 6B) mapped north of station 9 contained a pod of organic material interpreted to have been derived from the upthrown side of the fault. This pod was most likely part of the pre-fault A-horizon developed across the site. Fault rupture displaced the surface, and an intact block of soil fell off the free face of the scarp and was incorporated in the colluvial wedge. The amount of organic material in the soil was considered insufficient to provide a reliable age. Accordingly, no radiometric data are available from the Upper Little Burn trench which constrain ages of surface rupture.

Following the last surface rupture, normal slope colluviation produced a veneer of material across the scarp surface. A weak A/C soil profile is present across the slope, suggesting a mid- to late Holocene surface rupture consistent with other trenches in the project area.

Interpretation: The Upper Little Burn trench shows evidence of at least two surface-faulting events displacing tills and overlying glaciofluvial sediments in a complex en echelon transition zone between two adjacent fault scarps. The possibility that more than two events occurred cannot be discounted based on trench stratigraphy alone. No radiometric ages were obtained from the trench; thus ages of faulting must be inferred. The lack of strong soil profile development across the scarp suggests that surface ruptures occurred in late Holocene time and are consistent with surface displacements in the main Bear River fault zone. Total tectonic displacement estimated from scarp profiles (tables I-2 and I-3; in appendix I) and stratigraphic offset ranges from 6.4 to 14.4 feet (2.0 to 4.4 m) suggesting each of the two events produced surface offsets of 3.2 to 7.2 feet (1.0 to 2.2 m) per event (table 6). The location of the trench in the transition zone between two scarps and the possibility of more than two events, however, increases uncertainty in these estimates.

Lower Little Burn Trench

The Lower Little Burn trench was excavated across the eastward extension of the same scarp exposed in the Upper Little Burn trench (figure 24 and plate I). The trench site is located about 100 feet (30 m) west of the Big Burn fault trace on the floor of a flat-bottomed ravine formed by a kame terrace to the west and a Pinedale lateral moraine to the east (figure 56). The head of the ravine is defined by the Big Burn scarp trending N. 20° W. and a second escarpment trending N. 55° E. parallel and possibly related to the Little Burn scarps. The Lower Little Burn scarp at the trench site is approximately 4.9 to 6.6 feet (1.5 to 2.0 m) in height, based on offset of the ravine floor, and can be traced across the ravine as a subtle but recognizable break in slope. The scarp is inferred to extend eastward to an intersection with the Big Burn scarp. Maximum scarp angle at the trench site is 13.0 degrees.

The geomorphology of the intersection between the Big Burn and Little Burn scarps is remarkable because it appears to be almost entirely a function of tectonic deformation with little modification by fluvial or mass-wasting processes. No evidence of a live stream is present in the ravine, suggesting it was formed by tectonic deformation.

The trench was intended to examine the modest scarp in the ravine floor and to provide additional information on the discordant family of scarps paralleling the North Flank fault zone. The

Figure 56. Excavation of the Lower Little Burn trench in section 34, T. 2 N., R. 10 E. The Big Burn scarp is visible behind the trench site.

trench was oriented in a N. 58° W. direction, was 59 feet (18 m) long and 4.9 feet (1.5 m) deep at the deepest point. Two detrital charcoal samples were recovered for radiometric dating.

Pre-fault stratigraphy: The stratigraphy of the Lower Little Burn trench is similar to the upper trench (plate IV). Tills are overlain by glaciofluvial deposits. Both the tills and the overlying meltwater deposits may be correlative with deposits in the upper trench but no conclusive relationship could be established. The tills consisted of gravels and cobbles in a pale-reddish-orange (2.5 YR 7/4) to bright brown (2.5 YR 5/6) silty sand matrix. Color banding, very thin internal bedding and locally graded bedding suggested a mixed ice-deposited and meltwater-deposited origin. The overlying glaciofluvial deposits consisted almost entirely of moderately well-sorted silty sand with minor stratification and thin to very thin internal stratification at the south end of the trench.

A soil-forming period is inferred from the presence of clay films on sand grains in the till. No clay films, however, were present in the overlying glaciofluvial materials.

Structure and post-fault stratigraphy: Two faults, defined by zones of loose sand truncating till and overlying glaciofluvial deposits were noted in the trench. Both fault zones were ill-defined due to the coarse-grained nature of deposits. The northern fault, between stations 11 and 12, appeared to exhibit the greatest displacement. Two colluvial wedges, one overlying the other, were mapped on the downthrown side of the fault. The base of the lowermost wedge was not exposed in the trench. The southern fault, between stations 12 and 13, displaced the upper surface of the till 0.7+ feet (0.2+ m) but no distinct colluvial wedge was associated with it.

The colluvial wedges on the north side of the main fault were overlain by colluvium believed to be of slope origin. A large boulder about 3 feet (1 meter) in maximum dimension was present in the base of the unit but was dislodged during the trenching operation. This boulder probably rolled into place from steeper slopes to the east. Near the faults, slope colluvium was composed of about 75 percent sand and 25 percent silt. To the north away from the faults, the percentage of silt increased to 50 percent at the expense of sand-sized material. The lateral change in composition is depicted on the trench log. The increase in silt is interpreted to be the result of loess deposition against the scarp.

Fragments of detrital charcoal up to several millimeters in dimension were noted in unit 5B at the north end of the trench. Two samples of this charcoal were collected and dated by radiocarbon methods. A sample obtained from just above the contact with the underlying unit produced a laboratory age of about 4,100 yr B.P. The sample from a stratigraphically higher position produced a laboratory age of about 5,900 yr B.P. Neither age represents a stratigraphic time line; thus, the apparent inversion of ages has little significance. The enveloping deposit, however, must be younger than the minimum laboratory age of about 4,100 yr B.P. The underlying, scarp-derived colluvial wedges (units 3 and 4) must be older than the overlying unit (5) but not significantly so.

Interpretation: The Lower Little Burn trench disclosed evidence of two(?) surface-faulting events displacing tills and glaciofluvial deposits associated with Bull Lake and Pinedale glaciations. Age of latest surface rupture cannot be established because no geologic time lines (buried soils) were found within the trench. The colluvium (units 5A and 5B) overlying interpreted scarp-derived colluvial wedges contains detrital charcoal fragments with laboratory ages of about 5,900 and 4,100 yr B.P. If the age of the enveloping colluvial deposits is coeval to the laboratory charcoal ages, the surface-faulting events are pre-5,900 yr B.P. Alternatively, the colluvial deposits may be younger than the detrital charcoal and, if so, no minimum age can be placed on surface rupture. The mid-Holocene radiometric ages obtained from the colluvial deposits are generally consistent with estimates of latest surface rupture from other trenches in the Bear River fault zone. This would support the interpretation that the Little Burn scarps are mid to late-Holocene features and formed at the same time as the Big Burn scarp and the rest of the Bear River fault zone. Intimate association with the Big Burn scarp implies that rupture on the Little Burn scarps was simultaneous with surface rupture in the Bear River fault zone.

Tectonic displacements per event can be estimated from total

surface offset and/or colluvial-wedge stratigraphy. Assuming total vertical displacement of 2.6 to 4.6 feet (0.8 to 1.4 m; table 2) and two surface-faulting events, resulting tectonic displacement per event would be about 1.3 to 2.2 (0.4 to 0.7 m) per event. Assuming colluvial-wedge thickness represents approximately half the surface displacement for each event (Ostenaa, 1984), the two (?) successive wedges exposed in the trench were derived from surface displacements of 3.3 to 5.9 feet (1.0 and 1.8 m), respectively (table 6).

Fault Rupture Characteristics

Rupture Length

Data from this study indicate the Bear River fault zone has ruptured twice during the Holocene over a distance of at least 21 miles (34 km) along strike. Associated deformation represented by the short scarp in sections 10 and 15, T. 14 N., R. 118 W. increases apparent rupture length to at least 25 miles (40 km).

Net Vertical Tectonic Displacements

Mapping of the Bear River fault zone indicates scarp heights increase from north to south along the fault zone, reaching their maximum development near the south end where normal faults impinge on the Uinta Mountain block. Presumably, single-event displacements at the south end of the fault zone could be on the order of 49 to 65 feet (15-20 m), although the relative amounts of tectonic displacement versus secondary deformation are unknown. Moreover, it is conceivable that large scarps at the south end of the fault zone were produced by more than the two post-mid-Holocene events recorded in the northern portion of the Bear River fault zone.

Figure 57 shows alternative mechanisms which could produce increasing displacements from north to south along the Bear River fault zone. A trench excavated across scarps in the north-central part of the fault zone would show evidence of two surface-faulting events in all cases. I prefer the interpretation shown in figure 57B: multiple events with increasing rupture lengths to the north. Unfortunately, no data are available to characterize displacements associated with possible earlier events in the southern part of the fault zone. In any case, surface-faulting events probably nucleated in the southern part of the fault zone, at or near the intersection with the Uinta Mountain buttress, and propagated unidirectionally to the north.

Trench exposures indicate vertical tectonic displacements per event indeed increase from north to south, although probably not enough to account for total apparent surface displacements (49 to 100+ feet [15 to 30+ m]) at the south end of the fault zone. The Big Burn scarp and the major, northeast-striking scarps south of Lily Lake are so large as to defy exploration by conventional trenching methods. The number of events that formed these scarps and net vertical tectonic displacements are unknown. No direct evidence, other than the size of the scarps, suggests the scarps were formed by more than two events.

To the north, scarps in the Bear River fault zone decrease in height and ultimately disappear altogether. Part of the decrease in scarp height may be related to increasing amounts of oblique or strike-slip component of movement associated with change in strike of the underlying Darby-Hogsback ramp from almost due north to northeast. In spite of these problems, vertical tectonic displacements obtained from scarp profiles and trench stratigraphy in the central sector of the Bear River fault zone provide reasonable estimates for use in hazard assessment and are considered representative averages for the fault zone.

Table 2 summarizes total net vertical tectonic displacements calculated from scarp-profile data (appendix I). The range in values results from uncertainties in parameters used in the calculations (fault dip and surface-slope angle among others). Estimates of net vertical tectonic displacements per event based on total displacement divided by the number of surface-faulting events are presented in table 3. Tables 4 and 5 summarize estimates of displacement per event based on stratigraphic offsets, number of surface-faulting events, and colluvial-wedge geometry exposed in trenches. Single-event displacement estimates from scarp-profile data, stratigraphic offsets, and colluvial-wedge geometry are compared in table 6. For each scarp/trench, the range and mean of single-event displacements are tabulated.

Mean vertical displacements per event based on scarp profiles and trench exposures range from 6.9 to 16.7 feet (2.1 to 5.1 m; table 6). These values were obtained from sites in the main part of the fault zone and probably do not represent extreme values at the north and south ends. Vertical displacements per event range from a minimum of 2.0 feet (0.6 m) in the Austin

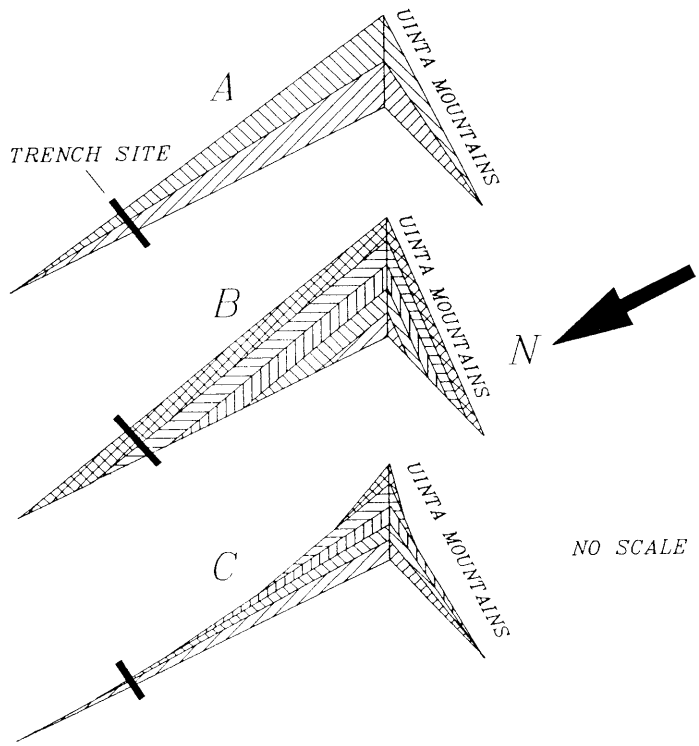

Figure 57. Models for increasing scarp height from north to south along the Bear River fault zone: (A) two events of increasing north to south displacement and equal rapture length; (B) multiple events with increasing rupture length; (C) multiple events with decreasing rupture lengths. In all cases, a trench excavated in the northern part of the fault zone would consistently show two surface faulting events.

Reservoir irrigation ditch exposure to a maximum of 23.6 feet (7.2 m) per event in the Sulphur Creek trench (table 6). The Austin Reservoir ditch exposure may be misleading because it is located near the southern end of the scarp where displacements are stepping over to the Sulphur Creek scarp.

Age of Movement and Recurrence Intervals

Ages of surface rupture and recurrence intervals for the Bear River fault zone were estimated using the following procedure:

1. The surface characteristics (rupture length and vertical tectonic displacement) of the main fault zone were defined by field mapping and scarp profiling.
2. Trenches excavated along the fault zone created interpretable exposures and provided materials for radiometric and relative age dating. Special emphasis was placed on defining stratigraphic units that would define individual fault displacements (colluvial wedges) and stratigraphic time lines (soils). Interpretations of trench stratigraphy defined the original pre-fault surface soil, subsequent soils formed on tectonically-derived colluvial wedges, and the modern unfaulted soil formed on the present-day scarp slope.
3. The ages of tectonically-buried and modern, unfaulted surface soils (stratigraphic time lines) were determined by radiometric methods. Laboratory radiometric ages were calendar calibrated according to the methods outlined earlier in the section on Radiocarbon and Amino Acid Racemization Ages.
4. Stratigraphic position and calendar-calibrated ages (± 2 sigma) of tectonically-buried and unfaulted modern soils were compared and correlated graphically between trench exposures along strike of the Bear River fault zone. Tectonically-buried and unfaulted surface soils were separated spatially in trench exposures by scarp-derived colluvial wedges. Spatial separation was accompanied in most cases by a temporal separation in soil-forming intervals caused by fault displacement and scarp colluviation. The gap in time between soil-forming periods defines a window during which the surface-faulting event must have occurred.
5. Fault-event windows were defined in each subsurface exposure along strike. The age of each surface-faulting event was constrained by correlative windows in soil forming intervals, providing a rational basis for establishing the ages of surface-rupture events and recurrence intervals. Significant differences in age of faulting along strike, indicating fault segmentation, would also become apparent.

Figure 58 presents stratigraphically significant ^{14}C age determinations (±1 sigma and ±2 sigma error bars) for each trench exposure from north to south along the Bear River fault zone. The relationship of ^{14}C ages to trench stratigraphy and correlations between trenches are presented on figure 59. Soil-forming intervals defined from trench stratigraphy and ^{14}C ages are depicted on figure 60. The gaps or "windows" in soil-forming intervals are caused by scarp degradation and development of colluvial wedges resulting from surface-faulting events. Figure 61 highlights windows between soil-forming intervals during which surface-faulting events must have occurred.

Hypothetically, the age of surface-faulting events can be determined by drawing a "best-fit" straight line through correlative fault-event windows. A straight line should fit cleanly through each window if surface rupture is truly contemporaneous in all exposures. Significant discrepancies in the temporal position of fault-event windows (>1,000 ^{14}C years) would indicate segmentation of the fault zone along strike. Relatively small discrepancies (<1,000 ^{14}C years), such as those apparent on figure 61, are attributable to uncertainties in apparent mean residence time (AMRT) ^{14}C ages of the soils and limitations of the radiocarbon method. Fault-scarp morphology and pattern of surface rupture can be used to assess whether or not continuity or segmentation is likely. In the case of the Bear River fault zone, continuity of surface rupture between trench exposures is indicated based on the pattern of surface faulting, scarp morphology, and geomorphic effects. No evidence was found to suggest the Bear River fault zone is segmented. Coherent surface rupture apparently occurred along the length of the fault zone between the Big Burn area and the La Chapelle trench in each of the past two events.

Inspection of figures 60 and 61 shows that straight lines representing surface-faulting events do not pass cleanly through correlative event windows defined by AMRT soil ages. Nevertheless, the age range for surface-faulting events can be constrained by correlative fault-event windows. The maximum age of the earliest event is constrained by AMRT ages of pre-fault surface soils in the Lester Ranch and Lester Ranch South trenches. The minimum age limit is defined by the AMRT age of the intermediate buried A-horizon in the La Chapelle trench. The earliest surface-faulting event, therefore, is interpreted to have occurred between 3,930 and 5,310 yr B.P. The mean of the age range is 4,620 yr B.P. Uncertainty in the age of the first event can be expressed as 4,620± 690 yr B.P. The mean value of 4,620 yr B.P. is used in recurrence and slip rate calculations.

The second and last surface-faulting event is interpreted to have occurred between 1,320 and 3,420 yr B.P. The maximum limit to the age range is constrained by AMRT ages of the base of the modern A-horizons in the Lester Ranch and the Sulphur Creek trenches. The minimum limit is defined by the AMRT age of the base of the modern A-horizon in the Big Burn trench. The mean of the range is 2,370 yr B.P., and uncertainty in the age of the last surface-faulting event can be expressed as 2,370 ± 1,050 yr B.P. The mean value of 2,370 yr B.P. is used in recurrence and slip-rate calculations.

The recurrence interval between the mean ages of the two surface-faulting events is about 2,250 years. Using the mean ages of the surface faulting, no surface-faulting event has occurred since about 2,370 yr B.P., suggesting the maximum recurrence interval is greater than about 2,370 years. Calculation of a minimum average recurrence interval is based on (1) the time between the mean ages of the two documented surface-faulting events (about 2,250 years) and (2) the minimum time between the mean age of the last documented event and the next future event (>2,370 years). The minimum average recurrence interval, therefore, is 2,310 years. Significant uncertainties in ages of movement and recurrence intervals result from the use of AMRT soil ages, limitations of the radiocarbon method, and the fact that only two surface-faulting events are available to establish recurrence intervals.

Soil residence time is not taken into account in the discussion above. According to Matthews (1980), the age of any geologic

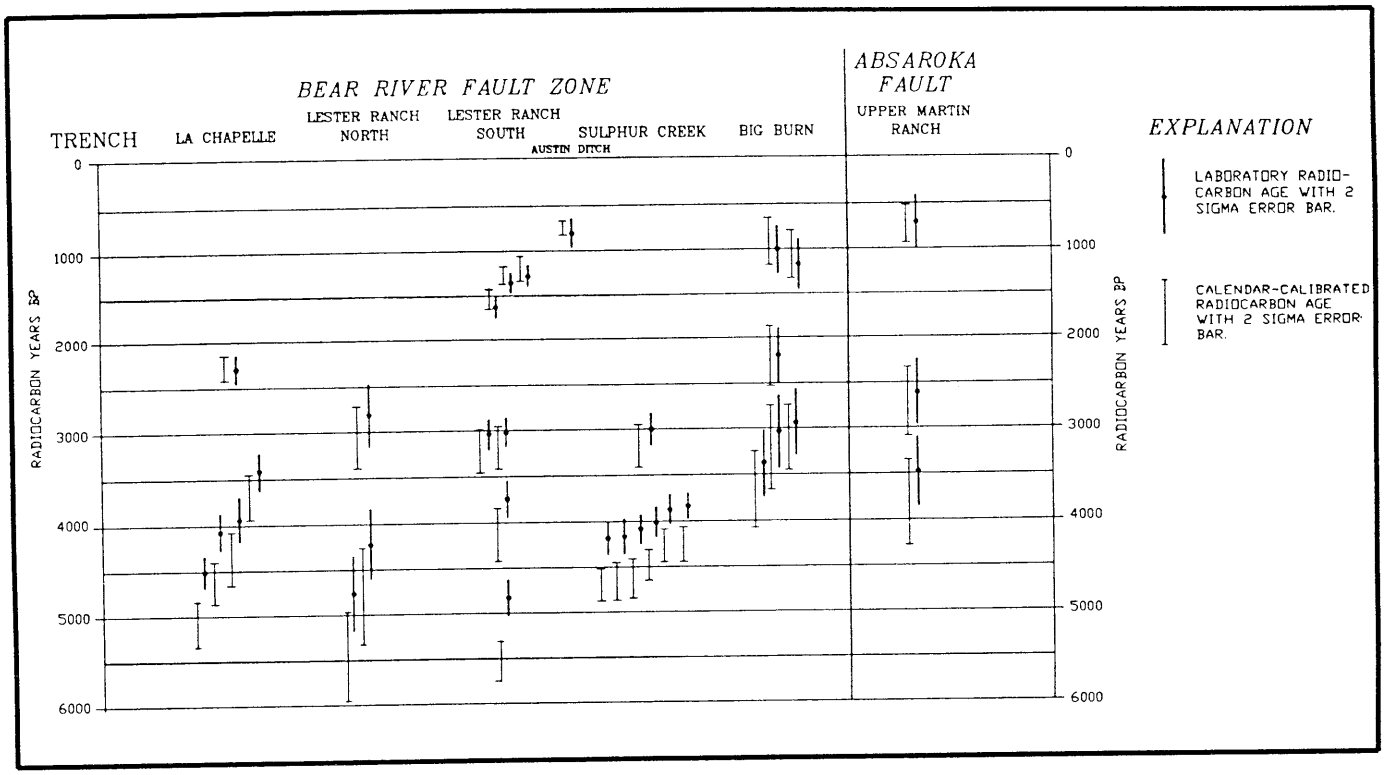

Figure 58. Laboratory and calendar-calibrated radiocarbon ages with 2 sigma error bars from trenches in the Bear River fault zone and the Martin Ranch scarp, Absaroka fault. Calendar-calibrated ages are shown to the left of the corresponding laboratory ages.

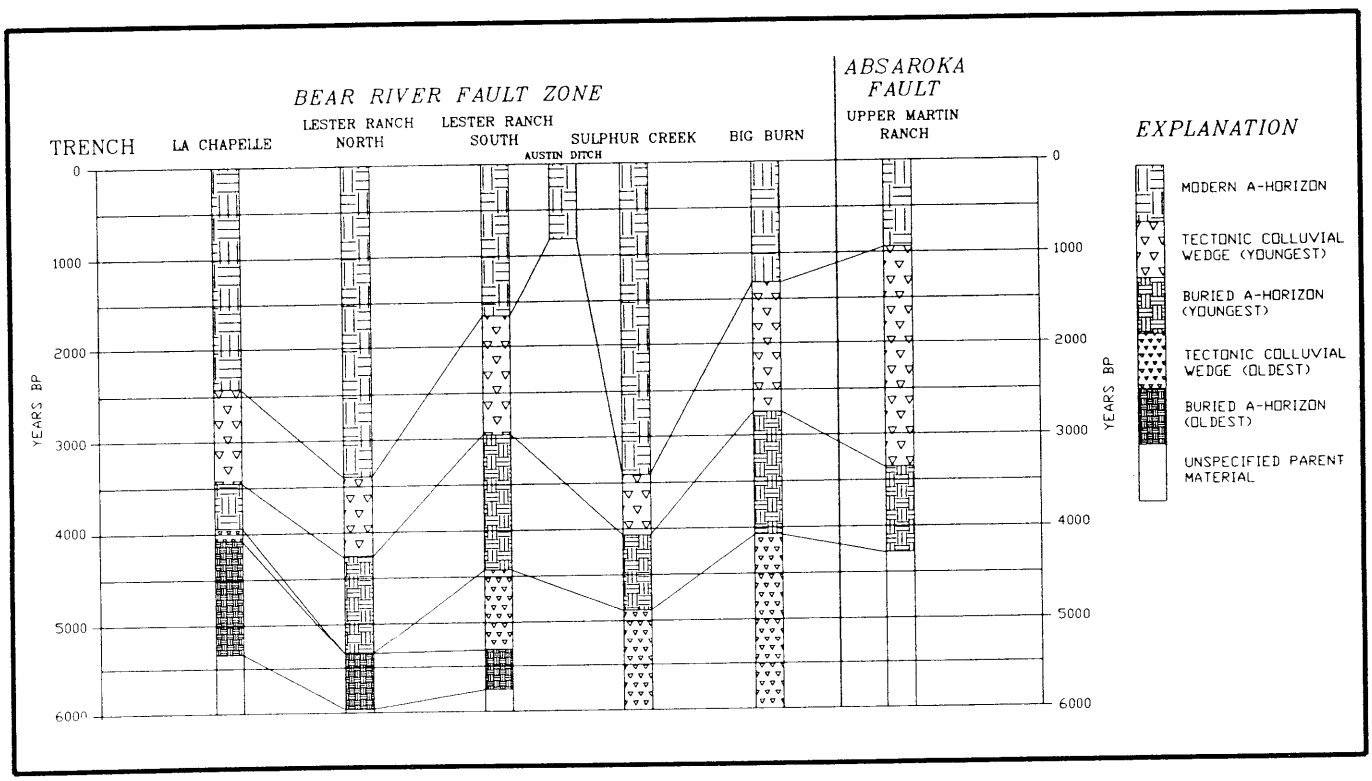

Figure 59. Development of soils and tectonically derived colluvial wedges with time in the Bear River fault zone and Martin Ranch scarp, Absaroka fault.

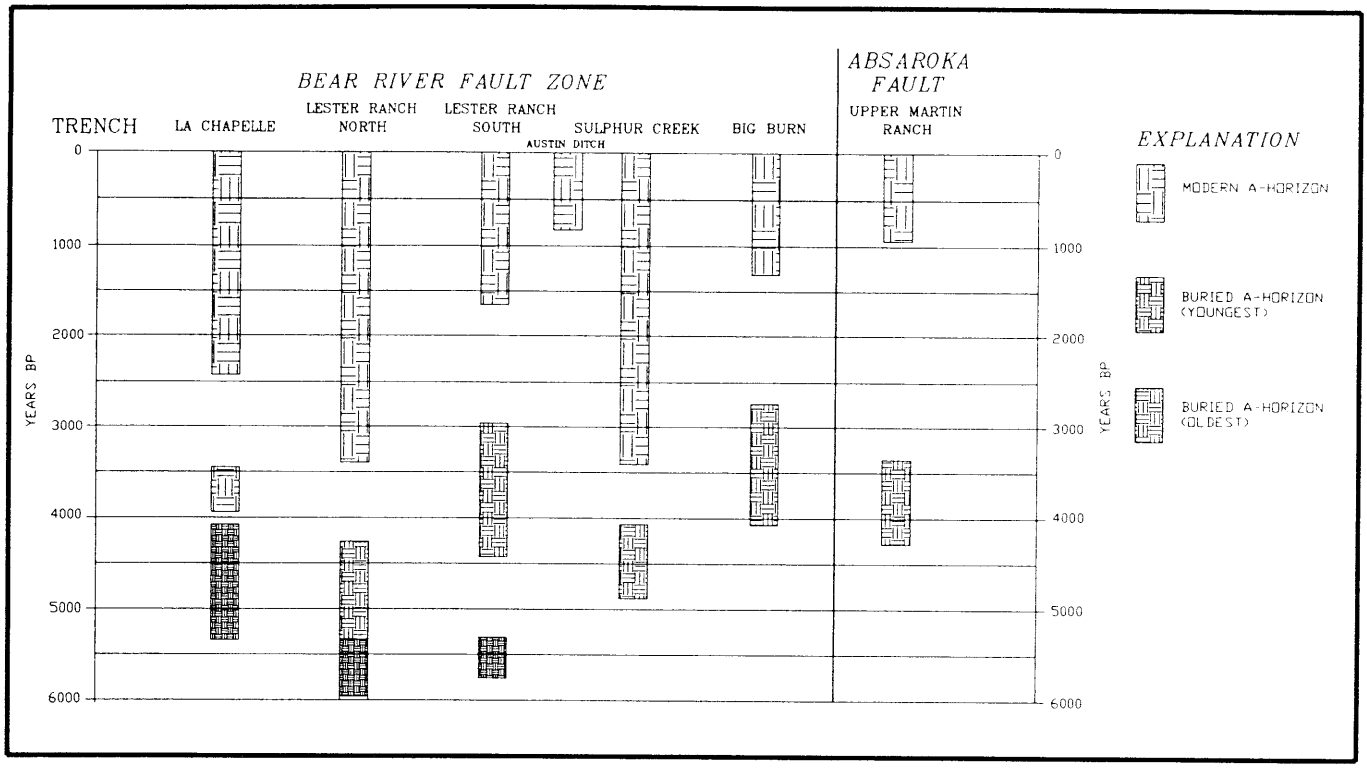

Figure 60. *Soil-forming intervals in the Bear River and Absaroka fault zones.*

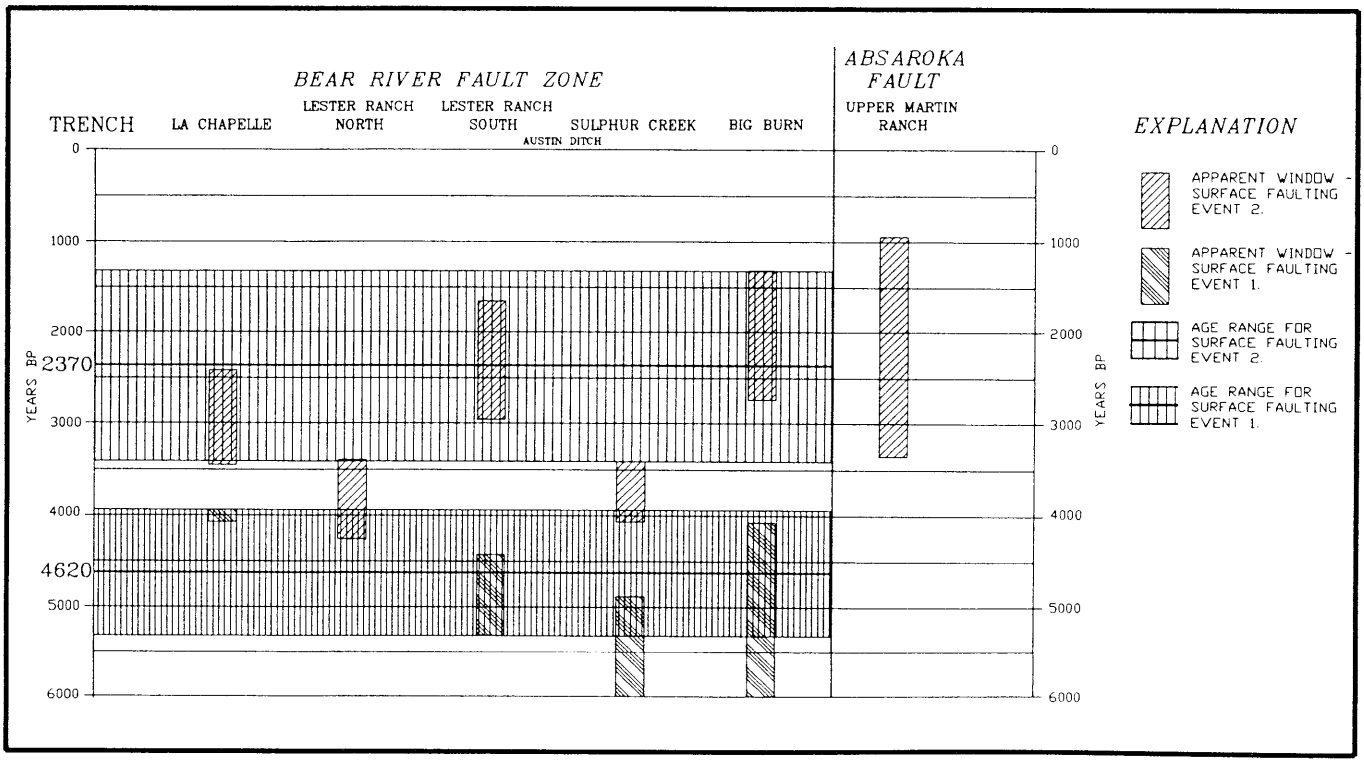

Figure 61. *Fault windows for first and second surface-faulting events in the Bear River and Absaroka fault zones. Mean ages of surface-faulting events and uncertainties are shown.*

Table 7.
Average slip rates based on total net vertical tectonic displacements and surface-faulting events at 4,620 ± and 2,370 ± yr B.P.

SCARP	NET VERT. DISPLACEMENT* (meters)	SLIP RATE (mm/yr)
La Chapelle	4.6 - 5.1	1.0 - 1.1**
Lester Ranch	3.9 - 11.3	0.8 - 2.4**
Sulphur Creek	6.7 - 8.6	1.5 - 1.9**
Big Burn	2.9 - 12.7	0.6 - 2.7**
Upper Little Burn	4.8 - 7.2	1.0 - 1.6**
Lower Little Burn	0.8 - 1.4	0.2 - 0.3**
	0.8 - 1. 4	0.3 - 0.6***

**See appendix I, tables I.2 and I.3 for explanation.*
***Assumes initial surface-faulting event at 4,620 yr B.P.*
****Assumes initial surface-faulting event at 2,370 yr B.P.*
To convert meters to feet multiply by 3.28.
To convert millimeters to inches divide by 25.4.

event (in this case surface faulting) based on the dating of buried A-horizons should take into account the apparent mean residence time (AMRT) of the soil according to the following relation:

Time elapsed since burial = ^{14}C age - AMRT

If residence time is not considered, the age of the soil must be considered a maximum estimate.

Apparent mean residence ages of modern A-horizons in the project area appear to range from about 1,000 to over 3,000 years based on radiometric ages of samples recovered from trenches (figure 60). The ages of surface-fault rupture defined by tectonically-buried soils can be reduced by the apparent mean residence time of the dated soils to arrive at geologically more reasonable ages. The estimation of apparent mean residence time for soils in the project area, however, is uncertain. Machette and others (1992) suggest apparent mean residence times of soils exposed in trenches excavated across the Wasatch fault zone are in the range of 200 to 300 years. The apparent mean residence time of soils in the project area appear to be longer but quantification is difficult. It is likely that estimated ages of surface-faulting events in the project area (4,620 ± 690 and 2,370 ± 1,050 yr B.P.) may be too old by at least several hundred years.

Tectonic Slip Rates

Estimates of total vertical tectonic displacements for each scarp in the Bear River fault zone are presented in table 7. Using these displacements and the mean value of the age of initial surface rupture documented in trench exposures, 4,620 yr B.P., tectonic slip rates along the fault zone can be calculated. From north to south, slip rates range from 0.04 in/yr (1.0 mm/yr) for the La Chapelle and 0.03 in/yr (0.8 mm/yr) for the Lester Ranch scarp to a maximum of 0.11 in/yr (2.7 mm/yr) for the Big Burn scarp. The relatively high slip rate on the Big Burn scarp is based on the assumptions that displacement is purely tectonic (no secondary mechanical component) and is produced by only two surface-faulting events. Uncertainties in these assumptions are discussed in the section on Net Vertical Tectonic Displacements.

Reliable slip rate estimates for the central part of the Bear River fault zone (La Chapelle to Sulphur Creek scarps) range from 0.03 to 0.07 in/yr (0.8 to 1.9 mm/yr). These values are comparable to slip rates on the Wasatch fault 0.004 to 0.07 in/yr (0.1 to 3.0 mm/yr) (Swan and others, 1983; Hays and Gori, 1992). Slip rates in the range of 0.04 to 0.4 in/yr (1 to 10 mm/yr) indicate a high rate of fault activity (Slemmons, 1981).

Summary

The Bear River fault zone ruptured the surface twice at 4,620 ± 690 and 2,370 ± 1,050 yr B.P. over a length of 21 to 25 miles (34 to 40 km) from the north flank of the Uinta Mountains northward into Wyoming. Calculated vertical tectonic displacements range from 6.6 to 17.4 feet (2.0 to 5.3 m) per event. Recurrence intervals, based on interpreted mean ages of surface faulting, range from about 2,250 to greater than about 2,370 years. Slip rates, based on total vertical tectonic displacements and mean age of initial surface rupture (4,620 ± 690 yr B.P.), range from 0.03 to 0.11 in/yr (0.8 to 2.7 mm/yr). Surface-rupture characteristics and recurrence intervals for the Bear River fault zone are comparable to similar parameters derived for the Wasatch fault (Swan and others, 1983; Hays and Gori, 1992), a major seismic source zone in the ISB.

ABSAROKA FAULT

Evidence for late Quaternary normal movement along the leading edge of the Absaroka thrust is three-fold: (1) the presence of a down-to-the-west fault scarp coincident with the leading edge of the thrust at Martin Ranch, (2) a 90° deflection in the Bear River channel where the river crosses the trace of the thrust, and (3) two(?) incised alluvial fans constructed in the Bear River floodplain coincident with the thrust trace.

Figure 62. Oblique aerial view to the northeast of the Martin Ranch scarp running across the photo from upper left to middle right. Small stock pond (section 16, T. 13 N., R. 119 W.) in middle ground is impounded against the scarp.

Martin Ranch Scarp

The Martin Ranch fault (figure 62) cuts two terrace levels on Hilliard Flat about 4.5 miles (7.2 km) west of the main Bear River fault zone (figure 24 and plate I). The scarp strikes N. 10-20° E. over a distance of about 2.5 miles (4.0 km). Apparent scarp height and slope angle on the upper terrace are 4.8 feet (1.45 m) and 14.5°, respectively. Apparent scarp height on the lower terrace ranges from 2.5 to 4.3 feet (0.75 to 1.3 m). The scarp terminates near the northeastern edge of the lower terrace and apparently does not cross Bazoo Hollow. To the south, the scarp disappears in gravel-cobble outwash/alluvium on the upper terrace level. The terrace surfaces are believed to be Bull Lake equivalent or older and are probably related to outwash deposition. The terrace surfaces offset by faulting merge in an upstream direction.

Geologic mapping for this study indicates the Martin Ranch scarp is coincident with the eastern ("young Absaroka" of Lamerson, 1982) trace of the Absaroka thrust (figure 24 and plate I). The eastern thrust trace is exposed along the channel of Sulphur Creek downstream of Sulphur Creek Reservoir. The thrust juxtaposes Frontier sandstones in the hanging wall against Hilliard shales and Frontier sandstones in the footwall along a fault plane striking N. 47° E. and dipping from 90° to 70° to the southeast. South of Sulphur Creek, the thrust trace passes beneath outwash and alluvium on Hilliard Flat. About 0.6 miles (1 km) south of Sulphur Creek, the Martin Ranch scarp appears along the projection of the thrust plane.

The coincidence of the Martin Ranch scarp with the leading edge of the Absaroka thrust indicates one of two possibilities. The first is that association of a down-to-the-west scarp with the thrust trace is fortuitous and has no tectonic significance. The second, and more likely possibility, is that the Martin Ranch scarp was produced by reactivation of the Absaroka thrust in a normal sense. The trace of the Absaroka fault and the Martin Ranch scarp could not be physically linked, however, in either a natural or trench exposure.

The explanation for the lack of continuity between the thrust plane and normal fault scarp may be related to characteristic rupture geometry along strike. For example, late Quaternary scarps in the Bear River fault zone to the east average about 1.9 miles (3.1 km) in length. The Martin Ranch scarp is 2.5 miles (4 km) in length and, therefore, may have reached its maximum development along strike. The absence of other scarps in the area presents another problem. The answer may be that either (1) other scarps were removed by erosion, or more likely, (2) scarp-producing ground rupture occurred only locally. Surface deformation north and south of the Martin Ranch scarp is expressed as a zone of warping rather than as distinct surface fault rupture.

Gibbons and Dickey (1983) excavated a trench across the Martin Ranch scarp near Martin reservoir but were hampered by high ground-water levels. Two trenches were excavated across the same scarp as part of this study.

Upper Martin Ranch Trench

The Upper Martin Ranch trench was excavated in 1983 across a scarp on the higher of two terrace surfaces on Hilliard Flat in the SW¼NW¼ section 4, T. 13 N., R. 119 W. (figure 24 and plate I). The trench extended from the terrace surface on the upthrown side of the scarp, across the scarp to the correlative surface on the downthrown side. The site was selected because

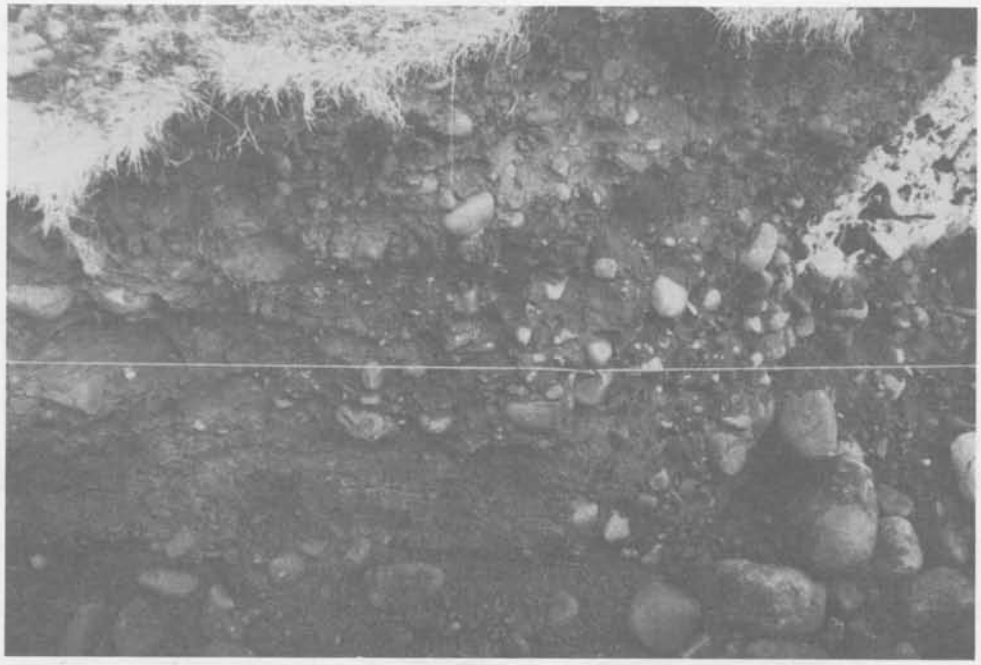

Figure 63. *Buried soil (unit 6) and overlying colluvial wedge (unit 7) exposed on the downthrown block in the Upper Martin Ranch trench. The fault zone is visible on the right side of the photo as a loose, disrupted zone with some suggestion of clast imbrication.*

of the well-defined, single-break nature of the scarp and ease of access. High ground water and irrigation ditches in the area, however, complicated trenching.

The scarp at the trench site is about 4.8 feet (1.45 m) high and exhibits a maximum scarp angle of 14.5 degrees. The trench was excavated in a N. 67° W. orientation. Length and maximum depth were 92 and 7.5 feet (28 and 2.3 m), respectively. Three samples of organic soils were collected for radiometric dating, and one soil profile was measured and described.

Pre-fault stratigraphy: The upper part of the trench (plate V) disclosed gravel-cobble outwash/alluvium with gravelly sand lenses overlying a cobble-boulder outwash/alluvium. A well-developed soil with textural B-horizon and a Stage II-III Bk-horizon is present on the upthrown terrace surface.

Structure and post-fault stratigraphy: At the mid-point of the scarp, the depositional fabric of the outwash/alluvium ended in a zone of disturbance marked by loose gravels, cobbles, and boulders. The walls of the trench tended to cave easily in this area. No shearing, however, could be detected in the disturbed zone due to the coarse-grained nature of the materials. A suggestion of imbrication was present in clasts on the west end of the disturbed area.

West of the disturbed zone, a colluvial wedge (units 7A and 7B) derived from outwash/alluvium in the upthrown block overlies a down-faulted soil horizon (figure 63). The buried soil appeared to be developed on older colluvium, although this interpretation could not be confirmed due to high ground water and the shallow depth of the trench. The buried soil could be traced laterally to the west where it merged with the modern surface soil. The disturbed zone and scarp-derived colluvial wedge were overlain by modern slope colluvium and the modern surface soil.

Although no shearing could be identified, disruption of depositional fabric in outwash/alluvium probably marks the position of the fault zone. The proximity of this zone to the buried soil and overlying colluvial wedge argues strongly for this interpretation. A trench excavated by Gibbons and Dickey (personal communication, 1983) about 1 mile (1.6 km) south of the Upper Martin Ranch site also revealed little evidence of shearing in coarse-grained deposits.

Samples for radiometric dating were collected from the buried soil, modern colluvium on the scarp slope, and from the base of the modern A-horizon. The buried soil yielded a laboratory age of about 3,500 yr B.P. Laboratory ages from the A-horizon and slope colluvium were about 700 and 2,600 yr B.P., respectively.

Interpretation: One surface-faulting event is clearly recorded by trench stratigraphy. An earlier event may be present but cannot be proven. Net vertical tectonic displacement during the last (and perhaps only) surface-faulting event is estimated to range from 4.3 to 5.2 feet (1.3 to 1.6 m; tables 8 and 9) with a mean of 4.9 feet (1.45 m) per event.

Lower Martin Ranch Trench

The Lower Martin Ranch trench was excavated across a 3+ foot (1+ m) high scarp on the lower of two terrace surfaces about 1,770 feet (540 m) north of the upper trench (plate I). The site was selected because of the well-defined nature of the scarp and distance from standing surface water. Boggy conditions were present along much of the scarp on the lower terrace surface.

The trench, in the N¼NW¼ section 4, T. 13 N., R. 119 W., was excavated from the terrace surface on the top of the scarp, down the slope to the terrace surface on the down-thrown side of the scarp. The trench was oriented in a N. 61° W. direction

Table 8.
Total and single-event net vertical tectonic displacement from scarp-profile data, Martin Ranch scarp, Absaroka fault.

TRENCH	TOTAL NET VERT. TECT. DISPLACEMENT* (meters)	NET VERT. DISPLACEMENT/EVENT (meters)
Upper Martin Ranch	1.3 - 1.6	1.3 - 1.6**
Lower Martin Ranch	- -	- -

*See appendix I, tables I.2 and I.3 for explanation.
**Assumes single scarp-forming event.
To convert meters to feet multiply by 3.28.

Table 9.
Comparison of vertical tectonic displacement per event summarized from scarp-profile, stratigraphic offset, and colluvial-wedge stratigraphic data, Martin Ranch scarp, Absaroka fault.

SCARP	VERTICAL TECTONIC DISPLACEMENT			MIN.	MAX.	MEAN
	SCARP PROFILES (meters)	STRAT. OFFSET (meters)	COLLUVIAL WEDGE STRAT. (meters)			
Upper Martin	1.3 - 1.6*	- -	- -	1.3	1.6	1.4
Lower Martin	- -	1.0*	0.7	0.7	1.0	0.9

*Assumes single scarp-forming event.
To convert meters to feet multiply by 3.28.

and was about 59 feet (18 m) long and 4.9 feet (1.5 m) deep near station 9. No material for dating was collected from the trench.

Pre-fault stratigraphy: A sandy gravel-cobble alluvium with scattered boulders was exposed in the upper part of the trench (plate V). The alluvium was crudely stratified and contained lenses of sand, gravel, and silt.

Structure and post-fault stratigraphy: At about the mid-point of the scarp, crude stratification in the upthrown block was terminated against a zone of loose, disturbed gravels and cobbles. A line of imbricated clasts defined the east or uphill side of the disturbed zone. On the downthrown side of the disturbed zone, a trough-like structure, defined by a concentration of gravels, cobbles, and intercalated organic material was present. This feature appeared to be similar to trough-like warping adjacent to the fault exposed in the Austin Reservoir irrigation ditch and probably represents displacement and back-tilting of the pre-fault terrace surface. Gravel-cobble alluvium underlying the trough appeared to be correlative with similar material on the upthrown side.

Interpretation: If the terrace deposits exposed in the upthrown and downthrown blocks are indeed correlative across the shear zone, the Lower Martin Ranch scarp ruptured once in mid- to late Holocene time, producing a scarp about 3+ feet (1+ m) high. Surface rupture on the lower terrace probably occurred simultaneously with latest rupture in the Upper Martin Ranch trench. Net vertical tectonic displacement for the single event is estimated to range between 2.3 to 3.3 feet (0.7 to 1.0 m; tables 10 and 11).

Deflection of the Bear River

About 6.5 miles (10.5 km) south of the Martin Ranch scarp, the Bear River abruptly changes course 85 degrees from N. 25° W. to S. 30° W. (figure 24 and plate I). The river flows to the southwest for about 1.2 miles (2 km) from the point of deflection before resuming a northwesterly course. The point at which the Bear River is deflected coincides with the mapped trace of the "young" Absaroka thrust (Lamerson, 1982), indicating a tectonic influence. Holocene normal movement (surface rupture or warping) on the leading edge of the Absaroka thrust similar to that observed along the Martin Ranch scarp would produce significant deflections in the course of the Bear River.

False-color infrared air photos show a subtle tonal lineament roughly corresponding to the inferred trace of the Absaroka thrust. The lineament coincides with the initial deflection point in the Bear River channel. Upstream of the lineament, both floodplain deposits and higher outwash terraces are remarkably uniform. Downstream of the lineament, however, normal fluvial deposition appears to have been interrupted by two(?) episodes of fan deposition in the floodplain (figure 64). The headward parts of the fans are coincident with the tonal lineament and the trace of the Absaroka thrust. The older fan appears to have been

Table 10.
Vertical displacement per event for total vertical stratigraphic offset, Martin Ranch scarp, Absaroka fault.

TRENCH	TOTAL VERT. STRAT. OFFSET (meters)	NET VERT. DISPLACEMENT/EVENT (meters)
Upper Martin Ranch	- -	- -
Lower Martin Ranch	1.0	1.0*

*Assumes single scarp-forming event.

Table 11.
Vertical displacement established from colluvial-wedge stratigraphy, Martin Ranch scarp, Absaroka fault.

TRENCH	EST. VERT. TECT. DISPLACEMENT EVENT 1 (meters)	EST. VERT. TECT. DISPLACEMENT EVENT 2 (meters)	VERTICAL DISPLACEMENT PER EVENT (meters)
Upper Martin Ranch	- -	0.5 - 1.1	0.5 - 1.1
Lower Martin Ranch	NA	0.7	0.7

NA = Not applicable
To convert meters to feet multiply by 3.28.

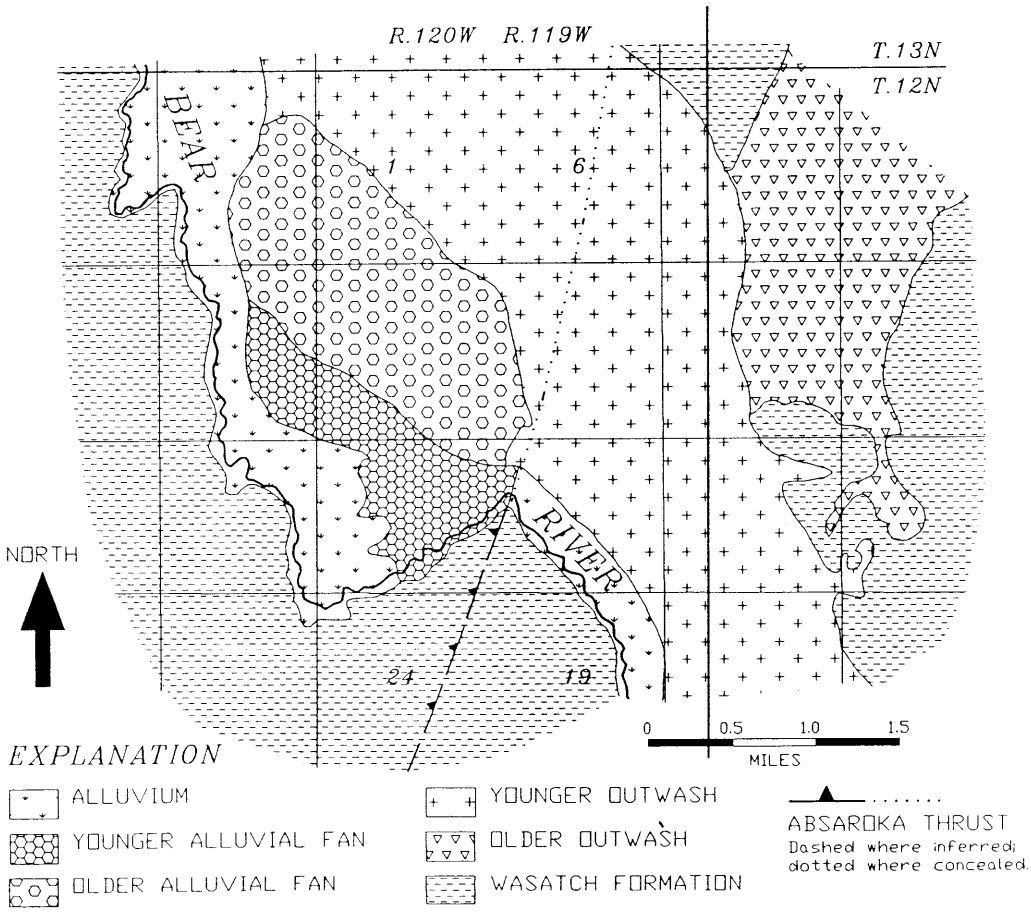

Figure 64. Sketch map showing deflection of the Bear River along the trace of the Absaroka thrust in the north half of T. 12 N., R. 119-120 W. The trace of the thrust across the floodplain is delineated by a tonal lineament and the heads of incised alluvial fans.

partially eroded by subsequent fan development. The younger fan is clearly related to the deflection and present channel of the Bear River. Circumstantially, the fans are consistent with the idea that the Absaroka thrust was reactivated in a normal sense in Holocene time. The morphology of the river channel through this area, however, is not easily explained by any simple theory involving the effect of faulting on a major river system. Clearly, a complex relationship has existed between river/floodplain dynamics and tectonic events.

Examination of valley slopes adjacent to the floodplain provided little insight into the tectonic development of the area. Some evidence of faulting was found in Wasatch beds on the southwest side of the floodplain along the projection of both the tonal lineament and the trace of the Absaroka thrust. Stratigraphic throw could not be determined but is believed to be minor, perhaps a few feet or tens of feet. No evidence of scarps or other tectonic features was found on either valley slope, suggesting that if tectonic movements indeed occurred along this portion of the Absaroka, displacements were either small or were manifested by warpage without distinct surface rupture.

Fault Rupture Characteristics

Rupture Length

The leading edge of the Absaroka thrust has been reactivated in a normal sense in response to the same regional stresses responsible for development of the Bear River fault zone. Geologic mapping indicates scarp-forming surface rupture occurred over a distance of 3.1 miles (5.0 km). Indirect evidence for associated surface deformation, principally deflection of the Bear River along the trace of the fault south of the Martin Ranch scarp, increases surface rupture length to 9.3 miles (15.0 km).

Net Vertical Tectonic Displacements

Two trenches were excavated along the Martin Ranch scarp coincident with the Absaroka thrust. Calculated mean net vertical tectonic displacements, assuming a single surface-faulting event, ranged from 4.9 feet (1.45 m) in the Upper Martin Ranch trench to 2.8 feet (0.85 m) in the Lower Martin Ranch trench (table 9).

Age of Movement and Recurrence Intervals

Age of fault movement and recurrence interval for the normally reactivated Absaroka fault were analyzed in the same manner described for the Bear River fault zone. Interpretation was limited by a single set of radiometric AMRT ages on buried and modern A-horizons from the Upper Martin Ranch trench. These data were plotted on figures 58 through 61 and were compared to AMRT ages of buried and modern A-horizons from the Bear River fault zone. Age of the last and perhaps only surface-faulting event exposed in the Upper Martin Ranch trench is consistent with age of latest surface rupture in the main Bear River fault zone, 2,370± 1,050 yr B.P. as shown on figure 62. This contemporaneity implies that normal displacement along the leading edge of the Absaroka fault was simultaneous with surface rupture to the east in the Bear River fault zone. Simultaneous movement suggests either (1) a sympathetic, mechanical response along a pre-existing zone of weakness or (2) tectonic reactivation of the Absaroka thrust in a normal sense due to regional extension localized along pre-existing thrust planes. The possibility that the Absaroka fault is independently seismogenic, however, cannot be precluded.

Tectonic Slip Rates

Total maximum vertical tectonic displacement for the Upper Martin Ranch scarp ranges from 4.3 to 5.2 feet (1.3 to 1.6 m; tables 8 and 9). Using the interpreted mean age of latest surface rupture of 2,370 yr B.P., tectonic slip rates of 0.02 to 0.03 in/yr (0.5 to 0.7 mm/yr) can be calculated for the scarp. These slip rates would classify the reactivated Absaroka fault as moderately high to highly active (Slemmons, 1981).

Summary

The leading edge of the Absaroka thrust has been reactivated in a normal sense for a distance of 3.1 to 9.3 miles (5.0 to 15.0 km) along strike. Scarp-forming surface rupture (ground breakage) is limited to about 3 miles (5 km); surface warping is apparently manifested over about 6 miles (10 km) south of the Martin Ranch scarp and has deflected the Bear River. Mean net vertical tectonic displacement at the Upper Martin Ranch site is 4.6 feet (1.45 m), assuming one surface-faulting event. Age of faulting is contemporaneous with surface rupture in the main Bear River fault zone. Continuity in time indicates that normal movement on the Absaroka fault was a response to regional extension localized along pre-existing thrusts. Tectonic slip rates range from 0.02 to 0.03 in/yr (0.5 to 0.7 mm/yr).

DARBY-HOGSBACK FAULT

Evidence for Quaternary movement on the Darby-Hogsback thrust includes: (1) regional deformation and tilting of alluvial/outwash terraces, (2) a distinct drainage lineament along East Muddy Creek and associated apparent Quaternary normal fault scarps, (3) scarps and topographic breaches in the Gilbert Peak erosion surface on Elizabeth Ridge, and (4) indirect evidence for separation of the Bear River and Green River drainage basins postulated by Hansen (1985).

Terrace Deformation

Streams draining the north flank of the Uinta Mountains generally flow from south to north. Well-developed alluvial/outwash terraces probably ranging from early or mid-Pleistocene to Holocene are associated with these drainages. Terrace gradients generally appear to be convergent in a downstream direction and slope from south to north in the same direction as stream flow. Many terraces, however, exhibit a strong component of tilt to the east at right angles to the direction of stream flow and depositional gradient (figure 65). Moreover, several terraces are either convergent in an upstream direction or tend to merge with younger terraces to the east while increasing in elevation relative to modern stream levels to the west.

Figure 65. Apparent eastward-tilted strath-terrace surfaces in the far middle ground (sections 25 and 36, T. 13 N., R. 119 W.). View is to the south. The main trace of the Bear River fault zone is approximately 2 miles (3 km) to the west (right).

This type of tilting indicates post-depositional tectonic deformation. Moreover, older terrace surfaces appear to be tilted more than younger terraces, indicating a recurrent deformational process.

Terraces in the vicinity of Bear River fault zone scarps show evidence of local back-tilting and warpage believed to be the result of displacement on these faults. Pronounced regional tilt, however, extends from west to east across the Bear River fault zone. Moreover, the vertical throw represented by the Bear River scarps, <3.3 to 49+ feet (<1.0 to 15+ m), does not account for either the magnitude of tilt or width of the tilted area. At most, the Bear River scarps account for local perturbation of regional eastward tilt.

A tectonic explanation requires the existence of a zone of down-to-the-west normal faulting east of the Bear River fault zone. Such faulting would account for the eastward tilt and possibly convergence of terraces in an upstream direction, particularly if displacements were increasing to the south similar to the Bear River scarps. Increasing tilt with age would suggest a recurrent process recording a cumulative effect. The rate of deformation could be established if the age and degree of tilt for each successive terrace surface were known.

Muddy Creek Lineament and Associated Scarps

A possible mechanism for eastward tilting of terrace surfaces involves normal reactivation of the Darby-Hogsback thrust, generally considered to be covered by several hundred meters of undisturbed Wasatch and Green River sediments in southwestern Wyoming. Interpretation of aerial photography indicated the presence of an almost linear stream drainage extending 6.0 miles (9.7 km) along the inferred subsurface trace of the Darby-Hogsback thrust (figure 24 and plate I). The drainage lineament follows East Muddy Creek from about 6.5 miles (10.5 km) north of Elizabeth Ridge to a point coincident with the abrupt northeast change in strike of the Darby-Hogsback thrust. The valley of Muddy Creek is asymmetrical with a ridge about 400 feet (122 m) above stream level on the east and rolling, dissected tablelands on the west.

The linear drainage and change in elevation and topography across the lineament are suggestive of down-to-the-west normal faulting and would account for terrace tilt to the east. Moreover, down-to-the-west normal faulting mapped by Lines and Glass (1975) and M'Gonigle and Dover (in press) is roughly coincident with both this lineament and the subsurface trace of the Darby-Hogsback thrust. The south end of the Darby-Hogsback thrust (Blackstone and Ver Ploeg, 1981; Dixon, 1982; Lamerson 1982) strikes to the southwest and is inferred to pass beneath Elizabeth Ridge. The top of Elizabeth Ridge, a remnant of the Gilbert Peak erosion surface, is breached in several places along and near the inferred trace of the Darby-Hogsback thrust. The origin of the apparent breaches in the Gilbert Peak erosion surface is critical to assessing the tectonic history of the Darby-Hogsback thrust.

Reconnaissance mapping along the Muddy Creek lineament identified a number of apparent down-to-the-west block faults and strong drainage alignments along the west side of Bigelow Bench east of Evanston (T. 13-14 N., R. 116-117 W.). These faults displace Pleistocene terrace gravels mantling the Bigelow surface and show a right-stepping, en echelon pattern similar to the Bear River fault zone (plate I). The normal-fault pattern is generally coincident with the inferred subsurface trace of the Darby-Hogsback thrust.

The most compelling evidence for down-to-the-west normal faulting is along the western edge of Bigelow Bench near I-80 (plate I). In this area, several normal faults displace the Bigelow

surface capped by Pleistocene gravels (figure 66). The gravel covered surface on the downthrown side of the faults is back-tilted to the east into the scarps (figure 67), and streams preferentially flow along the scarps. A major escarpment, up to 660 feet (200 m) high, forms the edge of Bigelow Bench. Below the edge of the escarpment, several eastward-tilted, gravel-capped surfaces are present. It is possible, but not proven, that these gravels are correlative with the gravels capping Bigelow Bench. The Muddy Creek lineament generally forms the western boundary of the zone of normal faulting. The elevation difference between the floor of Muddy Creek and Bigelow Bench, therefore, may approximate the maximum Pleistocene throw of normal faulting in this area.

South of Chapman Butte in section 4, T. 13 N., R. 117 W., the pattern of faulting becomes less distinct due in part to tectonic overprinting on glacial deposits/topography and perhaps due to poorly understood structural complexities. Normal faulting is believed to be manifested along linear drainages including Fish Creek, Clear Creek, and the East Fork of Muddy Creek. A consistent pattern of down-to-the-west topographic displacement is present across these drainages, suggesting that normal faulting continues to the south. Near the headwaters of East and West Muddy creeks, the drainage pattern swings to the southwest and drains the northern flank of Elizabeth Ridge. This drainage pattern is roughly coincident with breaches in the Gilbert Peak erosion surface.

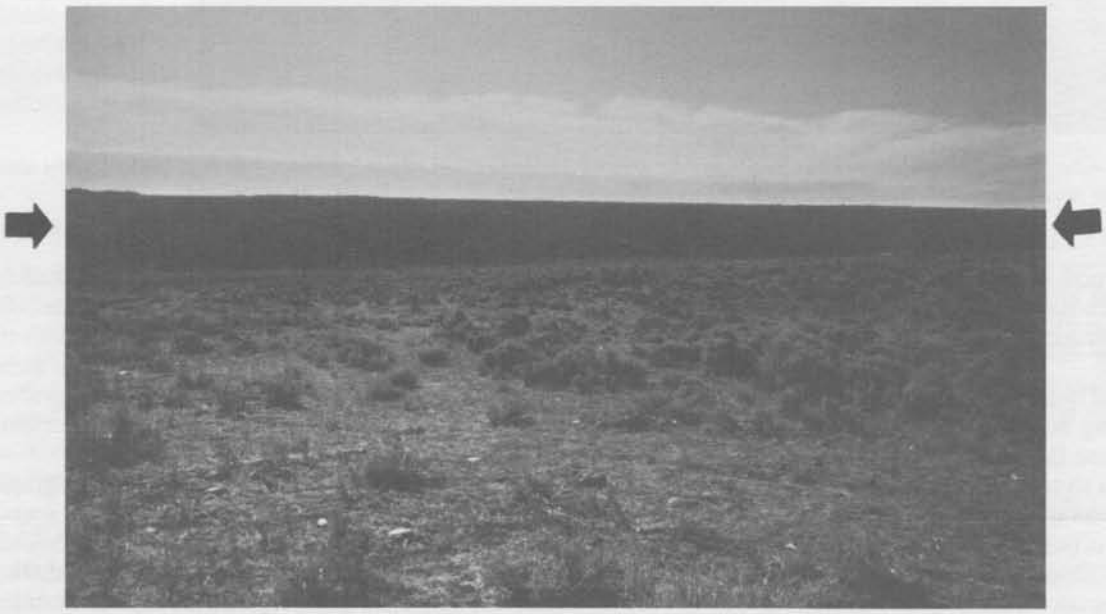

Figure 66. *Apparent down-to-the-west fault scarp displacing the Bigelow Bench surface and outwash/terrace gravels. View is to the east in section 7, T. 15 N., R. 116 W.*

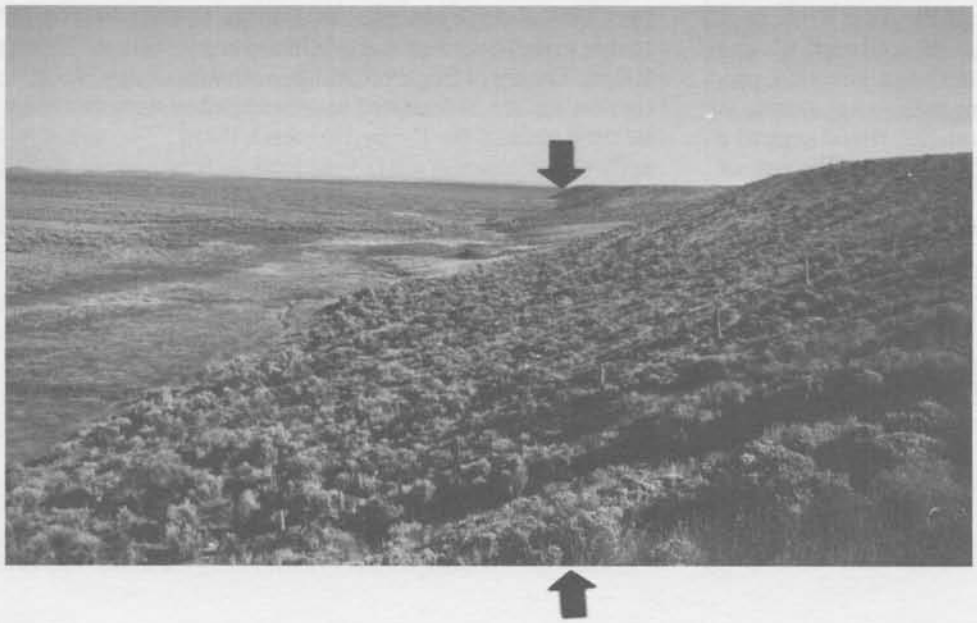

Figure 67. *View to the north along apparent fault scarp displacing the Bigelow Bench terrace/outwash surface in section 6, T. 15 N., R. 116 W. Surfaces are believed to be correlative across the scarp. Evidence of backtilting into the scarp is apparent on the downthrown (left) side. A modern stream flows preferentially along the base of the scarp.*

Despite circumstantial evidence for Quaternary normal displacement on the Darby-Hogsback thrust, no conclusive evidence, for example actual stratigraphic offset in the Wasatch and Green River Formations, has been found. Attempts to verify the normal fault mapped by Lines and Glass (1975) were unsuccessful. Unpublished mapping by M'Gonigle and Dover reportedly shows a zone of normal faulting along and west of Muddy Creek roughly coincident with the fault mapped by Lines and Glass (1975). No faults, however, are mapped along the west side of Bigelow Bench where the best evidence for displacement of the Pleistocene Bigelow surface and overlying gravels is preserved.

Elizabeth Ridge Scarps

Three linear scarps (figure 68), subparallel to the North Flank fault but about 4.0 miles (6.5 km) north of the fault trace, were noted on the crest and west flank of Elizabeth Ridge (T. 2 N., R. 11 E.; figure 24 and plate I). The easternmost of these three faults exhibits down-to-the-south displacement and cuts Bishop Conglomerate capping the Gilbert Peak erosion surface. The other two faults, although on the same linear trend 0.5 miles (0.8 km) to the west, show down-to-the-north displacements. Moreover, the western scarps appear to be younger, based on height and degree of preservation. The eastern scarp, although clear on air photos, is subdued on the ground, indicating it is older than its western counterparts.

In addition to the scarps described in the preceding paragraph, the Gilbert Peak erosion surface has been breached or displaced in several places between Elizabeth Pass and Elizabeth Mountain to the northwest (figure 68 and plate I). Maximum topographic relief across these features relative to the elevation of the erosion surface is about 295 feet (90 m). In general, the topographic breaches are generally linear with northeast to north-northeast trends and cut completely across the erosion surface. South of Elizabeth Pass to Table Top (plate I), the erosion surface exhibits a strong component of apparent down-to-the-west warping or tilting.

Three hypotheses explain the origin of the apparent breaches and scarps in the Gilbert Peak erosion surface on Elizabeth Ridge. The first argues that topographic breaches in the Gilbert surface and related scarp-like forms are related to erosional processes. In this hypothesis, headwardly eroding streams breached the Gilbert Peak erosion surface, creating the scarp-like forms visible across the top of Elizabeth Ridge. The breaches and related scarps, however, are not associated with drainages on the flanks of the ridge that would account for breaches through headward erosion.

The second hypothesis invokes landsliding as a cause of the breaches and scarp-like forms. The flanks of Elizabeth Ridge exhibit evidence of massive slope failures characterized by rotational (toreva) blocks, linear landslide scarps, and sag ponds. In virtually all cases, these mass movements parallel the topographic escarpment at the edge of the Gilbert Peak erosion surface, and movement is toward the free face of the slope. No evidence indicates that landsliding breached the erosion surface. It is possible, however, that continued landsliding obliterated drainage patterns on the flanks of the ridge.

Figure 68. Vertical aerial view (1:34,500) of short scarps on the west flank and top of Elizabeth Ridge (sections 2 and 3, T. 2 N., R. 11 E.) from natural color photography. The Gilbert Peak erosion surface forms the top of Elizabeth Ridge in the upper right part of the photo. The Elizabeth Ridge scarp is visible as tonal/color lineament in the lower right hand part of the photo. Linear breaches in the erosion surface are visible in the upper center.

The third hypothesis suggests the breaches and scarps are tectonic in origin. Tectonic features would cross-cut pre-existing drainages and topography. Since neither stream erosion nor landsliding offer a satisfactory explanation for geomorphic features on Elizabeth Ridge, a tectonic origin seems plausible. The tectonic hypothesis was tested by excavation of an exploratory trench across an anti-slope scarp on the Gilbert Peak erosion surface. The interpretation of this trench is described below.

Elizabeth Ridge Trench

The Elizabeth Ridge trench was excavated across a down-to-the-south scarp on Bishop Conglomerate and the Gilbert Peak erosion surface 0.6 miles (1 km) north of Elizabeth Pass (figure 24 and plate I) and 4.3 miles (6.9 km) east of the Bear River fault zone. The scarp, trends N. 70° E., and is anti-slope in aspect, opposite the north-sloping gradient of the erosion surface.

Trench excavation proved difficult because of large cobbles and boulders. The trench, completed in 1984, was oriented in a N. 8° W. direction, was 252 feet (77 m) long and 6.6 feet (2.0 m) deep at its deepest point. The scarp at the trench site is 8.2 feet (2.5 m) high with a maximum scarp angle of 5.5 degrees. Scarp profiles (appendix I) were not long enough to provide gradients on the undisturbed geomorphic surface away from the scarp. No material for radiometric dating was collected from the trench. Three soil profiles, however, were measured and described.

Pre-fault stratigraphy: The upper part of the trench (plate V) north of the scarp slope was excavated in coarse cobble-boulder alluvium and residuum interpreted to be part of the Bishop Conglomerate of Oligocene age. The matrix consisted of roughly equal percentages of sand and clay comprising 50 percent by volume of the total deposit. The clay fraction appeared as pedogenic clay films resulting from maximum development of a textural B-horizon. Colors ranged from reddish brown (2.5 YR 4/6 to 4/8) to dark reddish brown (2.5 YR 3/6). The B-horizon was overlain by an A-horizon developed on colluvium and residuum derived from the underlying material.

The Bishop Conglomerate exposed in the trench was poorly sorted with evidence of crude, lenticular stratification. Bedding, where visible, ranged from thin to thick. Stratification was interrupted locally by vertical or near vertical zones of loose, imbricated cobbles and gravels believed to be the result of frost wedging and related periglacial processes. Each of these zones was examined carefully for evidence of offset and/or shearing. No such evidence was found; hence, the preferred interpretation is frost wedging. Approximately 10 to 15 percent of clasts derived from quartzites and related lithologies of the Uinta Mountain Group exhibited evidence of weathering, but less than 5 percent were significantly grussified.

Structure and post-fault stratigraphy: No direct evidence of faulting was found in the Elizabeth Ridge trench. Distinct lateral changes in deposits and soil development across the scarp, however, are consistent with a tectonic interpretation. Alternative non-tectonic interpretations are also possible and are discussed below.

Near station 29, a wedge of material interpreted to be slope colluvium (unit 2) was deposited on the Bishop Conglomerate and resident textural B-horizon characterized by maximum clay film development and strong red colors. The younger colluvial material contained more sand and silt at the expense of pedogenic clay, although clay films were present. Colors were less strong and ranged from dull reddish brown (5 YR 5/3) to dull orange (5 YR 6/3) in a dry state to dark reddish brown (2.5 YR 3/3) in a moist state. The colluvium was very poorly to non-sorted and showed a hint of stratification near the top of the unit. About 5 to 15 percent of the clasts were significantly weathered. Frost wedging was apparent in the unit, and some frost wedges were observed to extend through the colluvial unit into the underlying Bishop Conglomerate. Near station 50.5, the Bishop Conglomerate disappeared into the trench floor. Pods of material derived from the Bishop were incorporated in the colluvial unit (unit 2) near stations 54 and 65. These pods were characterized by strong red colors and maximum clay film development.

Between stations 50 and 51, the colluvial unit (unit 2) was overlain by a third deposit (unit 3) interpreted to be either colluvium or alluvial channel-fill. This unit consisted of approximately 10 percent silt, 30 percent clay, and 40 percent sand with only 20 percent clasts mainly in the gravel size range. No pedogenic clay films were noted and colors were in the 5 YR to 7.5 YR range. The unit was poorly sorted to non-sorted and was generally non-stratified except near station 52. The base of the unit showed evidence of frost wedging, but no frost wedges, with the possible exception of a feature near station 69.7, completely penetrated the unit. No clear evidence of alluvial origin, except for the overall lenticular, channel-like nature of the deposit, could be found. A colluvial origin for this unit, therefore, is preferred. The entire surface exposed in the trench was mantled by slope colluvium and the modern A-horizon.

Interpretation: Both tectonic and non-tectonic interpretations were considered as part of this study. A stream erosion/channel fill interpretation requires the existence of a drainage which created the escarpment by erosion and replaced eroded Bishop Conglomerate with younger alluvial deposits. A small intermittent drainage is present along the scarp but was not intercepted by the trench. The gully drains to the east where, on crossing the edge of Elizabeth Ridge, it drops into a deep, headwardly-eroding ravine.

The gully at the base of the escarpment is underfit and has no appreciable drainage basin which could account for the amount of erosion and/or the volume of material and clast sizes found in the trench. The alluvial channel is asymmetrical, i.e. an escarpment exists on the north side of the drainage but not on the south. Stream erosion would form a symmetrical channel with escarpments on both sides of the channel. The drainage is also oriented in an east-northeast direction almost perpendicular to the main south-to-north regional drainage pattern. The gradient of the Gilbert Peak erosion surface is also south to north.

The headwardly eroding ravine in line with the escarpment on the east side of Elizabeth Ridge may be evidence for fluvial origin of the escarpment across the ridge crest. It is unclear, however, how a headwardly eroding stream on a steep slope would create a linear escarpment completely across a pre-existing geomorphic surface. A more plausible explanation suggests a fault displaced the erosion surface and the flanks of the ridge thereby controlling subsequent drainage development across the top of the ridge and on the steeper flanking slopes. The steep ravine on the east flank of the ridge is being eroded along the position of a former tectonic scarp, perhaps in loose shear zone materials. The small, underfit drainage on the ridge crest is a manifestation of drainage control by a pre-existing tectonic scarp.

Geomorphology and trench stratigraphy, even in the absence of direct evidence for faulting, are consistent with a surface fault interpretation. The anti-slope nature of the escarpment and discordance with drainage patterns reinforce the tectonic interpretation. Apparent colluvial deposits in the trench and the apparent step in the Bishop Conglomerate and the resident soil are consistent with surface faulting. Pods of Bishop-derived material incorporated in the colluvial deposits may have been derived from the upthrown block. The position and change in soil development from the very old soil developed on the Bishop

in the northern part of the trench to apparently younger soils in the southern part is also consistent with a tectonic interpretation. The Elizabeth Ridge scarp, therefore, is believed to be tectonic in origin and was formed during a surface-faulting event.

Important questions remain as to the age of faulting and its relationship to regional tectonic features. The distance of the Elizabeth Ridge scarps from the Bear River fault zone indicates they are not related structurally or temporally. Sub-parallelism with the North Flank fault suggests a circumstantial relationship. A closer, although discordant relationship, exists between the Elizabeth Ridge scarps and the southern end of the Darby-Hogsback thrust (plate I). The apparent relationship may be analogous to the relationship between discordant scarps and the southern end of the Bear River fault zone.

The subdued nature of the Elizabeth Ridge scarp and possible tectonically-derived deposits exposed in the trench indicate surface faulting in the area is significantly older than mid to late Holocene and, therefore, is not comparable, at least in age, to the Bear River fault zone. No absolute dates were obtained from the Elizabeth Ridge trench; thus, no constraints can be placed on the minimum or maximum age of surface rupture. The evidence suggests, however, that surface rupture in the area pre-dates latest surface ruptures along the Bear River fault zone.

Trench stratigraphy was inadequate to define the number of surface-faulting events or net vertical tectonic displacements per event. Maximum vertical displacement is on the order of 4.9 to 8.1 feet (1.5 to 2.47 m) based on scarp-profile data and estimated vertical stratigraphic displacement (appendix I).

Drainage Basin Separation

Hansen (1985) commented on drainage basin development in southwestern Wyoming. His principal observations relate to warm-and cold-water fish biotas and their apparent relationships to paleo and modern drainages. The crux of Hansen's hypothesis is that cold-water fish species were transferred from the Snake and Bear Rivers to the Green River drainage basin. Several possible transfer sites are located in southwestern Wyoming and involve the former courses of the Bear River, Muddy Creek, and Stowe Creek. According to Hansen, the ancestral Bear River may once have drained into the Green River by way of Hilliard Flat and Muddy Creek. A map accompanying Hansen's article, reproduced as figure 69, shows the course of the Bear River trending northeastward to confluence with Muddy Creek and thence to the Green River. Hansen invokes basin-and-range faulting as the mechanism by which the Bear and Green River drainage basins were separated. Examination of figure 69 suggests diversion took place along or east of Muddy Creek. Faulting is also invoked as mechanism for lowering the base level of the Bear River and increasing stream competence relative to tributaries of the Green River.

Comparison of terrace profiles in the Bear River and Blacks Fork drainages indeed shows a lower base level and locally steeper gradient for the Bear as compared to the Blacks Fork, a modern tributary of the Green River. Moreover, the apparent separation of the ancestral drainage basins took place along the Muddy Creek lineament and the inferred subsurface trace of the Darby-Hogsback thrust precisely at the location expected if indeed the Darby-Hogsback thrust was reactivated in a normal sense. Figure 70 shows the traces of the Absaroka, Darby-Hogsback, and Bear River faults superimposed on Hansen's drainage map.

According to Hansen (1985), cold-water fish species probably entered the Green River from the Snake River after the Green had been diverted to the south in mid-Pleistocene time about 600,000 years ago. Transfer of species from the Snake and/or Bear Rivers took place during an interglacial period following diversion of the Green River post-600,000 years ago. Separation of the Green River and Bear River drainage basins, therefore, did not occur until less than 600,000 years after the transfer had taken place. Maximum age of the onset of basin-and-range faulting according to Hansen's interpretation would be about 600,000 years ago.

Fault-Rupture Characteristics

The Darby-Hogsback thrust shows evidence of normal reactivation in mid- to late Quaternary time. No substantive evidence indicates movement occurred within the last 5,000 years comparable to the Bear River and Absaroka faults.

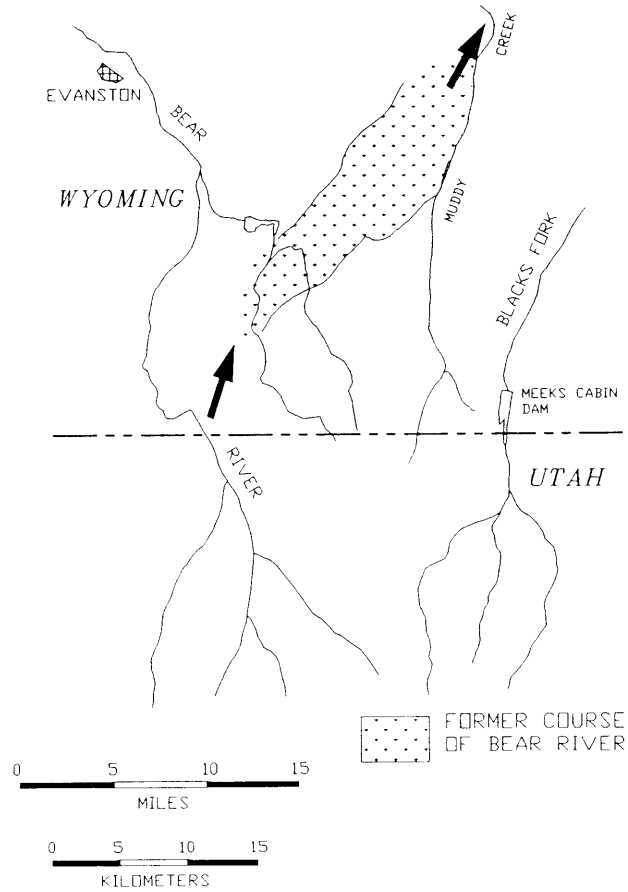

Figure 69. Map showing the postulated course of the Bear River prior to separation of the Bear River and Green River drainage basins post-600,000 years ago (Hansen, 1985). Hansen infers tectonic separation may have occurred along or near Muddy Creek.

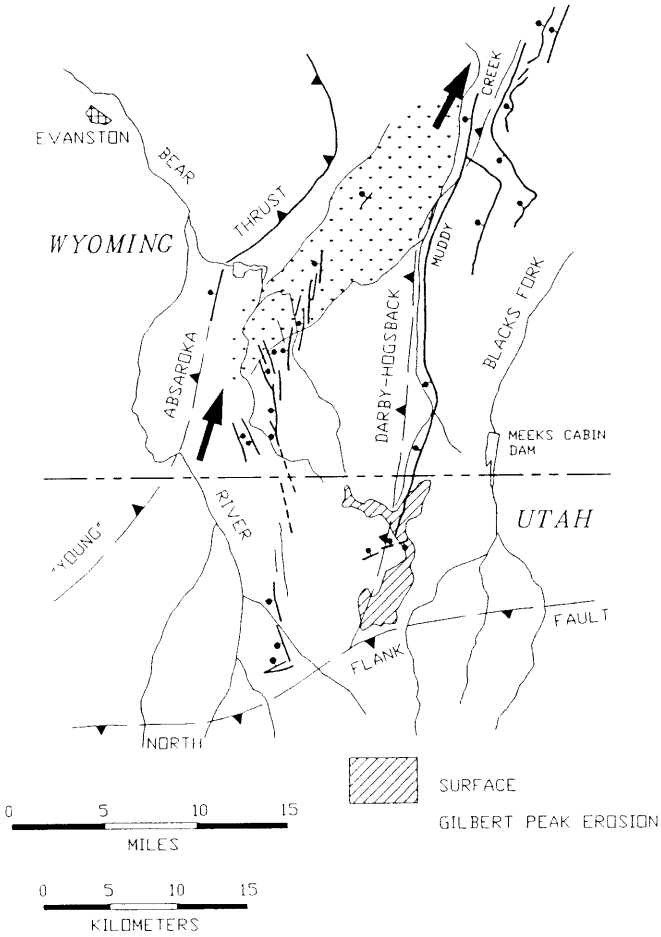

Figure 70. Map showing relationship of neotectonic features to former course of the Bear River and Muddy Creek. The Darby-Hogsback thrust is coincident with the Muddy Creek lineament. Normal reactivation of the Darby-Hogsback thrust may be responsible for separation of the Bear and Green River drainage basins. Note also that the leading edge of the Absaroka thrust is coincident with a right-angle bend in the Bear River.

Rupture Length and Vertical Tectonic Displacements

The zone of apparent normal faulting and tectonic warping along the leading edge of the Darby-Hogsback thrust extends over at least 34.1 miles (55 km) along strike. The northern end of apparent normal reactivation was not identified but may end several miles north of I-80. Reconnaissance mapping of normal faults along the leading edge of the Darby-Hogsback fault indicates the zone is segmented. The pattern of faulting appears to be different north and south of the Chapman Butte area (section 4, T. 13 N., R. 117 W.; plate I), suggesting the entire length did not rupture in any single event.

The tectonic models presented in the following sections are based on coherent reactivation of pre-existing thrust faults and imply that surface-rupture parameters along the leading edge of the Darby-Hogsback thrust should be similar to surface-rupture parameters documented for the Bear River fault zone to the west, i.e., 21 to 25 miles (34 to 40 km) surface-rupture length and net vertical tectonic displacements of 6.6 to 16.4+ feet (2 to 5+ m) per event.

Age of Movement and Recurrence Intervals

No reliable data are currently available concerning either the onset, minimum age of faulting, or recurrence interval along the normally-reactivated Darby-Hogsback fault. Initial surface displacement probably occurred after development of Bigelow Bench, which appears to grade into glacial deposits of possible Bull Lake age. The age of Bigelow Bench, based on dating of correlative glacial deposits in Yellowstone Park, may be about 150,000 years old (Pierce, 1979). Schlenker (personal communications, 1987, 1989) suggests the Bigelow surface is pre-Bull Lake in age. This would imply faulting may be considerably older than 150,000 years.

The minimum age of faulting is also poorly constrained but appears to be no younger than late Pleistocene to early Holocene based on the dissected nature of the scarps and well-adjusted drainage patterns. No morphotectonic features similar to those in the Bear River fault zone were identified that would indicate a mid- to late Holocene age. Recurrence intervals are inferred to be similar to the Bear River fault zone and probably ranged from about 1,000 to several thousand years between major surface-faulting events.

Tectonic Slip Rates

Total vertical tectonic displacement on the reactivated leading edge of the Darby-Hogsback fault is approximated by the elevation difference between the floor of the East Muddy Creek Valley and Bigelow Bench, about 660 feet (200 m). Using a tectonic slip rate of 0.06 in/yr (1.5 mm/yr) consistent with the north-central Bear River fault zone, 133,000 years would have been required for total apparent displacement of 660 feet (200 m) to have occurred.

According to Hansen (1985) separation of the Bear River and Green River drainage basins occurred post-600,000 years ago. Using 600,000 years as a maximum for onset of surface rupture and 660 feet (200 m) of vertical displacement, a slip rate of 0.01 in/yr (0.33 mm/yr) can be calculated. Assuming Bigelow Bench is Bull Lake in age, initial surface rupture occurred less than about 150,000 years ago (Pierce, 1979). Using 150,000 years as the maximum age of surface rupture, a slip rate of 0.05 in/yr (1.33 mm/yr) results. This slip rate is slightly lower than values obtained from the Bear River fault zone but is in reasonable agreement.

Summary

The leading edge of the Darby-Hogsback thrust was reactivated in a normal sense during mid- to late Quaternary time. Normal faults are apparent over a distance of more than 34.1 miles (55 km) along the subsurface trace of the pre-existing Darby-Hogsback thrust. Age of initial surface rupture is poorly constrained, but probably resulted in postulated separation of the Bear and Green River drainage basins less than 600,000 years ago (Hansen, 1985). Displacement of Bigelow Bench and tectonic slip rates derived from the Bear River fault zone suggest initial surface rupture could have occurred less than about 150,000 years ago. Latest normal movement on the Darby-

Hogsback fault appears to be late Pleistocene to early Holocene and probably pre-dates surface rupture in the Bear River fault zone. Past surface-faulting events along the Darby-Hogsback fault were probably similar in dimension to more recent events recorded in the Bear River fault zone.

Northeast-trending scarps paralleling the North Flank fault at the south end of the Bear River fault zone and near Elizabeth Ridge at the south end of the Darby-Hogsback fault are believed to result from mechanical adjustment to down-to-the-west displacement on north-striking normal faults.

PART IV - TECTONIC MODELS AND HAZARD ASSESSMENT

NEOTECTONIC MODELS

The Bear River fault zone and related deformation are products of late Quaternary extension along the eastern margin of the Basin and Range Province. Although the relationship of extensional tectonics to pre-existing structure is somewhat problematical, the presence of recurrent late Quaternary normal faulting on the Darby-Hogsback thrust plate, alignment of the Martin Ranch scarp with the leading edge of the Absaroka thrust, and other regional neotectonic features suggest more than a coincidental relationship. The well-defined nature of neotectonic deformation in the project area and the areal and subsurface configurations of pre-existing thrust faults provide a basis for tectonic interpretations.

Subsurface Structure

Published geologic sections prepared from high-density reflection seismic data (Dixon, 1982; Lamerson, 1982) provide the main source of subsurface data for the project area. These sections along with unpublished oil company seismic lines (Hunt Oil Company, personal communication, 1986; Marathon Oil Company, personal communication, 1986; Exxon USA, personal communication, 1987) provide the basis for interpretation of subsurface structure depicted on figure 71.

Seismic data (Dixon, 1982; Lamerson, 1982) disclose a ramp structure on the Darby-Hogsback thrust about 5.6 miles (9 km) west of the inferred subsurface trace of the leading edge. This ramp cuts sharply up-section through competent beds, mainly Paleozoic and lower to mid-Mesozoic units. The thrust flattens abruptly in Cretaceous marine shales. The transition from the ramp to the upper flat lies almost directly below the Bear River fault zone at a depth of about 3.0 miles (4.9 km).

Both the Darby-Hogsback and Absaroka thrusts steepen abruptly as they approach the existing ground surface. The Darby-Hogsback is commonly portrayed as a single thrust plane covered by thousands of feet of Eocene Wasatch Formation and younger rocks. The Absaroka thrust splays into two or three distinct fault planes in the near subsurface and is locally exposed in windows eroded through the Tertiary cover.

Neotectonic Development of the Bear River Fault Zone

Three hypotheses are advanced for development of the Bear River fault zone. The first suggests normal faults, including the Bear River fault zone, are formed by simple mechanical relaxation in weak Cretaceous and Tertiary sediments. The second hypothesis suggests basement-penetrating, basin-and-range faulting displaces older structures as the contemporary margin of the Basin and Range Province migrates to the east into the Middle Rocky Mountains and Colorado Plateau. The third hypothesis invokes reactivation of pre-existing thrust faults in a normal direction and propagation of listric normal faults as the result of superimposed tectonic extension.

Mechanical Relaxation

Dixon (1982, personal communication, 1984) is an advocate of the mechanical relaxation hypothesis. Compressional stresses in the thrust belt produced intense deformation in weak units, salt beds and shales, in the shallow subsurface. Adverse geometries coupled with release of compression and weak bedrock units resulted in mechanical relaxation which produced shallow, listric normal faults soling into underlying thrust planes. According to Dixon, the faults have no tectonic significance beyond a local adjustment to adverse geometries in incompetent bedrock. Faults produced by mechanical relaxation would generally be considered either aseismic or capable of producing low to moderate magnitude earthquakes (M_L=<5.0±).

The Bear River fault zone, however, does not fit the relaxation hypothesis. First, the Bear River fault zone has experienced at least two scarp-forming surface ruptures fully characteristic of seismogenic basin-and-range faulting. Second, the Bear River fault zone ruptured the surface in the last 5,000± years as a "new" tectonic feature. The structural geometry conducive to mechanical relaxation was in existence for literally tens of millions of years prior to this time. If the Bear River fault zone is a product of mechanical relaxation, why then did the fault zone develop in late Quaternary time, when the geometry had existed for tens of millions of years? Third, the fault zone is traceable in a regular pattern over at least 21 miles (34 km). Faults produced by relaxation would be strongly influenced by local stratigraphic and structural controls and would be less con-

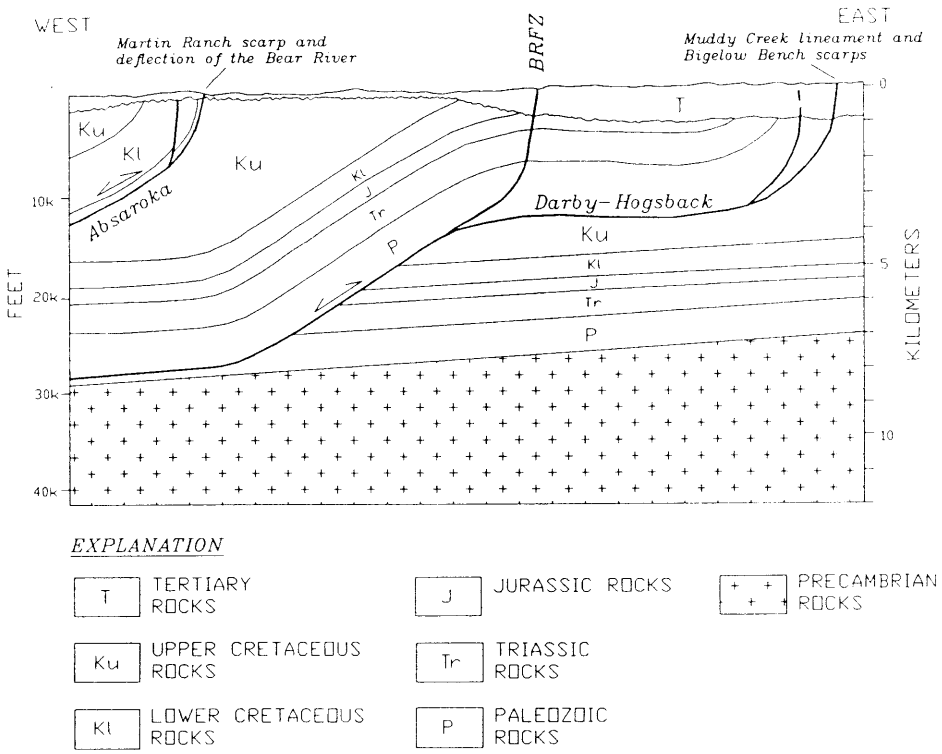

Figure 71. *Geologic cross section A-A′ (plate I) showing subsurface of the Darby-Hogsback thrust plate in the project area. Section is based on published geologic sections and reflection seismic data.*

tinuous and more irregular in pattern. Relaxation, therefore, does not offer a suitable explanation for development of the Bear River fault zone.

Basement-Penetrating Faults

Basement-penetrating normal faults associated with eastward migration of the Basin and Range Province appear to offer the most satisfactory explanation for the Bear River fault zone. This hypothesis eliminates the problems of timing and geometry. Extension could be imposed relatively late, for example in late Quaternary time, and would be consistent with the concept of an eastward migrating tectonic boundary encroaching on the Middle Rocky Mountains Province. Moreover, few if any geometric constraints exist, since the faulting would cut all older structure and penetrate to seismogenic depths. Deep-seated normal faults would also produce recurring surface rupture in the Bear River fault zone.

Although this hypothesis is straightforward, available subsurface data do not support it. No evidence from reflection seismic studies or drilling indicates that normal faults cut older structures or penetrate the basement. In fact, available oil company data show normal faults to be closely associated with ramp structures.

An unpublished reflection seismic line (Hunt Oil Company, personal communication, 1986) crossing the southern Bear River fault zone shows a down-to-the-west normal fault coinciding with the trace of surface rupture. Sediments to the west appear to sag between the main zone of normal faulting and what appears to be an antithetic fault to the west. The main and antithetic faults intersect at depth forming a half-graben. The main normal fault (Bear River fault zone) can be traced to the top of the Darby-Hogsback ramp where it merges with the pre-existing thrust plane as depicted on figure 71. No evidence indicates the normal fault continues down-dip and displaces either the Darby-Hogsback thrust plane or basement rocks. Couples (1986), however, suggests the position of thrust fault trailing edges and ramps are controlled by underlying basement structure including steeply-dipping normal or high-angle reverse faults.

On the other hand, it can be argued that (1) the seismic reflection technique lacks the resolution to "see" fine structure at great depth, and (2) high velocity reflectors such as the Cambrian Flathead Quartzite effectively mask underlying structure if it exists. The continuity of the Flathead Quartzite as a seismic reflector throughout the region, however, is cited (Dixon, 1982) as proof that faults penetrate neither the Flathead nor the underlying basement.

Reactivation of Thrust Faults

The third hypothesis invokes reactivation of pre-existing thrust faults as the result of superimposed east-west extension. Extension would cause the sense of motion on the older thrust faults to change from up-to-the-west reverse/thrust movement to down-to-the-west normal movement. Extension would be manifested by normal faulting along the leading edges of the affected thrust faults and by propagation of new normal faults

over points of stress concentration along the thrust planes, for example, the transition from thrust ramp to flat. In fact, this hypothesis appears to best explain the association of the Bear River fault zone with the ramp on the Darby-Hogsback thrust (figure 71). The Bear River fault zone is listric to the Darby-Hogsback thrust plane at the transition between the ramp and the upper decollement. East-west extension is transmitted along the basal decollement up the ramp to the ground surface via listric normal faults in the Bear River fault zone as shown on figure 71.

In the context of this interpretation, northeast-striking scarps south of Lily Lake at the southern end of the Bear River fault zone (plate I) are related to down-to-the-west normal faulting. The northeast-striking, down-to-the-north faults simply accommodate normal faulting against the buttressing effect of the Uinta Mountains. A north-south hinge line is inferred to exist some distance to the west of the Bear River fault zone, accounting for decreasing throw to the west along northeast-striking faults.

Change in sense of displacement along pre-existing faults explains the Martin Ranch scarp as the reactivated leading edge of the Absaroka thrust. In this case, extension has been transmitted along the pre-existing thrust plane to the ground surface in a normal sense.

Building on this interpretation, it is possible to account for other neotectonic features in the project area including terrace deformation east of the Bear River fault zone, the Muddy Creek lineament, fault scarps along the west side of Bigelow Bench and the Elizabeth Ridge scarps. During the earliest stages of east-west extension, the Darby-Hogsback thrust was reactivated as a normal fault and ruptured the surface as a series of right-stepping, en echelon faults along and east of the Muddy Creek lineament. Continued extension and normal faulting tilted the area west of the surface trace to the east. Recurrent fault movement produced progressively greater tilt with time. This regional eastward tilt is manifested by deformed terrace surfaces (figure 65) observed between the Bear River fault zone and the Darby-Hogsback thrust and may have been responsible for the postulated separation of the Bear and Green River drainage basins less than 600,000 years ago (Hansen, 1985).

Simultaneous with normal reactivation of the Darby-Hogsback thrust, northeast-striking, down-to-the-north faults formed against the Uinta Mountains to accommodate normal faulting and regional tilt to the east in much the same manner that scarps accommodate movement in the Bear River fault zone. The Elizabeth Ridge scarp with down-to-the-south displacement is anomalous but may represent a local adjustment, possibly backsliding on an older Laramide structure.

Continuing extension caused propagation of a listric normal fault system, the Bear River fault zone, above the Darby-Hogsback ramp. As this system developed the leading edge of the Darby-Hogsback was tectonically beheaded and may have become dormant. In this interpretation, tectonic extension is transmitted along the ramp normal fault system to the ground surface with no requirement for continued movement on the former thrust plane to the east. Simultaneous with development of the normal fault system over the Darby-Hogsback ramp, the leading edge of the Absaroka fault was reactivated and ruptured the surface as a down-to-the-west normal fault.

Several other lines of evidence support normal reactivation of the Darby-Hogsback and Absaroka thrusts including (1) the surface pattern of late Quaternary faulting and (2) a body of existing literature on normal reactivation of thrust faults.

Inspection of plate I shows that both the Darby-Hogsback and the Absaroka thrusts abruptly change strike from about N. 7-13° E. to a more northeasterly strike of N. 35-40° E. in T. 14 N. Based on published structure contour maps of the Darby-Hogsback and Absaroka thrust planes (Dixon, 1982; Lamerson, 1982), the change in strike is not related to significant flattening of dip, but instead may be related to sub-decollement structure and geometry of the craton margin (Beutner, 1977; Couples, 1986). A straight line drawn between inflection points (from northerly to northeasterly strike) on the Darby-Hogsback and Absaroka thrusts defines the northern end of the main Bear River fault zone. In addition, the short late Quaternary fault in sections 10 and 15, T. 14 N., R. 118 W. is located in the same position as the Bear River fault zone relative to the Darby-Hogsback and Absaroka thrusts and shows a parallel change in strike to the northeast.

The areal geometry of late Quaternary faults in the project area supports the concept that neotectonic deformation is intimately related to pre-existing structure. Right, en echelon late Quaternary normal faults are consistent with east-west extension superimposed on north-northeast striking, pre-existing thrust faults. A slightly oblique orientation of the minimum principal stress to the Darby-Hogsback ramp would produce right en echelon normal faults with a small component of left-lateral strike slip. Late Quaternary normal faults die out at the point where the thrusts swing to the northeast and obliqueness between the extensional stress field and the pre-existing thrust faults decreases. At the inflection point from north-northeast to northeasterly strike, the dip-slip component of movement decreases with an increase in left-lateral, strike-slip component. Scarp heights, expressed primarily as a function of dip-slip, vertical displacements should decrease. The amount of extension and resulting lateral displacement, however, may not be sufficient to produce observable strike-slip movement at the ground surface.

In 1985, Exxon drilled a well on Mumford Ridge in section 21, T. 13 N., R. 117 W. (plate I) near the leading edge of the Darby-Hogsback thrust. Although the target of this well is confidential, Exxon (personal communication, 1987) indicated the well was plugged and abandoned because reservoir seals were broken by previously unrecognized normal faults. Comparison of normal faults defined by Exxon from the test well and reinterpreted seismic data showed close correspondence to Quaternary normal faults along the Muddy Creek lineament and west side of Bigelow Bench. A proprietary structure map prepared by Exxon (personal communication, 1987) showed down-to-the-west, step-faults roughly corresponding to the leading edge of the Darby-Hogsback thrust. Near the Uinta Mountains to the south, Exxon's interpretation suggests normal faults swing to the west-southwest and parallel the north flank of the Uintas.

Exploration efforts in the thrust belt generally rely on high resolution seismic data and test well drilling. From this perspective, it is interesting to note that a thrust fault reactivated in a normal sense remains a thrust by definition unless subsequent normal slip exceeds initial reverse slip. The Darby-Hogsback

and Absaroka faults, despite neotectonic normal movement of a few tens of feet to perhaps several hundred feet in the contemporary tectonic setting, would still be classified as thrust faults. Furthermore, the distinction between primary thrust movement and subsequent change in sense of displacement is transparent to conventional exploratory and interpretive techniques.

Re-occupation of pre-existing structures by subsequent and unrelated stress fields is well documented in the geological literature. Several authors note changes in sense of displacement on pre-existing thrust faults under superimposed extension elsewhere in the Cordilleran thrust belt. A classic example is the Flathead normal fault of northern Montana and southern British Columbia, Canada (Bally and others, 1966; Dahlstrom, 1970; Constenius, 1982, 1988). The Flathead fault and the Kishenehn basin to the west are interpreted to have formed as the result of tectonic extension and change of sense of displacement on the Lewis thrust. The Flathead fault preferentially occupies a ramp on the Lewis thrust plane and has tectonically beheaded the thrust's leading edge. The Kishenehn basin formed as an eastward tilted half-graben on the west or downthrown side of the Flathead fault. This interpretation of the Lewis-Flathead fault system is virtually identical to the model postulated for the Bear River and Darby-Hogsback faults (figure 71).

Other workers, including Royse and others (1975); McDonald (1976); Sprinkel (1979); Corbett (1982); Royse (1983); and Skipp (1985), note that pre-existing thrust faults in the Cordilleran thrust belt of Montana, Idaho, Wyoming, and Utah may change sense of displacement from thrust to normal movement under superimposed regional tectonic extension. Structures characteristic of superimposed extension include normal faults listric to underlying thrust planes, especially ramps, and eastward tilted grabens and half-grabens.

Figure 72 summarizes the model for development of neotectonic features on the Darby-Hogsback and Absaroka thrust plates with time. The sequence of events is described as follows:

A. *Development of the Absaroka thrust in latest Cretaceous time.*

B. *Development of the Darby-Hogsback thrust in latest Cretaceous to mid- to late Paleocene time.*

C. *Onset of east-west-directed tectonic extension in Miocene to Holocene time.* Age of normal fault surface rupture in southwestern Wyoming and north-central Utah suggests onset of extension occurred in mid- to late Pleistocene time. It is possible, however, that extension pre-dated actual surface rupture by a considerable length time, perhaps hundreds of thousands of years. The interval between onset of extension and surface fault rupture may have been characterized by warping, folding, and episodic propagation of incipient normal fault planes through unfaulted Eocene sediments in thrust hanging walls.

D. *Normal reactivation and initial surface rupture along the leading edge of the Darby-Hogsback thrust.* The west side of Bigelow Bench was faulted in a series of eastward tilted blocks. The postulated separation of the Bear River and Green River drainage basins occurred as displacements increased. Normal movement along the Darby-Hogsback thrust caused warping of the Gilbert Peak erosion surface along the north flank of the Uinta Mountains and development of northeast- striking scarps on Elizabeth Ridge. The Bear River fault zone began to develop

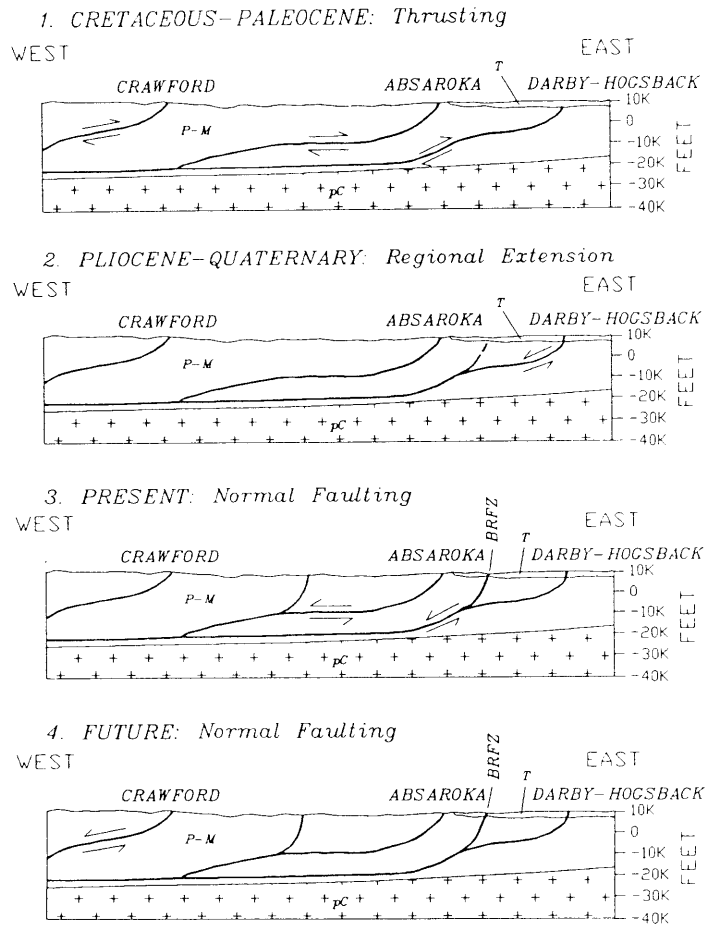

Figure 72. *Hypothetical model for neotectonic development of the Darby-Hogsback (D-H) and Absaroka thrust plates. (1) Development of the Crawford, Absaroka, and D-H thrust plates from west to east; (2) Normal reactivation of D-H thrust and propagation of the BRFZ over the thrust ramp; (3) BRFZ ruptures surface and Absaroka thrust is reactivated; (4) Absaroka ramp – normal faults rupture the surface and Crawford thrust is reactivated. Neotectonic deformation progresses from east to west, opposite sequence of thrusting.*

over the Darby-Hogsback ramp and propagate upward through unfaulted hanging wall sediments. It is conceivable that the Bear River fault zone may have nucleated along either a blind, imbricate thrust or a pre-existing "relaxation" normal fault. The precise age of initial movement on the Bear River fault zone is poorly constrained.

E. *Surface fault rupture along the Bear River fault zone and development of scarps against the Uinta Mountains as a mechanical response.* The leading edge of the Darby-Hogsback thrust was tectonically cut-off and may have become dormant or inactive.

F. *Reactivation of the Absaroka thrust and surface rupture along the Martin Ranch scarp at the leading edge.* The Bear River was deflected by normal movement on the Absaroka thrust south of the Martin Ranch scarp. Presumably, normal faults developed over ramps in the Absaroka thrust plane as the result of reactivation. The timing of Absaroka reactivation appears to

postdate reactivation of the Darby-Hogsback thrust. If this is indeed the case, reactivation due to tectonic extension proceeds from east to west, at least locally, opposite initial development of the thrusts from west to east in late Cretaceous to Paleocene time.

SEISMOGENESIS IN NORTH-CENTRAL UTAH, SOUTHWESTERN WYOMING, AND THE INTERMOUNTAIN SEISMIC BELT

Major earthquakes in the ISB occur on basement-penetrating, planar normal faults with 45° to 60° dips. This geometry, however, is not evident in southwestern Wyoming and north-central Utah where surface and subsurface geologic data indicate late Quaternary tectonic extension is accommodated along pre-existing thrust faults and related secondary listric structures. Reactivated thrust and listric normal faults show evidence of late Quaternary, recurrent, co-seismic surface rupture associated with large magnitude (M_L = 7.0 to 7.5) earthquakes. Critical questions are: are such faults truly seismogenic, or is surface rupture produced by non-seismogenic mechanical relaxation? If these faults are related to seismogenesis, what are the implications for seismotectonic hazard assessment in the ISB and eastern transition zone of the Basin and Range Province?

Seismogenesis in the ISB

The Borah Peak, Idaho earthquake of October 28, 1983 and re-evaluation of the Hebgen Lake, Montana earthquake of August 18, 1959, have produced a model for occurrence of large earthquakes accompanied by surface rupture in the ISB (Doser and Smith, 1982, 1983, 1985; Doser, 1984, 1985a, 1985b; Barrientos and others, 1985; Stein and Barrientos, 1985). The Hebgen Lake and Borah Peak events are the largest earthquakes of historic record in the ISB. Similar paleoseismic events accompanied by surface rupture are recorded by late Quaternary geomorphology and stratigraphy along the Wasatch fault zone of central Utah, the east flank of the Teton Range in northwestern Wyoming, and the east flank of Star Valley near Afton, among other locations.

The Hebgen Lake earthquake, assigned local magnitudes ranging from M_L = 7.1 to 7.7 (Bolt, 1984), was accompanied by 14.9 miles (24 km) of surface-fault rupture along the Red Canyon and Hebgen faults, and maximum vertical displacements of 22 feet (6.7 m). The Borah Peak earthquake has been assigned magnitudes of M_L = 7.2 and M_s = 7.3 (Doser, 1985b) and was accompanied by surface rupture over a length of 22.3 miles (36 km) with 8.9 feet (2.7 m) of maximum vertical displacement (Crone and others, 1985).

The Hebgen Lake and Borah Peak events are similar in magnitude, seismic moment, and surface-rupture characteristics. The characteristics of these historic events define a model for genesis of major earthquakes accompanied by surface rupture in the ISB. Analysis of seismological and geodetic data indicates:

1. Both earthquakes occurred on normal fault planes with dips in the range of 45° to 60°.
2. The events nucleated at depths of 7.4 to 9.9 miles (12 to 16 km).
3. Fault rupture propagated upward to the ground surface and in one direction along the causative fault.

These data imply paleoseismic events with surface rupture characteristics similar to Hebgen Lake and Borah Peak nucleated along moderately steeply dipping, planar faults penetrating to depths of 7.4 to 9.9 miles (12 to 16 km).

In contrast to major surface-faulting events in the ISB, historic earthquakes in the range of M_L = 6.0 to 6.5 do not produce surface rupture and apparently are not associated with known recurrent late Quaternary faulting (Doser, 1985b; Arabasz and others, 1987). The threshold for ground breakage in the ISB is inferred by Doser (1985b) to be M_L = 6.5 based on analysis of 15 events in the range of M_L = 6.0 to 7.0 recorded since 1870. The occurrence of historic events in the range of M_L = 6.5+ and apparent lack of association with known surface structure suggest these events nucleate on "blind" faults with no surface expression. Genesis of smaller events ($<M_L$ = 6.5 to 7.0) on blind structures follows a fundamentally different process than that for nucleation of M_L = 6.5-7.5 events accompanied by surface faulting.

Geological Versus Seismological Models

Despite seismological evidence outlined above, considerable debate exists over the geometry of normal faults in the ISB and the relationship of seismicity to surface and subsurface structure. Neotectonic research in north-central Utah and southwestern Wyoming bears directly on these issues. Geologic evidence indicates tectonic extension is accommodated along pre-existing thrust faults and secondary normal faults listric to stress points in thrust geometry. Late Quaternary extension is accompanied by co-seismic surface rupture comparable to the Hebgen Lake and Borah Peak events. No subsurface evidence exists in the study area, except by analogy to the Hebgen Lake/Borah Peak models, that paleoseismic events occurred on a 45° to 60° plane penetrating from the zone of surface rupture to depths of 7.4 to 9.9 miles (12 to 16 km).

Figure 73 shows major neotectonic features of the project area in cross-section. A hypothetical 45° rupture plane from an earthquake focus at a depth of 7.4 miles (12 km) to the zone of surface rupture along the Bear River fault zone, the locus of Holocene deformation, is also illustrated on figure 73. This hypothetical rupture plane, although consistent with seismological interpretations, does not account for reactivation of the Darby-Hogsback and Absaroka faults in a normal sense or the listric relationship of the Bear River fault zone to the Darby-Hogsback thrust.

Smith and Bruhn (1984) discuss intraplate extensional tectonics and the relationship of contemporary seismogenic faults to pre-existing tectonic structures. Their studies of the Wasatch Front indicate the areal position and subsurface geometry of the Wasatch fault are locally controlled by pre-existing thrust faults, ramps, and lateral transfer zones possibly related to extensional reactivation of these structures. Significant examples of this control include association of the Collinston-Ogden segment with a ramp anticline in the hanging wall of the Absaroka thrust

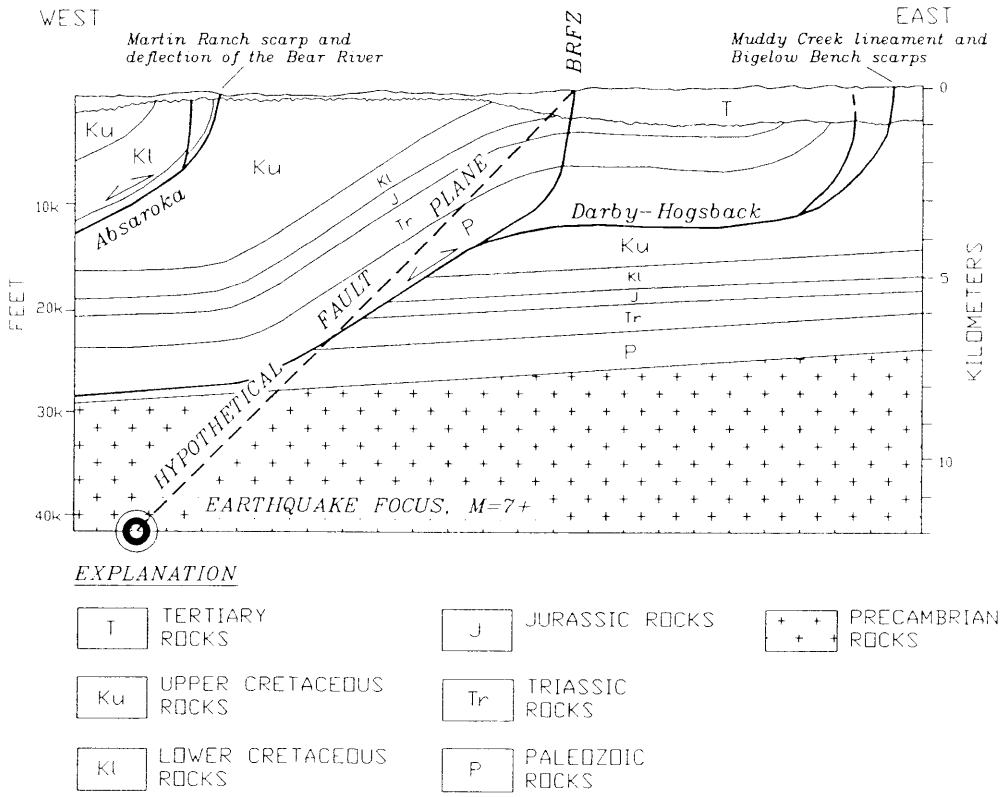

Figure 73. *Geologic cross section A-A'(plate I) showing relationship of hypothetical 45 degree fault plane and M=7.5 earthquake nucleating at a depth of 7.5 miles (12 km) to subsurface structure, the Bear River fault zone, and pre-existing thrust faults in the project area.*

and flattening of the Levan segment into the Pavant thrust plane at a depth of about 3.1 miles (5 km). The position of the Wasatch fault north of Salt Lake City is controlled by a ramp in the Absaroka thrust. Similar structural relationships between the Hoback and Star Valley faults and underlying thrust ramps are also noted by Smith and Bruhn (1984). In these latter cases, the normal faults flatten and merge into thrust planes at depth.

In other areas along the Wasatch fault zone, the association of normal faulting with pre-existing thrust geometry is not readily apparent; and in some areas, normal faults may actually cut thrusts at high angles. Smith and Bruhn (1984) conclude that although reactivation of thrust faults and ramps may occur along parts of the Wasatch fault zone, the hypothesis is not applicable for the entire length of the fault.

Smith and Bruhn (1984) also examined geometric evidence for extension in the Basin and Range of Utah and the transition zone into the Middle Rocky Mountains east of the Wasatch Front. They note that high-angle normal faults in the Sevier Desert appear to terminate at depth against a low-angle detachment fault. Moreover, they allow the possibility that Mesozoic thrust faults may have been reactivated during regional tectonic extension. East of the Wasatch Front, the East Cache Valley fault is interpreted as listric to the Willard thrust, although a possible high-angle interpretation cannot be precluded.

Reactivation of pre-existing thrust faults has been discussed and/or documented by a number of workers including Bally and others (1966); Dahlstrom (1970); Royse and others (1975); McDonald (1976); Sprinkel (1979); Wernicke (1981); Corbett (1982); Constenius (1982, 1988); Royse (1983); Bartley and Wernicke (1984); Skipp (1985); Wernicke and others (1985); and Hait (1988).

The apparent conflict in interpretation results from compelling seismological evidence for generation of large magnitude earthquakes accompanied by surface rupture along planar, basement-penetrating faults and equally compelling geological evidence for reactivation of pre-existing structures under regional tectonic extension. If the seismological interpretation is correct, no tectonic requirement would exist for reactivation of pre-existing, low-angle decollements and thrusts because seismogenic faults responsible for major earthquakes and surface rupture are planar, high-angle, and basement-penetrating. Conversely, reactivation of thrusts above a shallow, thin-skinned regional decollement would not account for observed seismological data recorded during the Hebgen Lake and Borah Peak events. The two hypotheses appear to be mutually incompatible even though evidence exists to show that both are correct, at least locally, in the ISB.

Smith and Bruhn (1984) attempted to reconcile geological evidence for listric, low-angle faulting and apparent reactivation of pre-existing thrusts with the seismological requirement for moderate to high-angle, basement penetrative, planar normal faults. They suggest several possibilities for reconciliation of apparent listric, low-angle fault geometries and moderate to high-angle, planar normal faults:

1. Planar normal faults extending below thrust faults and decollements are not recognized due to limitations of the seismic method.

2. Planar faults develop listric geometry as the result of strain compatibility requirements between brittle and ductile layers.

3. High-angle, planar faults are rotated to lower dips as the result of recurrent fault displacement.

4. Distributed movement across a broad, step-faulted zone mimics listric faulting.

Except for 2 above, these explanations suggest low-angle, listric geometries may not actually exist and, by implication, that reactivation of thrust faults may not occur.

In the conclusion to their article, Smith and Bruhn (1984) state:

> We suggest that the close spatial correlation between normal faults and thrust fault segmentation along the Wasatch Front reflects major east-trending structural and lithologic boundaries inherited from tectonic processes associated with the evolution of the cordilleran miogeocline, that began in the Precambrian. This hypothesis is significantly different from one in which thrust belt structures are thought to place primary structural control on subsequent normal fault systems.

The relationship between subsurface structure and seismicity in the ISB has been examined by Arabasz and Julander (1986). They note diffuse background seismicity is apparently controlled by variable mechanical behavior in vertically stacked thrust plates or low-angle detachments. Moderate earthquakes occur on blind structures without direct evidence of surface expression. Large magnitude earthquakes nucleate at depths of 9.3+ miles (15+ km) but rupture pathways to the surface are unclear.

The capability of low-angle faults to generate earthquakes is also addressed by Arabasz and Julander (1986). Focal plane solutions suggest seismic slip occurs along fault planes with moderate to high dip with only weak evidence for seismic slip on low-angle (<30°) fault planes. Arabasz and Julander (1986) find no evidence for clustering of earthquake foci on low-angle faults. Focal mechanisms, similarly, do not support seismic slip on either listric or low-angle normal faults. The presence of listric and low-angle normal faults in the ISB is considered problematical. Seismic slip in areas of pervasive listric and low-angle faulting is postulated to occur along (1) upper, steeply dipping parts of listric faults, (2) related antithetic faults, and/or (3) secondary faults in the interior of blocks bounded by listric or low-angle normal faults (Arabasz and Julander, 1986). They also suggest that future experience could indicate whether seismic slip can occur along low-angle normal faults.

Despite the lack of evidence for seismic slip on low-angle tectonic structures, Arabasz and Julander (1986) state:

> ... background seismicity is fundamentally controlled by variable mechanical behavior and internal structure of individual horizontal plates within the seismogenic upper crust.

Although seismic slip has not been proven to occur along listric or low-angle normal faults in the ISB, it seems clear that pre-existing low-angle structures including thrust faults and detachments exert a fundamental control on low to moderate level seismicity. Much of this seismicity cannot be associated with known surface structure including recurrent, late Quaternary faulting. Low- to moderate-level events (M = 6.0 to 6.5) occur along blind structures within blocks bounded by listric normal, low-angle normal, and thrust faults. Figure 74 (Arabasz and Julander, 1986) shows the relationship of seismicity to geological structure in the ISB.

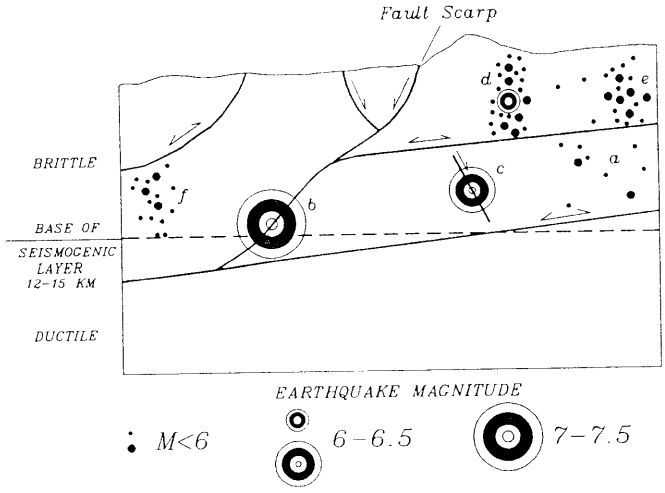

Figure 74. *Diagrammatic geologic cross section (Arabasz and Julander, 1986) showing relationship of seismicity to various types of geologic structures in ISB. Donuts=moderate to large earthquakes. Dots=microseismicity. Bi-directional fault-slip arrows indicate normal reactivation of thrust faults. Letters designate: a=predominance of local seismicity within a lower plate; b=nucleation of a large earthquake at the base of the seismogenic layer on an old thrust ramp; c=moderate-sized earthquake occurring on a blind structure; d=occurrence of a moderate earthquake and aftershocks with deformation restricted to an upper plate; e=diffuse block-interior seismicity within an upper plate; f=diffuse block interior seismicity in a lower plate with lower frequency of occurrence. The base of the seismogenic layer at 7 to 9 miles (12-15 km) divides the crust into an upper brittle layer and lower, quasiplastic, ductile layer.*

Arabasz and Julander (1986) also address the occurrence of large magnitude events accompanied by surface rupture. They conclude that major earthquakes occur along basement-penetrating, planar faults dipping 45° to 60°. Figure 74 shows a large magnitude surface-faulting event nucleating along a pre-existing thrust ramp with coseismic slip propagating to the surface along a listric normal fault. No vertical scale is provided but presumably the event would nucleate at a depth of 9.3± miles (15± km) consistent with the Hebgen Lake and Borah Peak events. Linkage of nucleation points of large magnitude earthquakes to surface rupture along pre-existing thrusts and listric normal faults is considered a possibility although the mechanics of such linkage are poorly understood. The hypothetical cross section presented by Arabasz and Julander (1986) on figure 74 is virtually identical to subsurface interpretations in the project area shown on figures 71 and 73.

In conclusion, Arabasz and Julander (1986) state:

> The possibility of initiating seismic slip on low-angle detachments remains an uncertain 'wild card'. Another key issue is the interaction of crustal extension at depth and that manifested in the uppermost crust, particularly

in the form of the shallow background seismicity that we observe.

Conclusions

Research in southwestern Wyoming and north-central Utah in comparison with the Hebgen Lake and Borah Peak areas suggests different levels of maturity and tectonic/structural relationships exist with time and location in the ISB/eastern Basin and Range transition zone. Hebgen Lake and Borah Peak represent evidence of mature seismogenesis manifested by imposing fault-bounded mountain blocks and evidence of recurrent normal fault movements with great displacements. The Bear River fault zone and normally-reactivated thrust faults represent an early, youthful stage of seismogenesis in a thrust-faulted terrain. Continued tectonic deformation may produce fault-bounded mountain ranges with remnants of thrust plates preserved within the block similar to the Wasatch Range east of Salt Lake City. Major seismogenic faults, which may be "blind" sub-decollement structures in early stages of extension, eventually rupture the surface as a 45° to 60° planar faults. The early tectonic relationship between regional extension and normally reactivated leading edges of thrust faults and ramp structures is destroyed with time. The idea that all late Quaternary surface faults in the ISB are steeply dipping and penetrate from ground surface to depths of 7.4 to 9.3 miles (12 to 15 km) may be an oversimplification that is applicable to certain seismically mature areas but cannot be applied unilaterally to all areas in the ISB/eastern basin-and-range transition zone.

SEISMOTECTONIC HAZARD ASSESSMENT

The Bear River and Absaroka faults exhibit clear evidence of Holocene surface rupture and would be considered seismogenic (active or capable) by widely accepted criteria. The reactivated leading edge of the Darby-Hogsback thrust also exhibits evidence of recurrent Quaternary movement but appears, at least circumstantially, to be older than normal faults to the west. Considering the absence of detailed studies, the normally reactivated leading edge of the Darby-Hogsback thrust could be considered independently seismogenic depending on the degree of conservatism required for engineering analyses.

Historic Seismicity

Review of historic seismicity data compiled by the University of Utah (1985) shows no coherent pattern of past earthquake occurrence in the project area (figure 75). In fact, the project area appears to be seismically quiescent with respect to surrounding areas. North of the project area, a north-northeast-trending belt of seismicity is spatially associated with the Darby-Hogsback and Absaroka thrust plates. This spatial association is potentially significant but has not been evaluated in light of evidence for late Quaternary faulting associated with normal reactivation of thrust faults. Smith (personal communication, 1985) of the University of Utah stated that apparent seismicity associated with the Darby-Hogsback and Absaroka thrust plates was assumed to be related to mining and petroleum exploration activities in the Kemmerer area. He added, however, that documented evidence for late Quaternary tectonic deformation south of Kemmerer would necessitate a re-evaluation of this assumption.

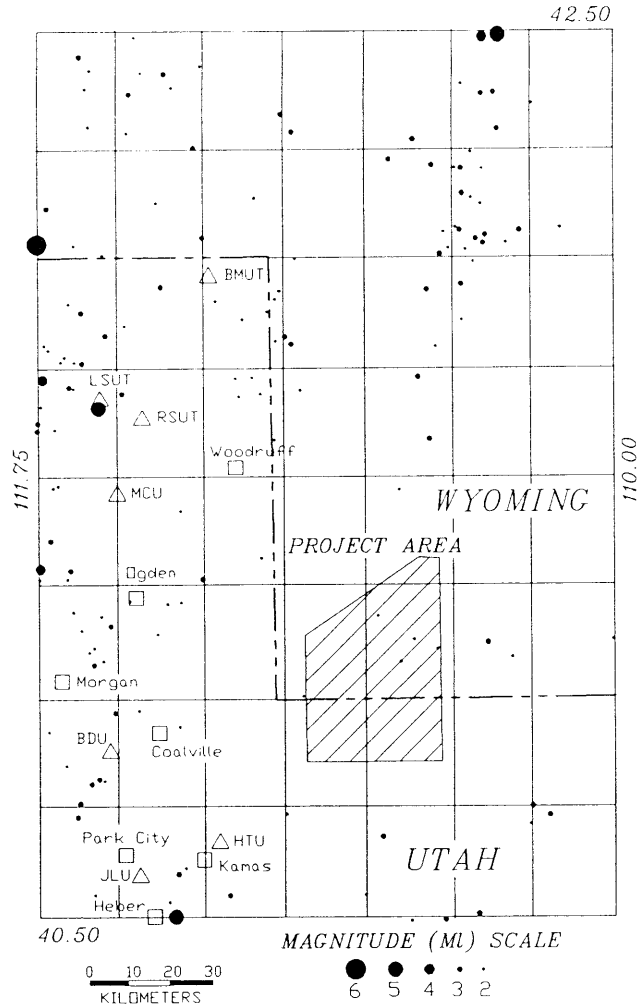

Figure 75. Seismicity map of north-central Utah and southwestern Wyoming compiled from the earthquake data base system, University of Utah Seismograph Stations (August 1985). Recording stations are indicated by triangles. Note the paucity of seismicity in the project area. Increased seismicity, however, appears to be associated with the projection of Darby-Hogsback and Absaroka thrusts to the north-northeast.

The largest earthquakes recorded near the project area are magnitude 4 or less. No known local historic events have caused damage or surface-fault rupture in the area. Small, infrequent tremors, however, have been reported by local ranchers. Historic seismicity does not illuminate late Quaternary faults in the project area and is considered of no value in characterizing hazard. In fact, over-reliance on historic seismicity could lead to the opposite conclusion: no significant hazard is present.

Table 12.
Paleoearthquake magnitudes.

SOURCE ZONE / STRUCTURE	PALEOEARTHQUAKE MAGNITUDE (M_S)
Bear River fault zone	6.9 - 7.4
Absaroka fault	6.3 - 6.9
Darby-Hogsback fault	6.9 - 7.4
Regional "floating" EQ	6.5

Paleoearthquakes and Hazard Assessment

In the absence of historic seismicity data, the surface-rupture parameters described earlier in the sections on the Bear River, Absaroka, and Darby-Hogsback faults were used to estimate the magnitudes of paleoearthquakes for each apparent seismogenic structure in the project area. Paleoearthquake magnitudes for each structure are summarized in table 12 and discussed in the following paragraphs. A regional "floating" earthquake is also possible based on the fact that events up to $M_L = 6.5\pm$ can occur on "blind" structures without surface manifestation.

The Maximum Credible Earthquake (MCE), defined as the largest event likely to occur on a seismogenic structure in the contemporary geologic/tectonic setting, is commonly used in earthquake-hazard assessment. Conservatism in engineering practice has generally dictated adding ¼ to ½ magnitude to the largest postulated paleoearthquake to arrive at the maximum "credible" event, or MCE. A number of workers, most notably Allen (personal communication, 1990) in review of this paper, argue strongly against the MCE concept for use in modern earthquake-hazard assessment. The fundamental objection is the subjective nature of the MCE. Simply stated: What is credible and what is not? The answer is largely in the eye of the beholder. To a public utility attempting to permit a large storage reservoir or to license a nuclear power plant, an MCE of M = 7.0 may seem incredibly large and result in significant increases in engineering and construction costs. To opponents of the same project, an MCE of M = 7.0 may seem incredibly small and a thinly veiled attempt by the utility to force an unsafe project on an unsuspecting public. Engineers, caught in the middle between owners/clients and the public, commonly adopt a maximum hazard design philosophy, which perpetuates the MCE concept. The engineer designs for the largest hazard reasonably conceivable and treats uncertainty with a conservative "factor of safety."

I concur with Allen; the MCE is a dying concept and has lingered too long. The future of earthquake-hazard assessment lies in probabilistic methods. The data in this report provides a partial basis for such an assessment. Further consideration of historic seismicity, in my opinion, would be required to arrive at a complete probabilistic earthquake hazard assessment for the study area in north-central Utah and southwestern Wyoming.

Bear River Fault Zone

Data from this study indicate the Bear River fault zone has ruptured the surface twice during the late Holocene. Surface rupture length and vertical tectonic displacements per event were used to estimate magnitudes of paleoearthquakes generated by the Bear River fault zone. Techniques outlined by Slemmons (1977); Wyss (1979); and Bonilla and others (1984) were used in the analyses. Surface-rupture lengths assumed for analysis ranged from 21 miles (34 km), the main zone of surface rupture, to 25 miles (40 km), the main zone of surface rupture extended to include the short scarp in sections 10 and 15, T. 14 N., R. 118 W. (plate I). Mean net vertical tectonic displacements from geomorphic offset, stratigraphic offset and colluvial-wedge stratigraphy were also used in the analyses. Mean minimum and maximum net vertical tectonic displacements per event were estimated to be 6.9 feet (2.1 m) and 16.7 feet (5.1 m; table 6), respectively.

Fault width (Wyss, 1979) was calculated using an assumed 45° dip and nucleation depth of 7.4 to 9.3 miles (12 to 15 km). Earthquake magnitudes derived from surface-rupture parameters and empirical techniques are summarized in tables 13 and 14.

Rupture length versus magnitude and displacement per event versus magnitude relationships for plate interior and all data compiled by Bonilla and others (1984) suggest the surface wave magnitude of each of the two documented surface-faulting events in the Bear River fault zone was in the range of $M_S = 7.0$ to 7.3. Earthquake magnitude (unspecified) versus rupture length multiplied by displacement per event or displacement per event squared compiled by Slemmons (1977) indicates prehistoric events ranged from M = 7.1 to 7.4. Wyss's (1979) fault-rupture width technique yields estimates of $M_S = 6.9$ to 7.1 depending on the depth of nucleation, 7.4 miles (12 km) versus 9.3 miles (15 km). The range of magnitudes derived from various techniques is generally consistent with the largest historic events to have occurred within the Basin and Range Province and the ISB. Comparison of surface rupture length, net tectonic displacement per event, and slip rates for the Bear River and Wasatch fault zones show surprisingly good agreement.

The estimation of paleoearthquakes for normal faults is based on empirical relationships established for basement-penetrating structures discussed in the section on Seismogenesis in North-Central Utah, Southwestern Wyoming, and the Intermountain Seismic Belt. This may not be the case in the Bear River fault zone where geologic evidence suggests extension is accommodated along pre-existing thrust faults. The Bear River fault zone and underlying decollements apparently do not penetrate to sufficient depths (>4.3 mi or 7 km) to produce large magnitude earthquakes (figure 73). The paleoearthquake magnitudes postulated for the Bear River fault zone (table 13), therefore, reflect

Table 13.
Estimates of paleoearthquake magnitudes from surface-rupture lengths and surface displacements, north-central Utah and southwestern Wyoming.

FAULT ZONE	SURFACE RUPT. LENGTH (km) MIN.	MAX.	VERT. DISPLACE. (m) MIN.	MAX.	LENGTH INT.* (M_S)	ALL*	DISPLACE. NORMAL ** (M_S)	SLEMMONS 1977 log LD (M)	log LDD (M)
Bear River	34	40	2.04	5.27	7.1 - 7.2	7.1 - 7.2	7.0 - 7.3	7.1 - 7.4	7.1 - 7.4
Absaroka	5	15	0.82	0.85	6.3 - 6.9	6.4 - 6.9	6.7 - 6.8	6.5 - 6.7	6.6 - 6.8
Darby-Hogsback	34	40	2.04	5.27	7.1 - 7.2	7.1 - 7.2	7.0 - 7.3	7.1 - 7.4	7.1 - 7.4

**Bonilla, Mark and Lienkaemper (1984) plate interior and all fault data.*
***Bonilla, Mark and Lienkaemper (1984) normal fault data.*
To convert kilometers to miles divide by 1.6.
To convert meters to feet multiply by 3.28.

Table 14.
Estimates of paleoearthquake magnitudes from rupture lengths and down-dip fault widths, north-central Utah and southwestern Wyoming (Wyss, 1979).

FAULT ZONE	FAULT WIDTH (km) MIN.	MAX.	FAULT LENGTH (km) MIN.	MAX.	FAULT AREA MIN.	MAX.	MAGNITUDE (M_S = log A + 4.15) MIN.	MAX.
Bear River	16.9	21.2	34	40	575	848	6.9	7.1
Absaroka	16.9	21.2	5	15	85	318	6.1	6.7
Darby-Hogsback	16.9	21.2	34	40	575	848	6.9	7.1

To convert kilometers to miles divide by 1.6.

maximum values, based on the assumption that faulting is planar and basement-penetrating.

Specification of focal depth and hypocentral location is problematical since the Bear River fault zone does not fit current models for seismogenic structures in the ISB. Seismologists (Stein and Barrientos, 1985; Arabasz and Julander, 1986) indicate that major earthquakes producing surface rupture nucleate along fault planes dipping at approximately 45° at depths of 7.4 to 9.3 miles (12 to 15 km). Using this interpretation arbitrarily for hazard-assessment purposes, earthquakes generated by the Bear River fault zone would nucleate down-dip along a hypothetical 45° plane at a minimum depth of 7.4 miles (12 km) as depicted on figure 73. This interpretation, however, is in conflict with geologic evidence for reactivation of thrust faults in the project area.

Absaroka Fault

The Absaroka thrust has been reactivated in a normal direction by the same regional stress field responsible for development of the Bear River fault zone. Minimum age of movement appears to be equivalent to the Bear River fault zone based on geomorphic expression and trenching of the Martin Ranch scarp. Direct evidence of surface rupture extends over a distance of 3.1 miles (5.0 km). Inclusion of indirect evidence for surface deformation south of the Martin Ranch scarp, (tectonic deflection of the Bear River) would increase maximum surface-rupture length to 9.3 miles (15.0 km). Maximum and minimum estimates of net vertical tectonic displacement per event range from 4.3 to 5.2 feet (1.3 to 1.6 m; table 11).

Evidence for surface rupture along the reactivated leading edge of the Absaroka fault and correlation with latest surface rupture in the Bear River fault zone imply movement on the two faults is related. The neotectonic model invoking coherent, normal reactivation of pre-existing thrust faults is compatible with movement on the Absaroka fault. Slip from a single seismic event nucleating at depth could propagate to the surface along pre-existing thrust planes. As an alternative, movement on the Absaroka could be a near surface mechanical response (relaxation) due to faulting and strong ground shaking elsewhere in the region. In either case, the reactivated leading edge of the Absaroka fault would not be considered independently seismogenic. If the Absaroka is assumed to be independently seismogenic, analyses of fault length-displacement versus magnitude relationships and fault rupture width (tables 13 and 14) indicate the fault may have produced paleoearthquakes in the maximum magnitude range of M_S = 6.3 to 6.9.

Darby-Hogsback Fault

The Darby-Hogsback fault shows evidence of normal reactivation in Pleistocene time (post 600,000 years). No substantive evidence was found to suggest movement occurred within the last 5,000 ± years comparable to the Bear River and Absaroka faults. Moreover, the model for neotectonic deformation in the project area suggests that the leading edge of the Darby-Hogsback fault was tectonically cut-off and became dormant or inactive with propagation of listric normal faults over the ramp to the west. Continued east-west extension was taken up by movement along the Bear River fault zone.

Based on lack of recent movement comparable to the Bear River fault zone and the proposed neotectonic model, the Darby-Hogsback fault may not be a seismogenic structure in the contemporary tectonic setting. Any conclusion regarding the

seismic potential of the leading edge of the Darby-Hogsback fault, however, must be tempered by the absence of detailed field study and reliable data on minimum age of faulting, recurrence intervals, and slip rates.

Using the neotectonic model as a unifying concept, rupture characteristics of the Bear River fault zone can be applied to the leading edge of the Darby-Hogsback fault. Paleoearthquake magnitudes for the normally-reactivated leading edge of the Darby-Hogsback fault are inferred to be similar to the Bear River fault zone. Accordingly,.the Darby-Hogsback fault may have generated Ms = 6.9-7.4 paleoevents accompanied by 21 to 25 miles (30 to 40 km) surface rupture and net vertical tectonic displacements of 6.6 to 16.4 + feet (2 to 5 + m) per event. Earthquake magnitudes are maximum values, however, and are based on the assumption that faulting is basement-penetrative.

Northeast-Striking Scarps

Northeast-striking scarps paralleling the North Flank fault at the south end of the Bear River fault zone and near Elizabeth Ridge at the south end of the Darby-Hogsback fault are believed to result from mechanical adjustment to down-to-the-west displacement on north-striking normal faults. Accordingly, these short scarps do not constitute evidence for reactivation of the North Flank fault and are not considered independently seismogenic.

Surface-Fault Rupture

Hazards due to surface-fault rupture are portrayed on plate I. In general, high surface-rupture hazard is present along the trace of the Bear River fault zone and along the leading edge of the Absaroka fault between Sulphur Creek and the Bear River floodplain to the south. Moderate surface-rupture hazard is present along the leading edge of the Darby-Hogsback fault, leading edge of the Absaroka fault north and south of the high risk area described above, and over the Darby-Hogsback ramp along the north-northeasterly extension of the Bear River fault zone. Within the high-risk zone, surface displacements of less than 3.3 feet (1 meter) to more than 16.4 feet (5 m) can occur. Surface displacements comprise both tectonic and secondary mechanical components. Displacements in moderate-risk areas, although less likely to occur, could be of similar magnitude.

Secondary Seismotectonic Hazards

Ground Tilt/Subsidence

Large magnitude earthquakes (>M = 7.0) produced by surface faulting in the Basin and Range and ISB are generally accompanied by ground tilt and subsidence extending considerable distances from the zone of surface rupture. For example, the Hebgen Lake earthquake of 1959 produced vertical ground/tilt subsidence of at least 1 foot (0.3 m) over an area extending 8.5 miles (13.7 km) from the surface-fault rupture. Maximum elevation changes adjacent to the fault were greater than 19.7 feet (6 m). Extreme tilting of the Hebgen Lake basin caused overtoppling of Hebgen Lake Dam by a series of waves.

Evidence of alluvial terrace deformation over large areas in southwestern Wyoming and north-central Utah indicates that similar widespread tilt/subsidence has accompanied normal-slip movement along the Darby-Hogsback, Bear River, and Absaroka faults. Qualitative comparisons with the 1959 West Yellowstone earthquake and postulated tilt associated with the Teton fault near Jackson Lake dam in northwestern Wyoming (USBR, 1983) suggest that ground deformation west of the Bear River fault zone could be on the order of ten feet or more during a major surface-faulting event (plate I). Generally, potential for ground deformation in the project area increases toward the surface trace of each late Quaternary fault and from north to south along strike with maximum potential deformation reaching 16.4+ feet (5+ m) at the zone of surface rupture.

Liquefaction

Strength and duration of ground motion from potential earthquakes in the project area are capable of causing liquefaction of susceptible soils, generally saturated cohesionless silts and sands. The north flank of the Uinta Mountains is underlain by relatively great thicknesses of unconsolidated deposits mainly of glacial origin. Present and former stream valleys north of the Uintas also are mantled by varying thicknesses of silts, sands, and gravels. These deposits, if saturated, may be subject to liquefaction in the event of a moderate to large earthquake in the region. Areas subject to high and moderate risks of earthquake-induced liquefaction are illustrated on plate I.

The normal effect of unconsolidated material overlying bedrock is to modify peak horizontal acceleration, peak velocity, and duration of ground shaking by some factor over base rock ground motions for a site founded on bedrock. These effects have significance in terms of structural and stability analyses but are difficult to characterize without extensive site and soil dynamics studies. Adding to the problem is the lack of empirical experience with site and dynamic soil response for earthquakes greater than M = 6.5, especially in the near field. Site-specific liquefaction and soil dynamics studies are recommended for critical structures or facilities.

Earthquake-Induced Landslides

Numerous landslides are present in southwestern Wyoming and north-central Utah, particularly in areas underlain by claystones and shales of the Wasatch Formation. A large segment of the Bear River fault zone, in fact, is obscured by post-fault landslide debris. Hansen (1969) reports that a large rockfall on the Middle Fork of the Blacks Fork River was possibly triggered by earthquake activity in the region. Whether or not this rockfall and/or other landslides are attributable to either strong ground motion or normal static instability is virtually impossible to determine. Clearly, moderate to strong earthquakes greater than magnitude M = 6.0 are capable of triggering landslides. A large-magnitude earthquake occurring on the Bear River fault zone could be expected, therefore, to produce landsliding in the region. Areas of existing landsliding in the project area are illustrated on plate I.

PART V - CONCLUSIONS AND RECOMMENDATIONS

CONCLUSIONS

Neotectonic deformation in north-central Utah and southwestern Wyoming is interpreted as resulting from regional east-west extension superimposed on the Darby-Hogsback and Absaroka thrust plates. Pre-existing thrust faults were reactivated in a normal sense and caused propagation of "new" listric normal faults over stress points, particularly at the transition from thrust ramps to flats in Jurassic salts and Cretaceous marine shales.

The Bear River fault zone developed above the Darby-Hogsback ramp and has experienced recurrent, Holocene movement over a length of 21 to 25 miles (34 to 40 km) with net vertical tectonic displacements ranging from less than 3.3 feet (1 m) to greater than 16.4 feet (5 m) per event. Two distinct surface-faulting events are represented by scarps and associated scarp-derived colluvial deposits.

Ages of surface rupture were estimated by radiocarbon dating of tectonically buried and modern A-horizons and other organic material exposed in trenches excavated across late Quaternary fault scarps. Calibrated radiometric ages indicate surface-faulting events occurred at 4,620±690 and 2,370±1,050 yr B.P. Estimates of recurrence intervals, based on these ages, range from 2,250 to over 2,370 years. Interpreted ages of surface-faulting events, however, have not been corrected for apparent mean residence time; thus, ages of surface-faulting events may be too old by several hundred years.

Surface-rupture lengths of 21 to 25 miles (34 to 40 km), vertical tectonic displacements of <3.3 to >16.4 feet (<1 to >5 m) per event, and slip rates of 0.04 to 0.1 in/yr (1.0 to 3.1 mm/yr) are comparable to the Wasatch fault, a major earthquake source zone in the ISB. The Bear River fault zone, based on criteria for seismogenic basement-penetrating normal faults, may have produced paleoearthquakes of M_S = 6.9-7.4. The mean age of latest surface rupture (2,370 yr B.P.) and minimum apparent recurrence interval (2,310 years) suggest a major earthquake could occur at any time in north-central Utah and southwestern Wyoming.

The Martin Ranch scarp is coincident with the leading edge of the Absaroka thrust about 4.5 miles (7.2 km) to the west of the Bear River fault zone. It developed in response to normal reactivation of the pre-existing thrust plane. Related tectonic deformation extending at least 6 miles (10 km) south of the Martin Ranch scarp deflected the channel of the Bear River. Scarp-derived colluvial deposits record one surface-faulting event over a length of 3.1 miles (5.0 km). Estimates of mean net vertical tectonic displacements for the single event range from 2.6 to 4.6 feet (0.8 to 1.4 m). The age of latest surface rupture is coeval with latest surface rupture in the Bear River fault zone, 2,370 ± 1,050 yr B.P. Similar ages of movement suggest displacement along the Martin Ranch scarp occurred as a simultaneous response to east-west extension superimposed on pre-existing thrust and ramp-normal faults. Slip rates on the normally reactivated leading edge of the Absaroka thrust range from 0.02 to 0.03 in/yr (0.6 to 0.7 mm/yr).

Fault scarps displacing Pleistocene geomorphic surfaces and associated outwash/alluvium, and a regional eastward tilt of terrace surfaces indicate the leading edge of the Darby-Hogsback thrust was also reactivated but now may be dormant or inactive due to development of the Bear River fault zone over the ramp structure to the west. Normal displacements along the leading edge of the Darby-Hogsback fault are believed responsible for apparent separation of the Bear and Green River drainage basins less than 600,000 years ago. Data concerning the independent seismogenic potential of the Darby-Hogsback fault are incomplete. Conservative treatment of earthquake hazards for engineering purposes may require that both the Absaroka and Darby-Hogsback faults be considered seismogenic structures.

Northeast-striking fault scarps sub-paralleling the north flank of the Uinta Mountains are believed to be mechanical adjustments related to reactivation of the leading edge of the Darby-Hogsback thrust and normal faulting in the Bear River fault zone. No evidence was found to suggest these scarps are related to independent tectonic movement on the North Flank fault.

Geologic evidence for late Quaternary deformation in southwestern Wyoming and north-central Utah is in apparent conflict with current seismological models for genesis of major earthquakes accompanied by surface rupture in the ISB. Analysis of seismological data from the 1983 Borah Peak (M = 7.2+) and the 1959 Hebgen Lake (M = 7.1+) events indicate major earthquakes accompanied by surface rupture nucleate along 45° dipping fault planes penetrating to depths of 7.4 to 9.3 miles (12-15 km).

Neotectonic deformation in north-central Utah and southwestern Wyoming is believed to represent the earliest stages of tectonic extension superimposed on a pre-existing thrust-faulted terrain. Borah Peak, Hebgen Lake, and the Wasatch Front represent late-stage development of the same process in a mature, active tectonic terrain. Intermediate stages of contemporary extensional tectonic development are inferred to be present along the eastern transition zone of the Basin and Range Province.

RECOMMENDATIONS

Tectonic deformation in north-central Utah and southwestern Wyoming has potentially significant implications for seismogenesis and earthquake-hazard assessment in the ISB. Additional studies are recommended to address the following issues:

1. Surface and subsurface relationships of late Quaternary tectonic deformation to pre-existing thrust faults and other Laramide structures.

2. History of Quaternary normal movement along the reactivated leading edge of the Darby-Hogsback thrust east of the Bear River fault zone.

3. Extent and degree of alluvial terrace deformation and relationship to late Quaternary tectonic deformation.

4. Tectonic evidence for Pleistocene separation of the Bear River and Green River drainage basins and Holocene deflection of the Bear River channel.

5. Comparison of models for occurrence of large-magnitude earthquakes in the ISB to structure and tectonics of the Darby-Hogsback and Absaroka thrust plates in southwestern Wyoming and north-central Utah.

6. Continued development of an integrated structural-tectonic model that accounts for all geologic/seismologic data in the study area and assessment of its implications for seismogenesis and earthquake hazard/risk.

7. Application of the conceptual tectonic model to other parts of the ISB/eastern Basin and Range transition zone.

SELECTED REFERENCES

Allen, C.R., 1968, The tectonic environments of seismically active and inactive areas along the San Andreas fault system, *in* Dickinson, W.R., and Grantz, Arthur, editors, Proceedings of the Conference on Geologic Problems of San Andreas Fault System: Menlo Park, Stanford University Publications, Geological Sciences v. XI, p. 70-82.

Anderson, L.W., and Miller, D.G., 1979, Quaternary fault map of Utah: Long Beach, California, Fugro, Inc., Consulting Engineers and Geologists, 35 p., scale 1:500,000.

Arabasz, W.J., and Julander, D.R., 1986, Geometry of seismically active faults and crustal deformation within the Basin and Range-Colorado Plateau transition in Utah, *in* Mayer, Larry, editor, Extensional tectonics of the southwestern United States - A perspective on processes and kinematics: Geological Society of America Special Paper 208, p. 43-74.

Arabasz, W.J., Pechmann, J.C., and Brown, E.D., 1987, Observational seismology and the evaluation of earthquake hazards and risk in the Wasatch Front area, Utah, *in* Gori, P.L. and Hays, W.W., editors, Assessment of regional earthquake hazards and risk along the Wasatch Front, Utah: U.S. Geological Survey Open-File Report 87-585, p. D-1 to D-58.

Arabasz, W.J., and Smith, R.B., 1979, Introduction - What you've always wanted to know about earthquakes in Utah, *in* Arabasz, W.J., Smith, R.B., and Richens, W.D., editors, Earthquake studies in Utah - 1850 to 1978: Salt Lake City, University of Utah Seismograph Station, Department of Geology and Geophysics, p. 1-15.

—1981, Earthquake prediction in the Intermountain seismic belt - An intraplate extensional regime, *in* Earthquake prediction - an international review: American Geophysical Union, Maurice Ewing Series, v. 4, p. 248-258.

Arabasz, W.J., Smith, R.B., and Richens, W.D., 1979, Earthquake studies in Utah – 1850 to 1978: Salt Lake City, University of Utah Seismograph Station, Department of Geology and Geophysics, 339 p.

—1980, Earthquake studies along the Wasatch Front, Utah - Network monitoring, seismicity, and seismic hazards: Seismological Society America Bulletin, v. 70, p. 1479-1500.

Armstrong, R.L., 1968, Sevier orogenic belt in Nevada and Utah: Geological Society of America, v. 79, p. 429-458.

Atwater, Tanya, 1970, Implications of plate tectonics for the Cenozoic tectonic evolution of western North America: Geological Society of America Bulletin, v. 81, p. 3513-3536.

Atwood, W.W., 1909, Glaciation of the Uinta and Wasatch Mountains: U.S. Geological Survey Professional Paper 61, 96 p.

Bally, A.W., Gordy, P.L., and Stewart, G.A., 1966, Structure, seismic data, and orogenic evolution of southern Canadian Rocky Mountains: Bulletin of Canadian Petroleum Geology, v. 14, no. 3, p. 337-381.

Barrientos, S.E., Ward, S.N., Gonzalez-Ruiz, J.R., and Stein, R.S., 1985, Inversion for moment as a function of depth from geodetic observations and long period body waves of the 1983 Borah Peak, Idaho, earthquake, *in* Stein, R.S., and Bucknam, R.C., editors, Proceedings of Workshop XXVIII on the Borah Peak, Idaho, earthquake: U.S. Geological Survey Open File Report 85-290, p. 485-518.

Bartley, J.M., and Wernicke, B.P., 1984, The Snake Range decollement interpreted as a major extensional shear zone: Tectonics, v. 3, no. 6, p. 647-657.

Beutner, E.C., 1977, Causes and consequences of curvature in the Sevier orogenic belt, Utah to Montana, *in* Heisey, E.L., editor, Rocky Mountain thrust belt; geology and resources: Wyoming Geological Association Guidebook No. 29, p. 353-366.

Blackstone, D.L., Jr., 1977, The Overthrust Belt salient of the Cordilleran fold belt - western Wyoming, southeastern Idaho, northeastern Utah, *in* Heisey, E.L., editor, Rocky Mountain thrust belt; geology and resources: Wyoming Geological Association Guidebook No. 29, p. 367-384.

Blackstone, D.L., Jr., and Ver Ploeg, A.J., 1981, Tectonic map of the overthrust belt, western Wyoming, southeastern Idaho, and northeastern Utah, showing current oil and gas drilling and development: Geological Survey of Wyoming, scale 1:316,800.

Blackwelder, Eliot, 1915, Post-Cretaceous history of the mountains of central western Wyoming: Journal of Geology, v. 23, p. 97-117, 193-217, and 307-340.

Bolt, B.A., 1984, The magnitudes of the Hebgen Lake 1959 and Idaho 1983 earthquakes: Earthquake Notes, v. 55, p. 13.

Bonilla, M.G., Mark, R.K., and Lienkaemper, J.J., 1984, Statistical relations among earthquake magnitude, surface rupture length, and surface fault displacement: Seismological Society of America Bulletin, v. 74, no. 6, p. 2379-2411.

Bradley, W.H., 1936, Geomorphology of the north flank of the Uinta Mountains: U.S. Geological Survey Professional Paper 185-I, p. 163-204.

Bryant, Bruce, 1985, Structural ancestry of the Uinta Mountains, *in* Picard, M.D., editor, Geology and energy resources, Uinta Basin of Utah: Utah Geological Association Publication 12, p. 115-120.

Cluff, L.S., Patwardhan, A.S., and Coppersmith, K.J., 1980, Estimating the probability of occurrence of surface-faulting earthquakes on the Wasatch fault zone, Utah: Seismological Society of America Bulletin, v. 70, no. 5, p. 1463-1478.

Colman, S.M., 1982, Clay mineralogy of weathering rinds and possible implications concerning the sources of clay minerals in soils: Geology, v. 10, no. 7, p. 370-375.

Colman, S.M., Pierce, K.L., and Birkeland, P.W., 1987, Suggested terminology for Quaternary dating methods: Quaternary Research, v. 28, p. 314-319.

Constenius, Kurt, 1982, Relationship between the Kishenehn basin and the Flathead listric normal fault system and Lewis thrust salient, *in* Powers, R.B., editor, Geologic studies of the Cordilleran thrust belt, Volumes I and II: Denver, Rocky Mountain Association of Geologists, p. 817-830.

—1988, Structural configuration of the Kishenehn basin delineated by geophysical methods, northwestern Montana and southeastern British Columbia: Mountain Geologist, v. 25, no. 1, p. 13-28.

Cook, W.R., 1977, The structural geology of the Aspen Tunnel area, Uinta County, Wyoming: Wyoming Geological Association Guidebook No. 29, p. 397-405.

Corbett, M.K., 1982, Superposed tectonism in the Idaho-Wyoming thrust belt, *in* Powers, R.B., editor, Geologic studies of the Cordilleran thrust belt, Volumes I and II: Denver, Rocky Mountain Association of Geologists, p. 341-356.

Couples, G.D., 1986, "Thrust belt" structures with "foreland" genesis [abs.]: Geological Society of America Abstracts with Programs, v. 18, no. 5, p. 349.

Crittenden, M.D., Jr., 1961, Magnitude of thrust faulting in northern

Utah: U.S. Geological Survey Professional Paper 424-D, p. D128-D131.

—1974, Regional extent and age of thrusts near Rockport Reservoir and relation to possible exploration targets in northern Utah: American Association of Petroleum Geologists Bulletin, v. 58, no. 12, p. 2428-2435.

Crone, A.J., Pierce, K.L., and Hait, M.H., 1985, The Borah Peak earthquake of October 28, 1983 - Surface-faulting, mass movements, and Quaternary tectonic setting: Field trip guide prepared for Geological Society of America 1985 Rocky Mountain Section Meeting, April 20-21, 1985, 23 p.

Dahlstrom, C.D.A., 1970, Structural geology in the eastern margin of the Canadian Rocky Mountains: Bulletin of Canadian Petroleum Geology, v. 18, no. 5, p. 332-406.

de Jong, A.F.M, Becker, Bernd, and Mook, W.G., 1986, High-precision calibration of the radiocarbon time scale, 3930-3230 BC, *in* Stuiver, Minze and Kra, R.S., editors, Radiocarbon, calibration issue - Proceedings of the 12th International Radiocarbon Conference, Trondheim, Norway: Radiocarbon, v. 28, no. 2B, p. 939-942.

Dixon, J.S., 1982, Regional structural synthesis, Wyoming salient of western overthrust belt: American Association of Petroleum Geologists Bulletin, v. 66, no. 10, p. 1560-1580.

Doser, D.I., 1984, The 1959 Hebgen Lake, Montana and the 1983 Borah Peak, Idaho earthquakes; examples of large normal fault events in the Intermountain region: Eastern Section of the Seismological Society of America, Earthquake Notes, 55, March 1984, p. 14.

—1985a, Source parameters and faulting processes of the 1959 Hebgen Lake, Montana earthquake sequence: Journal Geophysical Research, v. 90, no. 6, p. 4537-4555.

—1985b, The 1983 Borah Peak, Idaho and 1959 Hebgen Lake, Montana earthquakes; models for normal fault earthquakes in the Intermountain seismic belt, *in* Stein, R.S., and Bucknam, R.C., editors, Proceedings of Workshop XXVIII on the Borah Peak, Idaho earthquake: U.S. Geological Survey Open File Report 85-290, p. 368-384.

Doser, D.I., and Smith, R.B., 1982, Seismic moment rates in the Utah region: Seismological Society of America Bulletin, v. 72, no. 2, p. 525-551.

—1983, Seismicity of the Teton-southern Yellowstone region, Wyoming: Seismological Society of America Bulletin, v. 73, p. 1369-1394.

—1985, Source parameters of the 28 October, 1983, Borah Peak, Idaho earthquake from body wave analysis: Seismological Society of America Bulletin, v. 75, no. 4, p. 1041-1051.

Eardley, A.J., 1959, Review of geology in northeastern Utah and southwestern Wyoming: Intermountain Association of Petroleum Geologists Guidebook to the Geology of the Wasatch and Uinta Mountains Transition Area, 10th Annual Field Conference, p. 166-171.

—1968, Major structures of the Rocky Mountains of Colorado and Utah: University of Missouri at Rolla, UMR Journal No. 1, p. 79-100.

Eaton, G.P., 1979, Regional geophysics, Cenozoic tectonics, and geologic resources of the Basin and Range Province and adjoining regions: Salt Lake City, Rocky Mountain Association of Geologists and Utah Geological Association 1979 Basin and Range Symposium, p. 11-40.

Geyh, M.A., Benzler, J.H., and Roeschman, G., 1971, Problems of dating Pleistocene and Holocene soils by radiometric methods, *in* Yaalon, D.H., editor, Paleopedology - Origin, nature, and dating of paleosols: International Society of Soil Science and Israel University Press.

Gibbons, A.B., and Dickey, D.D., 1983, Quaternary faults in Lincoln and Uinta Counties, Wyoming and Rich County, Utah: U.S. Geological Survey Open-File Report 83-288, scale 1:100,000.

Gilbert, G.K., 1928, Studies of basin-range structure: U.S. Geological Survey Professional Paper 153, 92 p.

Hait, M.H., 1988, Preliminary reconstruction of the pre-extension configuration of Mesozoic thrust belt in east-central Idaho and southwest Montana [abs.]: Geological Society of America Abstracts with Programs, Rocky Mountain Section Meeting, v. 20, no. 6, p. 418.

Hait, M.H., Jr., and, Scott, W.E., 1978, Holocene faulting, Lost River Range, Idaho [abs.]: Geological Society of America Abstracts with Programs, v. 10, p. 217.

Hansen, W.R., 1969, The geologic story of the Uinta Mountains: U.S. Geological Survey Bulletin 1291, 144 p.

—1984, Post-Laramide tectonic history of the eastern Uinta Mountains, Utah, Colorado, and Wyoming: The Mountain Geologist, v. 21, no. 1, p. 5-29.

—1985, Drainage development of the Green River basin in southwestern Wyoming and its bearing on fish biogeography, neotectonics, and paleoclimates: Mountain Geologist, v. 22, no. 4, p. 192-204.

—1986, Neogene tectonics and geomorphology of the eastern Uinta Mountains in Utah, Colorado, and Wyoming: U.S. Geological Survey Professional Paper 1356, 78 p.

Hanson, K.L., Swan, F.H., and Schwartz, D.P., 1981, Study of earthquake recurrence intervals on the Wasatch fault, Utah (North Creek site): Sixth Semi-Annual Technical Report to the U.S. Geological Survey under contract no. 14-08-001-16827 by Woodward-Clyde Consultants, San Francisco, California.

Hays, W.W., and Gori, P.L., editors, 1992, Assessment of regional earthquake hazards and risk along the Wasatch Front, Utah: U.S. Geological Survey Professional Paper 1500 A-J, variously paginated.

Hintze, L.F., 1980, Geologic map of Utah: Utah Geological and Mineral Survey, scale 1:500,000.

Jackson, Michael, 1991, The number and timing of Holocene paleoseismic events on the Nephi and Levan segments, Wasatch fault zone, Utah: Utah Geological Survey Special Study 78, Paleoseismology of Utah Volume 3, 23 p., 3 plates.

Klein, Jeffrey, Lerman, J.C., Damon, P.E., and Ralph, E.K., 1982, Calibration of radiocarbon dates - tables based on the consensus data of the Workshop on Calibrating the Radiocarbon Time Scale: Radiocarbon, v. 24, no. 2B, p. 103-149.

Lamerson, P.R., 1982, The Fossil basin area and its relationship to the Absaroka thrust fault system, *in* Powers, R.B., editor, Geologic studies of the Cordilleran thrust belt, Volumes I and II: Denver, Rocky Mountain Association of Geologists, p. 279- 340.

Lines, G.C., and Glass, W.R., 1975, Water resources of the thrust belt of western Wyoming: U.S. Geological Survey Hydrologic Investigation Atlas HA-539, 3 sheets, various scales.

Linick, T.W., Long, Austin, Damon, P.E., and Ferguson, C.W., 1986, High-precision radiocarbon dating of bristlecone pine from 6554 to 5350 BC, *in* Stuiver, Minze and Kra, R.S., editors, Radiocarbon, calibration issue - Proceedings of the 12th International Radiocarbon Conference, Trondheim, Norway: Radiocarbon, v. 28, no. 2B, p. 943-953.

Lowell, J.D., 1977, Underthrusting origin for thrust-fold belts with application to the Idaho-Wyoming Belt: Wyoming Geological Association Guidebook, No. 29, p. 449-455.

Lund, W.R., Schwartz, D.P., Mulvey, W.E., Budding, K.E., and Black, B.D., 1991, Fault behavior and earthquake recurrence on the Provo segment of the Wasatch fault zone at Mapleton, Utah County, Utah: Utah Geological Survey Special Study 75, Paleoseismology of Utah Volume 1, 41 p.

Machette, M.N., Personius, S.F., and Nelson, A.R.,1992, Paleoseismology of the Wasatch fault zone: A summary of recent investigations, interpretations, and conclustions; *in* Hays, W.W. and Gori, P.L., editors, Assessment of regional earthquake hazards and risk along the Wasatch Front, Utah: U.S. Geological Survey Professional Paper 1500 A, p. 1-8.

Martel, Y.A., and Paul, E.A., 1974, The use of radiocarbon dating of organic matter in the study of soil genesis: Soil Science Society of America Proceedings, v. 38, p. 501-506.

Martin, R.A., Jr., Nelson, A.R., Weisser, R.R., and Sullivan, J.T., 1985, Seismotectonic study for Taskeech dam and reservoir site and Upper Stillwater dam and reservoir site, Central Utah Project, Utah: Denver, U.S. Bureau of Reclamation Seismotectonic Report 85-2, 95 p.

Matthews, J.A., 1980, Some problems and implications of ^{14}C dates from a podzol buried beneath an end moraine at Haugabreen, southern Norway: Geografiska Annaler 62 A (3-4), p. 185-208.

McCalpin, J.P., 1982, Quaternary geology and neotectonics of the west flank of the northern Sangre de Cristo Mountains, south-central Colorado: Colorado School of Mines Quarterly, v. 77, no. 3, 94 p.

—1987, Quaternary deformation along the East Cache Valley fault, north-central Utah [abs.]: Geological Society of America Abstracts with Programs, v. 19, no. 5, p. 320.

McDonald, R.E., 1976, Tertiary tectonics and sedimentary rocks along the transition Basin and Range Province to Plateau and Thrustbelt province, Utah, *in* Symposium of the geology of the Cordilleran hingeline: Denver, Rocky Mountain Association of Geologists, p. 281-317.

M'Gonigle, J.W., and Dover, J.H., in press, Geologic map of the Evanston 1:100,000 sheet: U.S. Geological Survey, 1 sheet.

Myers, W.B., and Hamilton, Warren, 1964, Deformation accompanying the Hebgen Lake earthquake of August 17, 1959, in the Hebgen Lake, Montana earthquake of August 17, 1959: U.S. Geological Survey Professional Paper 435, p. 55-98.

Nelson, A.R., and Martin, R.A., 1982, Seismotectonic study for Soldier Creek dam, Central Utah Project: U.S. Bureau of Reclamation, Seismotectonic Report 82-1, Denver, 102 p.

Nixon, R.P., 1955, Geology of the Hilliard Flat area, Uinta County, Wyoming: Salt Lake City, University of Utah, M.S. thesis, 50 p.

Ostenaa, D.A., 1984, Relationships affecting estimates of surface fault displacements based on scarp-derived colluvial deposits [abs.]: Geological Society of America, Abstracts with Programs, v. 16, no. 5, p. 327.

Parry, W.T., and Bruhn, R.L., 1987, Fluid inclusion evidence for minimum 11 kilometers vertical offset on the Wasatch fault, Utah: Geology, v. 15, p. 67-70.

Pearson, G.W., and Stuiver, Minze, 1986, High-precision calibration of the radiocarbon time scale, 500-2500 BC *in* Stuiver, Minze and Kra, R.S., editors, Radiocarbon, calibration issue - Proceedings of the 12th International Radiocarbon Conference, Trondheim, Norway: Radiocarbon, v. 28, no. 2B, p. 839-862.

Personius, S.F., 1991, Paleoseismic analysis of the Wasatch fault zone at the Brigham City trench site, Brigham City, Utah and the Pole Patch trench site, Pleasant View, Utah: Utah Geological Survey Special Study 76, Paleoseismology of Utah Volume 2, 39 p.

Pierce, K.L., 1979, History and dynamics of glaciation in the northern Yellowstone National Park area: U.S. Geological Survey Professional Paper 729-F, 90 p.

Porter, S.C., Pierce, K.L., and Hamilton, T.D., 1983, Late Wisconsin mountain glaciation in the western United States, *in* Wright, H.E., Jr., editor, Late Quaternary environments of the United States, Volume 1, the Late Pleistocene (Porter, S.C., editor): University of Minnesota Press, p. 71-111.

Richmond, G.M., 1957, Three pre-Wisconsin glacial stages in the Rocky Mountain region: Geological Society America Bulletin, v. 68, p. 239-262.

—1964, Three pre-Bull Lake tills in the Wind River Mountains, Wyoming - A reinterpretation: U.S. Geological Survey Professional Paper 501-D, p. D104-D109.

—1965, Glaciation of the Rocky Mountains, *in* Wright, H.E., editor, The Quaternary of the United States: Princeton, New Jersey, Princeton University Press.

Ritzma, H.R., 1971, Faulting on the north flank of the Uinta Mountains, Utah and Colorado: Wyoming Geological Association 23rd Annual Field Conference, p. 145-150.

Royse, Frank, 1983, Extensional faults and folds in the foreland thrust belt, Utah, Wyoming, Idaho [abs.]: Geological Society of America Abstracts with Programs, v. 15, no. 5, p. 295.

Royse, Frank, Warner, M.A., and Reese, D.L., 1975, Thrust belt structural geometry and related stratigraphic problems, Wyoming-Idaho-northern Utah: Denver, Rocky Mountain Association of Geologists 1975 Symposium, p. 41-54.

Schlenker, G.C., 1988, Glaciation and Quaternary geomorphology of the Blacks Fork drainage, high Uinta Mountains, Utah and Wyoming: Salt Lake City, University of Utah, M.S. thesis, 87 p.

Schoenfeld, M.J., 1969, Quaternary geology of the Burnt Fork area, Uinta Mountains, Summit County, Utah: Laramie, University of Wyoming, M.S. thesis, 75 p.

Scholz, C.H., Barzangi, Muawia, and Sbar, M.L., 1971, Late Cenozoic evolution of the Great Basin, western United States as an ensialic interarc basin: Geological Society of America Bulletin, v. 82, no. 11, p. 2979-2990.

Schwartz, D.P., and Coppersmith, K.J., 1984, Fault behavior and characteristic earthquakes - Examples from the Wasatch and San Andreas fault zones: Journal of Geophysical Research, v. 89, p. 5681-5698.

—1986, Seismic hazards - New trends in analysis using geologic data, *in* Active tectonics: National Research Council, National Academy Press, p. 215-230.

Schwartz, D.P., Hanson, K.L., and Swan, F.H., III, 1983, Paleoseismic investigations along the Wasatch fault zone - An update, *in* Gurgel, K.D., editor, Geologic excursions in neotectonics and engineering geology in Utah: Utah Geological and Mineral Survey Special Studies 62, p. 45-49.

Sears, J.W., Graff, P.J., and Holden, G.S., 1982, Tectonic evolution of lower Proterozoic rocks, Uinta Mountains, Utah and Colorado: Geological Society of America Bulletin, v. 93, no. 10, p. 990-997.

Shroba, R.R., and Birkeland, P.W., 1983, Trends in late Quaternary soil development in the Rocky Mountains and Sierra Nevada of the Western United States, *in* Wright, H.E., Jr., editor, Late Quaternary environments of the United States, Volume 1, the Late Pleistocene (Porter, S.C., editor): University of Minnesota Press, p. 145-156.

Skipp, Betty, 1985, Contraction and extension faults in the southern Beaverhead Mountains, Idaho, and Montana: U.S. Geological Survey Open-File Report 85-545, 170 p., 3 sheets, various scales.

Slemmons, D.B., 1977, Faults and earthquake magnitude: Vicksburg,

Mississippi, U.S. Army Engineer Waterways Experiment Station Miscellaneous Paper S-73-1, Report 6, 129 p.

—1981, Geologic considerations for earthquake zonation: U.S. - China Workshop on Microzonation for Earthquakes.

Smith, R.B., 1977, Intraplate tectonics of the western North American plate: Tectonophysics, v. 37, p. 323-336.

—1978, Seismicity, crustal structure, and intraplate tectonics of the interior of the western Cordillera *in* Cenozoic tectonics and regional geophysics of the western Cordillera: Geological Society of America Memoir 152, p. 111-144.

Smith, R.B., and Bruhn, R.L., 1984, Intraplate extensional tectonics of the eastern Basin-Range - Inferences on structural style from seismic reflection data, regional tectonics, and thermal-mechanical models of brittle-ductile deformation: Journal of Geophysical Research, v. 89, p. 5733-5762.

Smith, R.B., and Sbar, M.L., 1974, Contemporary tectonics and seismicity of the western United States with emphasis on the Intermountain seismic belt: Geological Society of America Bulletin, v. 85, no. 8, p. 1205-1218.

Sprinkel, D.A., 1979, Apparent reverse movement on previous thrust faults along the eastern margin of the Basin and Range Province, north-central Utah: Salt Lake City, Rocky Mountain Association of Geologists-Utah Geological Association Basin and Range Symposium, p. 135-142.

Stein, R.S., and Barrientos, S.E., 1985, The 1983 Borah Peak, Idaho earthquake - Geodetic evidence for deep rupture on a planar fault, *in* Stein, R.S., and Bucknam, R.C., editors, Proceedings of Conference XXVIII - The Borah Peak earthquake: U.S. Geological Survey Open-File Report 85-290, p. 459-484.

Stewart, J.H., 1971, Basin and range structure - A system of horsts and grabens produced by deep-seated extension: Geological Society of America Bulletin, v. 82, no. 4, p. 1019-1044.

Stokes, W.L., 1976, What is the Wasatch Line?: Denver, Rocky Mountain Association of Geologists 1976 Symposium on the Geology of the Cordilleran Hingeline, p. 11-25.

—1977, Subdivisions of the major physiographic provinces of Utah: Utah Geology, v. 4, no. 1, p. 1-17.

Stokes, W.L., and Madsen, J.H., 1961, Geologic map of Utah -Northeast quadrant: Utah Geological and Mineral Survey, scale 1:250,000.

Stuiver, Minze, and Kra, R.S., 1986, Calibration issue - Proceedings of the 12th International Radiocarbon Conference, Trondheim, Norway: Radiocarbon, v. 28, no. 2B, 225 p.

Stuiver, Minze, and Reimer, P.J., 1986, A computer program for radiocarbon age calibration: Radiocarbon, v. 28, no. 2B, p. 1022-1033.

Sullivan, J.T., Nelson, A.R., LaForge, R.C., Wood, C.K., and Hansen, R.A., 1988, Central Utah regional seismotectonic study for USBR dams in the Wasatch Mountains: U.S. Bureau of Reclamation Seismotectonic Report 88-5, Denver, 269 p.

Swan, F.H., III, Hanson, K.L., Schwartz, D.P. and Black, J.H., 1983, Study of earthquake recurrence intervals on the Wasatch fault, Utah (East Cache fault): Eighth Semi-Annual Technical Report prepared for the U.S. Geological Survey under contract no. 14-08-001-19842 by Woodward-Clyde Consultants, San Francisco, California, 20 p.

Swan, F.H., III, Schwartz, D.P., and Cluff, L.S., 1980, Recurrence of moderate to large magnitude earthquakes produced by surface faulting on the Wasatch fault zone, Utah: Seismological Society of America Bulletin, v. 70, p. 1431-1462.

Swan, F.H., III, Schwartz, D.P., Hanson, K.L., and Black, J.H., 1982, Study of earthquake recurrence intervals on the Wasatch fault zone, Utah, *in* Summaries of technical reports, Volume XIV: U.S. Geological Survey Open-File Report 82-840, p. 95-97.

Taylor, R.E., 1987, Radiocarbon dating - an archeological perspective: Orlando, Academic Press, Inc., 212 p.

Thenhaus, P.C., editor, 1983, Summary of workshops concerning regional seismic source zones of parts of the conterminous United States convened by the U.S. Geological Survey 1979-1980, Golden, Colorado: U.S. Geological Survey Circular 898, 36 p.

Thenhaus, P.C., and Wentworth, C.M., 1982, Map showing zones of similar ages of surface faulting and estimated maximum earthquake size in the Basin and Range Province and selected adjacent areas: U.S. Geological Survey Open-File Report 82-742, 18 p.

University of Utah, 1985, Listing and plot of seismicity data, August 30, 1962, through June 27, 1985, in the area bounded by 110.00° and 111.75° W. long. and 40.50° and 42.50° N. lat.: Salt Lake City, University of Utah Seismograph Stations Earthquake Data Base System.

U.S. Bureau of Reclamation, 1983, Seismotectonic study for Jackson Lake dam and reservoir, Minidoka Project, Idaho-Wyoming: Denver, U.S. Bureau of Reclamation Seismotectonic Report 83-8, 123 p.

Van Arsdale, R.B., 1979a, Geology of Strawberry Valley and regional implications: Salt Lake City, University of Utah, Ph.D. dissertation, 65 p.

—1979b, Geometry and most recent movement along the Strawberry normal fault, Wasatch County, Utah [abs.]: Geological Society of America Abstracts with Programs, v. 11, no. 7, p. 531-532.

Wallace, R.E., 1977, Profiles and ages of young fault scarps, north-central Nevada: Geological Society of America Bulletin, v. 88, no. 9, p. 1267-1281.

—1981, Active faults, paleoseismology and earthquake hazards in the western United States, *in* Earthquake prediction - An international review: Washington D.C., American Geophysical Union, p. 209-216.

Wernicke, B.P., 1981, Low-angle normal faults in the Basin and Range Province - Nappe tectonics in an extending orogen: Nature, v. 291, p. 645-647.

Wernicke, B.P., Walker, J.D., and Beaufait, M.S., 1985, Structural discordance between Neogene detachments and frontal Sevier thrusts, central Mormon Mountains, southern Nevada: Tectonics, v. 4, no. 2, p. 213-246.

West, M.W., 1978, Quaternary geology and reported surface faulting along east flank of Gore Range, Summit County, Colorado: Colorado School of Mines Quarterly, v. 73, no. 2, 66 p.

—1984, Recurrent late Quaternary (Holocene?) faulting, Bear River fault zone, Uinta County, Wyoming and Summit County, Utah [abs.]: Geological Society of America Abstracts with Programs, v. 16, no. 4, p. 259-260.

—1986a, Quaternary extensional reactivation of the Darby and Absaroka thrusts, north-central Utah and southwestern Wyoming: [abs.]: Geological Society of America Abstracts with Programs, v. 18, no. 5, p. 422.

—1986b, Earthquake hazards and dam safety in southwestern Wyoming and north-central Utah [abs.]: San Francisco, Association of Engineering Geologists, Abstracts with Program, 19th Annual Meeting, p. 68.

—1987, Surface rupture characteristics, recurrence intervals, and slip rates determined by trenching, Bear River fault zone, Wyoming and Utah [abs.]: Geological Society of America Abstracts with Programs, v. 19, no. 5, p. 341-342.

—1992, An integrated model seismogenesis in the Intermountain Seismic Belt: Seismological Society of America Bulletin, v. 82, n. 3, p. 1350-1372.

—1993, Extensional reactivation of thrust faults accompanied by coseismic surface ruture, southwestern Wyoming and north-central Utah: Geological Society of America Bulletin, v. 105, p. 1137-1150.

Wiltschko, D.V., and Dorr, J.A., 1983, Timing of deformation in overthrust belt and foreland of Idaho, Wyoming, and Utah: American Association of Petroleum Geologists Bulletin, v. 67, no. 8, p. 1304-1322.

Winkler, G.R., 1970, Sedimentology and geomorphic significance of the Bishop Conglomerate and the Browns Park Formation, eastern Uinta Mountains, Utah, Colorado, and Wyoming: Salt Lake City, University of Utah, M.S. thesis, 115 p.

Witkind, I.J., 1975, Preliminary map showing known and suspected active faults in Wyoming: U.S. Geological Survey Open-File Report 75-279, 36 p., scale 1:500,000.

Wyss, Max, 1979, Estimating maximum expectable magnitude of earthquakes from fault dimensions: Geology, v. 7, no. 7, p. 336-340.

Yaalon, D.H., editor, 1971, Paleopedology - Origin, nature and dating of paleosols: International Society of Soil Science and Israel University Press.

Zoback, M.L., 1983, Structure and Cenozoic tectonism along the Wasatch fault zone, Utah, *in* Tectonics and stratigraphy of the eastern Great Basin: Geological Society of America Memoir 157, p. 3-28.

Zoback, M.L., Anderson, R.E., and Thompson, G.A., 1981, Cenozoic evolution of the state of stress and style of tectonism of the Basin and Range Province of the western United States: Royal Society of London Philosophical Transactions, series A, v. 300, p. 407-434.

APPENDIX I

Table I.1
Scarp-Profile Data

SCARP/LOCATION	SURFACE DATUM	MAX. SCARP ANGLE (Degrees)	SCARP HEIGHT (Meters) GROUND	SURFACE	SURFACE OFFSET (Meters) MEAS.	EST.	FAULT DIP (Degrees) MEAS.	EST
La Chapelle	Upper	12.0	5.6	5.1	--	5.0	89-90	--
Lester Ranch 1	Upper	15.0	4.2	4.0	--	4.1	76	90
Lester Ranch 2	Upper	20.5	5.6	5.4	--	5.5	80-87	--
Lester Ranch 3	Lower	20.5	4.0	3.9	--	3.9	80-87	--
Lester Ranch 4	Upper	24.0	12.3	12.2	--	11.2	--	90
Lester Ranch 5	Upper	14.0	9.4	9.5	--	7.5	--	90
Sulphur Creek	Upper	15.0	4.6	5.7	--	6.7-8.5	--	90
Big Burn 1	Upper	31.0	12.3	3.3-11.8	--	2.8-10.1	62-86	--
Big Burn 2	Lower	28.0	12.3	12.1	--	12.7	62-86	--
Big Burn 3	Lower	29.5	9.7	9.7	--	9.7	62-86	--
Upper Little Burn 1								
Upper Scarp	Upper	11.5	0.8	0.9	--	0.7	--	90
Lower Scarp	Upper	24.5	4.9	4.7		4.3	71-90	--
Total						5.4		
Upper Little Burn 2								
Upper Scarp	Upper	27.5	2.6	2.8	--	2.7	--	90
Lower Scarp	Upper	16.0	3.3	3.5	--	3.4	71-90	--
Total						7.1		
Lower Little Burn	Upper	13.0	2.1	1.5	--	0.8	74-82	--
Elizabeth Ridge 1	Upper	5.0	2.5	2.3	--	1.5	--	90
Elizabeth Ridge 2	--	5.5	2.5	2.5	2.0	--	--	90
Upper Martin Ranch	Upper	14.5	1.5	1.3	--	1.3	85	

To convert meters to feet multiply by 3.28

Table I.2
Vertical tectonic displacement calculated from scarp height, maximum scarp angle, surface-slope angle, and fault dip.

SCARP/LOCATION	SURFACE DATUM	SCARP HT. MAX. (Meters)	SCARP HT. MIN. (Meters)	MAX. SCARP ANGLE (Degrees)	SLOPE ANGLE DATUM (Degrees)	FAULT DIP MEAS. (Degrees)	FAULT DIP EST. (Degrees)	FAULT THROW MIN. MAX. (Meters)
La Chappelle	Upper	5.6	5.1	12.0	1.0	89	--	4.6 - 5.1
						90	--	4.6 - 5.1
Lester Ranch 1	Upper	4.2	4.0	15.0	0.0	76	90	4.0 - 4.2
Lester Ranch 2	Upper	5.6	5.4	20.5	0.5	80	--	5.3 - 5.5
						87	--	5.3 - 5.5
Lester Ranch 3	Lower	4.0	3.9	20.5	-0.5	80	--	3.9 - 4.1
						87	--	3.9 - 4.1
Lester Ranch 4	Upper	12.3	12.2	24.0	2.0	--	90	11.2 - 11.3
Lester Ranch 5	Upper	9.5	9.4	14.0	3.0	--	90	7.4 - 7.5
Sulphur Creek	Upper	5.7	4.6	15.0	-8.0	--	90	6.9 - 8.6
Big Burn 1	Upper	12.3	3.3 to 11.8	31.0	5.0	62	--	3.0
								10.5 - 11.0
						86	--	2.8
								10.1 - 10.6
Big Burn 2	Lower	12.3	12.1	28.0	-1.5	62	--	12.5 - 12.7
						86	--	11.2 - 11.4
Big Burn 3	Lower	9.7	9.7	29.5	0.0	62	--	9.7 - 9.7
Upper Little Burn 1								
Upper Scarp	Upper	0.9	0.8	11.5	2.5	--	90	0.6 - 0.7
Lower Scarp	Upper	4.9	4.7	24.5		--	90	4.2 - 4.4
Total								4.8 - 5.1
Upper Little Burn 2								
Upper Scarp	Upper	2.8	2.6	27.5	1.0	--	90	2.4 - 2.6
Lower Scarp	Upper	3.5	3.3	16.0	3.0	--	90	2.7 - 2.9
Total								5.1 - 5.5
Lower Little Burn	Upper	2.1	1.5	13.0	6.5	--	90	1.0 - 1.4
Elizabeth Ridge 1	Upper	2.5	2.3	5.0	2.0	--	90	1.6 - 1.8
Elizabeth Ridge 2	--	2.5	2.5	5.5	1.0	--	90	2.0 - 2.0
Upper Martin Ranch	Upper	1.5	1.3	14.5	-1.0	85	--	1.3 - 1.6

To convert meters to feet multiply by 3.28

Table I.3

Vertical tectonic displacement calculated from surface offset, surface-slope angle, and fault dip.

SCARP/LOCATION	SURFACE DATUM	SURFACE OFFSET MEAS. (Meters)	SURFACE OFFSET EST. (Meters)	SLOPE ANGLE OF DATUM (Degrees)	FAULT DIP MEAS. (Degrees)	FAULT DIP EST. (Degrees)	FAULT THROW (Meters)
La Chappele	Upper	--	5.0	1.0	89-90	--	5.0
Lester Ranch 1	Upper	--	4.1	0.0	76	90	4.1
Lester Ranch 2	Upper	--	5.5	0.5	80-87	--	5.5
Lester Ranch 3	Lower	--	3.9	-0.5	80-87	--	3.9
Lester Ranch 4	Upper	--	11.2	2.0	--	90	11.2
Lester Ranch 5	Upper	--	7.5	3.0	--	90	7.5
Sulphur Creek	Upper	--	6.7 to 8.5	-8.0	--	90	6.7 - 8.5
Big Burn 1	Upper	--	2.8 to 10.1	5.0 5.0	62 86	-- --	2.9 - 10.5 2.8 - 10.1
Big Burn 2	Lower	--	12.7	-1.5	62-86	--	12.5 - 12.7
Big Burn 3	Lower	--	9.7	0.0	62.86	--	9.7
Upper Little Burn 1							
Upper Scarp	Upper	--	0.7	2.5	--	90	0.7
Lower Scarp	Upper	--	4.3	2.5	71-90	--	4.3
Total			5.4	2.5	71-90	--	5.4 - 5.5
Upper Little Burn 2							
Upper Scarp	Upper	--	2.7	1.0	--	90	2.7
Lower Scarp	Upper	--	3.4	3.0	71-90	--	3.4
Total			7.1	3.0	71-90	--	7.1 - 7.2
Lower Little Burn	Upper	--	0.8	13.0	74-82	--	0.8
Elizabeth Ridge 1	Upper	--	1.5	2.0	--	90	1.5
Elizabeth Ridge 2		2.0	--	1.0	--	90	2.0
Upper Martin Ranch	Upper	--	1.3	-1.0	85	--	1.3

To convert meters to feet multiply by 3.28

Scarp Profiles

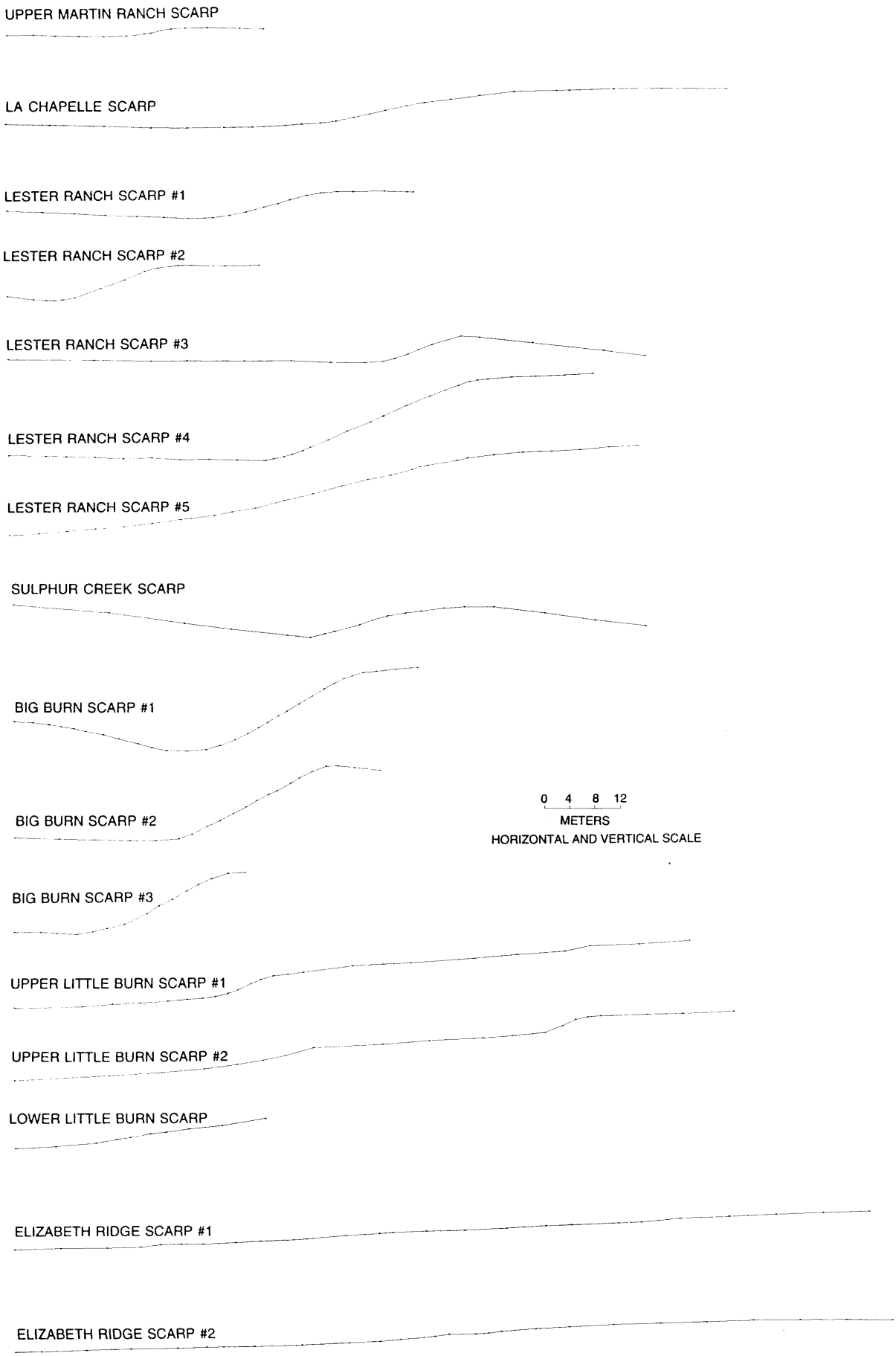

APPENDIX II

Radiocarbon Age Determinations

TRENCH LOCATION	LAB NO.	FIELD NO.	% ORGANIC CARBON < 125 MICRONS	WT. ORGANIC CARBON grams	^{14}C yr B.P.	$^{13}C/^{12}C$	ADJUSTED ^{14}C yr B.P.	REMARKS
La Chapelle								
	BETA-11666	MW-LC-1	--	--	4100±100	-26.35	4080±100	Soil
	BETA-11667	MW-LC-2	--	--	3950±120	-25.55	3940±120	Soil
	BETA-11668	MW-LC-3	--	--	3430±100	-25.79	3420±100	Soil
	BETA-11669	MW-LC-4	--	--	4530±90	-26.22	4510±90	Soil
	BETA-11670	MW-LC-5	--	--	2300±80	-25.30	2300±80	Soil
	BETA-11671	MW-LC-6	--	--	16,310±200	- 8.78	16,580±200	Organics
	BETA-11672	MW-LC-7	--	--	9630±480			Charcoal*
	BETA-11673	MW-LC-8	--	--	4230±180	-20.30	4310±170	Soil
Lester Ranch								
	GX-10251	MW-LR-1	2.75	1.91	--	-23.9	2820±170	Soil
	GX-10252	MW-LR-2	2.08	1.77	--	-24.3	4220±190	Soil
	GX-10253	MW-LR-3	2.90	2.44	--	-24.0	4770±205	Soil
Lester Ranch South								
	BETA-11657	MW-LRS-1	--	--	3770±100	-25.79	3750±100	Soil
	BETA-11658	MW-LRS-2	--	--	4840±130	-25.39	4830±100	Soil
	BETA-11659	MW-LRS-3a	--	--	3050±80	-25.86	3040±80	Soil
	BETA-11660	MW-LRS-3b	--	--	3020±80	-25.17	3020±80	Soil
	BETA-11661	MW-LRS-4	--	--	1280±60	-25.71	1270±60	Soil
	BETA-11662A	MW-LRS-5a	--	--	1330±60	-24.25	1350±60	Soil
	BETA-11662B	MW-LRS-5b	--	--	1660±60	-26.75	1630±60	Soil
Austin Reservoir								
	BETA-11665	MW-AR-6	--	--	820±80	-26.00	800±80	Soil
Sulphur Creek								
	BETA-11650	MW-SC-1	--	--	4140±80	-28.24	4090±80	Soil
	BETA-11651	MW-SC-2	--	--	4190±90	-25.33	4190±90	Soil
	BETA-11652	MW-SC-3	--	--	4040±80	-26.35	4020±80	Soil
	BETA-11653	MW-SC-4	--	--	3850±80	-23.63	3870±80	Soil
	BETA-11654	MW-SC-5	--	--	3730±70	-18.24	3840±70	Soil
	BETA-11655	MW-SC-6	--	--	3000±90	-25.33	3000±90	Soil
	BETA-11656	MW-SC-7	--	--	4230±100	-21.60	4170±100	Charcoal**
Big Burn								
	GX-10052	MW-BB-1	--	--	--	-23.90	1000±135	Charcoal
	GX-10375	MW-BB-2	4.95	4.14	--	-23.60	1170±140	Soil
	GX-10376	MW-BB-3	2.71	0.98	--	-23.60	800±130	Soil
	GX-10377	MW-BB-4	3.74	2.07	--	-23.60	2195±150	Soil
	GX-10378	MW-BB-5	1.64	0.70	--	-23.70	2930±180	Soil
	GX-10379	MW-BB-6	2.71	1.50	--	-24.10	3030±200	Soil
	GX-10380	MW-BB-7	2.75	1.02	--	-25.40	3375±180	Soil
Lower Little Burn								
	BETA-11663	MW-LLB-1	--	--	5830±110	-23.60	5860±110	
	BETA-11664	MW-LLB-2	--	--	4050±150	-21.76	4110±150	Organics*
Upper Martin Ranch								
	GX-10254	MW-UMR-1	3.96	3.13	--	-25.70	700±145	Soil
	GX-10255	MW-UMR-2	1.09	1.66	--	-23.30	2610±180	Soil
	GX-10256	MW-UMR-3	1.16	1.59	--	-23.00	3480±190	Soil

**Extended counting*

***Accelerator Mass Spectrometry (AMS)*

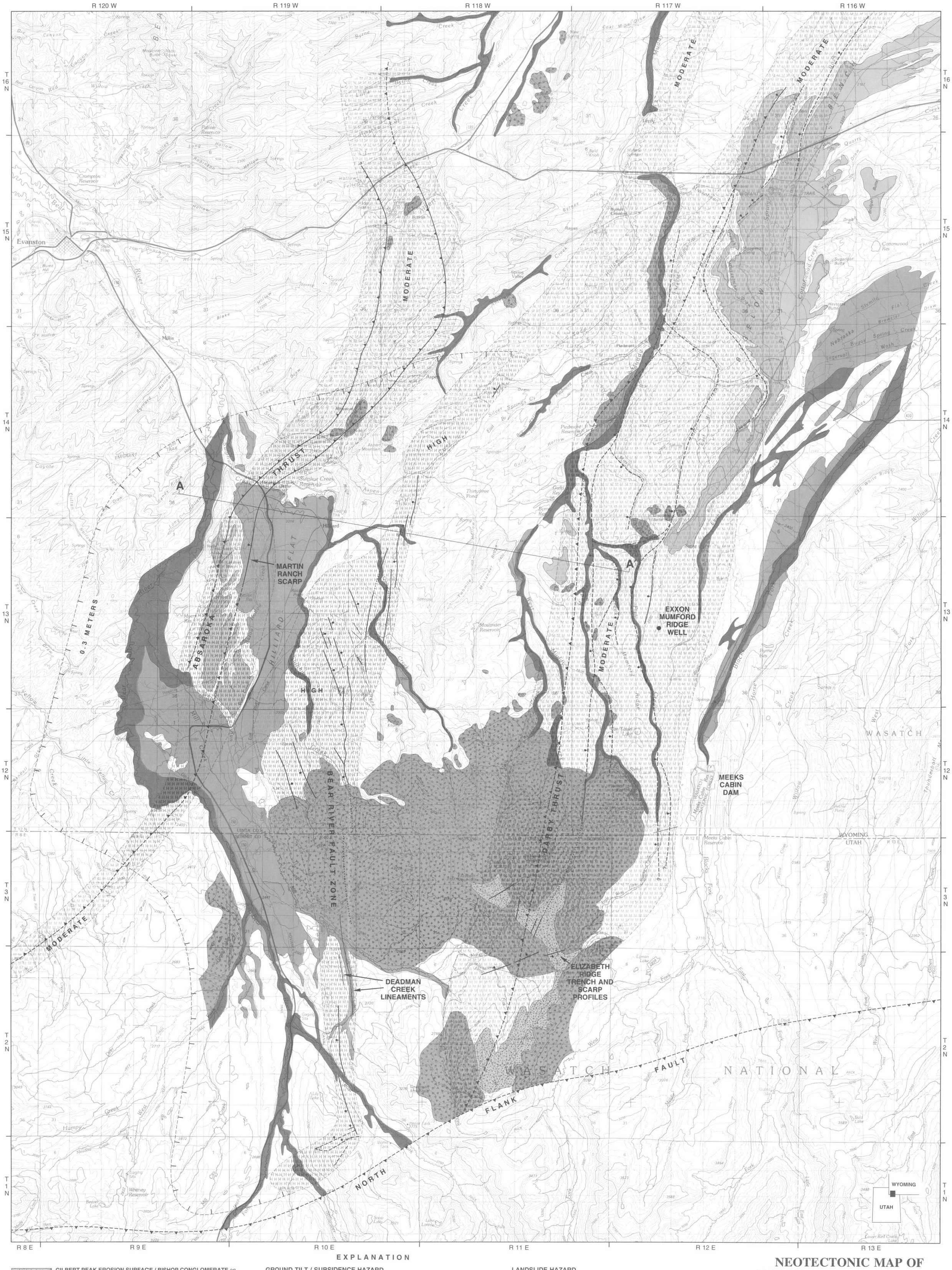

EXPLANATION

GILBERT PEAK EROSION SURFACE / BISHOP CONGLOMERATE on Elizabeth Ridge and Table Top.

THRUST FAULT-- Teeth on upper plate, dashed where covered.

NORMAL FAULT-- Ball and bar on downthrown side, dashed where inferred, dotted where covered.

PHOTOGEOLOGIC LINEAMENT-- Believed to be related to surface faulting.

A — A' **GEOLOGIC CROSS SECTION--** See figures 71 and 73 in text.

FAULT SURFACE RUPTURE HAZARD

HIGH-- Evidence of recurrent surface rupture within 6,000 years before present.

MODERATE-- Evidence of recurrent surface rupture between 6,000 and 600,000 years before present and/or areas of potential future surface rupture based on existing pattern of faulting and apparent directions of fault propagation.

GROUND TILT / SUBSIDENCE HAZARD

Area enclosed by hachured line may be subject to significant (1 foot or 0.3 meters) ground tilt / subsidence associated with surface faulting. Areas adjacent to normal fault scarps in the Bear River fault zone could experience deformations of ≥20 feet (≥6 meters). Ground tilt / subsidence potential generally decreases away from the fault zone.

LIQUEFACTION HAZARD

HIGH-- Alluvial deposits containing high percentages of saturated, low-density, cohesionless silts and sands. Generally equivalent to Holocene alluvium and low terrace surfaces along perennial drainages.

MODERATE-- Alluvial and glaciofluvial deposits containing high percentages of partially and/or intermittently saturated, low-density, cohesionless silts and sands. Generally associated with poorly drained and/or irrigated, intermediate-level alluvial terraces and glacial outwash plains.

LOW-- Alluvial and glaciofluvial deposits containing variable percentages of well-drained, low-density, cohesionless silts and sands. Generally associated with high-level, alluvial terraces and glacial outwash plains.

LANDSLIDE HAZARD

Areas of existing landslides and debris flows considered susceptable to reactivation during a major earthquake. Strong ground motion and/or surface fault rupture may trigger additional slope failures in areas not shown as existing landslides on this map.

NOTES

1. Mapping in Wyoming modified from Gibbons, A.B., 1986, Surficial materials map of the Evanston 30′ x 60′ quadrangle, Uinta and Sweetwater counties, Wyoming: U.S. Geological Survey Coal Investigations Map C-103.
2. This map portrays seismotectonic hazards based on detailed fault studies, regional reconniassance mapping, and work by others. It is intended as a general guide to seismotectonic hazard assessment and is subject to the limitations and explanations contained in the attached paper. Site-specific assessment of seismotectonic hazard / risk requires consideration of existing or planned facilities, site geologic mapping, and subsurface investigations to determine the presence of potentially liquefiable materials.

N

SCALE 1:100,000

0 1 2 3 4 5 MI

0 1 2 3 4 5 6 7 KM

NEOTECTONIC MAP OF NORTH-CENTRAL UTAH AND SOUTHWESTERN WYOMING, WITH HAZARD OVERLAYS

by
Michael W. West

1994

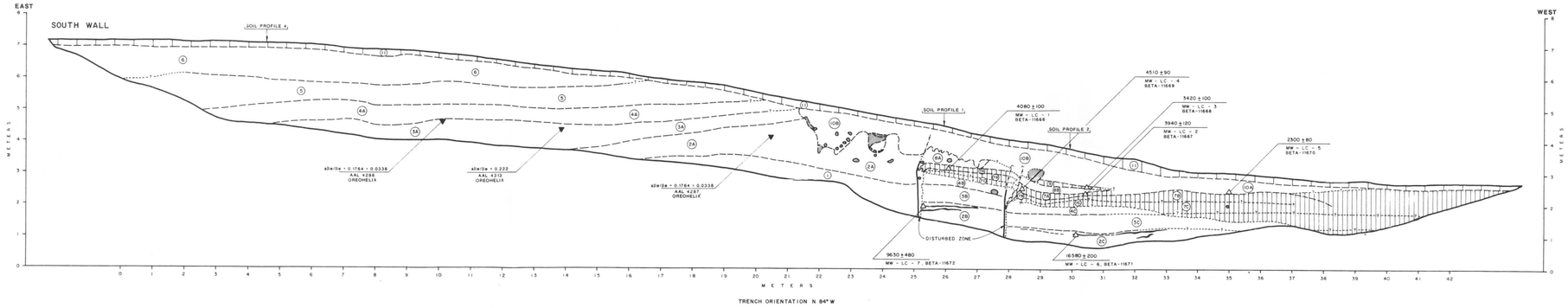

EXPLANATION

LITHOSTRATIGRAPHIC UNITS	SOIL STRATIGRAPHIC UNITS	AGE
10 LOESS	11 MODERN A HORIZON	2300±80
10A LOESS		
10B BIOTURBATED LOESS		
FAULT EVENT		
	9 BURIED A-HORIZON	3420±100
8 SCARP COLLUVIUM		
8A INTERMEDIATE DOWNTHROWN BLOCK		
8B DOWNTHROWN BLOCK		
FAULT EVENT		
	7 BURIED SOIL	
	7A BURIED A-HORIZON	3940±120 4080±100 4510±90
	7B BURIED ARGILLIC B-HORIZON	
	7C BURIED CARBONATE-RICH HORIZON	
FLUVIAL DEPOSITS (UNITS 1-6)		
6 CLAY		
5 INTERBEDDED CLAYS AND SANDS		

EXPLANATION (CONT.)

LITHOSTRATIGRAPHIC UNITS	SOIL STRATIGRAPHIC UNITS	AGE
4 CLAY		
4A UPTHROWN BLOCK		
4B INTERMEDIATE DOWNTHROWN BLOCK		
4C DOWNTHROWN BLOCK		
3 INTERBEDDED SILTS, CLAYS AND SANDS		
3A UPTHROWN BLOCK		
3B INTERMEDIATE DOWNTHROWN BLOCK		
3C DOWNTHROWN BLOCK		
2 CLAY		
2A UPTHROWN BLOCK		
2B INTERMEDIATE DOWNTHROWN BLOCK		9630±480
2C DOWNTHROWN BLOCK		16580±480
1 INTERBEDDED GRAVELLY SANDS AND CLAYS		

LOG OF
LA CHAPELLE
TRENCH
BEAR RIVER FAULT ZONE
BY
M.W. WEST, C. KRINSKY

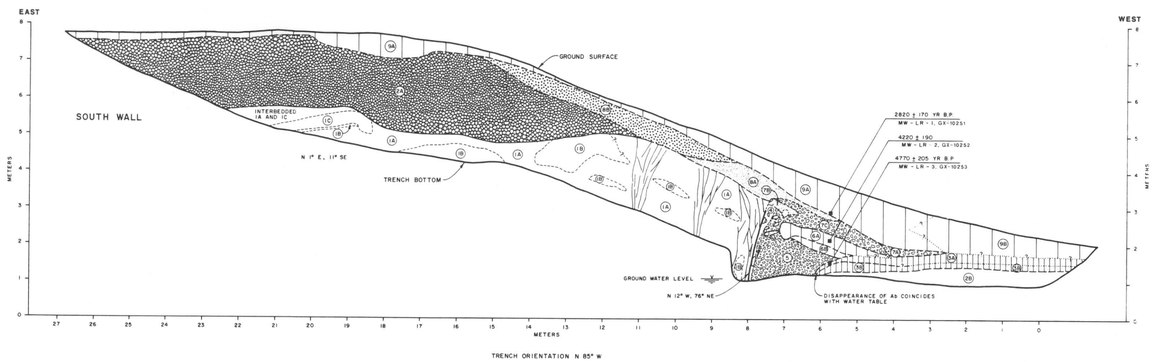

EXPLANATION

LITHOSTRATIGRAPHIC UNITS	SOIL STRATIGRAPHIC UNITS	AGE
	9 MODERN A-HORIZON	2820±170
	9A A-HORIZON	
	9B MOLLIC A-HORIZON	
8 SLOPE COLLUVIUM		
8A FROM WASATCH FORMATION		
8B FROM TERRACE ALLUVIUM		
7 SCARP COLLUVIUM		
7A DISTAL		
7B PROXIMAL, FROM WASATCH FORMATION		
7C PROXIMAL, FROM TERRACE ALLUVIUM		
FAULT EVENT		
	4 BURIED SOIL	
	4A A-HORIZON	4220±190
	4B ARGILLIC HORIZON	
5 SCARP COLLUVIUM		
4 SHEAR ZONE		
FAULT EVENT		
	3 BURIED SOIL	
	3A A-HORIZON	4770±205
	3B ARGILLIC HORIZON	

EXPLANATION (CONT.)

LITHOSTRATIGRAPHIC UNITS	SOIL STRATIGRAPHIC UNITS	AGE
2 TERRACE ALLUVIUM		
2A UPTHROWN BLOCK		
2B DOWNTHROWN BLOCK		
UNCONFORMITY		
1 WASATCH FORMATION		
1A FRIABLE SANDSTONE		
1B INDURATED SANDSTONE		
1C SANDY SHALE		

LOG OF
LESTER RANCH TRENCH
BEAR RIVER FAULT ZONE
BY
M.W. WEST, C. KRINSKY

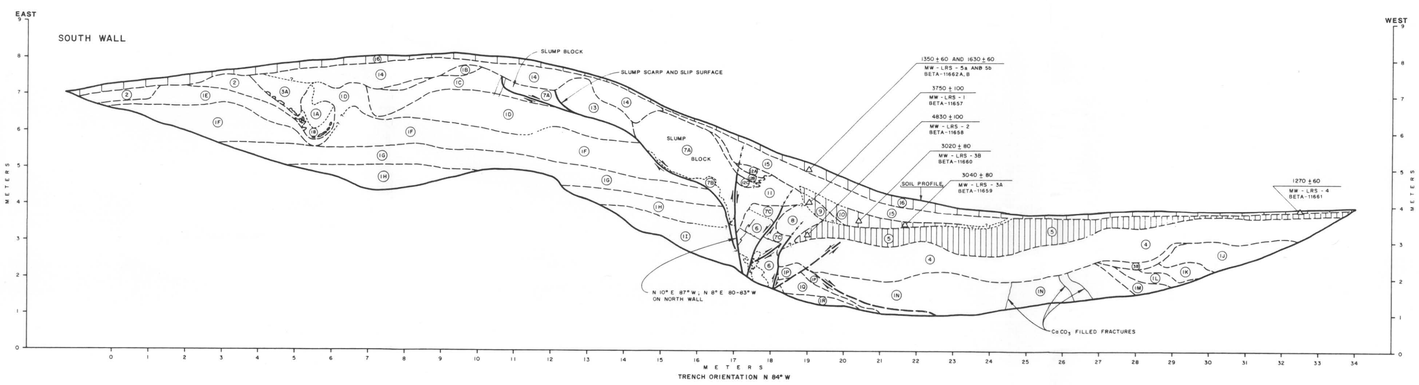

EXPLANATION

LITHOSTRATIGRAPHIC UNITS	SOIL STRATIGRAPHIC UNITS	AGE
	16 MODERN A-HORIZON	1270±60 1350±60 1630±60
15 SLOPE COLLUVIUM		
14 TERRACE LAG/COLLUVIUM		
13 COLLUVIUM/FISSURE FILL		
12 SCARP COLLUVIUM, FROM WASATCH FORMATION		
11 SCARP COLLUVIUM, FROM TERRACE ALLUVIUM		
FAULT EVENT		
	10 BURIED A-HORIZON	3020±80 3040±80
	9 BURIED A/B-HORIZON	3750±100
8 SCARP COLLUVIUM		
7 SLUMP BLOCK		
7A SLUMP		
7B BASAL SLUMP		
7C SLUMP ON DOWNTHROWN ROCK		
6 SHEARED BEDROCK AND FAULT GOUGE		
FAULT EVENT		
	5 BURIED A-HORIZON	4830±100
4 ALLUVIUM		
3 ALLUVIAL CHANNEL FILL		
3A UPTHROWN BLOCK		
3B DOWNTHROWN BLOCK		

EXPLANATION (CONT.)

LITHOSTRATIGRAPHIC UNITS	SOIL STRATIGRAPHIC UNITS	AGE
2 COLLUVIUM, LOESS AND BEDROCK LAG		
UNCONFORMITY		
1 WASATCH FORMATION		
UPTHROWN BLOCK		
1A PALEO-CHANNEL FILL		
1B PALEO-CHANNEL FILL		
1C SILTY CLAYSTONE		
1D SILTY CLAYSTONE		
1E SILTY CLAYSTONE - PALEOSOL		
1F SILTY CLAYSTONE		
1G CLAYSTONE		
1H SANDY SILT/CLAYSTONE		
1I SANDY SILT/CLAYSTONE DOWNTHROWN BLOCK		
1J CLAYSTONE		
1K SILTY CLAYSTONE		
1L SILTSANDSTONE		
1M CLAYEY SILTSTONE		
1N SILTY CLAYSTONE		
1P SILTY CLAYSTONE		
1Q SILTSANDSTONE		
1R CLAYSTONE		

LOG OF
LESTER RANCH
SOUTH TRENCH
BEAR RIVER FAULT ZONE
BY
M.W. WEST, C. KRINSKY

M.W. WEST

PLATE II

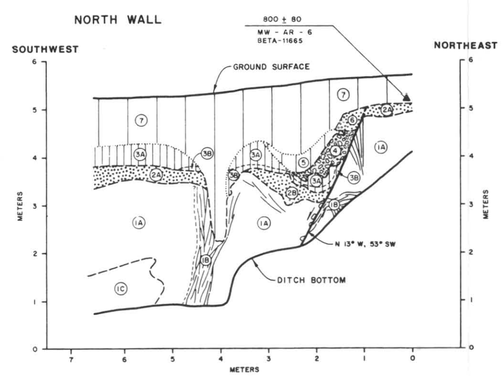

DITCH WALL ORIENTATION N 37° E

EXPLANATION

LITHOSTRATIGRAPHIC UNITS	SOIL STRATIGRAPHIC UNITS	AGE
	7 MODERN A-HORIZON AND FISSURE-FILL	800±80
6 SCARP COLLUVIUM		
FAULT EVENT		
	5 BURIED A-HORIZON	
4 SCARP COLLUVIUM		
FAULT EVENT		
	3 BURIED A-HORIZON	
	3A UPPER	
	3B BASAL	
2 COLLUVIUM		
2A FINE-GRAINED FACIES		
2B COARSE-GRAINED FACIES		
UNCONFORMITY		
1 WASATCH FORMATION		
1A WEATHERED BEDROCK		
1B SHEARED BEDROCK		
1C INTACT BEDROCK		

LOG OF
IRRIGATION DITCH WALL
AUSTIN RESERVOIR
SCARP
BEAR RIVER FAULT ZONE
BY
M W WEST, E BALTZER

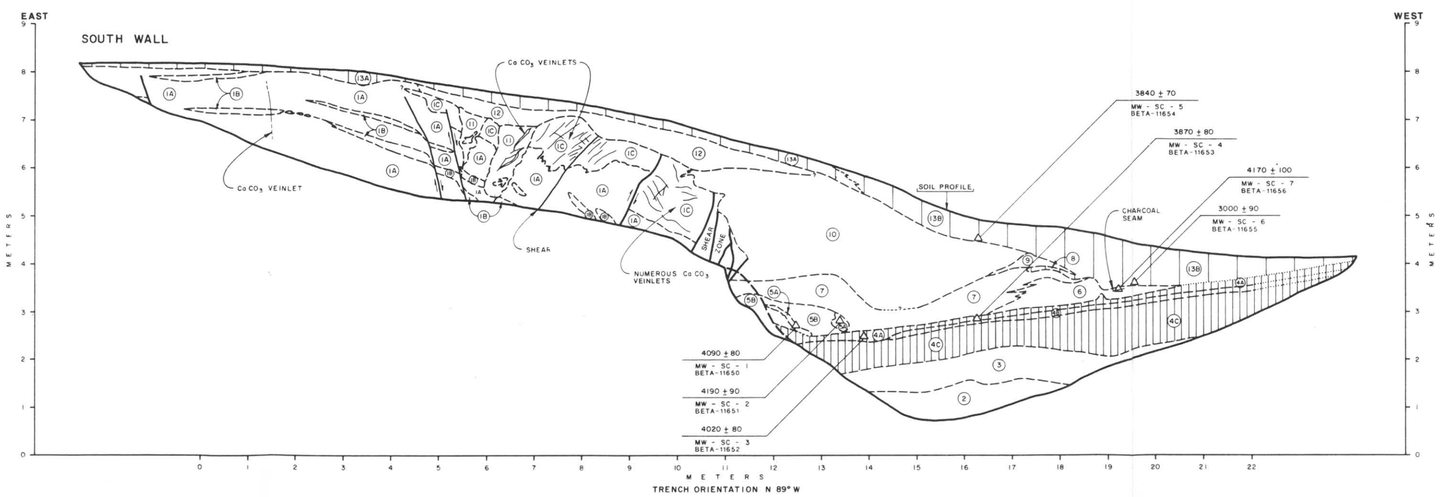

TRENCH ORIENTATION N 89° W

EXPLANATION

LITHOSTRATIGRAPHIC UNITS	SOIL STRATIGRAPHIC UNITS	AGE
	13 MODERN A-HORIZON	
	13A ON COLLUVIUM	
	13B ON LOESS	3000±90 3840±70
12 SLOPE COLLUVIUM		
11 FISSURE-FILL/COLLUVIUM		
10 SCARP COLLUVIUM		
9 SLOPE COLLUVIUM		
UNCONFORMITY		
	8 BURIED A-HORIZON	
7 SCARP COLLUVIUM		
6 SLOPE COLLUVIUM		4170±100
5 SCARP COLLUVIUM		
5A DERIVED FROM A-HORIZON		4090±80 4190±90
5B DERIVED FROM ALLUVIUM/COLLUVIUM		
FAULT EVENT		
	4 BURIED SOIL	
	4A A-HORIZON	3870±80 4020±80
	4B B1-HORIZON	
	4C ARGILLIC HORIZON	

EXPLANATION (CONT.)

LITHOSTRATIGRAPHIC UNITS	SOIL STRATIGRAPHIC UNITS	AGE
3 SAG POND SEDIMENTS		
2 SCARP COLLUVIUM		
? FAULT EVENT ?		
ALLUVIUM/COLLUVIUM		
UNCONFORMITY		
1 WASATCH FORMATION		
1A CLAYSTONE		
1B CLAY/SILTSTONE		
1C SANDSTONE		

LOG OF
SULPHUR CREEK
TRENCH
BEAR RIVER FAULT ZONE
BY
M.W. WEST, C. KRINSKY

M.W. WEST

PLATE III

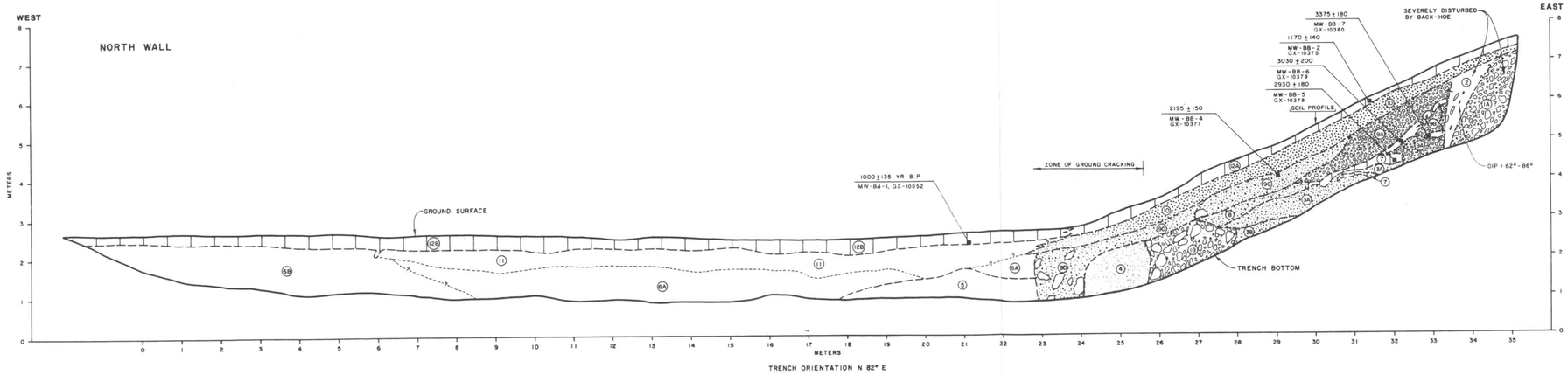

EXPLANATION

LITHOSTRATIGRAPHIC UNITS	SOIL STRATIGRAPHIC UNITS	AGE
	12 MODERN A-HORIZON	
	12A ON SCARP	1170±140
	12B IN SAG POND	1000±135
11 SAG POND SEDIMENTS		
10 SLOPE COLLUVIUM		
9 SCARP COLLUVIUM		
9A PROXIMAL		
9B PODS OF A-HORIZON		3030±200 3375±180
9C INTERMEDIATE		2195±150
9D DISTAL AND FISSURE-FILL		
FAULT EVENT		
8 SLOPE COLLUVIUM		
	7 BURIED A-HORIZON	2930±180
6 SAG POND SEDIMENTS		
6A ORGANIC SILT AND SAND		
6B GRAVELLY SAND		
5 COLLUVIUM		
4 FISSURE FILL		
3 SCARP COLLUVIUM		
3A SCARP COLLUVIUM		
3B SCARP COLLUVIUM/ FISSURE-FILL		
2 SHEAR ZONE		
FAULT EVENT		
1 TILL		
1A UPTHROWN BLOCK		
1B DOWNTHROWN BLOCK		

LOG OF
BIG BURN TRENCH
BEAR RIVER FAULT ZONE
BY
M.W. WEST, C. KRINSKY

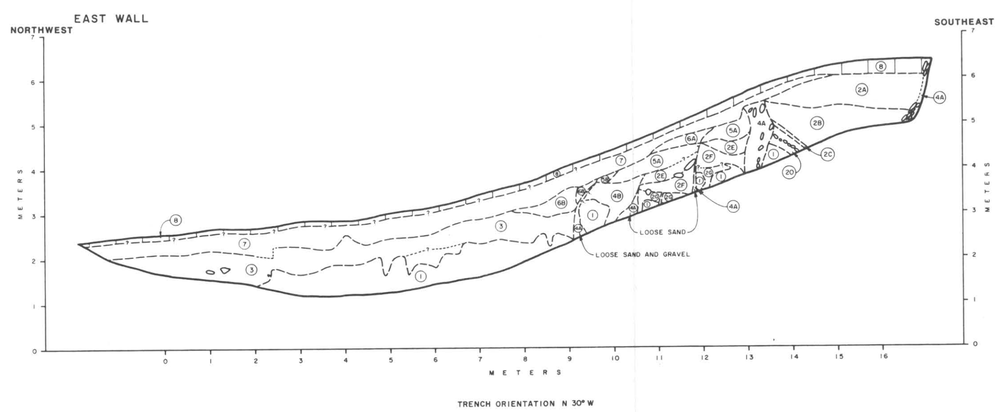

EXPLANATION

LITHOSTRATIGRAPHIC UNITS	SOIL STRATIGRAPHIC UNITS
	8 MODERN A-HORIZON
7 SLOPE COLLUVIUM	
6 SCARP COLLUVIUM	
6A COLLUVIUM	
6B COLLUVIUM	
6C A-HORIZON(?) POD	
FAULT EVENT	
	SOIL-FORMING PERIOD
5 SCARP COLLUVIUM	
5A PROXIMAL	
5B DISTAL	
4 SHEAR ZONE/FISSURE-FILL	
4A SHEAR ZONE	
4B FISSURE-FILL	
FAULT EVENT	
	SOIL-FORMING PERIOD
3 COLLUVIUM/RESIDUUM	
UNCONFORMITY	
2 GLACIO-FLUVIAL DEPOSITS	
UPTHROWN BLOCK	DOWNTHROWN BLOCK
2A SAND	2E SAND
2B SAND	2F SAND
2C SANDS AND GRAVELS	2G SANDS AND GRAVELS
2D SANDS AND GRAVELS	
1 TILL	

LOG OF
UPPER LITTLE BURN
TRENCH
BEAR RIVER FAULT ZONE
BY
M.W. WEST, C. KRINSKY

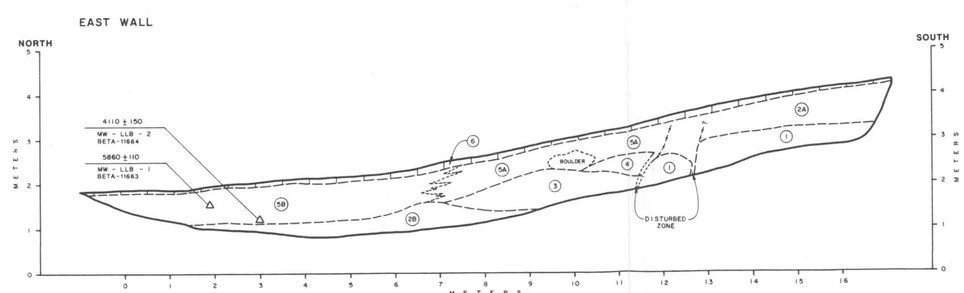

EXPLANATION

LITHOSTRATIGRAPHIC UNITS	SOIL STRATIGRAPHIC UNITS	AGE
	6 MODERN A-HORIZON	
5 SLOPE COLLUVIUM		
5A COLLUVIUM FROM GLACIO-FLUVIAL DEPOSITS		
5B LOESS AND COLLUVIUM		4110±150 5860±110
4 SCARP COLLUVIUM		
FAULT EVENT		
	SOIL FORMING PERIOD (?)	
3 SCARP COLLUVIUM (?)		
? FAULT EVENT ?		
UNCONFORMITY		
	SOIL-FORMING PERIOD	
2 GLACIO-FLUVIAL DEPOSITS		
2A UPTHROWN BLOCK		
2B DOWNTHROWN BLOCK		
1 TILL		

LOG OF
LOWER LITTLE BURN
TRENCH
BEAR RIVER FAULT ZONE
BY
M.W. WEST, C. KRINSKY

M.W. WEST

PLATE IV

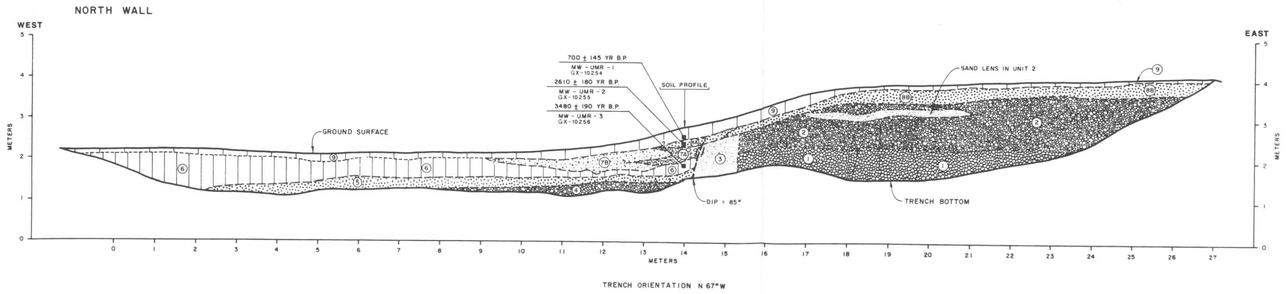

EXPLANATION

LITHOSTRATIGRAPHIC UNITS	SOIL STRATIGRAPHIC UNITS	AUE
	5 MODERN A-HORIZON	700±145
8 SLOPE COLLUVIUM		2610±180
8A 7.5 YR 5/4 DULL BROWN		
8B 5 YR 4/8 REDDISH BROWN		
7 SCARP COLLUVIUM		
7A PROXIMAL		
7B DISTAL		
FAULT EVENT		
	6 BURIED A/B HORIZONS	3480±190
5 SLOPE COLLUVIUM		
4 SCARP COLLUVIUM (?)		
3 SHEAR ZONE		
FAULT EVENT		
2 GRAVEL, COBBLE ALLUVIUM		
1 GRAVEL, BOULDER ALLUVIUM		

LOG OF
UPPER MARTIN RANCH
TRENCH
BEAR RIVER FAULT ZONE
BY
M.W. WEST, C. KRINSKY, E. BALTZER

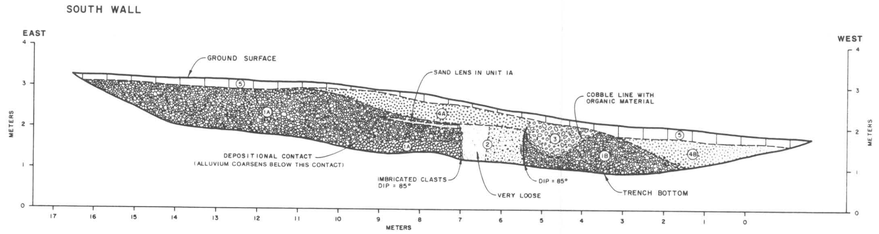

EXPLANATION

LITHOSTRATIGRAPHIC UNITS	SOIL STRATIGRAPHIC UNITS
	5 MODERN A-HORIZON
4 COLLUVIUM/RESIDUUM	
4A UPTHROWN BLOCK	
4B DOWNTHROWN BLOCK	
3 SCARP COLLUVIUM	
2 SHEAR ZONE	
FAULT EVENT	
	SOIL-FORMING PERIOD
1 ALLUVIUM	
1A UPTHROWN BLOCK	
1B DOWNTHROWN BLOCK	

LOG OF
LOWER MARTIN RANCH
TRENCH
BEAR RIVER FAULT ZONE
BY
M.W. WEST, C. KRINSKY

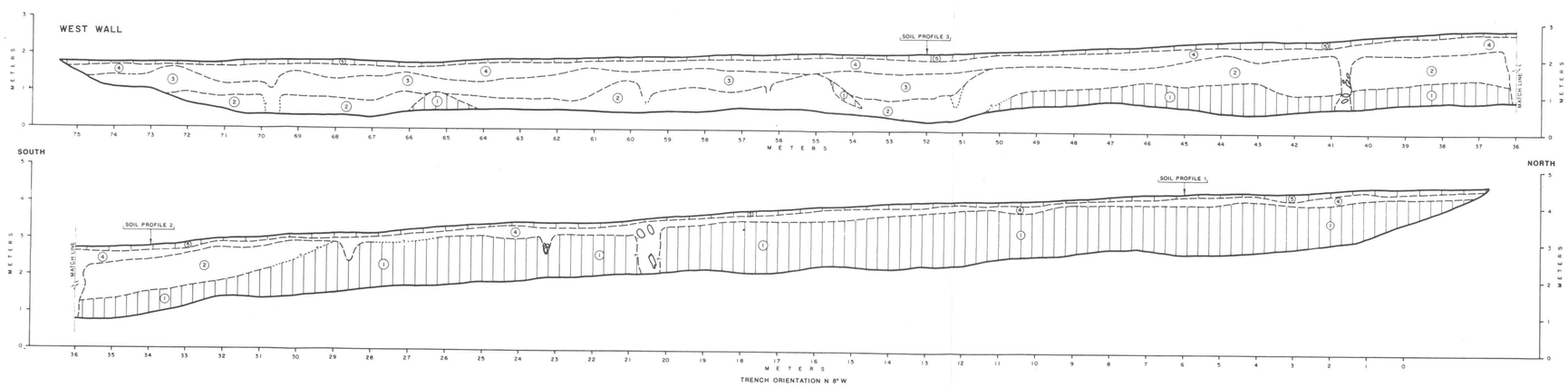

EXPLANATION

LITHOSTRATIGRAPHIC UNITS	SOIL STRATIGRAPHIC UNITS
	5 MODERN A-HORIZON
4 COLLUVIUM	
3 COLLUVIUM/CHANNEL-FILL	
2 SLOPE COLLUVIUM	
	1 ARGILLIC HORIZON SUPERIMPOSED ON BISHOP CONGLOMERATE
UNCONFORMITY	
1 BISHOP CONGLOMERATE, RESIDUUM	

LOG OF
ELIZABETH RIDGE TRENCH
BY
M.W. WEST, C. KRINSKY

M.W. WEST

PLATE V